The functional characterisation of MOB1-regulated Hippo core cassette kinase signalling

Yavuz Kulaberoglu

University College London

Cancer Institute

PhD Supervisor: Dr. Alexander Hergovich

A thesis submitted for the degree of Doctor of Philosophy

2017

Declaration

I, Yavuz Kulaberoglu, have read and understood the University Regulations on Cheating and Plagiarism and by submitting this work confirm that it is my own and does not contain any unacknowledged work from any other handwritten, printed or Internet source. I further confirm that I have acknowledged all sources used and quoted in this work. I understand that penalties can be applied in cases of proven cheating and plagiarism. If this work is to be submitted in both electronic and paper copy I certify that both copies are the same. I understand that this work may now or in future be submitted for checking by the TurnitIn plagiarism detection service.

Abstract

The Hippo tumour suppressor pathway regulates tissue growth by co-ordinating cell death, proliferation and differentiation. The central Hippo core cassette consists of MST1/2, LATS1/2, NDR1/2 and MOB1, with recent studies of MOB1 knockout mice indicating MOB1 functions as the central hub of Hippo signalling. However, it has remained unknown which interactions of MOB1 with the Hippo core cassette kinases MST1/2, LATS1/2 and NDR1/2 are required for normal life and tumour suppression. Therefore, my PhD project focused on deciphering the complex protein-protein interactions of MOB1 with MST1/2, LATS1/2 and NDR1/2. To do so, we generated a series of MOB1 variants that are selectively impaired in their binding to NDR1/2 (Trc), MST1/2 (Hippo), or LATS1/2 (Warts) in human (fly) cells. Using these selective loss-of-interaction (SLOI) variants we studied the effects of MOB1 overexpression on the proliferation and anchorage-independent growth of human cancer cell lines, thereby establishing which MOB1 interactions are required for the tumour suppressive role of MOB1. Equally importantly, we found that human MOB1 can restore the survival of *mats* loss-of-function (LOF) in *Drosophila.* By generating and studying transgenic flies expressing our SLOI MOB1 variants combined with Mats LOF, we discovered that the Hippo/MOB1A interaction is dispensable for fly development and reproduction, while the Trc/MOB1A and Wts/MOB1A interactions are essential. Taken together, my PhD thesis defined a completely novel panel of MOB1 SLOI variants to study the importance of MOB1 interactions. By studying transgenic human cells lines and flies expressing these SLOI variants we delineated which MOB1 interactions are essential for life of a complex multicellular organisms and for tumour suppression in human cancer cells. Collectively, our findings suggest that the Hippo/MOB1 interaction is neither required for life nor for tumour suppression, while the other interactions of MOB1 with Hippo core cassette kinases are essential in a context-dependent manner.

Acknowledgements

First of all, I would like to thank so much to Alex, for being such a supportive, motivational supervisor, for giving me an opportunity I would have never obtained in my life to work in such a motivating scientific environment and for being such a patient and tolerant to my "weak" English at the very beginning. I remember the first time I came in to meet Alex about my PhD project. At that time, Alex was outlining the PhD project and I remember well that I did not understand even one single word. Then, I remembered the famous saying from Richard Branson *"If someone offers you an amazing opportunity and you are not sure you can do it, say YES, and then learn how to do it later"*. All of a sudden, someone came in and asked Alex "Who is he", after seeing me. He replied, "He is a new PhD student". She answered, "Oooo, he is a new victim, then", while smiling Alex replied again, "No, he is a new victor". And, I started thinking, like "Am I going to achieve it?". My gut feeling was telling me, "Yes, you can". And I listened to my gut feeling.

Also, I would like to thank all the members of the Hergovich Lab, especially to Ramazan, for being such a friendly and supportive. Also, my big thanks go to Nic Tapon, Ivana Bjedov, and Maxine Holder for being such a helpful in my *Drosophila* studies.

Lastly, my big thanks go to the folks of Arnos grove house for being supportive. It would be shame for me if I forget to thank Ufuk Ucar for supporting me physiologically.

Turkish Acknowledgements

Değerli Annecim, Babacım ve Amcacım (Metin Kulaberoglu),

Size nasıl teşekkür edeceğimi gerçekten bilmiyorum. Daha doğrusu size ne kadar teşekkür etsem, bu yeterli olmaz. Anadolu lisesine kazandığımda, daha iyi eğitim alabilmem için, yediklerinden kısarak beni özel okula gönderdiğinizi, anneciğimin altınlarını satıp, bizlerin eğitimine verdiğini unutamam. Alinlerin terleriyle kazandıkları kazançları, eğitimime yatirdiğiniz hiç unutulur mu? Yaptığınız bu fedakârlıklar her zaman aklımda ve hiç unutmayacağım. Bende sizlerin bu fedakârlıklarına karşılık, Allah şahittir, canimi dişime takip calistim ve elimden geleni yaptım. Hiç şüpheniz olmasın, size utandıracak hiçbir şey yapmadım. Dünyanın en iyi 25. Üniversitesinde yüksek lisans eğitimimi tamamladım ve dünyanın en iyi 10. Üniversitesinde, an itibariyle doktora eğitimimi bitirmek üzereyim. Ve dünyanın en iyi 4. Üniversitesi olan Cambridge Üniversitesinden 3 sene, post-doc teklifi aldım. Bu basarilari elde ederken, Allah`tan başka kimseden yârdim talep etmedim.

Baba yarim olan, Metin amcamın, ailemin bu zorlu süreçlerinde hem maddi hem de manevi olarak yanında olmasını da unutmak çok büyük vefasızlık olur. Amca, bu elde edilmiş başarılarda, senin de çok büyük payın var ve sana nasıl teşekkür edeceğimi bilmiyorum!!! Ve bu basarilari elde etmemde, maddi ve manevi olarak yanımda olan, Yasin abimi, kardeşim Beyza'yı, babaannemi, Gülay yengemi unutmak ise büyük vefasızlık olur. Hepinizi çok seviyorum ve teşekkür ediyorum… Son olarak, Aziz Türkiye Cumhuriyeti Devleti`ne, bana sponsorluk yaptığı için çok teşekkür ediyorum. Aziz milletimin, alin terlerinden akıtarak vermiş olduğu vergilerle almış olduğum eğitimle, basta insanlığa sonra Aziz Türk milletine hizmet edeceğimden kimsenin kuskusu olmasın.

Abbreviations

AGC…… Protein kinase A (PKA)/PKG/PKC-like.

AS……..... Activation segment motif

CRB……. Crumbs

DKO……. Double knock-out

EMT…….. Epithelial-mesenchymal transition

ErbB4……. Receptor tyrosine-protein kinase erbB-4

Ex…… Expanded

GPCR…….. G-protein coupled receptor

HID…….. Head involution defective

HIPK…… Homeodomain interacting protein kinase

HM……... Hydrophobic motif

HP……. Hematoporphrin

Hpo……... Hippo

Hppy……. Happyhour

IAP……..... Inhibitors of apoptosis protein

KO……. Knock-out

LATS1/2…… Large tumour suppressor 1/2

LIFR…….. Leukemia inhibitory factor receptor

LPA……... serum-borne lysophosphatidic acid

MAP…… Microtubule affinity-regulating kinase 1

MAP4K……... Mitogen-activated protein kinase

mats……. Mob as a tumour suppressor

MEN…… Mitotic exit network

MOB1…….. Mps-one binder 1

MST1/2…… Mammalian Ste20-like serine/threonine kinases 1/2

NDR…… Nuclear dbf2 related

NF2…….. Neurofibromatosis-2

NTR……. N-terminal regulatory domain

OA…… Okadaic acid

PAR…….. Protease-activated receptors

PP2A……. Protein phosphatase type 2A

PPI……. Protein-protein interaction

RASSF……... RAS association domain family

RUNX1/2……... Runt-related transcription factor 1

S1P……. Sphingosine 1-phosphate

SAV……... Salvador

SIK……. Salt-inducible kinase

SIN……. Septation initiation network

TAO1……. Serine/threonine-protein kinase

TAZ…… Transcriptional co-activator with PDZ-binding motif

TBX5…… T-box transcription factor 5

TEAD…… TEA domain family member

Trc…….. Tricornered

TSG…… Tumour suppressor gene

VGLL4……... Vestigial-like family member 4

VP…….. Verteporfin

Wts…….. Warts

YAP…… Yes associated protein

Yki……... Yorkie

β-TrCP……. beta-transducin repeat containing E3 ubiquitin protein ligase

Table of Contents

1. Introduction 1
1.1. General introduction 1
1.2. The Core kinase network of the Hippo Pathway 4
1.3. Upstream regulators of the Hippo pathway 12
1.4. Hippo signalling in diseases 14
1.4.1. The Hippo pathway and cancer 14
1.4.2. Hippo signalling in non-cancer pathologies 18
1.4.3. Hippo Signalling as a therapeutic target 20
1.5. MOB Proteins 23
1.5.1. MOB proteins in budding and fission yeast 24
1.5.2. MOB proteins in *Drosophila* 26
1.5.3. MOBs in mammalian cells 31
1.5.4. Regulation of MOB1/Mats Proteins in *Drosophila* and Mammals 32
1.5.4. Mats/MOB1A in cancer 36
1.6. Research Aims 40
2. Materials and Methods 41
2.1. Materials 41
2.1.1. Reagents 41
2.1.2. Antibodies 47
2.1.3. Buffers and Solutions 48
2.1.4. Plasmids 60
2.1.5. Oligonucleotides 61
2.2. Methods 63
2.2.1. Molecular Biology Techniques 63
2.2.2. Biochemistry methods 79
2.2.3. Cell biology methods 85
2.2.4. Structural Studies Methods (performed in collaboration with the Wu Laboratory) 90
2.2.5. Fly genetics 92
3. Results 104
3.1. Structural and biochemical definition of the importance of MOB1A-NDR, MOB1A-LATS, and MOB1A-MST complex formation 104
3.1.1. Abstract 104
3.1.2. Introduction 105

3.1.3. Results - Structural definition of MOB1-NDR2 and MOB1-LATS1 complex formations 107
3.1.4. Results - Characterization of MOB1A mutants with selective binding to MST/NDR/LATS kinases in mammalian cells 115
3.1.5. Discussion 123
3.2. Defining the importance of complex formation of MOB1A with the Hpo, Wts, and Trc kinases in fly cells 126
3.2.1. Abstract 126
3.2.2. Introduction 127
3.2.3. Results - Characterization of MOB1A mutants with selective binding to the Hpo/Wts/Trc kinases in fly cells 128
3.2.4. Discussion 134
3.3. Defining phosphorylation patterns of our MOB1A variants by human MST1/2 and fly Hpo kinases 135
3.3.1. Abstract 135
3.3.2. Introduction 136
3.3.3. Results - Testing selective MOB1A mutants as MST1/2 substrates 137
3.3.4. Results - Testing selective MOB1A mutants as Hpo substrates 144
3.3.5. Discussion 147
3.4. Defining the tumour suppressive roles for MOB1A interactions with Hippo core kinases in human cancer cells 148
3.4.1. Abstract 148
3.4.2. Introduction 149
3.4.3. Results 151
3.4.4. Discussion 156
3.5. Defining the tumour suppressive roles of MOB1A interactions with the Hippo core kinases in *Drosophila melanogaster* 158
3.5.1. Abstract 158
3.5.2. Introduction 159
3.5.3. Results – The characterisation of Mats loss-of-function and transgenic flies expressing MOB1A variants 161
3.5.4. Results – The characterisation of transgenic flies expressing MOB1A variants in mosaic fly tissues 165
3.5.3. Discussion 176
4. Final discussion 179
4.1. Final discussion - from structural biology to cell culture 179
4.2. Final discussion - from human cells and *Drosophila melanogaster* 182
4.3. Future outlook 185

5. References 187
Supplementary Data 200
Supplementary Table S1 Data collection and refinement statistics. 200
Appendix 1 205
Appendix 2 215

Table of Figures

Figure 1.1. The involvement of the Hippo pathway in different cellular processes. 2
Figure 1.2. Schematic illustration of the human Hippo pathway. 9
Figure 1.3. Schematic illustration of the Drosophila Hippo pathway. 11
Figure 1.4. Hippo (MST1/2) loss-of-function phenotypes in Drosophila and mice. 14
Figure 1.5. Conservation of the Mats gene. 30
Figure 1.6. A proposed model for Wts activation. 34
Figure 1. 7. The implications of the Mats loss-of-function in cancer-related phenotypes. 37
Figure 2.1. Cloning of MOB1A into pcDNA3.1_myc. ____ 71
Figure 2.2. The cloning of myc-MOB1A cDNAs, Drosophila myc-Mats, HA-Hpo, HA-Trc, HA-Warts into pENTR3C. ____ 73
Figure 2.3. The cloning of myc-hMOB1A cDNAs, Drosophila myc-Mats, HA-Hpo, HA-Trc, HA-Wts into pAW. ____ 74
Figure 2.4. The cloning of MOB1A cDNAs into pMAL-2C. ____ 76
Figure 2.5. The cloning of MOB1A cDNAs into PKC26W pUbi. ____ 78
Figure 2.6. A Schematic representation of ΦC31-mediated insertion. ____ 94
Figure 2.7. Differences between wild type and TM6B balancer flies. ____ 95
Figure 2.8. The generation of the balanced flies. ____ 96
Figure 2. 9. Recombination of Roo transposon. ____ 97
Figure 2.10. Recombination of FRT sites. ____ 99
Figure 2.11. The FLP/FRT system. ____ 102
Figure 3.1. The MOB1A/NDR2 structure reveals that MOB1A and NDR2 interact through conserved interfaces. ____ 108
Figure 3.2. NDR2 and LATS2 bind to MOB1A through different key residues/mechanisms. ____ 111
Figure 3. 3. Characterization of MOB1A(D63V) and MOB1A(K104E/K105E) binding to NDR2, LATS1 and MST2 by gel filtration chromatography. ____ 113
Figure 3.4. Characterization of the interaction of MOB1A variants with MST1/2. 116
Figure 3.5. Characterization of the interaction of MOB1A variants with the LATS1/2 kinases. ____ 118
Figure 3.6. Characterization of the interaction of MOB1A variants with NDR1/2. 119
Figure 3.7. Generation of MOB1A variants to dissect the importance of MOB1A interactions with mammalian Hippo core cassette kinases. ____ 122
Figure 3.8. Characterization of the interaction of MOB1A variants with the fly Hippo kinase ____ 129

Figure 3.9. Characterization of the interaction of MOB1A variants with the Wts kinase. _____ *130*
*Figure 3.10. Characterization of the interaction of MOB1A variants with the Trc kinase*_____ *131*
Figure 3.11. Generation of MOB1 variants to dissect the importance of MOB1 interactions with Drosophila Hippo core cassette kinases. _____ *133*
Figure 3.12. Bacterially expressed and purified MAL-MOB1A variants. _____ *137*
Figure 3.13. Phosphorylation of MOB1A mutants by MST1/2. _____ *138*
Figure 3.14. Characterization of the anti-Thr12-P and anti-Thr35-P antibodies in the context of MST1/2-mediated phosphorylation of MOB1A. _____ *140*
*Figure 3.15. Characterization of the MST1/2-mediated phosphorylation of MOB1A variants.*_____ *142*
Figure 3.16. Characterization of the anti-Thr12-P and anti-Thr35-P antibodies in the context of Hippo-mediated phosphorylation of MOB1A. _____ *144*
Figure 3.17. Characterization of the MST1/2(Hippo)-mediated phosphorylation of MOB1A variants. _____ *145*
Figure 3.18. MOB1A functions as tumour suppressor by decreasing cell proliferation. _____ *152*
Figure 3. 19. MOB1A can suppress proliferation and anchorage-independent growth of human cancer cells through different interactions with Hippo core cassette kinases. _____ *154*
*Figure 3.20. Confirmation of the homozygous lethality caused by Mats loss-of-function.*_____
Figure 3. 21. Ubiquitous expression of human MOB1(wt) or MOB1(K104E/K105E) rescues larval lethality of Mats deficient flies. _____ *163*
*Figure 3.22. Ubiquitous expression of human MOB1(wt) or MOB1(K104E/K105E) rescues tissue overgrowth phenotype driven by Mats loss-of-function*_____ *166*
Figure 3.23. Ubiquitous expression of the MOB1A(wt) transgene restores expanded upregulation in Mats^{roo} mutant clones in wing imaginal discs. _____ *168*
Figure 3.24. Ubiquitous expression of MOB1A(wt) transgene rescues Expanded upregulation in Mats^{roo} mutant clones in the eye imaginal discs. _____ *170*
Figure 3.25. Expression of MOB1A(KEKE) restores normal Ex levels in Mats^{roo} mutant clones in the wing imaginal disc, while expression of MOB1A(DV) or MOB1A(DVKEKE) does not. _____ *172*

Figure 3.26. Expression of MOB1A(KEKE) restores normal Ex levels in Mats^{roo} mutant clones in the eye imaginal disc, while expression of MOB1A(DV) or MOB1A(DVKEKE) does not. 174

Figure 2.1. Cloning of MOB1A into pcDNA3.1_myc. *71*
Figure 2.2. The cloning of myc-MOB1A cDNAs, Drosophila myc-Mats, HA-Hpo, HA-Trc, HA-Warts into pENTR3C. *73*
Figure 2.3. The cloning of myc-MOB1A cDNAs, Drosophila myc-Mats, HA-Hpo, HA-Trc, HA-Wts into pAW. *74*
Figure 2.4. The cloning of MOB1A cDNAs into pMAL-2C. *76*
Figure 2.5. The cloning of MOB1A cDNAs into PKC26W pUbi. *78*
Figure 2.6. A Schematic representation of ΦC31-mediated insertion. *94*
Figure 2.7. Differences between wild type and TM6B balancer flies. *95*
Figure 2.8. The generation of balanced stocks. *96*
Figure 2.9. Recombination of Roo transposon. *97*
Figure 2.10. Recombination of FRT sites. *99*
Figure 2.11. The FLP/FRT system. *102*

Figure 3.1. The MOB1A/NDR2 structure reveals that MOB1A and NDR2 interact through conserved interfaces. *108*
Figure 3.2. NDR2 and LATS2 bind to MOB1A through different key residues/mechanisms. *111*
Figure 3. 3. Characterization of MOB1A(D63V) and MOB1A(K104E/K105E) binding to NDR2, LATS1 and MST2 by gel filtration chromatography. *113*
Figure 3.4. Characterization of the interaction of MOB1A variants with MST1/2. ..... *116*
Figure 3.5. Characterization of the interaction of MOB1A variants with the LATS1/2 kinases. *118*
Figure 3.6. Characterization of the interaction of MOB1A variants with NDR1/2. ..... *119*
Figure 3.7. Generation of MOB1A variants to dissect the importance of MOB1A interactions with mammalian Hippo core cassette kinases. *122*
Figure 3.8. Characterization of the interaction of MOB1A variants with the fly Hpo kinase. *129*
Figure 3.9. Characterization of the interaction of MOB1A variants with the Wts kinase. *130*
Figure 3.10. Characterization of the interaction of MOB1A variants with the Trc kinase *131*
Figure 3.11. Generation of MOB1 variants to dissect the importance of MOB1 interactions with Drosophila Hippo core cassette kinases. *133*
Figure 3.12. Bacterially expressed and purified MAL-MOB1A variants. *137*
Figure 3.13. Phosphorylation of MOB1A mutants by MST1/2. ..... *138*
Figure 3.14. Characterization of the anti-Thr12-P and anti-Thr35-P antibodies in the context of MST1/2-mediated phosphorylation of MOB1A. *140*
Figure 3.15. Characterization of the MST1/2-mediated phosphorylation of MOB1A variants. *142*
Figure 3.16. Characterization of the anti-Thr12-P and anti-Thr35-P antibodies in the context of Hippo-mediated phosphorylation of MOB1A. *144*
Figure 3.17. Characterization of the MST1/2(Hippo)-mediated phosphorylation of MOB1A variants. *145*
Figure 3.18. MOB1A functions as tumour suppressor by decreasing cell proliferation. *152*
Figure 3. 19. MOB1A can suppress proliferation and anchorage-independent growth of human cancer cells through different interactions with Hippo core cassette kinases. *154*
Figure 3.20. Confirmation of the homozygous lethality caused by mats loss-of-function. *161*
Figure 3.21. Ubiquitous expression of human MOB1(wt) or MOB1(K104E/K105E) rescues larval lethality of mats deficient flies. *163*

Figure 3.22. Ubiquitous expression of human MOB1(wt) or MOB1(K104E/K105E) rescues tissue overgrowth phenotype driven by Mats loss-of-function 166
Figure 3.23. Ubiquitous expression of the MOB1A(wt) transgene restores ex upregulation in mats^{roo} mutant clones in wing imaginal discs. 168
Figure 3.24. Ubiquitous expression of MOB1A(wt) transgene rescues Ex upregulation in mats^{roo} mutant clones in the eye imaginal discs. 170
Figure 3.25. Expression of MOB1A(KEKE) restores normal Ex levels in mats^{roo} mutant clones in the wing imaginal disc, while expression of MOB1A(DV) or MOB1A(DVKEKE) does not. 172
Figure 3.26. Expression of MOB1A(KEKE) restores normal Ex levels in mats^{roo} mutant clones in the eye imaginal disc, while expression of MOB1A(DV) or MOB1A(DVKEKE) does not. 174

Publications

Bold and # indicate first or equally contributed authorship.

Hoa, L.[#], **Y. Kulaberoglu[#]**, R. Gundogdu, D. Cook, M. Mavis, M. Gomez, V. Gomez and A. Hergovich. "The Characterisation of Lats2 Kinase Regulation in Hippo-Yap Signalling." *Cellular Signalling* 28, no. 5 (2016): 488-497.

Kulaberoglu, Y.[#],Gundogdu, R., and Hergovich, A. Role of p53/p21/p16 in DNA damage signalling and DNA repair. ***Genome Stability*** **(in press)**. http://store.elsevier.com/Genome-Stability/isbn-9780128033098/

Kulaberoglu, Y.[#], Gomez, M., Assefa Shifa, B., Hoa, L., Tapon, N. and Hergovich, A. The functional characterisation of the regulatory MOB1 interactions in Hippo kinase signalling reveals essential roles for MOB1-containing complexes. (*planned submission to* ***Nature Structural and Molecular Biology*** (in 2016)

Chisnall, B., C. Johnson, Y. Kulaberoglu and Y. W. Chen. "Insoluble Protein Purification with Sarkosyl: Facts and Precautions." *Methods Mol Biol* 1091, (2014): 179-86.

Conference attended

2015 (between 21th and 24th August): Oral Presentation**,** 4th National Molecular biology and Biotechnology Conference, Afyonkarahisar, Turkey

Leadership experiences

2014-2015: Personal tutor for Onur Kahraman and Mustafa Taher (Master students in UCL Cancer Institute)

2015-2016: Personal tutor for Annabel Tran and Angela Li (Master students in UCL Cancer Institute)

2014-2015: Supervision for Merdiye Mavis (Master student in UCL cancer Institute, passed with Merit, Thesis title: Biochemical and Structural Definition of MOB1 Loss of Interaction Variant

Awards

- A full scholarship for Master and PhD study abroad awarded by Ministry of National Education of Turkey
- Post-doctorate research associate, sponsored by Cancer-Research UK for 3 years, under supervision of Dr Ewan St. John Smith, University of Cambridge in the department of pharmacology (Expected start date: 6 October 2016)

Outreach/public engagement activities

2014 – Present: Exhibitor at London Innovation Society in Inspiring Science Scheme

- I am exhibitor of London Innovation Society (LIS) and run public engagement activity named "Who do you think you are?" in collaboration with LIS. The public engagement activity takes 55 minutes and includes the following hands-on activities;
  - **Building up the model DNA using play-dough**
  - **Extracting pupil`s DNA from their saliva and sequencing their DNA**
  - **Tracing their possible ancestor using sequence analysis**
- The public engagement activities performed so far are listed below;
  - **2015: North London Grammar School (NLGS), student aged 11-16.**
  - **2016: King Fahad Academy, Girls Grade 9G1 (Yr 10)**
  - **2016: King Fahad Academy, Boys Grade 9B1 (Yr 10)**
  - **2016: Ashmole Academy, Student year 10**

1. Introduction

1.1. General introduction

The regulation of cell proliferation, death and differentiation is regarded as one of the most fundamental biological processes not only to ensure proper organ size during development but also to sustain tissue homeostasis during postnatal life. The coordination of these processes is considered crucial for physiological and pathological conditions (Galliot and Ghila 2010). Cell proliferation and differentiation is needed to ensure proper organ size and differentiation of multiple cell types, allowing to function accurately, during development (Gomez, Gomez et al. 2014). In adult animal, most tissues are subjected to continuous cell turnover to sustain functionality. Aged and/or damaged cells undergo apoptosis (also known as programmed cell death), followed by replacement of these aged and/or damaged cells by differentiating adult stem cells, which can replenish dysfunctional cells. Under normal conditions, wound healing and organ regeneration is tightly controlled and regulated by cell division and differentiation of tissue specific progenitor cells. However, deregulation of cell proliferation and death result in hyperplasia or tumorigenesis (Yu and Guan 2013). Intensive research efforts have been invested to uncover the detailed mechanism underlying cell proliferation, death and differentiation. However, how multicellular organisms coordinate the growth of their individual cells and the size of their organs is poorly understood.

Research carried out over the past decade has discovered the Hippo pathway as an evolutionally and functionally conserved signalling network, which has been shown to be a master regulator of cell proliferation, death and differentiation (Yu and Guan 2013, Gomez, Gomez et al. 2014). Current evidence strongly suggests that the Hippo pathway may play pivotal roles in coordinating these cellular processes **(Figure 1.1)**.

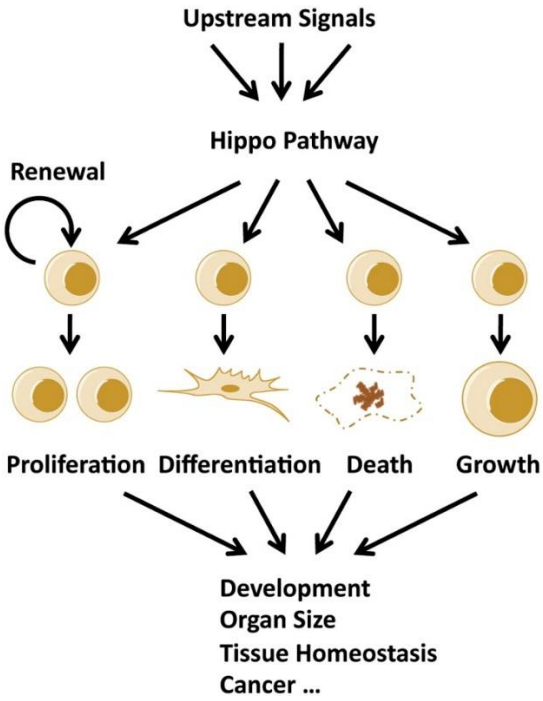

Figure 1.1. The involvement of the Hippo pathway in different cellular processes.

The Hippo pathway can regulate cell proliferation, differentiation, and death. The modulation of these cellular processes by the Hippo pathway may contribute to different physiological and pathological conditions including development, tissue homeostasis, and cancer development (Adapted from (Yu and Guan 2013).

The Hippo pathway is a highly conserved growth inhibitory signalling cascade. This pathway was initially discovered in *D. melanogaster* by genetic mosaic screens to identify genes whose loss-of-function mutations result in severe overgrowth phenotype (Meng, Moroishi et al. 2016). For example, genetic inactivation of Hippo components, such as Warts (Wts) (Justice, Zilian et al. 1995, Xu, Wang et al. 1995), Hippo (Hpo) (Harvey, Pfleger et al. 2003, Wu, Huang et al. 2003), Salvador (Sav) (Tapon, Harvey et al. 2002), and Mats (Lai, Wei et al. 2005), all lead to similar severe overgrowth phenotype. Significantly, follow up studies revealed that the Hippo pathway is highly conserved from flies to human. Each member of the Hippo pathway in *D. melanogaster* possesses functional orthologs in mammals. In flies, Hpo (Harvey, Pfleger et al. 2003, Jia, Zhang et al. 2003, Pantalacci, Tapon et al. 2003, Udan, Kango-Singh et al. 2003, Wu, Huang et al. 2003), Sav (Kango-Singh, Nolo et al. 2002,

Tapon, Harvey et al. 2002), Wts (Justice, Zilian et al. 1995, Watson 1995, Xu, Wang et al. 1995, Justice, Woods et al. 1999, Tapon, Harvey et al. 2002) and Mats (Lai, Wei et al. 2005) organize a kinase network which phosphorylates and negatively regulates Yki, which together with Sd (Hong and Guan 2012) mediates the major physiological functions of the pathway. In mammals, a classical view of the core of the Hippo pathway organizes a kinase network in which mammalian Ste20-like serine/threonine kinases 1/2 (MST1/2) (Dan, Watanabe et al. 2001) are activated by multiple upstream branches. The activated MST1/2 then interact with their scaffolding partner SAV (Avruch, Zhou et al. 2012), which is in turn followed by phosphorylation of the large tumour suppressor 1/2 serine/threonine protein kinases (LATS1/2) (Hergovich, Stegert et al. 2006, Praskova, Xia et al. 2008, Li, Li et al. 2014, Meng, Moroishi et al. 2015, Hoa, Kulaberoglu et al. 2016) and MOB1 (Hergovich 2011), leading to increased LATS/MOB1 complex formation and ultimately LATS1/2 activation. Phosphorylation of YAP/TAZ by activated LATS1/2 kinases result in YAP/TAZ cytoplasmic retention and/or degradation (please see **Table 1.1** for the nomenclature of core components of the Hippo pathway in *Drosophila* and mammals).

While this traditional linear signalling network has been serving for the initial studies of Hippo signalling, recent studies have identified the AGC serine/threonine NDR1/2 kinases (Zhang, Tang et al. 2015) and members of the Ste-like MAP4K as a new members of the core Hippo pathway (Meng, Moroishi et al. 2015). More specifically, in addition to MST1/2 kinases, members of MAP4K kinases can induce the phosphorylation and activation of LATS1/2 to negatively regulate YAP/TAZ via LATS1/2-stimulated-phosphorylation (Hergovich 2016). Furthermore, a recent study revealed that NDR1/2 can act as YAP kinases (Zhang, Tang et al. 2015). Taken together, MST1/2 as well as members of MAP4K kinases can regulate and activate NDR1/2 and LATS1/2 kinases, consequently negatively regulating YAP/TAZ (Hergovich 2016).

Following the identification of MAP4K as new upstream regulator of LATS1/2 and NDR1/2 kinases, another recent study discovered the ste-20 kinase Happyhour (Hppy) (counterpart of mammalian MAP4K kinases)

as an alternative kinase which phosphorylates and activates Wts in *Drosophila* (Zheng, Wang et al. 2015).

Table 1.1. Hippo core components in humans and *D. melanogaster* (adapted from (Johnson and Halder 2014)

Human proteins	*D. melanogaster* protein	Protein function	Domain composition
Core components			
MST1, MST2	Hpo	Serine/threonine kinase, STE20 family	Kinase domain, SARAH domain
SAV1 (also known as WW45)	Sav	Adaptor protein	FERM domain-binding motif, two WW domains, SARAH domain
LATS1, LATS2	Wts	Serine/threonine kinase, NDR family	Kinase domain
MOB1A, MOB1B	Mats	Cofactor	MOB domain
YAP, TAZ	Yki	Transcriptional co-activator	Two WW domains, 14-3-3 binding motif, TEAD-binding motif, PDZ-binding motif
TEAD1–TEAD4	Sd	Transcription factor	TEAD DNA-binding domain, vestigial binding domain

1.2. The Core kinase network of the Hippo Pathway

The mammalian Hippo pathway consists of a core kinase cassette compromising mammalian sterile 20-like serine/threonine kinases 1 and 2 (MST1 and MST2, also known as STK4 and STK3), MAP4Ks (Mitogen-activated kinases), the large tumour suppressor 1 and 2 (LATS1/2) serine/threonine protein kinases, nuclear dbf2-related kinases 1 and 2 (NDR1/2), the adaptor protein Salvador homologue 1 (SAV1, also known as WW45), the signal transducer Mps-one binder 1 (MOB1), and the downstream effectors compromising the transcriptional co-activators Yes-associated protein and transcriptional co-activator with PDZ-binding motif (TAZ). The physiological output of Hippo signalling is to negatively regulate the activities of YAP and TAZ (Gomez, Gomez et al. 2014). MST1/2, MAP4Ks, LATS1/2, NDR1/2, SAV1, MOB1, and YAP/TAZ correspond to Hpo, Hppy, Wts, Trc, Sav, Mats, and Yki in flies, respectively. The inactivation of YAP/TAZ plays an important role in maintaining cell quiescence. Dysregulation of YAP/TAZ activities significantly contributes to cancer initiation and development **(Figure 1.1)**

through various mechanisms (Meng, Moroishi et al. 2016). The main mediator of YAP/TAZ is believed to be TEAD1-4 transcription factors, though other transcription factors, such as RUNX1/2, p63/p73, ErbB4, can also associate with YAP/TAZ (Hansen, Moroishi et al. 2015).

Our traditional understanding of the regulation of core Hippo signalling can be summarised as follows: the Hippo pathway is activated by pro-apoptotic kinases MST1/2 by the binding of SAV1 through the SARAH domains (Hwang, Ryu et al. 2007). MST1/2 (Hippo) can be activated through different mechanisms. The activation of MST1/2 is also performed by binding to Ras association domain family (RASSF) proteins (Oh, Lee et al. 2006). Furthermore, recent studies have revealed that the thousand-and-one (TAO) amino acids kinase or TAOK1-3 can also phosphorylate and activate Hpo or MST1/2 (Boggiano, Vanderzalm et al. 2011, Poon, Lin et al. 2011). In contrast to mammals, *Drosophila* homologous RASSF has been shown to inhibit Hpo (homologues of human MST1/2), possibly owing to competition with Sav for Hpo binding (Polesello, Huelsmann et al. 2006) and the recruitment of the dSTRIPAK-PP2A complex **(Figure 1.3)** (Ribeiro, Josue et al. 2010). Following the activation of MST1/2, LATS2 is in turn phosphorylated at Thr1041 (known as hydrophobic motif (HM) site) (Hoa, Kulaberoglu et al. 2016). MOB1 is phosphorylated by MST1/2 at Thr12 and Thr35 sites, which leads to an enhanced affinity of MOB1 for LATS1/2, leading to the phosphorylation of LATS1/2 at Ser872 (known as T loop) and Thr1041 (HM sites) (Praskova, Xia et al. 2008, Hoa, Kulaberoglu et al. 2016). Activated LATS1/2 in turn phosphorylates YAP in HXRXXS motif at Ser127 residue (Yorkie at Ser168 residue), creating a 14-3-3 binding site, which result in cytoplasmic retention of YAP. (Gomez, Gomez et al. 2014). TAZ is regulated in a similar fashion as YAP. TAZ is phosphorylated by LATS2 in HXRXXS motif at Ser89, generating a 14-3-3 binding site, therefore resulting in its inactivation **(Figure 1.2)** (Johnson and Halder 2014). YAP and TAZ do not contain any DNA binding domain. However, they are able to bind to the vicinity of promoters of target genes by associating with DNA-binding transcriptional factors, such as TEAD1-4 (Goulev, Fauny et al. 2008), Smad1/2/3 (Alarcon, Zaromytidou et al. 2009),

p63/p73 (Strano, Munarriz et al. 2001), T-box transcription factor 5 (TBX5) (Murakami, Nakagawa et al. 2005), RUNT-related factor 1 and 2 (RUNX1/2) (Murakami, Nakagawa et al. 2005) . The association of YAP/TAZ with the transcriptional factors triggers changes in the expression of genes involved in cell proliferation, cell death, differentiation (Meng, Moroishi et al. 2016).

In addition to traditional regulation of core Hippo signalling, recent studies discovered new additional kinases MAP4Ks and NDR1/2 as novel members of the core cassette of Hippo signalling. More specifically, MAP4Ks were shown to function as important physiological LATS-activating kinases in addition to MST1/2 kinases (Meng, Moroishi et al. 2015). Furthermore, the involvement of NDR1/2 kinases in core Hippo signalling made the regulation more and more complex. NDR1/2 interact with MOB1 (Bichsel, Tamaskovic et al. 2004, Hergovich, Bichsel et al. 2005, Hergovich, Kohler et al. 2009) and act as YAP kinases (Zhang, Tang et al. 2015). Interestingly, it was shown that NDR1/2 is regulated by MST1, MST2, and MST3 (Stegert, Hergovich et al. 2005, Cornils, Kohler et al. 2011). More interestingly, recent studies revealed that MAP4Ks are the upstream regulator of NDR1/2 kinases (Selimoglu at al., 2014). Taken together, NDR1/2 can be regulated by MST kinases and function as upstream regulator of YAP. Furthermore, MOB1-NDR1/2 and MOB1-LATS1/2 complex formation seems to play pivotal role for the regulation of Hippo signalling **(Figure 1.2)**. In addition to MST kinases, MAP4Ks can also act as upstream regulator of NDR1/2 as well as LATS1/2. NDR1/2 and LATS1/2 kinases initiate the phosphorylation of YAP to negatively regulate YAP **(Figure 1.2)**.

Phosphorylation of YAP and TAZ at Ser127 and Ser89, respectively, plays a pivotal role in generating the 14-3-3 binding side, leading to their cytoplasmic sequestration and subsequent inactivation. In addition, YAP and TAZ are phosphorylated by LATS1/2 at Ser381 and Ser311, respectively, which primes YAP and TAZ for subsequent phosphorylation by CK1 (casein kinase 1), which generates a phospho-degron that can recruit β-TrCP (beta-transducin repeat containing E3 ubiquitin protein

ligase) and hence promote YAP and TAZ ubiquitination and degradation (Liu, Zha et al. 2010, Zhao, Li et al. 2010, Huang, Lv et al. 2012). YAP/TAZ can be also phosphorylated at other serine sites by LATS1/2 (YAP on Ser61, Ser109, Ser164, TAZ on Ser66, Ser89, Ser117, Ser311). However, their functions are unknown. In addition to the phosphorylation-dependent degradation, YAP and TAZ also can be suppressed through phosphorylation-independent manner by protein-protein interactions with transmembrane complexes-related proteins, leading to YAP and TAZ cytoplasmic sequestration (see **section 1.3) (Figure 1.2)** (Santucci, Vignudelli et al. 2015).

The regulation of the Hippo pathway is highly conserved from *Drosophila* to mammals. In tradition to fashion as observed in mammals, the *Drosophila* Hippo pathway is "turned on" by the activation of Hpo, in association with an adaptor protein Sav, which in turn phosphorylates and activates the kinase Wts. Furthermore, Mats is then phosphorylated by Hpo, leading to enhanced binding of Mats for Wts. The activated Wts then phosphorylates Yki as downstream effector, which in turn leads to its cytoplasmic retention via 14-3-3 **(Figure 1.3)** (Meng, Moroishi et al. 2016). As reported in mammalian Hippo signalling, the regulation of *Drosophila* core Hippo signalling is also more complex than it has been thought. Recent research discovered Tricornered (Trc) and Happyhour (Hppy) as novel components of core *Drosophila* signalling. Trc and Hppy correspond to NDR1/2 and MAP4Ks in mammals. There are some connections that link Trc to the regulation of core *Drosophila* Hippo signalling. First connection, Hippo (counterpart of human MST1/2) functions as upstream regulator of Trc and Wts in fly neurons (Emoto, Parrish et al. 2006). Second connection, Trc and Wts mutant cells exhibit increased levels of F-actin (He, Emoto et al. 2005, Fang and Adler 2010), a phenotype also detected upon Yki overexpression or Hippo loss-of-function (Fang and Adler 2010). Third connection, Trc and Wts mutant cells display upregulation of DE-Cadherin expression, which was also reported in Mats mutant cells (Fang and Adler 2010). Fourth connection, Trc as well as Wts have been shown to physically and genetically associate with Mats (He, Emoto et al. 2005, Lai, Wei et al.

2005). Furthermore, the complex formation of Wts or Trc with Mats might play important roles in fly wing development. These findings suggest that Trc and Wts, together with Mats, might function together to phosphorylate and ultimately inactivate Yki **(Figure 1.3)**. However, it has not been addressed yet whether Trc could directly phosphorylate and inactivate Yki. On the other hand, another key player Hppy was identified as novel component of core *Drosophila* Hippo signalling (Zheng, Wang et al. 2015). Hppy was found to function as upstream regulator of Wts by phosphorylating the hydrophobic motif of Wts (Zheng, Wang et al. 2015).

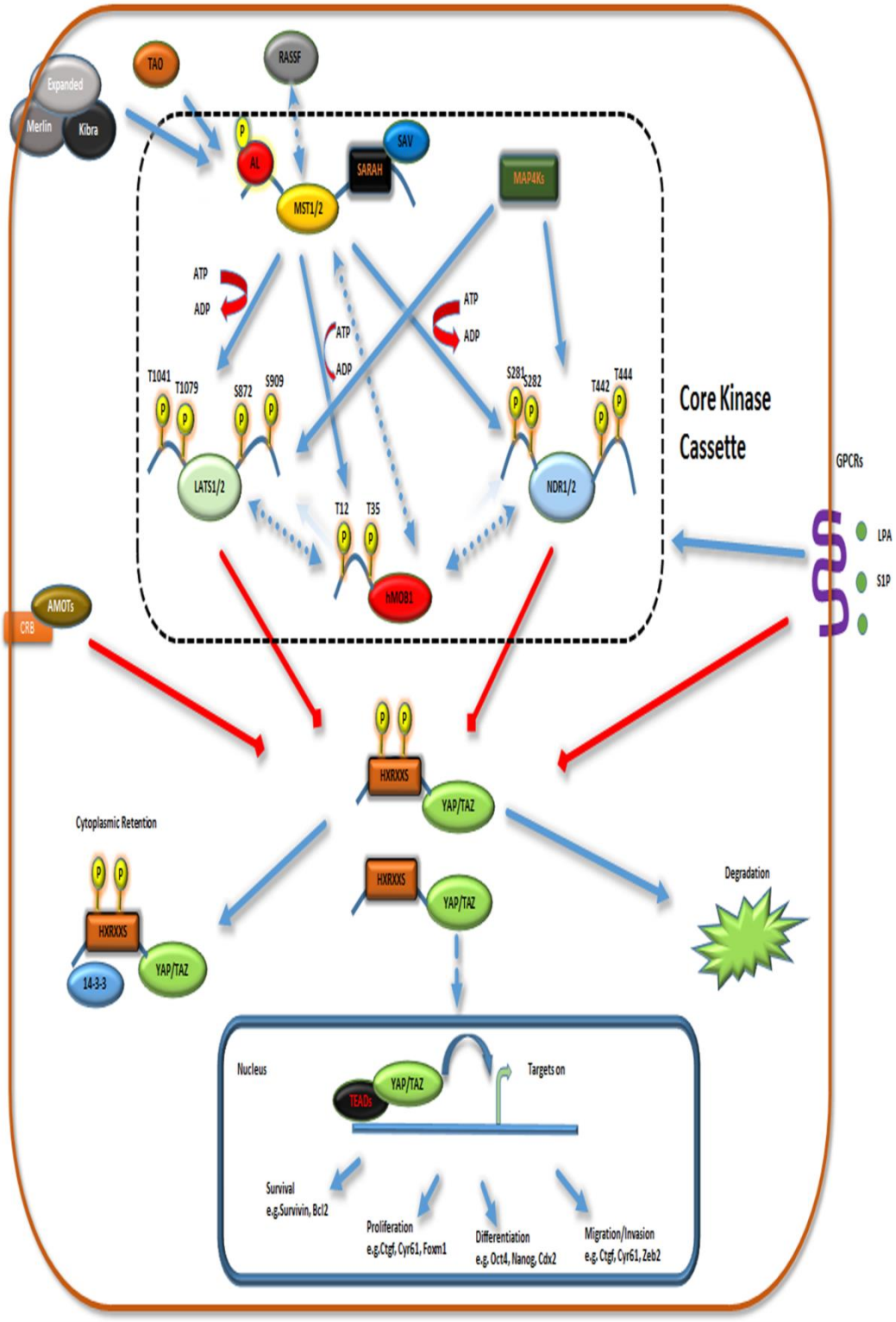

Figure 1.2. Schematic illustration of the human Hippo pathway.

The Hippo pathway is activated by pro-apoptotic kinases MST1/2 by the binding of SAV1 through the SARAH domains. The activation of MST1/2 is also performed by binding to Ras association domain family (RASSF) proteins. Furthermore, recent studies have revealed that the thousand-and-one (TAO) amino acids kinase or TAOK1-3 can also phosphorylate and activate MST1/2. Following the activation of MST1/2, LATS2 is in turn

phosphorylated at Thr1041. MOB1A is phosphorylated by MST1/2 at Thr12 and Thr35 sites, which leads to an enhanced affinity of MOB1A for LATS1/2, leading to the phosphorylation at Ser872 and Thr1041. Activated LATS1/2 in turn phosphorylates YAP in HXRXXS motif at Ser127 residue, creating a 14-3-3 binding site, which lead inactive Ser127-phosphorylated YAP to be sequestered in the cytoplasm. TAZ is regulated in similar fashion with YAP. The association of YAP/TAZ with the transcriptional factors triggers changes in the expression of genes involved in cell proliferation, cell death, and differentiation. MAP4Ks function as important physiological LATS-activating kinases in addition to MST1/2 kinases. Furthermore, the involvement of NDR1/2 kinases in core Hippo signalling made the regulation more and more complex. NDR1/2 interacts with MOB1 and act as YAP kinases. NDR1/2 is regulated by MST1, MST2, and MST3. Recent studies revealed that MAP4Ks can be the upstream regulator of NDR1/2 kinases.

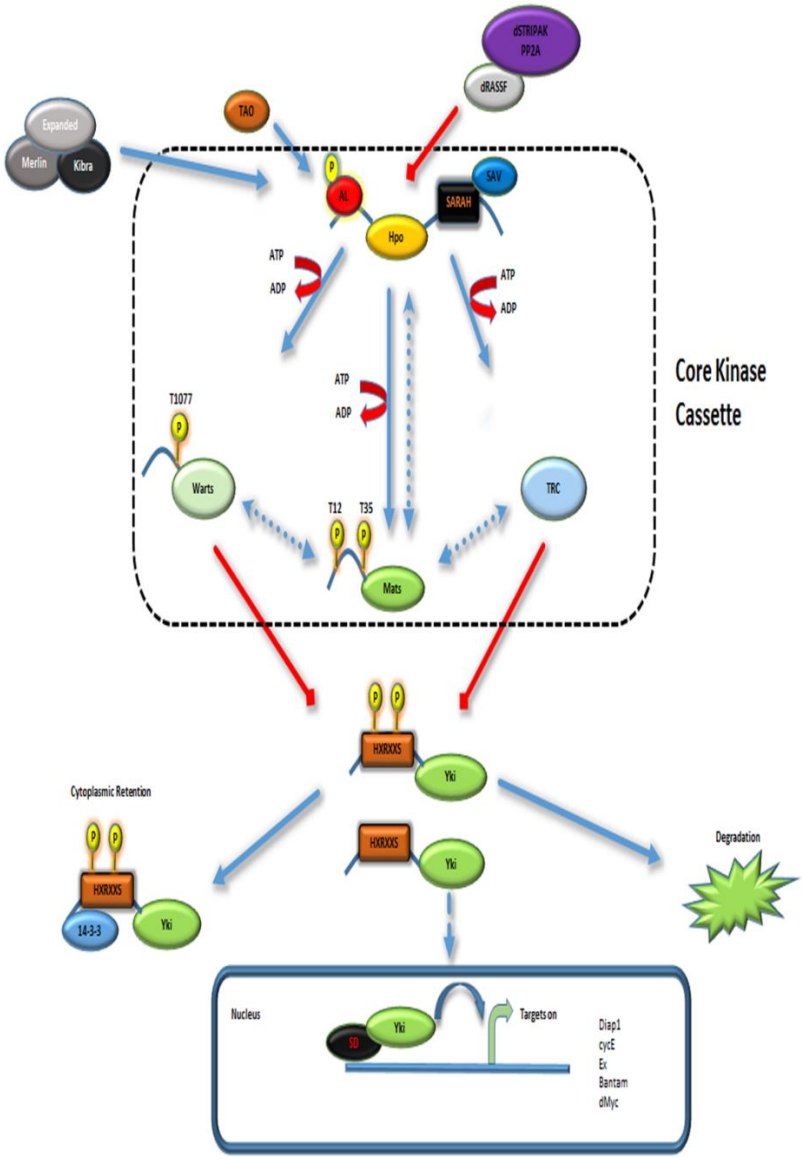

Figure 1.3. Schematic illustration of the *Drosophila* Hippo pathway.

At the centre of the Hippo signalling pathway in *Drosophila* is a kinase cascade which consists of Wts and Hpo. This kinase cascade, together with their co-factors Sav and Mats, forms the core of the Hippo signalling pathway in *Drosophila*. The functional output of this core kinase cascade is to regulate the Yki transcriptional co-activator. Mechanistically, Hpo forms a complex with Sav. The Hpo-Sav complex phosphorylates Warts at Thr1077 and Mats at Thr12/35. Phosphorylation residues of Mats are conserved from *Drosophila* to human. The activated Warts, together with Mats, then phosphorylates Yki, thus leading to cytoplasmic retention and ultimately degradation of Yki by binding to 14-3-3 phosphopeptide binding proteins. Mats also genetically interacts with serine/threonine-protein kinase Trc, the second NDR/LATS kinase in flies. The *Drosophila* Hippo signalling pathway is also regulated by multiple upstream branches.

1.3. Upstream regulators of the Hippo pathway

So far, more than 20 upstream regulators have been discovered which somehow affect either Hippo core signalling or downstream targets of the Hippo pathway (Harvey, Zhang et al. 2013). Here, we provide an overview of selected upstream regulators.

Research performed over last 10 years has showed that YAP/TAZ (Yki in *Drosophila*) is directly or indirectly controlled by multiple upstream branches of the Hippo signalling pathway. These upstream regulators mainly regulates the Hippo pathway in 2 major pathways: by initiating the activation of the core kinase cassette which ultimately suppresses YAP/TAZ (Yki); and by bypassing and interfering with the core kinase cassette by directly forming physical complexes with YAP/TAZ(Yki), thereby sequestering them at cell-cell junctions and leading to nuclear exclusion (Harvey, Zhang et al. 2013).

The Kibra-Expanded-Merlin Complex: Merlin (also termed NF2 for neurofibromatosis-2) and Expanded are members of the FERM (4.1, Ezrin, Radixin, and Moesin) domain-containing family of proteins. In *Drosophila*, both Merlin and Expanded loss-of-function resulted in severe overgrowth phenotype similar to that of Hpo mutants (Hamaratoglu, Willecke et al. 2006). Following that, Kibra (a WW and C2 domain containing protein) was discovered to physically associate with both Merlin and Expanded. Moreover, it has been shown that Sav and Hpo physically interact with Merlin and Expanded and Kibra associates with Wts, thereby activating Wts in a cooperative manner (Baumgartner, Poernbacher et al. 2010, Genevet, Wehr et al. 2010, Yu, Zheng et al. 2010) **(Figure 1.3)**. In mammals, Kibra interacts with Merlin, leading to enhanced phosphorylation of LATS1/2 *in vitro* (Xiao, Chen et al. 2011). Association of Kibra with LATS2 prevents LATS ubiquitination and subsequent proteasomal degradation, thus resulting in decreased proliferation (Xiao, Chen et al. 2011).

Apical-basal polarity proteins: Crumbs (CRB, a transmembrane apical-basal polarity determinant) has been classified as a cell surface regulator of the Hippo pathway in *Drosophila* (Robinson, Huang et al. 2010). In

Drosophila, CRB interacts with Expanded. The complex formation of CRB and Expanded regulates the localization and stability of Expanded, thereby modulating the activity of the Hippo pathway kinases and Yki **(Figure 1.3)** (Chen, Gajewski et al. 2010).

Upstream regulators of the Hippo core kinase cassette: Hippo signalling can be also activated by TAO (thousand and one amino acid protein) kinases and the cell polarity kinase MAP/microtubule affinity-regulating kinase 1 (MARK1; also termed PAR1). TAO kinases have been shown to phosphorylate the activation loop of MST1/2, thereby regulating the activity of the core kinase cassette **(Figure 1.2 and 1.3)** (Yu and Guan 2013). Additionally, two groups of MAP4Ks (mitogen-activated protein kinase), MAP4K1/2/3/5 and MAP4K4/6/7 have been shown to enhance phosphorylation of LATS1/2 at HM, resulting in LATS1/2 activation (Li, Li et al. 2014, Meng, Moroishi et al. 2015, Zheng, Wang et al. 2015). In this context, triple knock-out of MAP4K4/6/7 in HEK293A cells resulted in the phosphorylation of YAP/TAZ more dramatically comparing to that of MST1/2 double knock-out (Meng, Moroishi et al. 2016), suggesting that MAP4Ks are the main regulators of YAP phosphorylation in the tested cell lines.

GPCR Signalling: Recent studies have reported that GPCR signalling can mediate the Hippo pathway activity in cultured cells by serum-borne lysophosphatidic acid (LPA) and sphingosine 1-phosphate (S1P) (Miller, Yang et al. 2012). As a mechanism of action, they showed that LPA or S1P bind to their corresponding GPCRs and act through Rho GTPase to initiate the activation of YAP/TAZ. Thrombin, known to activate protease-activated receptors (PARs; a GPCR), has also been shown to stimulate YAP/TAZ activity through Rho GTPase **(Figure 1.2)** (Miller, Yang et al. 2012, Yu, Zhao et al. 2012). In contrast, activation of GPCRs by epinephrine and glucagon can boost LATS kinase activities and subsequently inactivate YAP/TAZ in a Protein Kinase A (PKA) dependent manner (Yu, Zhang et al. 2013). Thus, GPCRs can either stimulate or restrain LATS kinase activities to trigger or repress YAP activity dependent on the nature of GPCRs.

1.4. Hippo signalling in diseases

1.4.1. The Hippo pathway and cancer

Several lines of evidence show that the disruption of the Hippo pathway is related to several human cancers as well as tumour formation/tissue overgrowth in *Drosophila* **(Figure 1.4)**. Indeed, dysregulation of Hippo signalling has been shown at a high frequency in different carcinomas **(Table 1.2)**, such as lung, colorectal, ovarian, liver and prostate cancer (Harvey, Zhang et al. 2013).

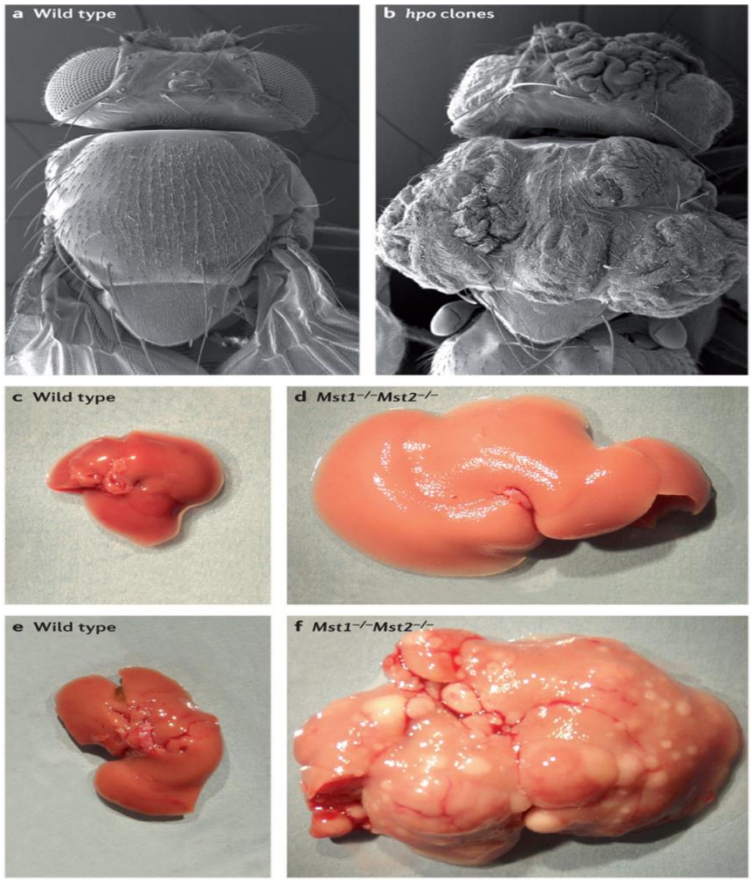

Figure 1.4. Hippo (MST1/2) loss-of-function phenotypes in *Drosophila* and mice.

Scanning electron micrographs (SEM) of a wild-type (wt) *Drosophila* **(panel a)** and a *Drosophila* with clonal loss of *hpo* **(panel b)** are indicated. *Drosophila* with loss of *hpo* exhibits overgrowths in head cuticle. Panel c indicates a mice liver from wt animal aged 2 months, while panel d represent a mice liver from *MST1/2* conditional knock-out mice aged 2 months. Panel e and f also shows mice livers from wt and *MST1/2* conditional knock-out mice aged 6 months, respectively (adapted from (Johnson and Halder 2014).

Uncontrolled cell proliferation and ultimately dramatic overgrowth phenotype are regarded as a fundamental aspect of neoplasia. The loss of the core Hippo pathway components resulted in severe overgrowth phenotype in *Drosophila* **(Figure 1.4)**, sparking the idea that the Hippo pathway might play a pivotal role in controlling organ growth and it might act as a tumour suppressor (Hansen, Moroishi et al. 2015). In *Drosophila*, loss-of-function of Hpo, Mats or Wts, or overexpression of Yorkie (*Drosophila* homolog of YAP and TAZ) leads to severe overgrowth of the corresponding adult structures, such as adult eye. It has been observed that these overgrowth phenotypes are caused by two defects. First, cell proliferation was deregulated; proliferation of mutant clones are faster than that of wild type clones and after organ size have reached their proper size, mutant cells continue to proliferate while wild type clones stop proliferating. Second, mutant clones are resistant to the apoptotic signals that usually trigger removal of extra wild-type cells (Johnson and Halder 2014).

Table 1.2. Hippo signalling deregulation in cancer (adapted from Harvey et al., 2013)

Mouse model	Tumour type
Nf2 hemizygote*	Osteosarcoma
	Hepatocellular carcinoma
	Malignant mesothelioma
Nf2 conditional null	Schwannoma
	Meningioma
	Renal carcinoma
	Hepatocellular carcinoma
	Cholangiocarcinoma
	Bile duct hamartoma
Lats1 null	Soft tissue sarcoma
	Ovarian carcinoma
Mst1, *Mst2* double conditional null	Hepatocellular carcinoma
	Cholangiocarcinoma
	Colonic adenoma
	T cell acute lymphoblastic leukaemia
Sav1 conditional null	Hepatocellular carcinoma
	Cholangiocarcinoma
	Gastrointestinal hyperplasia
Mob1a, *Mob1b* null or heterozygote‡	Skin cancer
	Osteosarcoma and fibrosarcoma
	Liver cancer
	Breast cancer
Yap1 overexpression	Hepatocellular carcinoma
	Gastrointestinal dysplasia
	Pancreatic ductal metaplasia
	Squamous cell carcinoma

This is further supported by recent researches performed in mice, which showed that loss of MST1/2 (Camargo, Gokhale et al. 2007, Dong, Feldmann et al. 2007, Zhou, Conrad et al. 2009, Lu, Li et al. 2010, Zhou, Zhang et al. 2011), SAV (Lee, Kim et al. 2008), or MOB1 (Nishio, Hamada et al. 2012, Nishio, Sugimachi et al. 2016) in mice lead to the development of different tumour types **(Figure 1.4)**, while YAP overexpression has been implicated in a wide range of human cancers including lung cancer (Lau, Curtis et al. 2014), breast cancer (Di Agostino, Sorrentino et al. 2016), colorectal cancer (Lee, Lee et al. 2015), liver cancer (Tao, Calvisi et al. 2014), and gastric cancer (Jiao, Wang et al. 2014). The overexpression of YAP and its relation to human cancer are broadly reviewed in (Zanconato, Cordenonsi et al. 2016)

In addition to the roles of the Hippo pathway in the control of cell growth and proliferation, it has been suggested that Hippo signalling might also play a prominent role in tumour invasion and metastasis (Cordenonsi, Zanconato et al. 2011, Zhao, Li et al. 2012). Metastasis is defined as spread of cancer to distant parts of the body and is responsible for the majority of cancer-associated mortalities. Metastasis consists of multiple steps including an epithelial-mesenchymal transition (EMT) of cells, which confers these cells with the ability to resist anoikis (a form of apoptosis) during dissemination (Simons and Mlodzik 2008). Concordantly, it has also been demonstrated that overexpression of YAP has a pronounced effect on cellular growth by promoting EMT of cultured cells (Hao, Chun et al. 2008) (Overholtzer, Zhang et al. 2006), suggesting a potential role for the Hippo pathway in human cancer metastasis. Consistent with this notion, it has been shown that TAZ activity is enhanced in metastatic breast cancer comparing to non-metastatic breast cancer (Cordenonsi, Zanconato et al. 2011). Moreover, expression of LATS1/2, which can function as inhibitors of YAP/TAZ, was considerably decreased in metastatic prostate cancer comparing to non-metastatic prostate cancer (Zhao, Li et al. 2012). In addition, recent studies reported that overexpression of LIFR (leukemia inhibitory factor receptor) dramatically decreases metastases formation in

metastatic breast cancer cell line in collaboration with YAP-Hippo signalling (Chen, Sun et al. 2012).

Although the activity of the Hippo pathway is clearly disrupted at a high frequency in a broad range of different human cancers, the exact mechanism by which dysregulation of Hippo signalling activity drives tumour formation remains to be answered. Considerable effect of YAP or Yorkie overexpression has been observed on organ size control, strongly suggesting that YAP or Yorkie functions as growth-promoting activity. Studies linking disruption of Hippo activity to human neoplasia are mostly based on immunohistochemical detection of nuclear YAP in the tumour tissue nucleus, which is likely to induce growth-promoting transcriptional programme. In full support for nuclear localization of YAP in different cancers, it has been observed that YAP is nuclear in about 60% of hepatocellular carcinoma, 15% of ovarian cancers, and 65% of non-small-cell lung cancer. On the other hand, in normal tissues, YAP is infrequently observed in the nucleus (Johnson and Halder 2014). Although the Hippo pathway can modulate YAP/TAZ (Yorkie in *Drosophila*) by restricting their access to the nucleus, its cancer-related mechanism is poorly understood and remains to be answered.

To date, few germline or somatic mutations of the Hippo signalling components have been discovered in human malignancies, with exception of mutations of the *NF2* locus. The *NF2* encodes the tumour suppressor protein Merlin that modulates the Hippo pathway by regulating the activity of the LATS kinases to mobilize them to the plasma membrane, and YAP/TAZ amplification (Gomez, Gomez et al. 2014, Johnson and Halder 2014). *NF2* loss of function is related to schwannomas, meningiomas, and mesotheliomas (Evans 2009, Harvey, Zhang et al. 2013). Loss of function of Merlin and the Hippo pathway components LATS2 or SAV1 is also seen in malignant mesothelioma (Murakami, Mizuno et al. 2011). Furthermore, inactivation of *NF2* in the mouse liver lead to HCC, and more interestingly, deletion of one allele of YAP gene completely blunts tumour formation (Zhang, Bai et al. 2010, Johnson and Halder 2014). Last but not least, a recent study has revealed that mammalian Merlin represses tumorigenesis

by suppressing the E3 ubiquitin ligase $CRL4^{DCAF1}$, which regulates transcription activity of genes including TEAD. (Li, Cooper et al. 2014). Mechanistically, they observed that $CRL4^{DCAF1}$ directly associates with and then prime LATS1/2 to ubiquitin for proteasome-dependent degradation in *NF2*-mutants cells, thereby leading to loss of kinase activity. As a consequence, active YAP and TAZ accumulate in nucleus, thereby resulting in TEAD-dependent transcription (Li, Cooper et al. 2014). Although these observations suggest that YAP has a critical role for the progression of cancers driven by NF2 deletion, the mechanism of action is not clearly understood.

1.4.2. Hippo signalling in non-cancer pathologies

The role for the Hippo pathway in tumour formation is gaining more and more popularity. On the other hand, the research over the role of the Hippo pathway in non-cancer abnormalities is growing day by day. Several lines of evidence have linked the Hippo signalling pathway to non-cancer pathologies **(Table 1.3, Table 1.4)**. These evidences are largely based on the manipulation of YAP/TAZ and MST1/2 (Gomez, Gomez et al. 2014).

Table 1.3. The involvement of MST1/2 kinases in non-cancer mammalian pathologies (adapted from (Gomez, Gomez et al. 2014)

Tissue	Protein	Model	Pathology
Liver	MST1/2	MST1/2 mutant conditional mouse	Hepatomegaly
Heart	MST1	Mouse model of Arrhythmogenic Cardiomyopathy and human samples	Arrhythmogenic Cardiomyopathy
		Neonatal rat ventricular myocytes	Heart failure, ischemic heart disease, dilated cardiomyopathy and cardiomyocyte apoptosis
		Dominant negative MST1 mice and MST1 −/− mice	Cardiac dysfunction
Muscle	MST1	MST1 deficient mice	Neurogenic muscle atrophy
Brain	MST1	Mouse model of Amyotrophic Lateral Sclerosis	Amyotrophic lateral sclerosis (ALS)
Pancreas	MST1/2	MST1/2 mutant conditional mouse	Reduction of pancreatic mass, exocrine pancreas disorganization and pancreatitis-like autodigestion
Thymus	MST1	MST1 deficient patients or with homozygous mutations	Immunodeficiency, T and B cells lymphopenia
		MST1 deficient mice	Defective lymphocyte trafficking and thymocyte egress. Autoimmune-like disorders. Impaired development and function of regulatory T cells. Low numbers of mature naïve T cells.
	MST1/2	MST1 and MST2 deficient mice	Autoimmune disease (skin lesions around the eyes, lymphocytes infiltration, colitis)
Lung	MST1/2	MST1/2 mutant conditional mouse	Respiratory distress syndrome
	MST1	Rat model of Hypoxic pulmonary vascular remodelling	Pulmonary arterial hypertension

Altered MST1 and YAP/TAZ activities were shown to result in heart defects **(Table 1.3, Table 1.4)**. Furthermore, MST1/2 and YAP knock-out mice were shown to exhibit defective heart development during embryonic development (Heallen, Zhang et al. 2011, Xin, Kim et al. 2011). Moreover, it was shown that the overexpression of YAP result in enhanced proliferation of cardiomyocytes (Del Re, Yang et al. 2013, Xin, Kim et al. 2013). To further support the role of the Hippo signalling pathway in heart regeneration, Olson and colleagues have shown that YAP conditional knock-out in the heart impede neonatal heart regeneration (Xin, Kim et al. 2013), while mice with heart specific LATS1/2 or SAV deletion display promoted regenerative capacities (Heallen, Morikawa et al. 2013). Taken together, these studies suggest that the Hippo pathway can play pivotal roles in modulating the potential of myocardial regeneration after injury. Therefore, an in-depth understanding of the Hippo pathway has the potential to significantly improve our knowledge regarding non-cancerous diseases, in addition to accelerating translational cancer research efforts.

Table 1.4. The involvement of YAP/TAZ proteins in non-cancer mammalian pathologies (adapted from (Gomez, Gomez et al. 2014))

Tissue	Protein	Model	Pathology
Liver	YAP	Mouse models of inducible active YAP1 in the liver	Increase in liver size
Heart	YAP/TAZ	SCA-1–/– human cardiac progenitor cell line	Infarct
		Cardiac-specific YAP or TAZ knockout mice. Mouse model of inducible active YAP1 in the heart	Loss of function results in impaired neonatal heart regeneration and lethal cardiomyopathy. Activated YAP enhances cardiac regeneration and improves function of ischemic hearts
	YAP	Mouse models of arrhythmogenic cardiomyopathy and human samples	Arrhythmogenic Cardiomyopathy
		Mouse models of cardiomyocyte-specific homozygous inactivation of YAP in the postnatal heart	Increased myocyte apoptosis and fibrosis, dilated cardiomyopathy, and premature death.
Muscle	YAP	Mouse models of inducible active YAP in the skeletal muscle cells	Loss of body weight, gait impairments and kyphosis. Skeletal muscle atrophy.
Brain	YAP/TAZ	Rat model of chronic constriction sciatic nerve injury	Neuropathic pain
	YAP/TAZ	Mammalian cell lines	Alzheimer's disease
Pancreas	YAP	MST1/2 mutant conditional mouse	Reduction of pancreatic mass, exocrine pancreas disorganization and pancreatitis-like autodigestion
		Mouse models of inducible active YAP1 in the pancreas	Pancreas increased in total size and acinar cells showed penetrant ductal metaplasia
Skin	YAP/TAZ	Mice model of wound healing	Wound healing
	YAP	Mouse models of inducible active YAP1 in the skin	Thickening of the epidermis and increased number of proliferating cells
Eye	YAP/TAZ	Primary human trabecular meshwork cells	Glaucoma
Ovary	YAP/TAZ	Mouse model of ovarian fragmentation, ovarian explant and follicle cultures. Primary ovarian insufficiency patients	Primary ovarian insufficiency and polycystic ovarian syndrome

1.4.3. Hippo Signalling as a therapeutic target

The widespread involvement of the Hippo pathway in cancer (summarized above) makes this pathway crucial for targeting as an anti-cancer therapy. Given the fact that human malignancies are linked to the enhanced activity of YAP/TAZ, it is tempting to develop strategies that aim to suppress YAP/TAZ activities. However, although mounting evidence suggests that pharmacological manipulation of the Hippo pathway components and YAP/TAZ activities seems promising for anti-cancer targets, there are problems that needs to be solved. First is that the core components of the Hippo pathway negatively regulates the pathway`s transcriptional output, creating a conceptual problem, because pharmacological inhibitors targeting the core components would lead to enhanced YAP activity, thus promoting cancer-related properties. Another disadvantage is that manipulation of YAP/TAZ as well as of Hippo components might result in deleterious side effects in normal tissues. For example, it seems tempting to inhibit MST kinase activity to recover from myocardial injury. However, it needs to be considered that MST deficiency has detrimental effects on the human immune system (Abdollahpour, Appaswamy et al. 2012, Nehme, Pachlopnik Schmid et al. 2012). Thus, any manipulation of YAP/TAZ and the Hippo signalling components should be addressed very cautiously to ensure that any vital organs or tissues are not dramatically affected.

Targeting GPCR signalling: GPCR signalling was shown to regulate the Hippo pathway activities through LAP, S1P and Thrombin to trigger YAP nuclear localization. Thus, agonists of LPA, S1P and thrombin-induced receptor signalling, such as adrenaline, glucagone, and the dopamine receptor agonist dihydrexidine, may lead to enhanced YAP phosphorylation and inactivation (Johnson and Halder 2014). Therefore, targeting GPCR, LPA, S1P and thrombin represent potential novel routes for therapeutic intervention. In this context, monoclonal antibodies highly specific to these molecules have been developed (Fleming, Wojciak et al. 2011). For example, the Sphinaomab (S1p-blocking antibody) has been found to attenuate lung tumour metastasis (Ponnusamy, Selvam et al. 2012). Additionally, Phenoxodiol, the isoflavone-derivative with SPHK1 inhibitor,

has been trialled in patient with platinum/taxane-refractory/resistant ovarium cancers, with limited single agent activity (de Souza, Liauw et al. 2006, Kelly, Mor et al. 2011).

Targeting protein-protein interactions in Hippo signalling: Extensive biological and clinical investigations have discovered protein-protein interaction (PPI) networks and nodes which play important roles in acquiring and maintaining cancer-related features fundamental for cellular transformation. In cancer, PPIs create signalling networks which deliver pathophysiological signals to complete an integrated biological output, ultimately leading to tumorigenesis, tumour progression, invasion, and/or metastasis (Ivanov, Khuri et al. 2013).

The large amount of evidence has shown that the Hippo pathway is involved in a large range of cancer. In this context, YAP/TAZ is regarded as the most attractive therapeutic in the Hippo pathway. However, pharmacologically inhibiting YAP/TAZ is challenging, as these proteins are transcriptional co-activators with no known enzymatic activity. Thus, YAP/TAZ needs to associate with transcription factors, such as TEAD, to regulate gene expression (Zhao, Ye et al. 2008). Furthermore, the transcription factors TEADs are largely redundant for normal development but necessary for YAP-driven tumorigenesis. All together, these make the targeting of YAP/TAZ-TEAD interaction the most direct and effective approach to stamp down YAP/TAZ-driven oncogenic events. To this end, Pan and colleagues investigated the role of YAP-TEAD interaction in murine tumours and found that a dominant-negative versions of TEAD2 (TEAD-DN, DNA-binding domain has been deleted) suppress YAP-driven transcription and YAP`s ability to drive soft-agar growth *in vitro* as well as YAP-induced cancer *in vivo* without resulting in severe liver abnormalities (Liu-Chittenden, Huang et al. 2012).

Having reached the conclusion that genetic disruption of the YAP-TEAD interaction can prevent YAP`s transforming activity, Pan and colleagues screened 3300 FDA-approved drugs to categorize compounds that can directly interfere with the YAP/TAZ-TEAD interactions, and

thereby suppress YAP/TAZ-triggered transcriptional activity (Liu-Chittenden, Huang et al. 2012). Significantly, they found that a group of the porphyrin family of compounds (Protoporphyrin IX (PPIX), hematoporphyrin (HP), and Verteporfin (VP) can impede the interaction of YAP/TEAD, ultimately inhibiting the transcription of YAP/TAZ target genes (Liu-Chittenden, Huang et al. 2012). Moreover, VP was shown to compete for TEAD to associate with YAP *in vitro* as well as to abolish liver overgrowth mediated by YAP overexpression and inactivation of NF2/Merlin *in vivo* (Liu-Chittenden, Huang et al. 2012), clearly demonstrating the therapeutic potential of disruption of YAP/TAZ-TEAD interaction.

As another alternative to target YAP/TAZ-TEAD interaction, one should take Vestigial-like (VGLL) proteins into account. There are four different VGLL proteins: VGLL1, VGLL2, VGLL3, and VGLL4. These proteins are transcriptional co-factors that are first identified in *Drosophila* as a master regulator of wing development (Zhang, Gao et al. 2014). Importantly, recent studies revealed that VGLL1 protein family increases cell proliferation (Pobbati, Chan et al. 2012). Similarly, VGLL3 is amplified in soft tissue sarcoma and its inhibition was shown to result in decreased cell proliferation and migration (Helias-Rodzewicz, Perot et al. 2010). However, VGLL4 seems to function differently. VGLL4 proteins are defined as a new group of TEAD-binding partners involved in tumorigenesis. Very interestingly, VGLL4 proteins were shown to promote apoptosis by negatively modulating inhibitors of apoptosis proteins (IAPs) (Jin, Park et al. 2011). Furthermore, recent research uncovered that VGLL4 associates with TEADs by competing for YAP, thereby suppressing lung cancer growth and progression (Zhang, Gao et al. 2014).

1.5. MOB Proteins

Considerable efforts have been invested to understand the regulation of Hippo signalling in Yeast, *Drosophila* and human. Recent studies have uncovered that MOB1A/Mats play essential role in the regulation of the Hippo core cassette through their regulatory interactions with NDR/LATS kinases in *Drosophila* and human.

The family of Mps One binder (MOB) co-activator proteins are evolutionally conserved from insects to human and constitute signal transducers in essential signalling network via their interactions with NDR/LATS kinases (Hergovich 2011). To date, several different MOB proteins have been discovered in every eukaryote. At the very beginning, key roles for Mob1p and Mob2p were revealed in the regulation of mitotic exit and cell morphogenesis. Four different MOB proteins (dMOB1A, dMOB2, dMOB3, and dMOB4) are encoded by *Drosophila*, with dMOB1 (also known as Mats) being the heart of the Hippo pathway and regulating cell proliferation and apoptosis (Lai, Wei et al. 2005, Staley and Irvine 2012). At least six different MOB proteins (MOB1A, MOB1B, MOB2, MOB3A, MOB3B, MOB3C) are expressed in mammalian genome, with MOB1A functioning as a master regulator of NDR/LATS kinases in mammalian Hippo signalling (Hergovich 2016) **(Figure 1.5)**. We will summarize current knowledge of this emerging protein family from yeast to human.

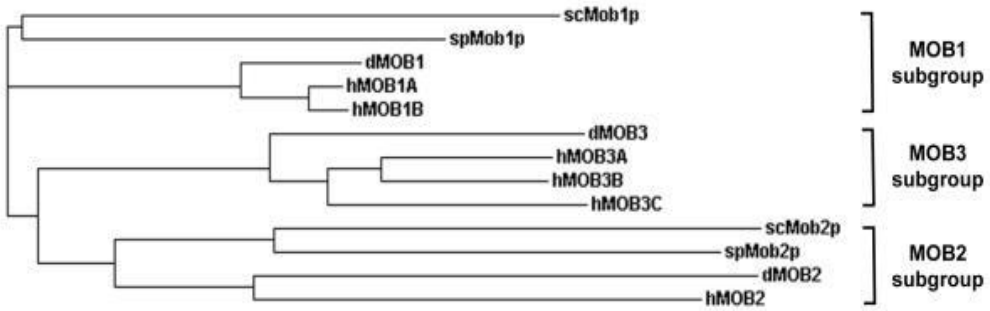

hMOB1A	100 %	-	-
hMOB1B	95 %	-	-
hMOB2	37 %	100 %	-
hMOB3A	50 %	30 %	100 %
hMOB3B	50 %	30 %	80 %
hMOB3C	49 %	29 %	72 %
scMob1p	48 %	31 %	35 %
scMob2p	35 %	27 %	32 %
spMob1p	57 %	35 %	42 %
spMob2p	38 %	32 %	30 %
dMOB1	86 %	39 %	48 %
dMOB2	34 %	45 %	30 %
dMOB3	51 %	28 %	64 %

Figure 1.5. Phylogenetic tree and sequence similarity within the MOB protein family.

(Top) Phylogenetic tree can be divided into three subgroups. *Saccharomyces cerevisiae* Mob1a (scMob1a) and *Schizosaccharomyces pombe* Mob1a (spMob1p) in budding and fission yeast, respectively, are grouped together with dMOB1 and MOB1A/B in MOB1 subgroup. scMob2p and spMob2p are classified together with dMOB2 and hMOB2 in MOB2 subgroup. dMOB3 fall into MOB3 subgroup together with MOB3A/B/C**. (Bottom)** Sequence similarities within the MOB protein family (adapted from (Hergovich 2012).

1.5.1. MOB proteins in budding and fission yeast

The MOB proteins were first identified in yeast by screening for novel interactors with Mps1p kinases, which is Mob1p typifying Mps one binder 1p (homologues of *Drosophila* Mats and Human Mob1) (Luca and Winey 1998). It has been reported that Mob1p has far reaching effects in yeast, such as the survival of cells, spindle pole body duplication, as well as the mitotic exit network (MEN) (Frenz, Lee et al. 2000) in budding yeast or septation initiation network (SIN) in fission yeast (Bardin and Amon 2001).

In summary, these studies (summarized in Hergovich, 2011) showed that the stimulation of Cdc15p kinase (counterpart of human MST1/2 and *Drosophila* Hippo) increases the activity of Mob1p towards Dbf2p or Sid2p (counterpart of human LATS1/2 and *Drosophila* Warts), which in turn phosphorylates the phosphatase Cdc14p, thus inducing mitotic exit of yeast cells **(Figure 1.6)**.

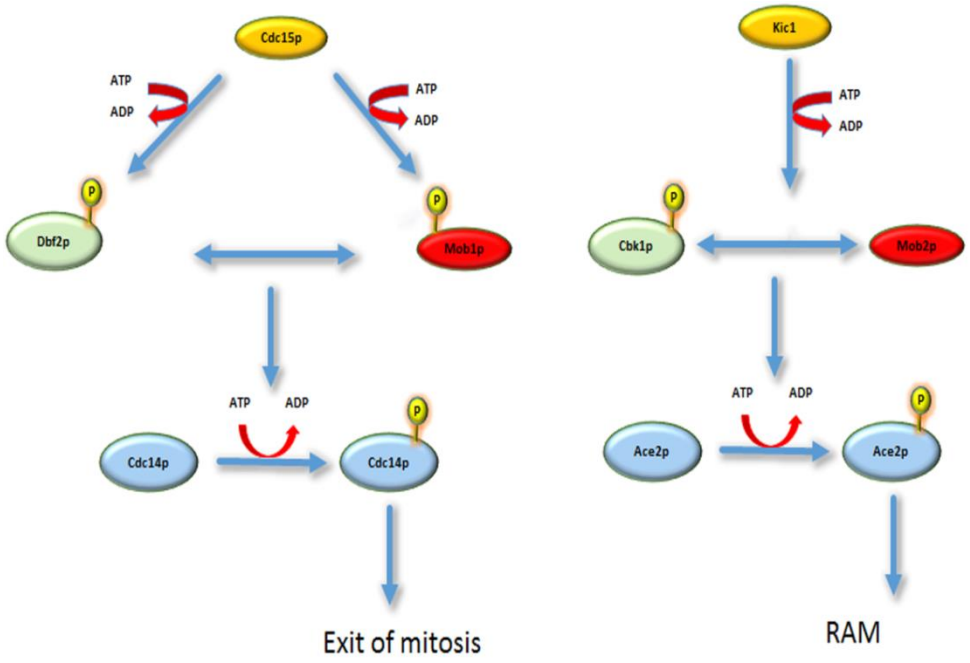

Figure 1.6. MOB-regulated intracellular signalling in *S.cerevisiae*.

(a) Mob1p is phosphorylated by Cdc15p. Phospho-Mob1p then activates the Dbf2p NDR/LATS kinase. Complex formation of Mob1p and Dbf2p subsequently phosphorylates Cdc14p, which in turn trigger mitotic exit of yeast cells. **(b)** Cooperation of Mob2p and Kic1p stimulates the Cbk1p NDR/LATS kinase. The association between Mob2p and Cbk1p targets Ace2p for phosphorylation to regulate Ace2p activity and cellular morphogenesis (RAM).

MOB1p has also been shown to play crucial roles in controlled exit of mitosis in *Schizosaccharomyces pombe* (Bardin and Amon 2001). SIN is also regulated by a similar signalling network as shown for MEN in *S. pombe*. Mob1p associates with the kinase Sid2p (counterpart of yeast Dbf2), thereby controlling and ultimately affecting the subcellular localisation of

Clp1p (Chen, Feoktistova et al. 2008) **(Figure 1.6)**. Taken together, association of Mob1p with the NDR/LATS kinases Dbf2p or Sid2p plays essential role in the functionality of MEN or SIN (Bardin and Amon 2001).

Importantly, in addition to establishing the first function of Mob1p, Mob2p was reported as a non-essential protein in yeast (Luca and Winey 1998). However, research uncovered that Mob2p is essential for the regulation of asymmetry in budding yeast by mediating Ace2p daughter-specific genetic programs (Colman-Lerner, Chin et al. 2001, Weiss, Kurischko et al. 2002). Additionally, association of Mob2p with Cbk1p (the second NDR/LATS kinase *S. cerevisiae*) regulates polarized growth in *S. cerevisiae*, which is termed RAM (Regulation of Ace2p and cellular Morphologies) (Jansen, Barry et al. 2006) **(Figure 1.6)**. Similarly, it was shown that Mob2p associates with the second NDR/LATS kinase Orb6p (Hou, Wiley et al. 2003). Research showed that Mob2p in complex with the Orb6p regulates a morphogenesis network in *S. pombe* (Hou, Wiley et al. 2003, Kanai, Kume et al. 2005).

Taken together, two different MOB proteins (Mob1p, Mob2p) are expressed in budding and fission yeast **(Figure 1.6)**. Association of Mob1p with Dbf2p and Sid2p, respectively, plays a central role in the control of exit from mitosis in yeast. On the other hand, Mob2p in complex with Cbk1p and Orb6p, respectively, play a pivotal role in the regulation of cell morphogenesis networks. Importantly, Mob1p does not associate with Orb6p, and Mob2p does not interact with Sid2p (Hou, Guertin et al. 2004, Kanai, Kume et al. 2005). Thus, yeast Mob1p and Mob2p regulate two separate biological processes by their association with the corresponding yeast NDR/LATS kinases **(Figure 1.6)**.

1.5.2. MOB proteins in *Drosophila*

In *Drosophila* genome, three different MOB proteins are expressed by independent genes **(Figure 1.5)**, namely dMOB1 (aka Mats), dMOB2, dMOB3, with Mats functioning as key regulator of the Hippo pathway in *Drosophila* Hippo signalling. Mats (known as Mob as a tumour suppressor)

is a protein-coding gene, corresponding to Mob1p in yeast and MOB1A in human. In the *Drosophila* genome, the *Mats* gene is located in third chromosome (3R:22421161..22423302**,** cytoplasmic map is 94A12). The *Mats* gene has 3 annotated transcripts and 3 polypeptides **(Figure 1.7)**. To date, nearly 15 mutant alleles of *Mats* have been reported whose phenotypes manifest in wing; denticle; trichogen cell; mesothoracic tergum; adult mushroom body; wing hair; imaginal disc **(Table 1.5)** (Attrill, Falls et al. 2016). dMOB2 is required for regulating neuromascular junctions and photoreceptor morphology (Campbell and Ganetzky 2013), while the biological role(s) of dMOB3 is not known.

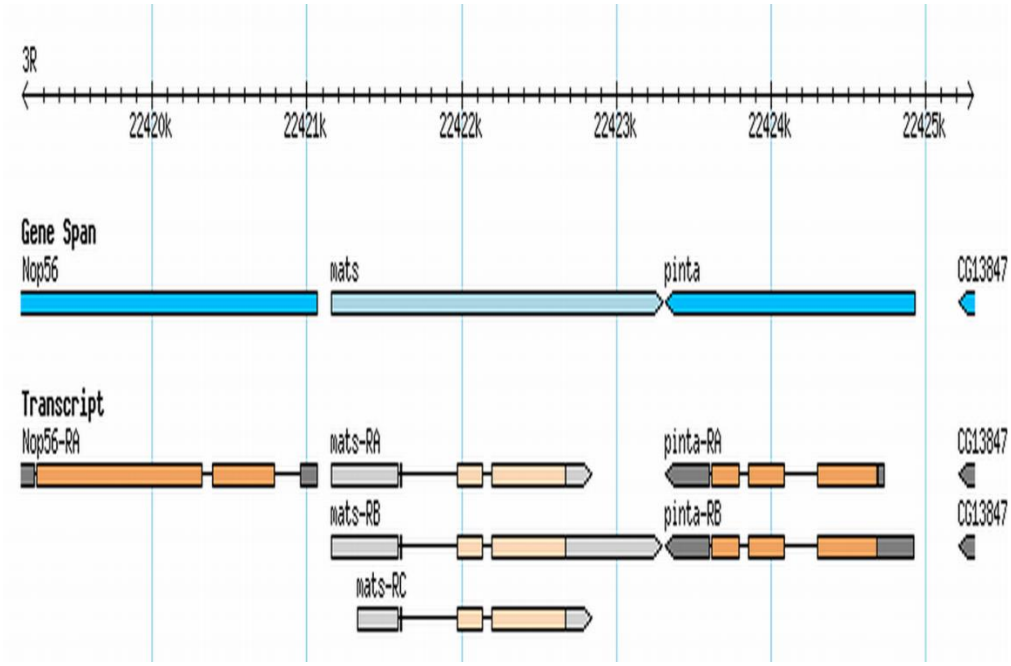

Figure 1.7. Schematic representation of the *mats* gene neighbouring nop56 in the *Drosophila* chromosome.

The *Mats* gene is located in 3.chromosome and its gene sequence location is 3R:22421161..2242330. The cytological map location of *mats* is 94A12. The *Mats* gene has 3 annotated transcripts (Mats RA, RB, RC) and 3 polypeptides (Mats PA, PB, PC) (Generated from http://flybase.org/).

Table 1.5. Mats alleles reported so far (adapted from http://flybase.org/)

Number	Allele (Symbol)	Mutagen	Reference(s)
1	*mats*^{e235}	P-element activity	(Lai, Wei et al. 2005)
2	*mats*^{roo}	transposable element activity	(Lai, Wei et al. 2005)
3	*mats*^{PBrv}	piggyBac activity	(He, Emoto et al. 2005)
4	*mats*^{unspecified}	-	(Schuldiner, Berdnik et al. 2008)
5	*mats*^{S113416}	P-element activity	(Deak, Omar et al. 1997)
6	*mats*^{A33}	ethyl methanesulfonate	(Liu, Zheng et al. 2016)
7	*mats*^{e03078}	piggyBac activity	(Thibault, Singer et al. 2004)
8	*mats*^{e03077}	piggyBac activity	(He, Emoto et al. 2005)
9	*mats*$^{Scer\UAS.cLa}$	in vitro construct	(Lai, Wei et al. 2005)
10	*mats*^{GD8136}	in vitro construct	(Neely, Kuba et al. 2010)
11	*mats*^{KK100140}	in vitro construct	(Rauskolb, Pan et al. 2011)
12	*mats*^{JF03246}	in vitro construct	(Jia, Soylemez et al. 2015)
13	*mats*^{HMS00475}	in vitro construct	(Jia, Soylemez et al. 2015)
14	*mats*^{e17}	Delta2-3 transposase	(Yang, Gupta et al. 2008)
15	*mats*$^{2236.T:Avic\GFP}$	in vitro construct	(Yang, Gupta et al. 2008)

After understanding the importance of Mob1p in yeast, Lai et al.(2005) embarked on the hunt for understanding the functions of MOB proteins in multicellular organism and found that Mats (the counterpart of human MOB1) is required for cell proliferation and death as central part of the Hippo pathway in *Drosophila* by functioning as an activator of Wts, one of two NDR/LATS kinases (Lai, Wei et al. 2005). Furthermore, Mats has been shown to be an essential gene which modulates proper mitotic division, possibly due to the requirement of Mats for proper chromosomal segregation (Shimizu, Hot et al. 2008). Even more interestingly, they showed that Mats and MOB1A proteins share 87% sequence identity and the loss of Mats is rescued by human MOB1A expression in the *Drosophila* eye **(Figure 1.8)**, suggesting that the function of Mats proteins is highly conserved from *Drosophila* to human (Lai, Wei et al. 2005). However, the current picture is getting more and more complicated, as recent studies showed that Mats can directly associate with Trc, the second NDR/LATS kinase in *Drosophila* (He, Emoto et al. 2005). Intriguingly, flies with Trc deficiency has enhanced negative phenotype in Mats mutant cells, indicating that Mats not only specifically associates with Wts and ultimately controls Wts signalling but also is required for Trc signalling in flies **(Figure 1.3)** (He, Emoto et al. 2005).

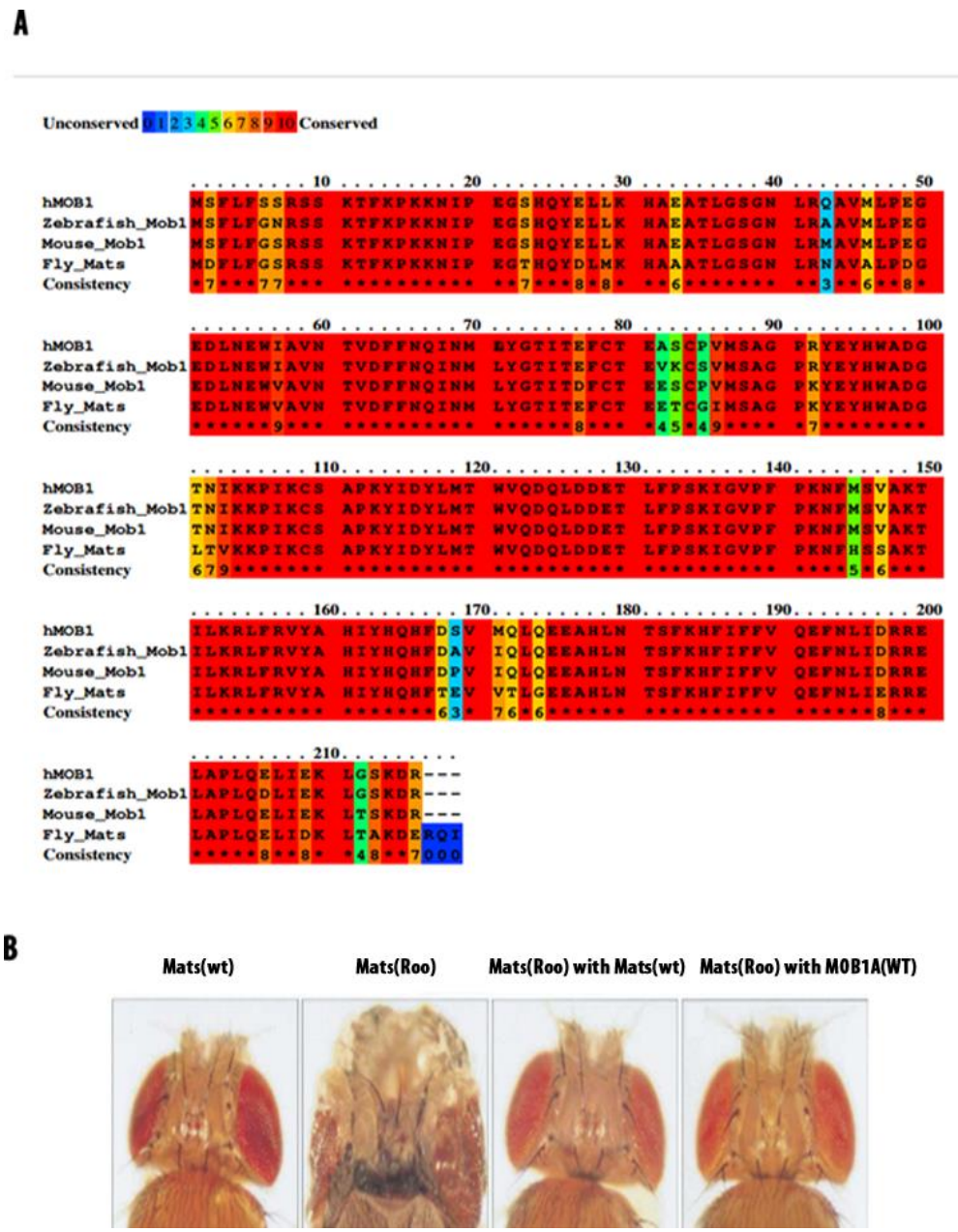

Figure 1.5. Conservation of the Mats gene.

(A) Illustration of the conservation of the Mats protein across species. Mats is highly conserved from *Drosophila* to human. Human MOB1 and *Drosophila* Mats proteins share 87% sequence identity. **(B)** Panel showing that MOB1A can rescue for Mats loss-of-function. Eyes with wild-type clones are shown as control. Eyes with *mats* mutant is shown to be larger and develop tumour formation. Mats expression in *mats* mutant clones is shown to suppress defective eye phenotype and tumour formation. MOB1A expression in *mats* mutant clones shows that MOB1A can rescue defective eye phenotype, as does Mats expression. (**A** is t generated from http://www.ebi.ac.uk/Tools/msa/clustalo/) and **B** is adapted from (Lai, Wei et al. 2005).

In addition to Mats (dMOB1), two additional and different MOB proteins (dMOB2, dMOB3) are expressed in flies. Little is known about the biological roles of dMOB2 and dMOB3. On the one hand, it was shown that dMOB2 is required for regulating neuromuscular junctions and photoreceptor morphology (Campbell and Ganetzky 2013). On the other hand, dMOB2 was shown to associate with Trc, thereby regulating wing hair morphogenesis (He, Emoto et al. 2005). Significantly, the biological functions of dMOB2 seem to be different from that of Mats, as mutations in the dMOB2 gene seem not to synergise with loss or gain of Trc kinase in the enhanced morphological phenotype (He, Emoto et al. 2005). However, overexpression of dMOB2 results in fly wing phenotype similar to the Trc mutant (He, Emoto et al. 2005), indicating a potential dominant-negative role in flies. In this context, it is tempting to speculate that Trc signalling is negatively regulated by dMOB2, as reported for human counterpart **(see section 1.5.3)**. Therefore, the mechanism of action of dMOB2 is yet to be determined. The biological functions of dMOB3 are currently not known.

1.5.3. MOBs in mammalian cells

Comparing to yeast and *Drosophila*, the complexity is higher in mammals, as mammals express at least six different MOB proteins (MOB1A, MOB1B, MOB2, MOB3A, MOB3B, and MOB3C) **(Figure 1.5)**.

MOB1A and MOB1B (also termed as MOB1) can associate with NDR/LATS kinases (Bichsel, Tamaskovic et al. 2004, Ponchon, Dumas et al. 2004, Hergovich, Bichsel et al. 2005, Hergovich, Schmitz et al. 2006, Hergovich, Kohler et al. 2009, Kohler, Schmitz et al. 2010, Hoa, Kulaberoglu et al. 2016). Interestingly, a conserved domain in NDR/LATS kinases mediates these interactions (Hergovich, Stegert et al. 2006). Furthermore, MOB1A has been shown to interact with various proteins, such as DOCK8, Praja2, and S100A8 (Ewing, Chu et al. 2007, Lignitto, Arcella et al. 2013, Rock, Lim et al. 2013).

MOB2 can associate with NDR1/2 kinases, not LATS1/2 kinases (Bothos, Tuttle et al. 2005, Hergovich, Schmitz et al. 2006, Kohler, Schmitz et al.

2010). Importantly, MOB2 associates with the same domain on NDR1/2 as MOB1 and seems to compete for NDR1/2 interaction with MOB1 and negatively regulate NDR1/2 signalling (Hergovich 2013).

MOB3A/B/C (also termed as MOB3) does not interact with and activate NDR1/2 and LATS1/2, despite of high sequence identity between MOB3A/B/C and MOB1 **(Figure 1.5)**. MOB3B seems to bind to Mitogen activated protein kinase p38 alpha (MAPK14) (Bandyopadhyay, Chiang et al. 2010), DNK2/KSR2 (Ewing, Chu et al. 2007), and NT5C2 (Rual, Venkatesan et al. 2005). These interactions have not tested experimentally yet.

1.5.4. Regulation of MOB1/Mats Proteins in *Drosophila* and Mammals

At the centre of the Hippo pathway in *Drosophila* is a kinase cascade which consists of the Ste20-like kinase Hpo, the nuclear Dbf2-related (NDR) family kinase Wts. This kinase cascade, together with a co-factor Sav (Salvador) and a key signal transducer Mats (Mob as a tumour suppressor), forms the core of the Hippo pathway in *Drosophila* (Yu and Guan 2013). The functional output of this core kinase cascade is to negatively regulate the Yorkie (Yki) transcriptional co-activator. Mechanistically, Hpo forms a complex with Sav (Wu, Huang et al. 2003). The Hpo-Sav complex activates Wts and Mats by phosphorylation (Wu, Huang et al. 2003). The activated Wts, together with Mats, then phosphorylates Yki, thus leading to cytoplasmic retention and ultimately degradation of Yki by binding to 14-3-3 phosphopeptide binding proteins (Meng, Moroishi et al. 2016).

However, recent studies have revealed that the current picture of the core *Drosophila* Hippo pathway is more complicated, as Mats also can genetically interacts with serine/threonine-protein kinase tricorner (Trc) (the counterpart of human LATS1/2), the second NDR/LATS kinase in flies, and is required for Trc signalling in flies (Hergovich 2011, Hergovich 2016), indicating that Trc is linked to the Hippo pathway and should be considered as novel core component of the Hippo pathway. However, the complex

interactome of Mats with the Hippo core kinases Hpo, Wts, and Trc is yet to be determined. And, its molecular mechanism remains to be answered.

The fact that Mats is highly conserved from *Drosophila* to human and human MOB1A can compensate for tissue overgrowth phenotype driven by Mats loss-of-function **(Figure 1.5)** suggests that the role and mechanism of Mats is also conserved.

The Hippo pathway in mammals is very similar to that of *Drosophila*. The mammalian Hippo pathway creates a kinase cascade which consists of MST1/2, LATS1/2, and NDR1/2. A recent structural study proposes new molecular role for MOB1A in LATS1/2 phosphorylation (Ni, Zheng et al. 2015). According to this model (Ni, Zheng et al. 2015), the auto-phosphorylation of MST2 at its long linker results in generation of a phosphor-docking motif, thereby recruiting MOB1A. Subsequently, LATS1 associates with the MOB1A-phospho-MST2 complex which ultimately forms the MST2-MOB1A-LATS1 ternary complex. This ternary complex subsequently enhances the phosphorylation of MOB1A at its N-terminal tail and LATS1 at its hydrophobic motif by MST2. Furthermore, auto-phosphorylation of LATS1 is further promoted by phosphorylated MOB1A, as it is required for LATS1 activation (Ni, Zheng et al. 2015). The activated LATS then phosphorylates YAP/TAZ, thereby resulting in cytoplasmic retention by binding to 14-3-3 proteins and proteasome-mediated degradation of YAP/TAZ. Taken together, this structural study proposes that MOB1 binding to MST1 plays a crucial role in activating LATS1 by MST2 (Ni, Zheng et al. 2015). However, in a recent comprehensive study, Stuhl *et al.* challenged the notion that the association of MOB1 with MST1 (the counterpart of fly Hpo) is crucial for the activation of LATS (the counterpart of Wts). They showed using conformation sensors that Wts/Mats complex formation is required for Wts activation, while the Hpo/Mats interaction seem to be dispensable (Struhl et al., 2015) **(Figure 1.6)**.

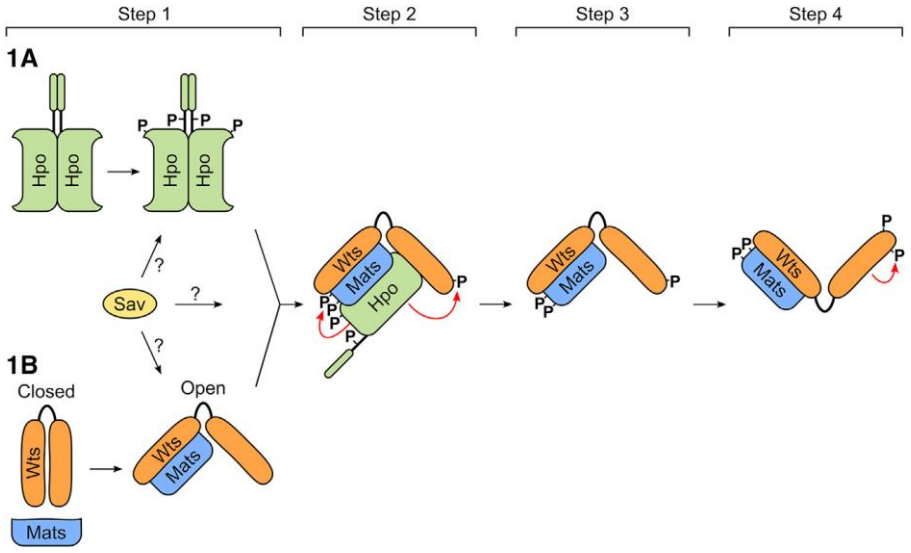

Figure 1.6. A proposed model for Wts activation.

(Step 1A) Hpo is activated by upstream components. **(Step 1B)** The conformation state of Wts is shifted from closed state to open state by the binding of Mats to Wts. **(Step 2)** Hpo associates with Wts as well as Mats and phosphorylates the Wts hydrophobic motif and Mats. **(Step 3)** This enhances Mats-Wts association and Hpo is then disassociated from the ternary complex. **(Step 4)** A further Mats-mediated allosteric change to Wts subsequently initiates activation loop phosphorylation. Active wts can initiate the phosphorylation of its substrate, such as Yki (Manning and Harvey 2015).

On the other hand, recent studies have revealed that the AGC serine/threonine NDR1/2 kinases (also termed as STK38/STK38L) function as novel members of the core cassette of the Hippo pathway, suggesting that the mammalian Hippo pathway is more diverse and complex. The first NDR serine/threonine kinaseDbf2p was identified in budding yeast (Johnston, Eberly et al. 1990). Follow up research then discovered NDR1/2 in human cells (Millward, Cron et al. 1995), while the Trc , the fly homolog of mammalian NDR1/2 kinases, was discovered later (Geng, He et al. 2000). To date, extensive efforts have been invested to reveal the molecular regulation of NDR1/2 kinases (Hoa, Kulaberoglu et al. 2016). It was shown that MST1/2 and MST3, another member of the MST kinase family, can initiate phosphorylation of NDR1/2 on Thr444/442 (Stegert, Hergovich et al. 2005, Hergovich, Kohler et al. 2009), while binding of MOB1 to the NTR domain of NDR1/2, which is located to the catalytic domain NDR1/2,

mediates the autophosphorylation of NDR1/2 at Ser281/282 in their T-loop (summarised in (Hergovich 2013). The overexpression of NDR1/2 did not lead to changes in YAP phosphorylation in the cultured mammalian cells, unlike LATS1/2 overexpression (Hao, Chun et al. 2008). Thus, it was thought that NDR1/2 does not regulate YAP kinases in mammalian cells. However, Zhang *et al*. discovered that NDR1/2 can directly mediate phosphorylation of YAP at Ser61/109/127/164, which is also phosphorylated by LATS1/2 (Zhao, Wei et al. 2007, Hao, Chun et al. 2008), strongly establishing that NDR1/2 functions as novel *bona fide* upstream kinases of YAP in mammalian cells. Intriguingly, NDR1/2-stimulated phosphorylation of YAP at Ser127 gave rise to cytoplasmic retention and ultimately inactivation of YAP (Zhang, Tang et al. 2015), as shown for the LATS1/2-stimulated phosphorylation of YAP at Ser127 (Zhao, Wei et al. 2007). Although it has been established that NDR1/2 functions as key upstream kinase of YAP, the exact molecular mechanism is yet to be determined. Therefore, it is significant to understand complex protein-protein interaction networks involving MST-SAV-MOB1A-LATS-NDR signalling.

In this context, Struhl and colleagues have recently reported that the activation of Wts by Mats does not appear to be dependent on phosphorylation by Hpo and is essential for Hippo signalling in flies. Furthermore, they also showed that the association of Mats with Hpo seems to be dispensable for activation of Wts (Vrabioiu and Struhl 2015). In contrast to these findings, it was shown that phosphorylation of MOB1 at Thr12 and Thr35 by MST1/2 is essential for the formation of NDR/MOB1 and LATS/MOB1 complexes (Praskova, Xia et al. 2008, Ni, Zheng et al. 2015). Although MOB1 has clearly been interconnected with NDR/LATS (Trc/Wts) signalling in mammalian cells and fly tissues, future studies are needed to uncover the biological importance of MOB1 associations with the MST1/2, NDR1/2 and LATS1/2 kinases in the Hippo pathway.

1.5.4. Mats/MOB1A in cancer

Loss-of-function of Mats in *Drosophila* results in homozygous lethality at early second larval stage and tumours (tissue overgrowth) in mosaic clones (Lai, Wei et al. 2005), leading an idea that Mats might play an important role in controlling cancer-related properties, such as cell proliferation and survival. To further support this idea, it was shown that these overgrowth phenotypes arise because of two main mechanisms (Johnson and Halder 2014). Firstly, they observed that *mats* mutant clones generated in larval eye disc has increased Yki activity and they proliferate exponentially when *mats* wild type clones quiescence. Furthermore, they also observed that *mats* mutant clones induced in larval eye disc overexpress *diap1*, making *mats* mutant clones resistant to the apoptotic signals which are triggered to get rid of the extra cells (Lai, Wei et al. 2005). The combination of deregulated cell proliferation and survival therefore results in dramatic overgrowth phenotypes **(Figure 1.10)**, ascribing a tumour suppressor role to Mats. Even more interestingly, Lai et al. (2005) showed that expression of MOB1A in Mats mutant clones generated in larval eye disc compensates for the Mats loss-of-function, further suggesting that the function of Mats is highly conserved from *Drosophila* to human.

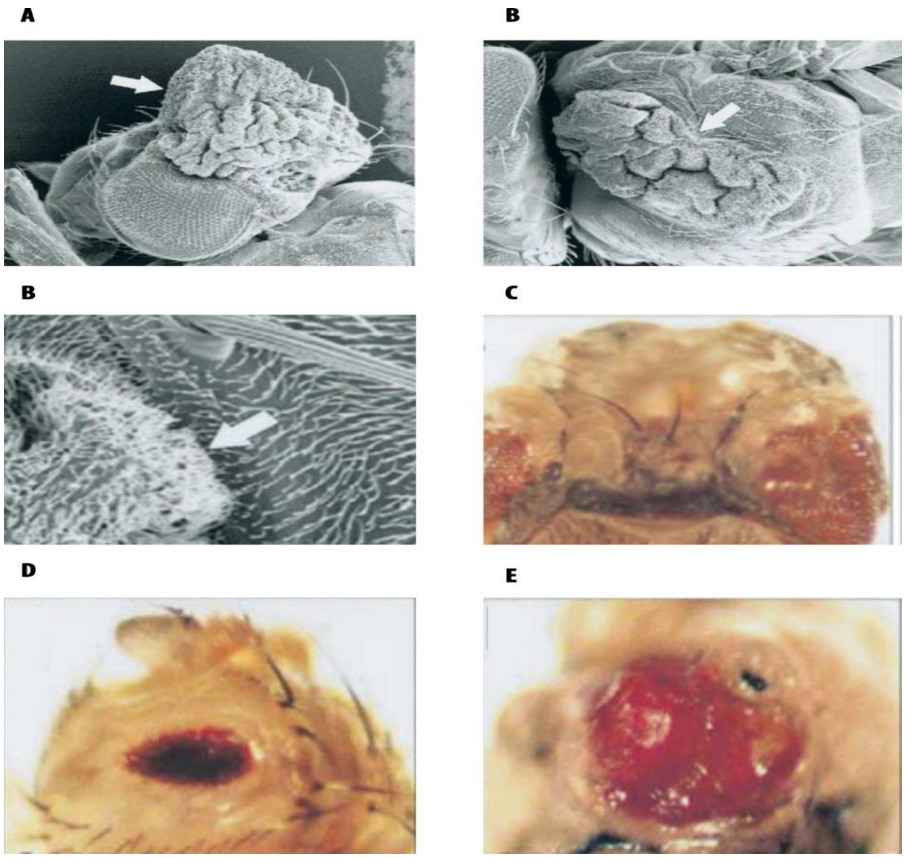

Figure 1. 7. The implications of the Mats loss-of-function in cancer-related phenotypes.

(A)(B)(C)(D) From mosaic flies with *mats* clones, large tumour in the head, notum, shoulder area and eye can be induced, respectively. **(D)** shows reduced eye phenotype due to hid-induced photype.(E) shows reduced eye phenotype in Mats mutant clones (Taken from (Lai, Wei et al. 2005). In addition to these phenotypes, Mats loss-of-function causes embryonic lethality. $Mats^{e235}$ and $Mats^{roo}$ are two independent alleles which cause Mats loss-of-function. $Mats^{e235}$ failed to complement the recessive lethality of $Mats^{roo}$.

Similarly, in mice, MOB1 loss-of-function has been linked to cancer. Recent studies revealed that MOB1 deficient mice display the most severe phenotype comparing to that of other Hippo component (Nishio, Hamada et al. 2012). Moreover, it was also shown that MOB1B heterozygous mice lacking MOB1A result in partial embryonic lethality and tumour formation in liver, while MOB1A heterozygous mice lacking MOB1B are all embryonically viable and free of liver tumours (Nishio, Hamada et al. 2012), implying that MOB1A might be key protein and more important than MOB1B. More importantly, keratinocyte-specific homozygous-null mutations of MOB1A and MOB1B (kDKO) mice

keratinocytes displayed over-proliferation, impaired apoptosis and contact inhibition, enhanced centrosomes, and increased progenitor self-renewal, thereby driving trichilemmal carcinoma in the skin (Nishio, Hamada et al. 2012).

In addition to these findings (Nishio, Hamada et al. 2012), Nishio et al. (2015) showed that conditional double knock-out of MOB1 in mouse liver cause hyperplasia of oval cells and immature cholangiocytes and half of mutant mice die within 3 weeks. Survival mice were observed to develop hepatocellular adenomas, intrahepatic cholangiocellular carcinoma (ICC), cholangiocarcinomas (cHC-CCs). Furthermore, they observed that liver conditional double knock-out of MOB1A exhibits dramatic phenotypes comparing to that of Nf2 (Benhamouche, Curto et al. 2010), Sav1 (Lu, Li et al. 2010), or Mst1/2 (Song, Mak et al. 2010) knockout mice, making MOB1A the most important elements of the Hippo pathway. They have also clarified that all these phenotypic changes in MOB1 double knock-out mice are genetically linked to YAP activation (Nishio, Sugimachi et al. 2016). Based on these results, they propose that MOB1 loss-of-function initiates the activation of YAP, leading to impaired cell contact-dependent growth inhibition, increased cell proliferation and migration, EMT, and liver tumour formation. However, it is unknown how MOB1 regulates YAP in these settings. From the general concept of the Hippo pathway (as outlined in **section 1.2**), one can conclude that LATS tumour suppressor proteins cannot be activated in MOB1-deficient mice. The inactive LATS proteins would not be able to inactivate and then inhibit YAP onco-proteins, which would ultimately trigger target genes leading to tumour formation. Furthermore, the fact that tumour formation observed in MOB1 deficient mice displayed more severe phenotype than those of the other Hippo components (MST1/2, LATS1/2, SAV) implies that MOB1 may have different molecular targets. In this context, the involvement of NDR1/2 kinases in these processes cannot be ruled out, since MOB1 can interact with NDR1/2 as well as LATS1/2 and MST1/2 kinases (Hergovich 2011, Hergovich 2016) and NDR1/2 functions upstream of YAP kinases (Zhang, Tang et al. 2015).

Taken together, involvement of Mats/MOB1 in cancer-related properties has clearly been shown in both *Drosophila* and mice. The involvement of Mats in cancer-related properties is shown in Mats loss-of-function *Drosophila*. The molecular mechanism how Mats loss-of-function results in overgrowth phenotype and impaired apoptosis is not completely known and remains to be uncovered. Importantly, the observation that Wts loss-of-function flies exhibit similar overgrowth phenotype implies that Wts-Mats signalling are important for tissue growth regulation in *Drosophila*. Even more importantly, the overgrowth phenotype in Mats mutant flies are stronger than Wts loss-of-function, indicating that Mats is master tumour suppressor in Hippo signalling. Moreover, it was also shown that Mats is required for Trc functions (He, Emoto et al. 2005). More importantly, Vrabioiu *et al*. showed that complex formation between Wts and Mats is required for Wts activation. On the other hand, they also showed that Hippo-Mats interactions seem to be indispensable. In this context, experimental evidence using full-length proteins carrying selective manipulations is yet outstanding and will help us to understand how tissue growth is regulated in *Drosophila*.

Involvement of MOB1 has been linked to human cancer (Gomez, Gomez et al. 2014). MOB1 loss-of-function can play pivotal role in the tumour formation. Intriguingly, recent research revealed that MOB1A is involved in a broader range of activities including association with MST1/2, LATS1/2 and NDR1/2. Importantly, it was revealed that double knockout of MOB1 in mice represents more severe tumour formation than that of LATS, Sav, MST deficiency (Harvey, Zhang et al. 2013), suggesting that MOB1 might function as tumour suppressor independent of LATS possibly including MOB1/MST or MOB1/NDR complexes. Complex interactions of MOB1 with its binding partners MST1/2, LATS1/2, and NDR1/2 are not yet investigated. In this context, the selected variants of MOB1A affecting binding properties to MST1/2, LATS1/2, and NDR1/2 will uncover the molecular mechanism of tumour formation driven by MOB1.

1.6. Research Aims

The Hippo signalling pathway has emerged as a key signalling pathway regulating tissue growth and organ size during *Drosophila* development. Recent studies have identified Mats (the counterpart of human MOB1A) as a tumour suppressor protein which functions as a key component of the Hippo pathway. The same study has also shown that loss of *mats* gave rise to uncontrolled tissue overgrowth in *Drosophila.* Very interestingly, it has also been shown that loss-of-function of *mats* can be functionally rescued by expression of wild-type MOB1A to suppress tissue overgrowth in the eye. Moreover, Wei et al. (2007) showed that Hpo phosphorylates Mats, which in turn results in the activation of Mats, thus upregulating Wts kinase activity. MOB1A has been shown to bind to NDR1/2, LATS1/2 and MST1/2. However, the importance of these interactions with respect to biological functions has so far only been tested in isolation without considering the context of these diverse PPIs. More importantly, none of these interactions have actually been tested in the context of tumour suppression and the regulation of YAP (Yki). Therefore, the aim of this project is to decipher the key PPIs of MOB1A with the Hippo core kinases MST1/2(Hpo), LATS1/2(Wts), and NDR1/2(Trc) which are essential for tumour suppression.

2. Materials and Methods

2.1. Materials

2.1.1. Reagents

Molecular biology reagents

Reagents	Company	Catalogue Number
1kb DNA Ladder	Fisher Scientific Ltd	FQ-SM0311
1.5ml PP Eppendorf tubes	Fisher UK	10509691
2.0ml PP Eppendorf tubes	Fisher UK	10038760
GelRed Nucleic Acid Gel Stain	Biotium	41003
Falcon Tubes (15ml and 50 ml)	Appleton Woods	BC031
Pfu DNA polymerase	MBL / supplier Caltag Med	RK-02-031-5
QIAquick Gel extraction kit	Qiagen	28706
NucleoSpin Plasmid	Fisher-MN	NZ740588250
Midi prep kit (MN)	Fisher UK	NZ740410100
T4 DNA ligase	NEB	M0202G
PCR Tubes	VWR	732-0676
BamH I - HF	New England Biolabs	R3136M
Dpn I	New England Biolabs	R0176L

EcoR I - HF	New England Biolabs	R3101L
EcoR V - HF	New England Biolabs	R3195L
Hind III	New England Biolabs	R0104S
Kpn I - HF	New England Biolabs	R3142S
Not I	New England Biolabs	R0189S
Pme I	New England Biolabs	R0560L
Xho I	New England Biolabs	R0146L
Taq DNA polymerase	New England Biolabs	M0273L
Alkaline phosphatase CIP	New England Biolabs	M0290S
5ml pipettes sterile	Fisher UK – Corning	TKV-670-051R
10ml pipette sterile	Fisher UK – Corning	TKV-670-071L
25ml pipette sterile	Fisher UK – Corning	TKV-670-091F

Biochemistry reagents

Reagents	Company	Catalog Number
ProtoGel (30%) Acrylamide	Fisher Scientific UK	12381469
Ammonium persulphate	Sigma	A3678-100G
Ampicillin	Sigma	A9393-25G
2-mercaptoethanol	Sigma	M3148-100ml
1.6ml plastic cuvettes	Fisher UK	11547692
Luminol	Sigma	123072-25G
pCoumaric acid	Sigma	C9008-10G
H_2O_2 30% solution	VWR	23622.260
X-ray films	SLS	MOL7016
EDTA	Sigma(fluka)	10617201
Ethanol	VWR	20827.365
Isopropanol (2-propanol)	VWR	1.09634.1000
Kanamycin	Sigma	K1377-5G
LB broth base	Sigma	L3022-1KG
LB agar	Sigma	L2897-1KG
MgSO4	Sigma	M7506-1KG
Glycine	Sigma	G7126-5KG
Boric acid	Sigma	B6768-1KG
Borax	Sigma	71998-250G
NaCI	Sigma	S3014-5KG
Na_2HPO_4	Sigma	S3264-500G
KCl	Sigma	P9541-500G
EGTA	Sigma	E3889-100G
IPTG	Sigma	I6758-10G
Glycerol	Sigma	G5516-1L
Na3VO4	Sigma	S6508-50G
Leupeptin	Enzo Life Sciences	ALX-260-009-M025
DTT	Enzo Life Sciences	ALX-280-001

Benzamidine	Sigma	12072-10G
Microcystin-LR	Enzo Life Sciences	ALX-350-012-C500
1M Hepes pH7.5 solution	Invitrogen	15630-056
10% SDS solution	Fisher UK	BPE2436-1
20% SDS solution	Fisher UK	BPE1311-1
Skim milk powder	Sigma	70166-500G
DMP	Fisher UK	PN21667
ATP (adenosine 5'-triphosphate)	Fisher UK - GE Healthcare	GZ27100603
TEMED	Fisher UK - National Diag.	ELR-420-010P
Bio-Rad protein assay	Bio-rad	500-0006
gamma-P32-ATP	Hartmann Analytic	SRP-301/37
Peptone from casein	Sigma	70172-500G
Yeast Extract	Sigma	70161-500G
Citric acid monohydrate	Sigma	C1909-500g
PMSF	Sigma	P7626-5G
NP40 substitute	Sigma	74385-1L
Coomassie Brilliant Blue	Sigma	B4921-20TAB
Tween 20	Bio-rad	170-6531
NaF	Sigma	S7920-500G
Triton X-100	Sigma	T9284-1L
Crystal violet	Sigma	C3886-100G
NaOH	Sigma	S5881-1KG
EDTA (IDRANAL)	Sigma	31064-1KG
Ponceau S	Sigma	P7170-1L
Protein A sepharose CL-4B beads	VWR	17-0780-01

Cell biology reagents

Reagents	Company	Catalog Number
DMEM	Sigma	D6429-24X500ML
DMSO	Sigma	D8418-1L
15ml PS tubes (for TC)	VWR - BD Falcon	734-0450
Tetracycline	Sigma	87128-25G
Gelatin	Fisher UK	G/0150/53
Polybrene/hexadimethrine bromide	Sigma	H9268-5G
Lipofectamine 2000	Invitrogen	11668-019
Opti-MEM	Invitrogen	31985-047
Fetal Bovine Serum (tet tested)	Invitrogen	16000-044
Trypsin 0.25%	Invitrogen	25050-014
D-MEM powder	Invitrogen	52100-039
D-PBS	Invitrogen	14040-174
Schneider's Drosophila medium	Invitrogen	21720-024
Penicillin G potassium salt	VWR	A1837.0010
Streptomycin sulfate	VWR	A1852.0025
Fugene-6	Roche	11814443001
Metafectene Pro	CamBio - Biontex UK	T040-1.0 or 2.0 or 5.0
Puromycin	Autogen - Invivogen	ant-pr-1
Zeocin	Autogen - Invivogen	ant-zn-5
Hygromycin B	Autogen – Invivogen	ant-hm-1
Blasticidin S	Autogen – Invivogen	ant-bl-1
G418 - Geneticin	Autogen -	ant-gn-5

	Invivogen	
RPMI 1640 with L-Glutamine	Invitrogen	21875034
D-PBS Ca/Mg free	Invitrogen	14190-169
Horse Serum	Invitrogen	16050122
DMEM/F12 medium Hepes	Invitrogen	31330038
EGF	Peprotech	AF-100-15-1000
Hydrocortisone	Sigma	H0888-10G
Cholera toxin	Sigma	C8052-1MG
Insulin	Sigma	I1882-100MG
0.05% trypsin plus 0.53mM EDTA	Invitrogen	25300096
Effectene transfection reagent	Qiagen	301425
HI-FBS	Invitrogen	10082147
Lipofectamine RNAiMAX	Invitrogen	13778150
Tissue culture 60mm dish 6cm	Appleton Woods	BC151
175cm tissue culture flasks T175	Greiner	660175
12-well TC plate	VWR	391-0006
6-well TC plates	VWR	734-1596
24-well TC plates	Fisher UK - Corning	TKT-520-090B
6cm TC plates	Fisher UK - Corning	TKV-160-034S
10cm TC plates	Fisher UK - Corning	TKV-160-049F
CryoTubes 2.0ml	Sarstedt	72.380.992

2.1.2. Antibodies

Primary Antibody	Species	Usage	Supplier	Catalog Number	Blocking Solution
HA-tag (C29F14)	Rabbit	1:1000	Cell Signalling	3724	5% Milk
HA-tag (42F13)	Mouse	1:500	Home-made		5% Milk
Myc-tag (71D10)	Rabbit	1:1000	Cell Signalling	2278	5% Milk
Myc-tag (9E10)	Mouse	1:50	Home-made		5% Milk
Alpha-tubulin (YL1/2)	Rat	1:100	Home-made		5% Milk
YAP (total)	Rabbit	1:1000	Cell Signalling	4912	5% Milk
Phospho-YAP(S127)	Rabbit	1:1000	Cell Signalling	4911S	5% Milk
Phospho-YAP(S397)	Rabbit	1:1000	Cell Signalling	13619	5% Milk
Anti-Actin (I-19)	Goat	1:1000	Santa Cruz	sc-1616	5% Milk
Anti-GAPDH (6C5)	Mouse	1:1000	Millipore	Mab374	5% Milk
Anti-MOB1	Rabbit	1:250	Home-made		5% Milk
anti-MOB1 (T12-P)	Rabbit	1:1000	NEB	8843	5% Milk
anti-MOB1 (T35-P)	Rabbit	1:1000	NEB	8699	5% Milk

2.1.3. Buffers and Solutions

Unless otherwise stated, buffers and solutions were kept at room temperature

5 x Laemmli SDS Sample buffer

Main Stock	Amount Taken	Final Concentration
1 M Tris-HCI pH 6.8	12.5ml	125mM
20% SDS solution	25ml	5)
autoclaved ddH2O	57.5ml	57.5%
beta-mercaptoethanol	5ml	0.05
Total Volume	100ml	

Western blot stripping solution*

Main Stock	Amount Taken	Final Concentration
Glycine	1.877 g	25mM
20% SDS solution	50ml	1% SDS
autoclaved ddH2O	Fill up to 1000 ml	
Total Volume	1000ml	

* **pH is adjusted to 2.5 with 37% HCI**

Standard 150mM Lysis Buffer*

Main Stock	Amount Taken	Final Concentration
1 M Tris pH 8.0	20 ml	20 mM
5 M NaCl	30 ml	150 mM
100 ml pure glycerol	100 ml	10%
10 % NP-40	100 ml	1%
0.5 M EDTA pH 8.0	10 ml	5 mM
0.5 M EGTA pH 8.0	1 ml	0.5 mM
0.5 M NaF	100 ml	50 mM
beta-glycerophosphate	4.32 g	20 mM
200 mM Na_3VO_4	5 ml	1 mM
autoclaved ddH2O	Fill up to 1000 ml	
Total Volume	1000 ml	

***Store at 4 ºC, Protease and phosphatase inhibitors; 1 mM benzamidine, 4 µM leupeptin, 0.5 mM phenylmethylsulfonyl fluoride [PMSF], and 1 mM dithiothreitol [DTT] were freshly added into buffer to prevent proteolysis, dephosphorylation and denaturation of proteins.**

Standard 1M lysis buffer (for IP washing)*

Main Stock	Amount Taken	Final Concentration
1 M Tris pH 8.0	20 ml	20 mM
5 M NaCl	100 ml	1 M
100ml pure glycerol	100 ml	10%
10 % NP-40	100 ml	1%
0.5 M EDTA pH 8.0	10 ml	5 mM
0.5 M EGTA pH 8.0	1 ml	0.5 mM
0.5 M NaF	100 ml	50 mM
beta-glycerophosphate	4.32 g	20 mM
200 mM Na3VO4	5 ml	1 mM
autoclaved ddH2O	Fill up to 1000 ml	
Total Volume	1 000ml	

***Store at 4 °C, Protease and phosphatase inhibitors; 1 mM benzamidine, 4 µM leupeptin, 0.5 mM phenylmethylsulfonyl fluoride [PMSF], and 1 mM dithiothreitol [DTT] were freshly added into buffer to prevent proteolysis, dephosphorylation and denaturation of proteins.**

MILB (low stringency MST Interaction Lysis Buffer)*

Main Stock	Amount Taken	Final Concentration
1 M HEPES pH 7.4	30 ml	30 mM
beta-glycerophosphate	4.32 g	20 mM
1 M KCl	20 ml	20 mM
0.5 M EGTA pH 8.0	2 ml	1 mM
0.5 M NaF	4 ml	2 mM
200 mM Na3VO4	5 ml	1 mM
Pure TX-100	10 ml	1%
autoclaved ddH2O	Fill up to 1000 ml	
Total Volume	1000 ml	

***Store at 4 ºC, Protease and phosphatase inhibitors; 1 mM benzamidine, 4 µM leupeptin, 0.5 mM phenylmethylsulfonyl fluoride [PMSF], and 1 mM dithiothreitol [DTT] were freshly added into buffer to prevent proteolysis, dephosphorylation and denaturation of proteins.**

10× MST1/2 (Hippo) kinase assay buffer*

Main Stock	Amount Taken	Final Concentration
1 M Tris pH7.5	2.5 ml	5 mM
beta-glycerophosphate	0.27 g	2.5 mM
0.5 M EGTA	1 ml	1 mM
0.2 M Na3VO4	2.5 ml	1 mM
1 M MgCl2	2 ml	4 mM

***1M DTT is freshly added to buffer at the final concentration of 0.01 mM. Store at 4 ºC**

Kinase Master Mix (KMM)

Main Stock	**Amount Taken**
10x Kinase Assay Buffer	1V
1 mM ATP	2V
ddH2O	2V

For SDS-PAGE

SDS Resolving Gel (for 10ml)

	8%	10%	12%
ddH_2O	4.6 ml	4.0	3.3 ml
30% Acrylamide mix	2.7 ml	3.3	4.0 ml
1.5 M Tris-HCl [pH 8.8]	2.5 ml	2.5	2.5 ml
10% SDS	0.1 ml	0.1	0.1 ml
10% APS	0.1 ml	0.1	0.1 ml
TEMED	0.006 ml	0.004	0.004 ml

Stacking gel (3 ml per gel)

ddH_2O	**2.1 ml**
30% Acrylamide mix	0.5 ml
1.0 M Tris-HCl [pH 6.8]	0.38 ml
10% SDS	0.03 ml
10% APS	0.03 ml
TEMED	0.003 ml

10 x SDS Running Buffer (for 2000ml)

Main Stock	**Amount Taken**	**Final Concentration**
Glycine	288.2 g	1.92 M
Tris base	60.6 g	250 mM
20% SDS solution	100 ml	
autoclaved ddH2O	Fill up to 2000 ml	

For Western Blotting

Tris-buffered saline-tween (TBS-T)

Tris-HCI [pH 7.5]	50 mM
NaCl	150 mM
Tween 20	0.1%

Chemiluminescent detection substrates

Solution 1

Tris-HCI [pH 8.5]	1 M
Luminol	250 mM
pCoumaric acid	90 mM

Solution 2

Tris-HCI [pH 8.5]	**1 M**
H_2O_2	30%

Coomassie staining solution

MeOH	25% (v/v)
Acetic acid	10% (V/V)
Coomassie	0.25% (w/v)

Destaining solution for Coomassie staining

EtOH	10%
Acetic acid	10%

10 x Western Blot Transfer Buffer (for 2000ml)

Main Stock	**Amount Taken**	**Final Concentration**
Glycine	288.2	1.92 M
Tris base	60.6	250 mM
autoclaved ddH2O	Fill up to 2000 ml	

10 x Tris-buffered saline (TBS) pH 7.4 (2000ml)

Main Stock	Amount Taken	Final Concentration
NaCl	175.32 g	3 M
Tris base	121.14 g	1 M
37% HCl	75 ml	
autoclaved ddH2O	Fill up to 2000 ml	

TBS-T (0.05 %)

Main Stock	Amount Taken
10x TBS	200 ml
Tween	10 ml
autoclaved ddH2O	Fill up to 2000 ml

10 x TBE (2000ml)

Main Stock	Amount Taken	Final Concentration
Tris base	216 g	0.89 M
Boric acid	110 g	0.89 M
0.5M EDTA pH8.0	80 ml	20 mM
autoclaved ddH2O	Fill up to 2000 ml	

1000 x Leupeptin stock (4mM)*

Main Stock	Diluted in
25 mg (Mw=475.6)	13.13 ml autoclaved ddH2O

***Store at -20**

1000 x DTT stock (1M)*

Main Stock	Diluted in
5 g (Mw=154.2)	32.43 ml autoclaved ddH2O

***Store at -20**

1000 x Benzamidine stock (1M)*

Main Stock	Diluted in
10 g (Mw=120.15)	83.23 ml autoclaved ddH2O

***Store at -20**

1000 x PMSF (0.5M)*

Main Stock	Diluted in
5 g (Mw=174.19)	57.4 ml DMSO

***Store at -20**

0.2M Sodium Orthovanadate stock (0.2M Na3VO4)*

Main Stock	Diluted in
9.2 g (Mw=183.91)	200 ml autoclaved ddH2O

* **Adjust pH to 10.0 with 37% HCl, Boil solution until it turns colourless; cool down to RT, Readjust pH to 10.0 with NaOH, Repeat boiling-cooling-adjusting procedure until the solution remains colourless with a stable pH of 10.0.**

200mM MBP lysis buffer (500ml)

Main Stock	Amount Taken	Final Concentration
20 mM Tris-HCI pH 7.5	10 ml	1 M
1 mM EDTA	1 ml	0.5 M
200 mM NaCl	20 ml	5 M
autoclaved ddH2O	Fill up to 500 ml	

1M MBP column washing buffer (500ml)

Main Stock	Amount Taken	Final Concentration
20 mM Tris-HCI pH 7.5	10 ml	1 M
1 mM EDTA	1 ml	0.5 M
1 M NaCl	100 ml	5 M
autoclaved ddH2O	Fill up to 500 ml	

0.2 M boric acid*

Main Stock	Diluted in
6.183 g (Mw=61.83)	500 ml autoclaved ddH2O

***Adjust pH to 4.0 with HCI, store at 4 °C**

0.05 M Na-Borax*

Main Stock	Diluted in
10.06 g (Mw=201.22)	1000 ml autoclaved ddH2O

*** Heat up in order to solve Borax completely**

0.2M Na-Borate buffer pH 9.0 (100ml)*

Main Stock	Diluted in
9 ml 0.2 M boric acid (pH4.0)	90 ml 0.05 M Borax

***Adjust pH to 9.0**

0.2 M Ethanolamine pH 8.0 (500 ml)*

Main Stock	Dissolved in
6 ml 16.6 M ethanolamine solution (99%)	450 ml autoclaved ddH2O

*** Adjust pH to 8.0 with HCl**

Bacteria culture buffers

LB medium* (1000 ml)

Main Stock	Amount Taken
Tryptone	10 g
Yeast Extract	5 g
NaCI	10 g
autoclaved ddH2O	Fill up to 1000 ml

***Adjust pH to 7.0 with NaOH and autoclave. Store at 4 °C. To prepare plates with amphicilin or kanamycin containing plates, add 100 mg/ml of amphicilin or 50 mg/ml of kanamycin.**

2 x YT medium* (1000 ml)

Main Stock	Amount Taken
Tryptone	16 g
Yeast Extract	10 g
NaCI	5 g
autoclaved ddH2O	Fill up to 1000 ml

***Adjust pH to 7.0 with NaOH and autoclave. Store at 4 ^{O}C.**

IGB buffer* (for competent *E.coli*) (500 ML)

Main Stock	Amount Taken	Final Concentration
PEG4000	50 g	10% (w/v)
$MgSO_4$	6.15 g	50 mM
$MgCI_2$	5.08 g	50 mM
DMSO	25 ml	5% (v/v)

***Dissolve solid chemicals in 400 ml LB medium, add DMSO, adjust pH to 6.5, and filter sterilise. Store at 4 ^{o}C**

LB plates*

Main Stock	Amount Taken
LB base	25 g
Agar	15 g
$MgSO_4$	1.204 g
10N NaOH	400 µl
autoclaved ddH2O	Solve in 1000 ml

***Adjust pH to 7.2-7.3 and autoclave. After autoclave, let it cool down to 45-50 and then store at 4 °C. To prepare plates with ampicilin or kanamycin containing plates, add 100 mg/ml of ampicilin or 50 mg/ml of kanamycin after cooling down to 45-50 °C.**

1000 x Ampicilin stock* (100 mg/ml)

Main Stock	Diluted in
1 g Ampicilin (349.41 g/mol)	9 ml autoclaved ddH2O

***Store at -20**

1000 x Ampicilin stock* (50 mg/ml)

Main Stock	Diluted in
0.5 g Kanamycin (484.499g/mol)	9 ml autoclaved ddH2O

***Store at -20**

100 mM IPTG*

Main Stock	Diluted in
10 g IPTG (238.3 g/mol)	419.6 ml autoclaved ddH2O

***Store at -20**

2.1.4. Plasmids

The following plasmids were kindly provided by the Hergovich Laboratory;

pCMV(R)neo_new MCS (New multiple cloning sides (MCS) were inserted into BamHI/XhoI to get new MCS: BamHI - MluI - PmeI - KpnI - HpaI - BglII – XhoI).

pcDNA3_neo_myc (with the myc-tag being in frame into KpnI/BamHI)

pcDNA3_neo_HA (with the HA-tag being in frame into KpnI/BamHI)

pMAL-2c_hMOB1A wt

pMAL-2c_hMOB1A T12A

pMAL-2c_hMOB1A T35A

pMAL-2c_hMOB1A E51K

pMAL-2c_hMOB1A D63V

pMAL-2c_hMOB1A K104E/K105E

pMAL-2c_hMOB1A E51K/K104E/K105E

pMAL-2c_hMOB1A D63V/K104E/K105E

pSuper.retro.puro shhMOB1A#1/shhMOB1B#3

pSuper.retro.puro shhMOB1A#4/shhMOB1B#3

pSuper.retro.puro_shLuc

pcDNA3_myc-RFP

pcDNA3_myc-RFP NDR1 1-80

pcDNA3_myc-RFP NDR1 18-82

pENTR-3C

pcDNA3_myc-RFP NDR1 20-82

pcDNA3_myc-RFP NDR1 22-82

pcDNA3_myc-RFP NDR1 25-82

pcDNA3_myc-RFP LATS2 568-661

pcDNA3_myc-RFP LATS2 603-661

pcDNA3_myc-RFP LATS2 580-661

pcDNA3_myc-RFP LATS2 590-661

pcDNA3_myc-RFP LATS2 595-661

pcDNA3_myc-RFP LATS2 600-661

Drosophila cell expression plasmid pAW was kindly provided by the Barbara Laboratory. Transgenic *drosophila* generation plasmid pKC26w pUbiq was kind gift for the Tapon Laboratory. The plasmid pSMT3-hMOB1A (33-216) was kindly provided by the Rice Laboratory. The plasmids pLEX (gateway casette inserted) were kind gift from the Rodriquez-Viciana Laboratory.

2.1.5. Oligonucleotides

Primers (5` to 3`)	**Sequence**
Universal T7	TAATACGACTCACTATAGGG
SP6	ATTTAGGTGACACTATAG
MOB1A (E51K) F	TTGCCTGAGGGAAAGGATCTCAATGAATGGATTGC
MOB1A (E51K) R	TCATTGAGATCCTTTCCCTCAGGCAACATAACAGC
MOB1A (D63V) F	GCTGTGAACACTGTGGTTTTCTTTAACCAGATCAACATGTTA
MOB1A (D63V) R	GATCTGGTTAAAGAAAACCACAGTGTTCACAGCAATCCATTCA
MOB1A (K104E/K105E) F	ACTAATATTGAAGAGCCAATCAAATGTTCTGCACC
MOB1A (K104E/K105E) R	TTTGATTGGCTCTTCAATATTAGTACCATCTGCCC
Roo Internal 1 R	GCCGCTCAAGATAGCCAGAT

Roo Internal 2 R	TATCTAAGGCGACATGGGTGC
Roo Internal Forward primer 4	ATCTGGCTATCTTGAGCGGC
Roo Internal Reverse Primer 4	CTAAGGCGACATGGGTGCAT
Roo Internal Forward primer 5	AATGGCCTACGGAGACCTAC
Roo Internal Reverse Primer 5	GCCGCTCAAGATAGCCAGAT
Primer 97	GCACACTTCCTGGAACCGCTCGCATC
Neo2 f	AGAGGCGCTTCGTCTACGGAGCGACA
hsp70_FRT r	CGGCAAGCAGGCATCGCCATGGGTC
pKC26-pUbiq F	CCCCAGCCAGGAAGTTAGTTTC
SV40 R	GGCATTCCACCACTGCTCCC

2.2. Methods

2.2.1. Molecular Biology Techniques

2.2.1.1. Preparation of Competent Cells

The *E. coli* strains XL1-Blue or BL21 were used to produce competent cells. XL1-Blue or BL21 were aseptically plated out on LB agar plates without any antibiotics, which in turn were incubated at 37 ^{o}C overnight. Single colonies were picked and inoculated into 5 ml of 2x YT. The following day, the overnight cultures were diluted into 500 ml 2x YT (1:100), which were then incubated in a shaking incubator at 37 ^{o}C until the optical density (OD) of the culture reached 0.4 at 600nm. The cultures were then centrifuged at 112 x g at 4 ^{o}C for 5 minutes. After removing the supernatant, the cell pellet was re-suspended in 1/10 volume ice cold IGB buffer. Then, cells were aliquoted into precooled tubes in a cold room at 4 ^{o}C, snap frozen in dry ice and stored at -80 ^{o}C.

2.2.1.2. Transformation of Competent cells

Bacterial transformation were performed as described by (Cohen, Chang et al. 1972), which reported that bacteria take up plasmids when treated with ice-cold $CaCl_2$ and subjected to a brief heat shock. Pre-prepared competent *E.coli* cells were thawed on ice. 1 µl of plasmid DNA were added to 100 µl competent cells and then incubated on ice for 30 minutes. The cells-DNA mixture was then heat-shocked at 42 ^{o}C by placing in pre-arranged thermomixer for 45 seconds, which were immediately transferred on ice for 5 minutes. Following the incubation on ice, 500 µl of LB medium without any antibiotics were added to the cells-DNA mixture and then incubated at 37 ^{o}C for 30 minutes. This so-called recovery step was only applied to the transformation after ligation. After the incubation at 37 ^{o}C, the cells-DNA mixture was plated out onto LB plates with corresponding antibiotics using sterile techniques. The plates were incubated at 37 ^{o}C overnight.

2.2.1.3. Preparation of plasmid DNA from competent *E.coli* cells

2.2.1.3.1. Small Scale preparation of plasmid DNA (Mini-Prep)

DNA minipreps were performed according to manufacturer`s instructions (Macherey-Nagel). Briefly, the plasmids were transformed and grown on LB plate with corresponding antibiotics. Single colony were then picked up and transferred into 3 ml LB medium in 15 ml falcon tubes with corresponding antibiotics and ultimately inoculated at 37 ^{o}C overnight with vigorous shaking. The following day, bacterial cells were pelleted by centrifugation at 12,000 x g for 1 minute. The supernatant was then removed and cell pellets were re-suspended in 250 µl pre-chilled buffer A1 (50 mM Tris-HCl, 10 mM EDTA, 100 µg/mL RNase A, pH 8.0; resuspension solution). 250 µl of the buffer A2 (200 mM NaOH, 1 % SDS; lysis buffer) were then added and incubated for 5 minutes at room temperature. 300 µl of the buffer A3 (2.8 M KAc, pH 5.1; neutralization solution) were ultimately added and mixed by inversion. The mixture was then spun down by centrifugation at 11,000 x g for 5-10 minutes, before transferring the supernatant to NucleoSpin® Plasmid column, followed by centrifugation at 11,000 x g for 1 minute to allow DNA to bind to silica membrane of NucleoSpin® Plasmid column. After discarding flow-through, silica membrane was then washed with the buffer A4 (100 mM Tris, 15% ethanol, 1.15 M KCl, adjusted to pH 6.3 with H_3PO_4, wash buffer) to remove any cellular debris. The NucleoSpin® Plasmid column was placed in a fresh 1.5 eppendorf tubes and 50 µl of autoclaved ddH_2O were added and finally centrifuged at 11,000 x g to elute DNA.

2.2.1.3.2. Large-scale preparation of plasmid DNA (Midi-prep)

DNA midipreps were performed according to manufacturer`s instructions (Macherey-Nagel). Briefly, the plasmids were transformed and grown on LB plate with corresponding antibiotics. Single colony was then picked up and transferred into 100 ml LB medium in 1000 ml Erlenmeyer flask with corresponding antibiotics and ultimately inoculated at 37 ^{0}C overnight with vigorous shaking. After the incubation overnight, bacterial cells were transferred to Nalgene® Centrifuge Tubes and then centrifuged at 5,000 x g

for 10 minutes at 4 ^{o}C. After centrifugation, the supernatant was discarded and cell pellets were then re-suspended in Cell Resuspension Solution (50 mM Tris-HCL (pH 7.5), 10 mM EDTA (pH 8.0), 100 µg/ml RNase A). Cell Lysis Solution (CLS) (0.2 M NaOH, %1 SDS) was added to the cell suspension and mixed by gently inverting the tube 3-5 times. After incubating the cell suspension-CLS mixture for 3 minutes at room temperature, Neutralization Solution (4.09 M guanidine hydrochloride (pH 4.2), 759 mM potassium acetate, and 2.12 M glacial acetic acid) were added to the lysed cells and mixed by gently inverting the tubes 3-5 times. The mixture was then centrifuged at 15,000 x g for 15 minutes to pellet the bulk of the cellular debris. During the centrifugation, a column stack was assembled by assembling a PureYield^{TM} Clearing Column (PCC) into the top of a PureYiald^{TM} Binding Column (PBC), which were ultimately placed onto the vacuum manifold. After centrifugation, the cleared lysate was decanted into PCC and the vacuum was applied to allow to not only pass through the clearing membrane in the PCC but also plasmid DNA to bind to the binding membrane in the PBC. To clean the PBC, 5 ml of Endotoxin Removal Wash was added and the vacuum was applied to allow the vacuum to remove the solution through the column. As a last step of washing, the PBC was washed with 20 ml of Column Wash Solution (60% Ethanol, 60 mM potassium acetate, 8.3 mM Tris-HCL and 0.04 mM EDTA). To elute plasmid DNA, 1.5 ml Eppendorf tube was placed in the base of the Eluator^{TM} Vacuum Elution Device in which PBC was previously placed. The Eluator^{TM} Device assembly were the placed into a vacuum manifold. 400 µl of Nuclease-Free Water were then added to the Eluator^{TM} Device Assembly to elute plasmid DNA into 1.5 ml eppendorf tubes.

2.2.1.4. Quantification of nucleic acids

The concentration of DNA was measured using NanoDrop^{TM} ND-1000. After setting up with Blank (Nuclease-Free Water), the concentration was quantified at 260nm. For example, a value of 39.019 at 260nm corresponded to 1950 ng of DNA per µl.

2.2.1.5. Agarose gel electrophoresis of nucleic acids

Agarose gel electrophoresis is widely used as a method of separating a mixed population of DNA based on length and size of DNA fragments. Negatively charged DNA molecules are run on an agarose matrix, with small DNA fragments running faster than large DNA fragment, when electric field is applied. DNA fragments were separated and visualized using agarose gel electrophoresis containing the Nucleic Acid Red Dye (VWR, cat# 730-2958). Nucleic Acid Red Dye helps to detect DNA or RNA with the reduced rate of mutagenicity, which make it safer than ethidium bromide. The agarose gels were prepared by mixing appropriate amount of agarose powder (see **Table 2.1**) (Sigma, cat# A2576) into appropriate amount of 10x TBE buffer, which were in turn microwaved to dissolve agar. Following cooling the agarose solution, appropriate amount of Nucleic Acid Red Dye (1:1000) were added into the solution to have DNA visualized after electrophoresis. The solution was then poured into a casting tray with a comb, subsequently allowing the solution to solidify for at least 20 minutes. After solidification of the gel, it was placed into electrophoresis chamber, immersed in 1x TBE and the comb was then removed. Appropriate amount of 6x DNA Loading Buffer was mixed with samples, which were subsequently loaded into wells. 1 µg of 1kb DNA Ladder (Fermentas, cat# SM0311) were exploited as a molecular weight marker. Electrophoresis was run at a constant voltage of 100 V for 50 minutes. The DNA were then visualized under UV light using Syngene G:BOX F3 Fluorescence Imaging System.

Table 2. 1

Percentage agarose gel (w/v)	DNA size resolution (kb=1000)
0.5%	1kb to 30 kb
0.7%	800 base pairs to 12 kb
1.0%	500 base pairs to 10 kb
1.2%	400 base pairs to 7 kb
1.5%	200 base pairs to 3 kb
2.0%	50 base pairs to 2 kb

2.2.1.6. Restriction endonuclease digestion, extraction and ligation of DNA fragments

In order to screen for inserts, right orientation of insert, or prepare for PCR products and plasmid DNAs for ligation, DNAs were digested in appropriate buffer with specific restriction endonucleases (please see **Figure 2.1, 2.2, 2.3**). For ligation of insert into vector backbones, 5 µg of inserts or vector backbones were digested in appropriate buffer with specific restriction endonucleases at the recommended temperature overnight. After the incubation overnight, the samples were run on appropriate percentage of agarose gel using electrophoresis. Following the separation of DNA fragments on agarose gel, QIAquick Gel Extraction Kit (Qiagen, cat#28704) was used to extract DNA if needed for subsequent cloning stages, according to the manufactures' protocol (Qiagen). Briefly, the DNA fragments were excised from the agarose gel with a clean and sharp scalpel. The gel slice was then weighed. According to weight, 3 volumes of Buffer QG were added to 1 volume gel (100 mg gel ~ 100 µl). The mixture was then incubated at 50 ^{o}C for 10 minutes. After the incubation, 1 volume of isopropanol was added to the sample and mixed. A QIAquick spin column was placed in a provided 2 ml collection tube. The sample were then applied to the QIAquick column and centrifuged at maximum speed for 1 minute to bind DNA. Then, flow-through was discarded and 750 µl of Buffer PE were added to the QIAquick column and centrifuged at maximum speed for 1 minute to wash. After the washing, the QIAquick column was placed into a clean 1.5 ml Eppendorf tube. To elute DNA, 50 µl of autoclaved ddH_2O were added and centrifuged at maximum speed for 1 minute. Following the extraction of DNA fragments (vector backbones, inserts or PCR products), 100 ng/µl of vector backbone and 10 µl of DNA inserts (5-10 ng) were mixed with 10 µl of 2X RLB and 1 µl of T4 DNA ligase (NEB, cat# M0202L) and the mixture was then incubated at room temperature for 20 minutes to ligate the insert into vector backbones. The ligation mixture was transformed into XL1-Blue *E.coli* to amplify the newly-ligated plasmid. After isolation of newly-ligated plasmids from XL1-Blue *E.coli*, the plasmids were screened for right insert using appropriate restriction

endonucleases. For example, as shown in Figure 1, plasmid C were digested with KpnI/XhoI in Buffer 4 overnight and run on agarose to screen for hMOB1 insert. The constructed plasmids were then sent for sequencing. 5 µl (100 µg/µl) of DNA and 5 µl (5 nmol) of necessary primers were sent for sequencing by SourceBioscience. For sequence analysis, the sequence results sent by SourceBioscience were blasted with corresponding cDNA sequence using ClustalW2 program.

2.2.1.7. Standard Polymerase Chain Reaction (PCR)

PCR is a most commonly used method in molecular biology as a tool of amplifying a single or several copies of a piece of DNA. PCR can be used to integrate specific restriction digestion sides to generate new multiple cloning sides in plasmid DNA. Briefly, all standard PCRs were performed as pointed in **Table 2.2**.

Table 2.2. Standard PCR reaction mix

Reagent	**Volume per reaction**
36 µl	Autoclaved ddH2O
5 µl	10 x buffer
5 µl	2.5mM dNTPs
1 ul	template (at 100 ng/µl)
1 µl	Forward primer (100 µM)
1 µl	Reverse primer (100 µM)
1 µl	*Pfu* DNA polymerase (2.5 U/µl)

PCR procedure consists of 3 main steps including denaturation, annealing, and extension, as pointed in

Table 2.3. *Pfu* PCR cycles*

Step	Temperature	Time	Description
Denaturation	98 ^{o}C	1 minute	dsDNA is exposed to high temperature, leading dsDNA to melt by disrupting the hydrogen bonds between complementary bases, thus generating single-stranded DNA.
Annealing	55 ^{o}C	1 minute	The temperature is reduced to 55 ^{0}C to enable the primers to anneal specifically and bind to the ssDNA. The temperature might differ according to primers. The best annealing temperature can be checked at http://tmcalculator.neb.com/#!/.
Extension	72 ^{o}C	2 minute per kb of template	DNA polymerases generate new DNA complementary to DNA template by adding the dNTPs to complementary base pairs on ssDNA.

***The temperature for Denaturation, Annealing, and Extension may vary according to the different enzymes. This PCR cycle is only for *Pfu* enzymes**

2.2.1.8. Site-directed PCR mutagenesis

Site-directed PCR mutagenesis is an *in vitro* molecular biology technique which introduces specific mutations into a vector at a particular position. All mutations created in this project were generated on pcDNA3.1- based plasmids and the mutant versions of cDNAs were then subcloned into other plasmids as specified. All site-directed mutagenesis were performed as pointed in **Table 2.2.**

Following the standard PCR procedure, 1 µl of *DpnI* enzyme (20 U/µl) were added to PCR products, mixed thoroughly and incubated for 2 hours at 37 ^{o}C to eliminate methylated DNA templates and select for newly-generated DNA including the desired mutation. 10 µl of *DpnI*-digested PCR products were then loaded on the corresponding percentage of agarose gel and subjected to electrophoresis at 80 V for 1 hour to detect the presence of the mutated DNA, as all non-mutated DNAs were digested and eliminated by *DpnI* enzyme. Ultimately, PCR products were transformed into *E.coli* competent cells **(Section 2.2.1.2),** and miniprep DNAs were prepared for the analysis of single clones **(Section 2.2.1.3.1)**. Full length of coding region was sequenced and analysed to confirm the desired mutations, as described in **Section 2.2.1.6**.

2.2.1.9. DNA vectors

2.2.1.9.1. Plasmids used for cloning and expression of hMOB1A variants, NDR1/2, MST1/2 and LATS1/2 cDNAs in COS-7 cells and HEK293 cells

All human NDR1/2, MST1/2, LATS2 and MOB1A cDNAs were subcloned into pcDNA3 and pcDNA3 derivatives containing a hemagglutinin(HA) or myc epitope using BamHI/XhoI restriction sites as described (Hergovich, Bichsel et al. 2005). Human LATS1 was subcloned into pcDNA3 containing a hemagglutinin (HA) epitope as described (Hergovich, Schmitz et al. 2006). All mutants of MOB1A were generated by PCR-based mutagenesis using pcDNA3-myc-hMOB1A(wt) as a template as outlined in s**ection 2.2.1.8**. The generated hMOB1A plasmids **(Figure 2.1)** were used for transient expressions in COS-7 and HEK-293 cells.

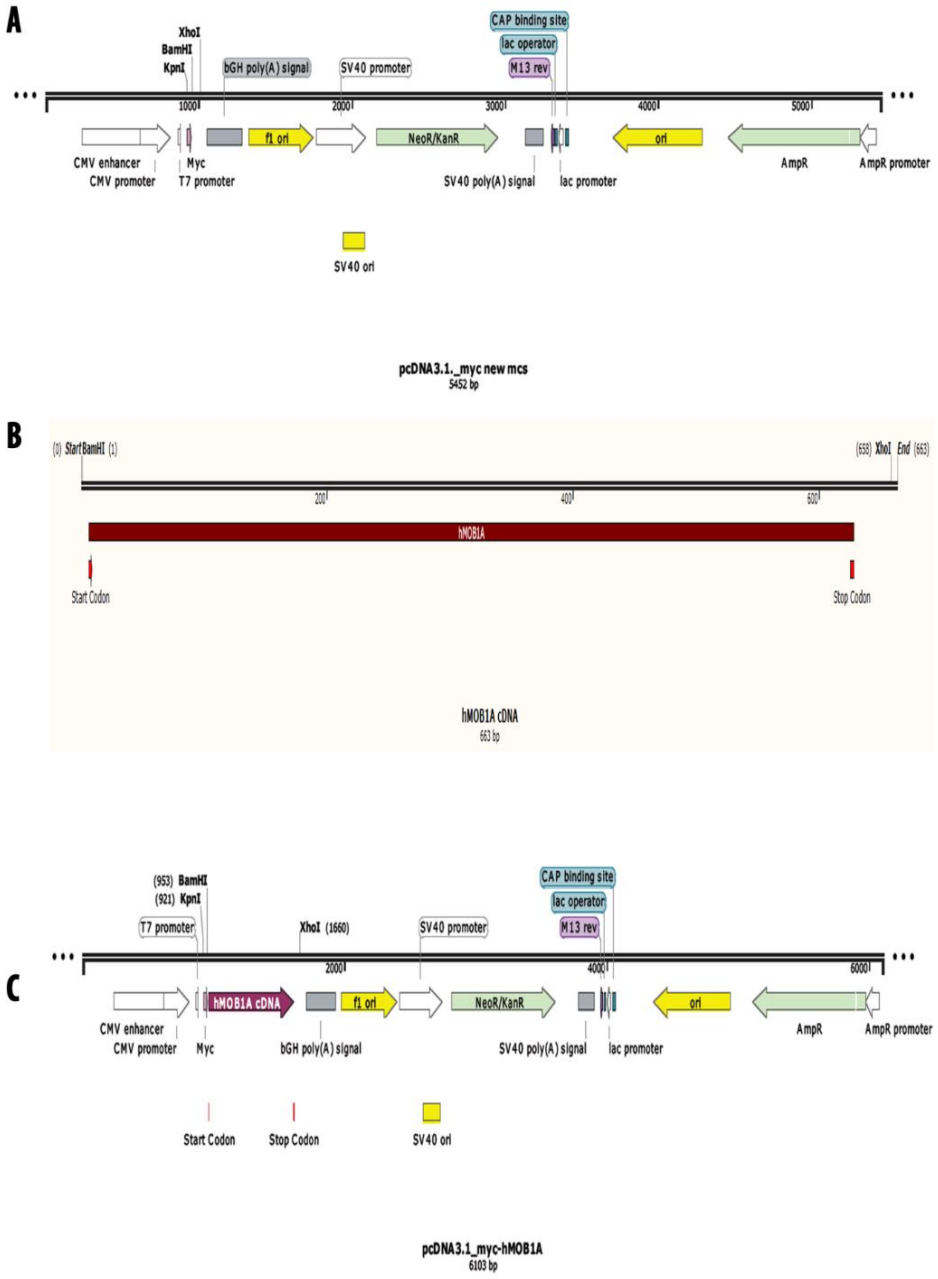

Figure 2.1. Cloning of MOB1A into pcDNA3.1_myc.

A (backbone) and **B** (insert) were digested with BamHI and XhoI restriction enzymes and **B** was ligated into **A** to generate pcDNA3.1_myc-MOB1A **(C)**. Plasmid C was used as a template to generate all MOB1A mutant versions. This figure is for representative purpose only. All plasmids are circular.

2.2.1.9.3. Plasmids used for cloning and transient expression of hMOB1A variants, Mats, Hpo, Warts and Trc cDNAs in S2R+ Drosophila cells

All fly Mats, Hpo, Trc and human MOB1A cDNAs were subcloned into pENTR-3C plasmids using KpnI/XhoI restriction sides. Fly Warts was subcloned into pENTR-3C using KpnI/NotI restriction sides. Following the construction of pENTR-3C-based plasmids, Gateway LR reactions were performed between pENTR-3C-based plasmids and pAW plasmid (destination plasmid). Gateway LR reactions are based on the recombination of ENTRY clone including attL sides with destination vector including attR sides, which results in the insertion of gene of interest placed in ENTRY clone between attL1 and attL2 into destination vector. The generated plasmids (**Figures 2.2 and 2.3**) were used for transient expression in *Drosophila* S2R+ cells**.**

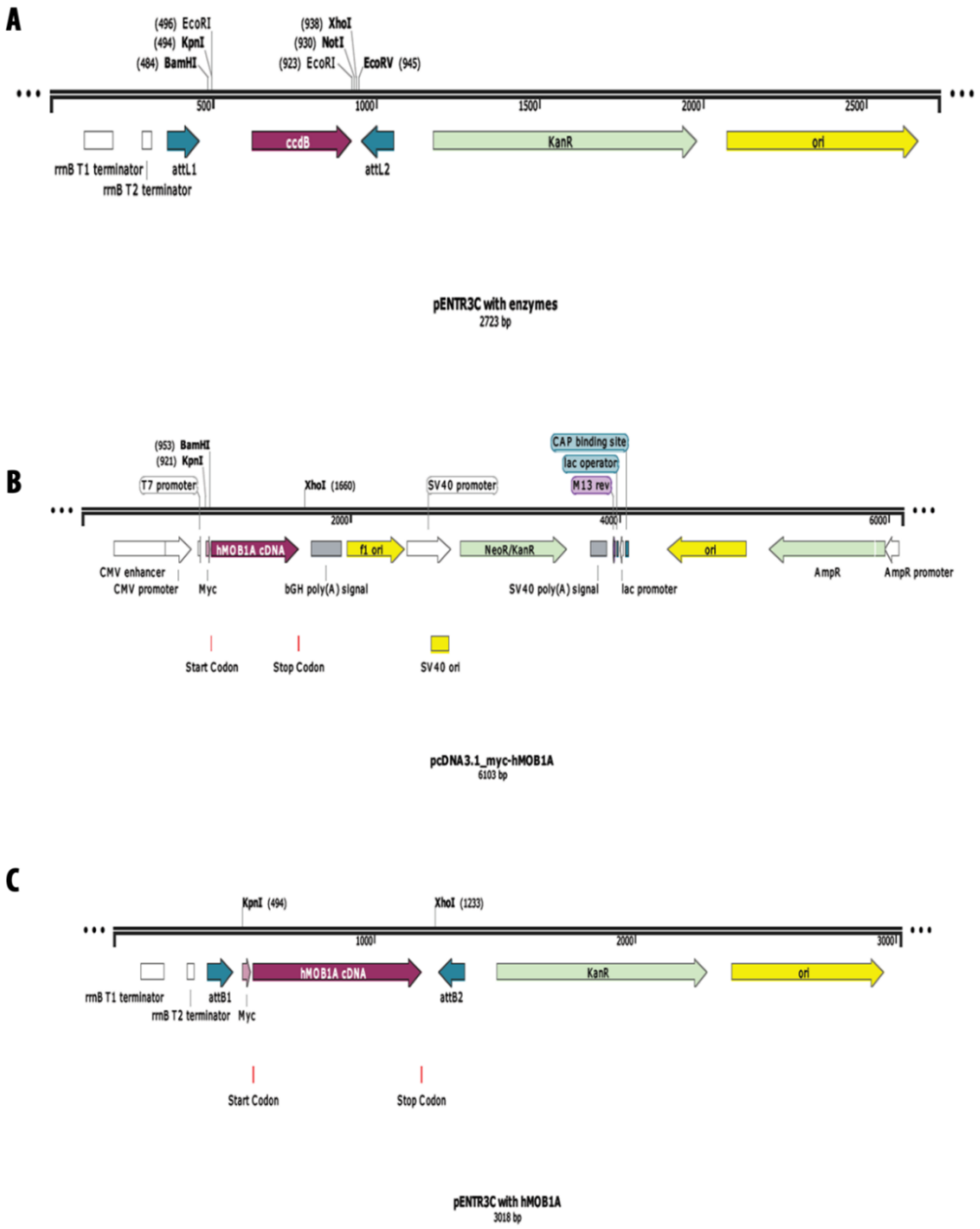

Figure 2.2. The cloning of myc-MOB1A cDNAs, *Drosophila* myc-Mats, HA-Hpo, HA-Trc, HA-Warts into pENTR3C.

Plasmid **A** and Plasmid **B** were digested with KpnI and XhoI restriction enzymes. The insert isolated from plasmid **B** were then ligated into plasmid **A**, resulting in Plasmid **C.** *Drosophila* Mats cDNA, Hpo, Trc and MOB1A mutant versions were generated with the same procedure. *Drosophila* Wts were subcloned into pENTR3C using KpnI/NotI restriction enzymes. The figure only shows MOB1A cDNA as an insert. This also applies to MOB1A mutant cDNAs, *Drosophila* myc-Mats, HA-Hpo, HA-Trc, HA-Wts. This figure is for representative purpose only. All plasmids are circular.

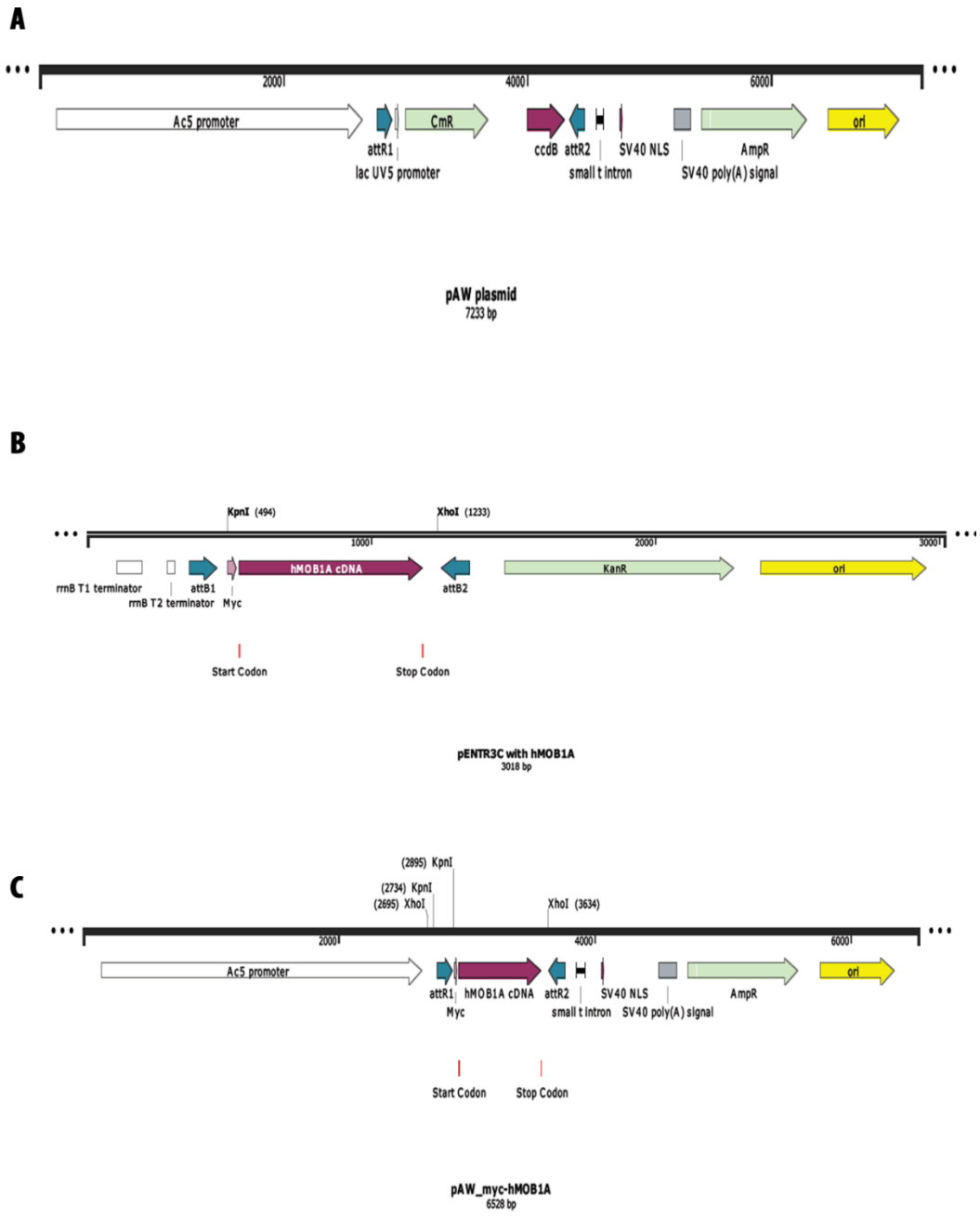

Figure 2.3. The cloning of myc-MOB1A cDNAs, *Drosophila* myc-Mats, HA-Hpo, HA-Trc, HA-Wts into pAW.

Gateway LR reaction were performed between plasmid **A** and **B**, resulting in plasmid **C**. The figure only shows MOB1A cDNA as an insert. This also applies to hMOB1A mutant cDNAs, *drosophila* myc-Mats, HA-Hpo, HA-Trc, HA-Warts. This figure is for representative purpose only. All plasmids are circular.

2.2.1.9.4. Plasmids used for cloning and stable expression of MOB1A cDNAs in MCF-7

All human MOB1A variants were subcloned into pCMV(R)neo_new MCS retroviral plasmids using PmeI/XhoI restriction sides. Also, all human MOB1A variants were subcloned into pENTR plasmids using KpnI/XhoI restriction sides, which were then subcloned into pLEX lentiviral plasmids using Gateway LR Reaction approach. The generated plasmids were used for stable expression of tagged MOB1A variants in MCF-7.

2.2.1.9.5. Plasmids used for cloning and recombinant protein production of MOB1A cDNAs in *E.coli* (BL21)

All human MOB1A variants were subcloned into pMAL-c2 (NEB) using BamHI/SalI restriction sides. The generated plasmids **(Figure 2.4)** were used for protein production in BL21 DE3 *E.coli*, and the purified recombinant proteins were subsequently used in kinase assays.

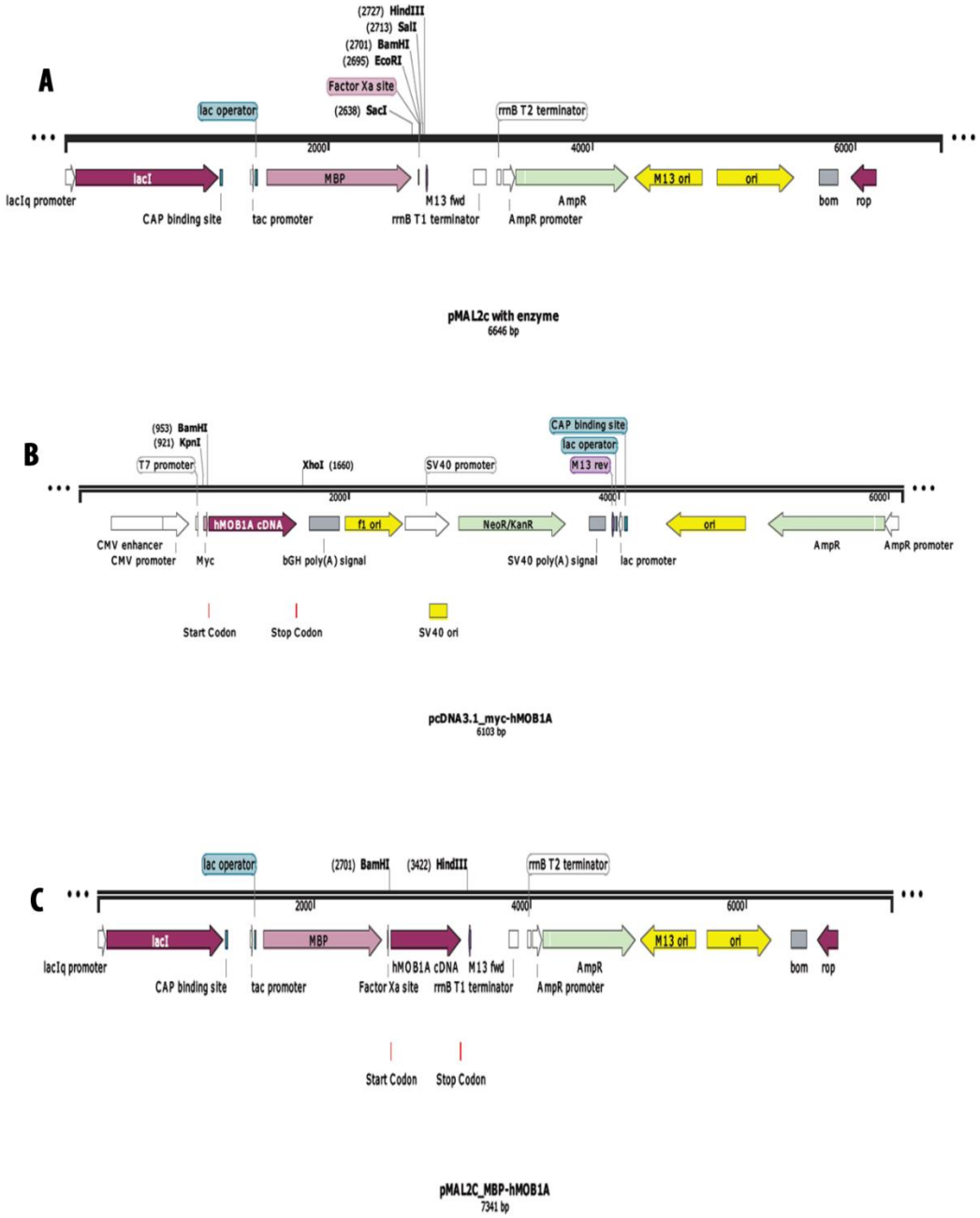

Figure 2.4. The cloning of MOB1A cDNAs into pMAL-2C.

Plasmid **A** and **B** were digested with BamHI/SalI and BamHI/XhoI, respectively. Then, the insert isolated from plasmid **B** were ligated into plasmid **A**, resulting in plasmid **C**. The figure only shows MOB1A cDNA as an insert. This also applies to MOB1A mutant cDNAs. This figure is for representative purpose only. All plasmids are circular.

2.2.1.9.6. Plasmids used for the generation transgenic flies expressing fly selected MOB1A variants in *D. Melanogaster*

All pENTR-3C-based plasmids of human MOB1A variants **(Figure 2.2)** were inserted into pKC26w pUbiq plasmids using Gateway LR reaction. All the generated plasmids **(Figure 2.5)** were screened for MOB1A inserts using KpnI/XhoI enzymes **(see section 2.1.6)**. After confirming the inserts, the identity of gene of interest was verified by sequencing using pUbiq and SV40 primers **(see section 2.2.1.6)**. Ultimately, the generated plasmids were expressed in S2R+ cells using Effectene Transfection **(See section 2.2.3.4.2)**, confirming the functionality of promoters. The generated plasmids were sent to BestGene Inc to generate transgenic *Drosophila* manipulating human MOB1A variants **(Figure 2.5) (More information can be found in section 2.2.5)**.

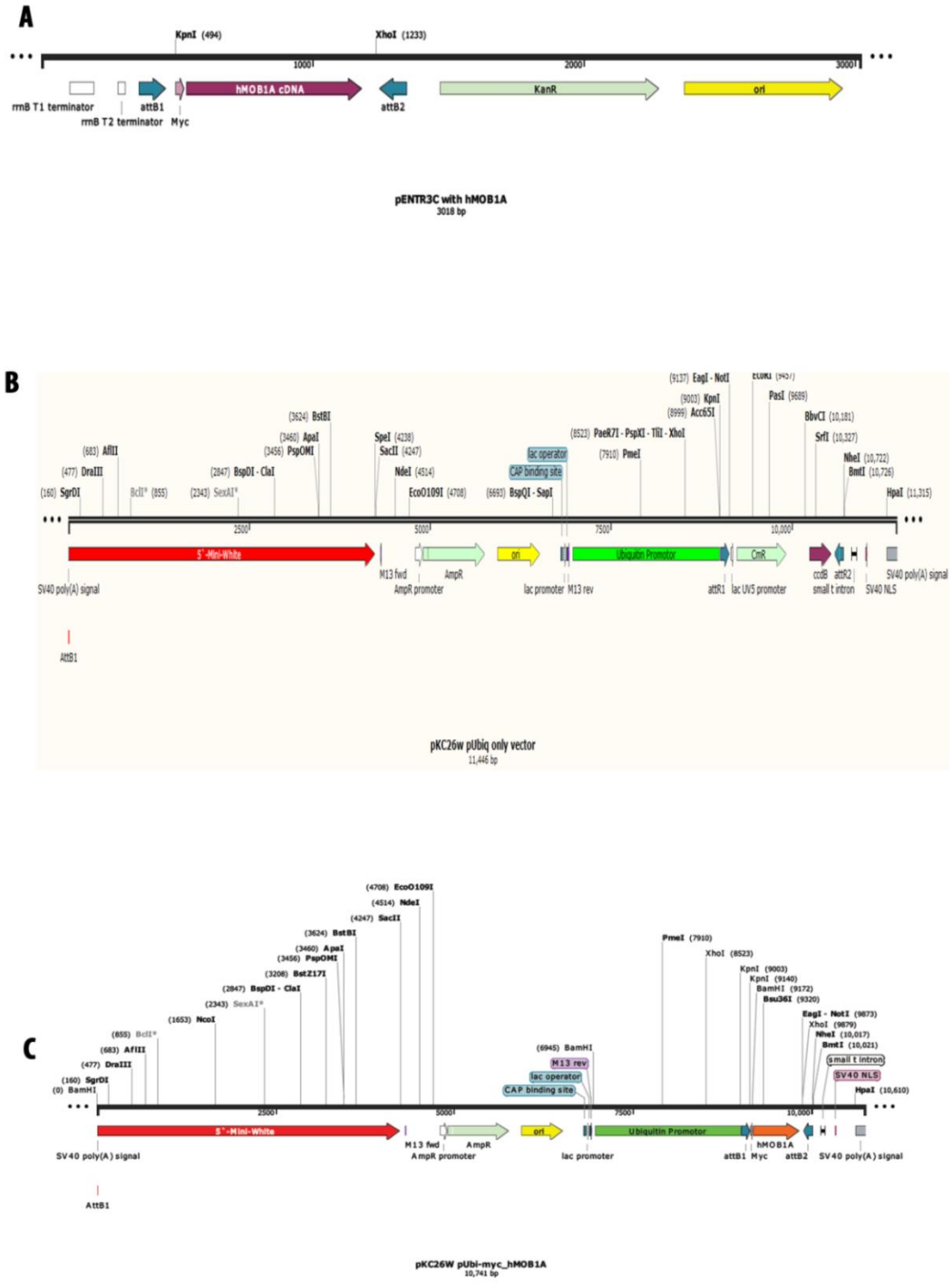

Figure 2.5. The cloning of MOB1A cDNAs into PKC26W pUbi.

Gateway LR reaction were performed between plasmid **A** and **B**, resulting in plasmid **C**. The figure only shows MOB1A cDNA as an insert. This also applies to MOB1A mutant cDNAs. This figure is for representative purpose only. All plasmids are circular.

2.2.2. Biochemistry methods

2.2.2.1. Cell lysis for protein extraction

Cells were gently washed with ice-cold PBS -Ca/-Mg, ice-cold 150 mM lysis buffer or MILB buffer was then added, which were subsequently followed by collecting cells in the lysis buffer using policeman scrapper. The cells were then transferred into pre-chilled 1.5 eppendorf tubes and incubated for 30 minutes on ice. After the incubation, the eppendorf tubes were centrifuged at 25,000 x g for 10 minutes at 4 ^{o}C, before supernatants were transferred into fresh-labelled eppendorf tubes on ice. The supernatants containing the cell lysate were used for either western blot analysis or processing as required (co-IP, Kinase assay).

2.2.2.2. Determination of protein concentrations using Bradford assay

Protein concentrations were determined by Spectrophotometer using Bradford assay. Briefly, Bradford reagent (Bio-Rad) was diluted in 1:5 ratio with distilled water. 5 µl of protein lysate or lysis buffer was mixed with 1 ml of the diluted Bradford reagent in spectrophotometer cuvettes, which were then measured at 595nm in spectrophotometer.

2.2.2.3. Preparation of Protein A-sepharose

Protein A-Sepharose CL-4B (1.5 g) (Fisher UK - GE Healthcare, cat#17-0780-01) was incubated overnight with 50 ml autoclaved ddH_2O at 4C on roller shaker. The following day, the beads were spun down by centrifugation at 1,100 x g for 4 minutes at 4C. Then, the supernatant was removed without touching the beads, before being washed twice with ddH_2O and with PBS minus, respectively. After washing the beads with PBS minus, they were transferred into 15 ml falcon tubes, which were in turn washed once with PBS minus, followed by centrifugation at 4 ^{o}C for 2 min at 1,100 x g and PBS minus was removed. Lastly, 3 ml PBS minus, 2 ml ethanol and 100 µl Na-Azide were added into 5 ml swollen beads to obtain slurry of 50% sepharose A beads, which was stored at 4 ^{o}C.

2.2.2.4. Anti-HA 12CA5 antibody coupling with Protein A-sepharose

To covalently couple anti-HA 12CA5 antibody with protein A-sepharose, anti-HA 12CA5 hybridoma supernatant (provided by the Hergovich Labaratory) was incubated with protein A-sepharose at 4 ^{o}C in 1 ml 10% NP-40 solution. Next day, beads were washed two times with PBS minus and three times with 0.2 M Na-Borate (pH: 9.0). 51.8 mg of dimethyl pimelimidate.2 HCL (DMP, from Fisher UK – Pierce, cat# PN21667) dissolved in 5 ml 0.2 M Na-Borate (pH: 9.0) was then added to antibody-beads slurry and incubated for at least 1 hour at room temperature. After the incubation, beads were washed twice with 0.2 M ethanolamine (pH: 8.0) and incubated for 3-4 hours at room temperature with 10 ml 0.2 M ethanolamine (pH: 8.0). Following the incubation, beads were washed twice with PBS minus and were kept at 4 ^{o}C in PBS minus containing 0.2% Na-Azide.

2.2.2.5. Co-immunoprecipitation (Co-IP)

Co-IP is a commonly used approach to study protein-protein interactions. In our studies, DNA sequences coding for short peptide tags, namely HA- and myc-tags, were inserted into N-terminus of our proteins of interest. After manipulation of the genes of interest in HEK293 cells, protein extracts were prepared in MILB buffer as described in **Section 2.2.2.1**. After preparation of protein extracts, 20 µl of the input lysate were collected into new tubes for equal loading, followed by denaturating at 95 ^{o}C with appropriate amount of Laemmli buffer. The remaining protein extracts were subjected to pre-clearing to remove unspecific binding to HA-beads. In the pre-clearing step, the protein lysate was incubated with Protein-A sepharose for 1 hour, rolling at 4 ^{o}C. After the incubation, the protein extract-Protein-A sepharose mixture was centrifuged at 25,000 x g at 4C for 1 minute. The supernatant was then transferred into pre-chilled tubes containing protein A sepharose coupled to anti-HA 12CA5 antibody **(see section 2.2.2.4)**, which were in turn incubated rolling overnight at 4 ^{o}C. The following day, the protein extract- anti-HA 12CA5 mixture was centrifuged at 25,000 x g for 30 seconds. After centrifugation, supernatant was removed without touching

the beads. The beads were then washed 3 times with MILB lysis buffer containing benzamidine, DTT, leupeptin and PMSF, before being denaturated at 95 ^{o}C with 20 µl of laemmli buffer.

2.2.2.6. Production of recombinant MAL-MOB1A variants

All pMAL-c2-based plasmids **(see Figure 2.4)** were re-transformed into BL21 DE3 *E.coli* as described in **Section 2.2.1.2**. The following day, one single colony was inoculated and incubated in 3 ml LB medium containing ampicillin for 8 hours at 37 ^{o}C with vigorous shaking. After 8 hours, the cultures were diluted in 100 ml LB medium containing ampicillin **(see section 2.1.3)** and were then incubated overnight at 37 ^{o}C with vigorous shaking. The following day, the cultures were again diluted in LB medium at a 1:10 ratio and then incubated for 1 hour, before IPTG (100 µM) **(see section 2.1.3)** was added and bacteria were incubated for another 3 hours at 37 ^{o}C. After 3 hours, the cultures were spin down by centrifugation at 1,400 x g for 10 minute, followed by processing each 1 litre culture with 50 ml lysis buffer. The suspension was then sonicated at 70% amplitude (Sonics Vibra Cell^{TM}, model:VCx 130), and the supernatant was clarified by filtration (40 µm cell strainer) before adding 2 ml amylose-resin (Biolabs, cat# E8021L), before the incubation overnight, rolling at 4C. The following day, protein-amylose resin mix were collected in yellow Bio-Rad columns (Bio-Rad, cat#737-4152) and washed with 20 ml 0.2 M Column Buffer, 10 ml 1M Column Buffer, 20 ml 0.2M Column Buffer. After the washing step, the elution of MAL bound proteins were performed in 2 ml maltose-containing buffer, followed by dialysis of eluted proteins overnight with 20 mM Tris pH 7.5 buffers. As a final step, 10% of glycerol was mixed with the collected proteins and the amount of proteins were analysed by SDS-PAGE running 1 µl, 5 µl and 10 µl of the purified proteins versus 0.1 µg, 0.5 µg, 1 µg and 2 µg of BSA.

Coomassie Staining and LiCor scan (680nM) were performed to quantify proteins. Briefly, LiCor macnine was used to scan acrylamide gel with the setting 700: 5; 800: 5 by including 100ng/500ng/1ug/5ug BSA as a reference. The quantified proteins were then stored until further use as a substrate for kinase assay.

2.2.2.6. *In vitro* kinase assays

In vitro kinase assays were used to identify phosphorylation status of MOB1A variants as MST1/2 (Hpo) substrate. In our project, two different approaches were used to identify the phosphorylation status: **(1)** Radioactive *in vitro* kinase assay and **(2)**, anti-phospho-antibody-based *in vitro* kinase assay. First approach is based on transferring a radioactive phosphate group from ATP to a substrate via [γ-^{32}P]-ATP (Hartmann Analytic, cat# SRP-301). The second approach is based on anti-phospho antibodies which are specific to human MOB1A proteins, which are phospho-MOB1A (Thr12) and phospho-MOB1A (Thr35).

In radioactive *in vitro* kinase assays, bacterially expressed and purified MAL- hMOB1A variants (kindly provided by Belul Assefa Shifa) were mixed with MST1 kinase buffer (50mM Tris,pH:7.5, 25 mM beta-glycerophosphatase, 10 mM EGTA,pH:8.0, 10 mM Na3VO4, 40 mM MgCI2, 0.1 mM DTT). The mixture was then resuspended in 10 µl kinase buffer including 200 µM [ϒ-32P] ATP, 20 ng/µl GST-MST1 (Sigma, cat# M9697) or GST-MST2 (Sigma, cat# S6573) (recombinant kinases expressed in insect cells; purchased from Sigma). After 30 min incubation at 30 ^{o}C, reactions were stopped with 20 µl SDS-Laemmli buffer, and samples were separated by SDS-PAGE, gels dried and finally analysed by autoradiography.

In anti-phospho-antibody-based *in vitro* kinase assays, we checked how hMOB1A mutants at Thr12 and Thr35 sites behave as substrate for both MST1/2 and Hpo using recombinant MOB1As, MST1/2 and S2R+-expressed HA-Hpo. To check the phosphorylation status of hMOB1A mutants by MST1/2, 500 ng of the bacterially expressed and purified MAL-MOB1A variants and 1× MST1/2 kinase assay buffer were mixed in a pre-chilled eppendorf tubes to a total volume of 10 µl. 1 µl of 10x kinase assay buffer and 2 µl of 2 mM ATP stock (f.c.200 µM ATP) were added to the mixture, before adding 500 ng of the bacterially expressed and purified GST-MST1 and GST-MST2 and 4.5 µl of ddH2O. KMM **(see section 2.1.3)** were finally added to all reactions, which were then incubated for 30 minutes at 30 ^{o}C. After 30 minutes, all reactions were stopped by adding 20

µl of laemmli buffer and then were separated by SDS-PAGE and analysed by Western Blotting. To check the phosphorylation status of hMOB1A mutants by Hpo, HA-Hpo were transiently expressed in *Drosophila* S2R+ cells using Effectene Transfection **(Section 2.2.3.4.2)** and the transfected cells were lysed and immunoprecipitated with anti-HA 12CA5 antibody as described in **(Section 2.2.2.5)**. After immunoprecipitating with anti-HA 12CA5 antibody**,** the beads were washed twice with 150 mM standard lysis buffer. The beads were then incubated with 1 M lysis buffer for 1 hour, rolling at 4 ^{o}C. After 1 hour incubation, the beads were washed once more with 150 mM lysis buffer and twice with 1x kinase assay buffer, followed by adding 500 ng of the bacterially expressed and purified MAL-MOB1A variants and ddH_2O to give a total volume of 15 µl. KMM were then added to IP-substrate mixture, which were then incubated for 30 minutes at 30 ^{o}C, followed by stopping the reaction with appropriate amount of laemmli buffer. The samples were separated by SDS-PAGE and analysed by western blotting.

2.2.2.8. Separation of proteins by SDS-PAGE

SDS-PAGE is routinely used to separate proteins based on their sizes. After the preparation of different percentage of SDS-PAGE gel **(see Table 2.4)**, gels were clasped into a MINIPROTEAN II electrode assembly and electrophoresis chamber (BIO-RAD). Equal amount of protein samples heat-denatured with Laemmli buffer at 95 ^{o}C for 5 minutes were loaded into the wells alongside pre-stained molecular marker (NEB), which were then run at 80V till samples had passed the stacking gel and reached to the resolving gel. The voltage was then increased to 100 V to run for another 90 minutes. Where appropriate, the gels were then either transferred to PVDF membrane **(Section 2.2.2.9)** or incubated with Coomassie Blue for staining.

Table 2.4. Gel percentage based on protein size (Adapted from Abcam.com)

Protein size	Gel acrylamide percentage
4–40 kDa	20%
12–45 kDa	15%
10–70 kDa	12.5%
15–100 kDa	10%
25–200 kDa	8%

2.2.2.9. Western blotting of SDS polyacrylamide gels

Following the separation of proteins on SDS-PAGE gels, the proteins were then transferred from polyacrylamide gels to PVDF membrane by Western blotting. Briefly, the polyacrylamide gels were soaked in transfer buffer and then placed on top of transfer buffer soaked-Whatman 3MM paper. PVDF membrane were pre-rinsed in methanol for 30 seconds, then washed with transfer buffer, which was subsequently placed on top of polyacrylamide gels, followed by more pre-soaked Whatman 3MM paper. The PVDF-membrane "sandwich" were then placed into electro-blotting apparatus cassette and then immersed in transfer buffer, followed by running at 0.40 A (per tank) for 1 hour alongside with an ice block. After transferring proteins from polyacrylamide PVDF membrane, proteins were direct-stained by Ponceau S staining solution to check the quality of protein transfer.

2.2.2.10. Immunodetection of proteins on Western blot membranes

Following checking the quality of the protein transfer, the blotted membrane was then washed with ddH_2O (2 times), and TBS-T (2 times), before blocking with 5% milk dissolved in TBS-T for at least 30 minutes. The membranes were then incubated overnight with primary antibody diluted in either 5% milk or BSA, rocking at 4 ^{o}C. The following day, the membranes

were washed three times with TBS-T at room temperature (each wash for 10 minutes) to remove any unbound antibodies, before being incubated with horseradish peroxidase-linked secondary antibodies **(see section 2.1.2)** specific to primary antibodies rocking at room temperature for at least 2 hours, followed by washing membranes three times with TBS-T (10 minutes per each wash). Following the washing step, chemiluminescent detection substrates were mixed in 1:1 ration and then added on top of membranes, which were then incubated for at least 30 seconds. Membranes were exposed to a film in the dark room and then developed by using a film processor (Konica Minolta, SRX-101A).

2.2.3. Cell biology methods

2.2.3.1. Tissue cell culture

MCF-7, Cos-7, HEK-293, HEK-293T and PT67 cells were maintained in Dulbecco`s modified Eagle`s medium (Sigma, cat# D6429) supplemented with foetal calf serum (Sigma, Cat no: F7524) to a final concentration of 10%. MCF10A (non-tumoral cell line) were cultured in a DMEM:- Nutrient Mixture F-12 (GIBCO® DMEM/F-12; cat# 11320-033) containing 5% horse serum (Gibco® HS; cat# 16050-122), 20 ng/mL epidermal growth factor (Peprotech EGF; cat# AF-100-15-1000), 0.5 μg/ml hydrocortisone (Sigma; cat# H0888-10G), 0.1 μg/ml cholera toxin (Sigma; cat# C8052-1MG), and 10 μg/ml insulin (Sigma; cat# I1882-100MG). *Drosophila* S2R+ cells were cultured in Schneider`s *Drosophila* Medium (Invitrogen, cat# 217200024) supplemented with heat-inactivated FBS (Invitrogen, cat# 10082147). Cells were grown in the presence of 100 units/ml penicillin (VWR, cat#A1837.0010) and 100 mg/ml streptomycin (VWR, cat# A1852.0025), at 37 ^{o}C with 5% CO_2 except for *Drosophila* S2R+ cells which were incubated at 24 ^{o}C.

2.2.3.2. Passaging of cells

After reaching approximately 80% confluency, cells were split to avoid overcrowding and prevent loss of epithelial morphology. Briefly, cell medium was removed and cells were washed once with PBS minus at 37 ^{o}C.

After removing PBS minus, a 0.25% trypsin/EDTA solution (0.05% trypsin/EDTA for MCF10A cells) were added to detach the cells (1 ml, 3ml and 5 ml of trypsin for 10cm plate, 75cm and 175cm flask, respectively). Briefly, trypsin was added to the cells and then trypsin-cells were incubated at 37 ^{o}C for trypsin to catalyse the reaction. Fresh medium containing serum was then added to the detached cells to neutralize the trypsin reaction, which were centrifuged at 94 x g after transferring the medium-trypsin-cell suspension into a 15 ml tube. After the centrifugation, the supernatant was aspirated and the cell pellet was resuspended in fresh medium. Subsequently, cells were seeded into fresh flasks or dishes at a 1:10 dilution. For S2R+ cells, no trypsin was used, since these cells do not attach to the flask so tightly. For passaging of these cells, cells were resuspended in 10 ml of Schneider medium and seeded into fresh flasks or dishes at a 1:15 dilution.

2.2.3.3. Freezing and thawing of cells

In order to store cell lines for long-term, cells were frozen. Briefly, cells were detached using trypsin/EDTA solution as described in **Section 2.2.3.2**. After the centrifugation, cells were then resuspended in freezing medium instead of complete medium. Then, 1ml of the cell suspension was aliquoted into cryotubes (Sarstedt, cat#72.380.992), which were immediately placed into Mr. Frosty before transferring to -80 ^{o}C. Next day, frozen cells were transferred to liquid nitrogen 2 in tower 10 (boxes 5 to 10).

To thaw frozen cells, cryotubes were taken out from liquid nitrogen and thawed at 37 ^{o}C for 40 seconds, before transferred the content into 15 ml falcon containing 5 ml complete medium. The medium with frozen cells was then spun down by centrifugation at 136 x g for 4 minutes. The cell pellet was resuspended in fresh complete medium and seeded into a flask.

2.2.3.4. Cell transfections

2.2.3.4.1. Fugene 6 transfection

Transient plasmid transfection of Cos-7 and HEK-293 cells was performed using Fugene 6 (Promega, cat# E2692) transfection reagent as outlined by the manufacturer. Briefly, Cos-7 and HEK-293 cells were seeded at a

consistent confluence (1 x 10^6 cells per 10-cm dish) 24 hours prior to transfection. Next day, plasmid DNAs mix was prepared in separate 1.5ml eppendorf tubes. After Fugene 6 and Optimem (Invitrogen, Cat no: 31985-047) had reached room temperature, Fugene 6 was diluted in 500 µl of Optimem. Following incubation of the Fugene-Optimem mixture for 5 minutes at room temperatures, the plasmid DNA mixture was added to the Fugene-Optimem mixture, which were then incubated for another 40 minutes at room temperature. Following 40 minutes incubation, the transfection complex was added to cells and the cells were incubated overnight at 37 ^oC. The following day, transiently transfected cells were processed as required.

2.2.3.4.2. Effectene transfection

Transient plasmid transfection of *Drosophila* S2R+ cells was mediated through Effectene (Qiagen, cat# 301425). Namely, 1.2 x 10^6 cells were seeded per well (6-well plate) 24 hours prior to transfection. On the day of transfection, appropriate amount of DNAs was added into 1.5ml ependorf tubes, followed by the addition of 150 µl of Buffer EC. The appropriate amount of Enhancer (the ratio of DNA to Enhancer was 1:8) was added and mixed by vortexing for 10 seconds. After incubating for 2-5 minutes at room temperature and brief centrifugation to collect drops from the top of the tube, 10 µl of Effectene was added to the DNA-Enhancer mixture. After vortexing for 10 seconds, the Effectene-DNA-Enhancer mixture was incubated for 30 minutes to allow transfection complex formation. Then, 500 µl of fresh Schneider`s *Drosophila* Medium were added to the transfection complex, and subsequently added onto cells. After 48 hours, the cells were processed as required.

2.2.3.5. Cell infection

2.2.3.5.1. Retroviral infection

To generate retroviral pools, transfection of the packaging cell line PT-67 (Clontech, Alto, CA) was mediated through the Lipofectamine 2000 transfection reagent (Life Technology, cat#11668-019). Briefly, 2 x 10^6 of PT67 cells were seed per 10cm plate 24 hours prior to transfection. On the

day of transfection, two sets of 2 ml eppendorf tubes were prepared. 30 µl of Lipofectamine 2000 was added into the first set of tubes containing 720 µl of pre-warmed Optimem, which were then mixed by continuous gentle inversion for 30 seconds, followed by incubation for 5 minutes at room temperature. In the meantime, 12 µg of plasmid DNA were mixed with Optimem to give a total volume of 750 µl. The DNA-Optimem mixture was added to the Lipofectamine 2000-Optimem mixture, which were then mixed by continuous gentle inversion and incubated for 30 minutes at room temperature to allow transfection complex formation. In the meantime, the medium of the cells was replaced with 5 ml fresh DMEM containing 10% tet-free FCS (Invitrogen, cat#26140079) without Pen-Strep. After 30 minutes incubation, the transfection complex was centrifuged briefly and added to the PT67 cells. 4 to 6 hours (preferentially 6 hours) after adding the DNA/Lipofectamine/Optimem, the medium was aspirated and replaced with fresh 6 ml medium DMEM containing 10% tet-free FCS without Pen-Strep, followed by incubation at 37 ^{o}C overnight. After 24 hours, supernatants were collected, filtered through a 0.45 µm filter (Sarstedt, cat#83.1826) in the presence of 0.8 µg/ml polybrene and subsequently added to 5 x 10^6 target cells for infection. After 2 days, the infected cells were selected by treatments with appropriate antibiotics. Stable cell pools of target cells were maintained in media supplemented with appropriate antibiotics **(see section 2.1.3)**.

2.2.3.5.2. Lentiviral Infection

To quickly generate cell lines stably expressing transgenes of interest, a lentiviral approach was used by transfecting HEK-293T cells with PEI transfection reagent (Polysciences, Inc, cat# 23966-2). 10 x 10^6 of HEK-293T cells were seeded per 10cm plate 4 hours prior to transfection. The following plasmids were mixed per 1.5 ml eppendorf tube:

Table 2. 5

	ratio	µg
pMD.G	1	2.4
p8.91	0.3	0.8
lentiviral vector	6	4.8

After mixing the DNAs in Eppendorf tubes, 800 µl of pre-warmed Optimem and 32 µl of PEI were added in a specific order, followed by continuous gentle inversion and then incubated for 30 minutes at room temperature. After the incubation, the transfection complex was added to HEK-293T cells. The cells were then incubated overnight at 37 ^{o}C. The following day, the medium of the cells was replaced with 5 ml fresh medium. In parallel, 1 x 10^{6} of target cells were seeded per 10 cm plate. The next day, virus containing supernatants were collected from the transfected HEK-293T cells, filtered through a 0.45µm filter (Nalgene) in the presence of 0.8 µg/ml polybrene and added onto the target cells after removing the medium of target cells. 24 hours later, the infected cells were selected by treatments with appropriate antibiotics **(see section 2.1.3)**. Stable cell pools of target cells were maintained in media supplemented with appropriate antibiotics.

2.2.3.6. Proliferation and colony formation assays

For cell proliferation analysis, cells were seeded at defined densities (5 x 10^{4} cells per well) in triplicates in 12-well plates, followed by non-invasive IncuCyte live cell imaging (Essen BioScience) to measure the kinetics of cell growth/proliferation based on area (confluence) metrics. Phase-contrast images were continuously collected on IncuCyte ZOOM (Essen BioScience) for at least one week. A specific processing definition (Phase-contrast processing module) was applied to count objects (cells) for the duration of the assay. The Phase object area was expressed as relative cell confluency for each well at each time point and subsequently exported into GraphPad (Prism Software) for final analysis. To evaluate colony formation, 1,000 cells were seeded per well (6-well format). After 8-12 days, colonies were fixed with methanol/acidic acid (3:1) for 5 minutes at room

temperature, stained with 0.5% (w/v) crystal violet for 15 minutes at room temperature, washed with water and finally scanned using the G:BOX HR gel documentation system (Syngene, cat# LCI-700-090R). Colonies composed of at least 50 cells were scored as positive.

2.2.3.7. Soft agar assays for anchorage-independent growth.

After trypsinization, cells were passed 4-5 times through a 21G syringe, before 1 x 10^4 cells were resuspended in complete medium (DMEM containing 10% FBS and appropriate antibiotics) with 0.6% agarose (Thermo Fisher Scientific, cat#16520050), and subsequently cultured in wells (6-well format) underlaid by a layer of 1% agarose in complete medium and overlaid with complete medium without agarose. Top layer media were replenished every 72 hours. After three weeks, colonies were stained with 2.5 mg/ml thiazolyl blue tetrazolium blue (MTT, Sigma, cat#M2128), scanned, and quantified. Cell clusters of at least 50 cells were scored as colonies.

2.2.4. Structural Studies Methods (performed in collaboration with the Wu Laboratory)

2.2.4.1. Protein expression and purification for structural and biochemical analyses.

cDNAs encoding human MOB1A (residues 33-216), NDR2 (residues 25-88), human LATS1 (residues 618-697 or 640-703), human MST2 (residues 2-392 or 2-308) were subcloned into a modified pET28a vector (Novagen), which were used to express N-terminally 6×His tagged proteins in the *E. coli* strain BL21 DE3. Bacteria carrying pET28a plasmids were grown at 37 ºC until they reached an optical density of 0.6 to 1.0 at 600 nm. Protein expression was induced by addition of 0.2 mM IPTG and cultures were incubated at 16 ºC for additional 12 to 16 hours. After cell lysis with a cell homogenizer (JNBIO) in lysis buffer (25 mM Tris pH 8.0, 300 mM NaCl, and 20 mM imidazole), followed by centrifugation, supernatants were subjected to Ni^{2+}-NTA affinity chromatography (Qiagen) as described by

the manufacturer. To form crystals of the MOB1A/NDR2 complex, NDR2 (25-88) and MOB1A (33-216) proteins were incubated at an 1:1 molar ratio at 4 °C in assembly buffer (20 mM Tris pH 8.0, 200 mM NaCl, and 5 mM DTT), prior to loading onto a HiLoad 16/60 Superdex 200 gel filtration column (GE Healthcare). Peak fractions were combined and concentrated to 10 to 15 mg/ml for crystallization experiments. Purified MOB1A (33-216) was phosphorylated as follows: in a total volume of 10 ml MOB1A (1 mg/ml) was incubated with MST2 (2-308, 0.002 mg/ml) at 30ºC for 90 minutes in phosphorylation buffer (40 mM Tris pH 7.5, 10 mM $MgCl_2$, 5 mM DTT, and 0.2 mM ATP). Completion of the phosphorylation reaction was verified by the shift of the MOB1A band in non-denaturing gel electrophoresis conditions (data not shown).

2.2.4.2. Crystallization and data collection.

Crystals of MOB1A (33-216) bound to NDR2 (25-88) were grown at 14C in crystallization buffer (17% PEG 3350, 0.1 M HEPES pH 7.5, and 150 mM magnesium chloride) by the hanging drop vapor diffusion method. Crystals were transferred to the crystallization buffer supplemented with 25% glycerol before freezing. Using an ADSC Quantum 315r CCD area detector an X-ray diffraction dataset at 2.10 Å was collected at the beamline BL17U1 at Shanghai Synchrotron Radiation Facility (Shanghai, China). Diffraction data were processed with the HKL2000 software (Otwinowski and Minor 1997).

2.2.4.3. Structure determination, refinement and molecular graphics.

The crystal belonged to the space group $P2_12_12_1$ and contained two MOB1A (33-216)–NDR2 (25-88) complexes in each asymmetric unit. MOB1 (33-216) molecules in the complex were located by the molecular replacement method with the CCP4 program Phaser (Mccoy, Grosse-Kunstleve et al. 2007)} using the published (Stavridi, Harris et al. 2003) structure of MOB1A (33-216) alone (PDB code: 1PI1) as the searching model. The model of the NDR2 (25-88) fragment was built manually with Coot (Emsley and Cowtan 2004). After refinement by the CCP4 program REFMAC5

(Winn 2003), the R_{work} and R_{free} factors were 15.3% and 24.4%, respectively. The quality of the final structure was verified by the CCP4 program PROCHECK (Laskowski, Macarthur et al. 1993), revealing good stereochemistry according to the Ramachandran plot (99.0%, 0.6%, and 0.4% for favored, allowed, and disallowed regions, respectively). The final models include residues 33-212 and 33-216 of MOB1A for chains A and B, respectively, and residues 25-85 and 25-87 of NDR2 for chains C and D, respectively. All figures displaying protein structures were generated with PyMOL (http://www.pymol.org). Sequence conservation of MOB1 mapped onto the surface of its crystal structure was generated by the ConSurf server (Landau, Mayrose et al. 2005).

2.2.4.4. Gel filtration chromatography.

Full-length MOB1A wild-type, D63V or K104E/K104E cDNAs were subcloned into the pET28a vector, expressed in bacteria and subsequently purified as described above for MOB1A (33-216). Purified full-length MOB1 proteins were incubated with NDR2 (25-88), LATS1 (618-697), or MST2 (2-392) protein at 4 ^{o}C for 20 minutes in assembly buffer, before the protein mixtures were loaded onto a HiLoad 16/60 Superdex 200 gel filtration chromatography column (GE Healthcare) and 1.4 ml fractions were collected. Samples from selected Superdex 200 fractions were analyzed by SDS-PAGE and Coomassie Blue staining. For the complex formation assay between MOB1A and LATS1, MOB1A protein was in vitro phosphorylated by MST2 (2-308) as described above before incubation with LATS1 (618-697).

2.2.5. Fly genetics

General Fly Husbandry

Flies were maintained in vials of standard fly food media. Generally, genetic crosses were performed using 5 virgin females and 3 males.

Fly food recipe (18L)

12600 ml H_2O

270g Agar

900g Sugar

3387 ml Extra water

540ml Nipagin

54 ml Propionic Acid

1800g Yeast

2.2.5.1. Generation of transgenic *D. melanogaster*

To generate transgenic flies expressing human MOB1A cDNAs, a full length of cDNAs of human MOB1A variants were subcloned into pKC26w pUBIQ plasmids as shown in **Figure 2.5**. The identities of our gene variants of interest were verified by sequencing using pUbiq and SV40 primers. The plasmids were transiently expressed in S2R+ cells using Effectene Transfection reagent **(see Section 2.2.3.4.2)**, confirming the functionality of promoters. The cloned plasmids were then sent to Best Gene (BestGene Inc 2140 Grand Ave., Suite#205 Chino Hills, CA 91709 U.S.A.) for injection into the germline of fly embryos carrying an attP site inserted at cytological location 89E11 (Bloomington stock number 9744; FlyBase ID: FBst0009744) for insertion into the *Drosophila* genome using the ΦC31 integrase system.

Site-specific integration using the *Streptomyces* phage ΦC31 integrase has been developed and subsequently applied to *D. melanogaster* system (Groth, Fish et al. 2004). Unlike a transposase, ΦC31 integrase mediates a sequence-specific recombination in which it catalyses the recombination between an engineered "docking" site, a phage attachment site (attP), in the fly genome, and a bacterial attachment site (attB) present in the injected plasmid **(Figure 2.6).** During the recombination, a plasmid carrying both a transgene and attB site is co-injected with ΦC31 integrase mRNA into attP-containing embryos in which attP acts as the receiving site, thus leading to the site-specific integration of the transgene into the attP site **(Figure 2.6)**. At least two independent stocks for each construct were kept.

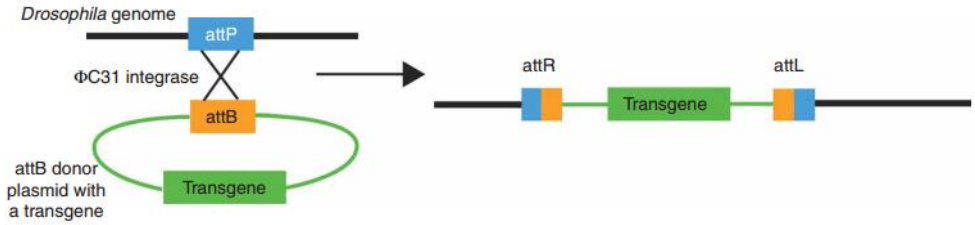

Figure 2.6. A Schematic representation of ΦC31-mediated insertion.

During the recombination, a plasmid carrying both a transgene and attB site is co-injected with ΦC31 integrase mRNA into attP-containing embryos in which attP acts as the receiving site, thus leading to the site specific integration of the transgene into the attP site (adapted from (Fish, Groth et al. 2007).

2.2.5.2. Generation of balanced fly stocks

Balancer chromosomes are modified chromosomes which carry multiple inversions, preventing the occurrence of crossing-over (genetic recombination) between two homologous chromosomes during meiosis. Balancer chromosomes used to stably maintain populations of *Drosophila* carrying homozygous lethal mutations across generations. Most balancers contain a dominant visible marker, which enables researchers to generate stocks carrying one copy of a mutation of interest over one copy of the balancer chromosomes. In our study, we used the balancer flies which have the *TMB6* (Third Multiple 6B) balancer on the third chromosome. *TM6B* balancer chromosome carries *Tubby (Tb)* and *Humeral* (*Hu*) as dominant markers **(see Figure 2.7)**.

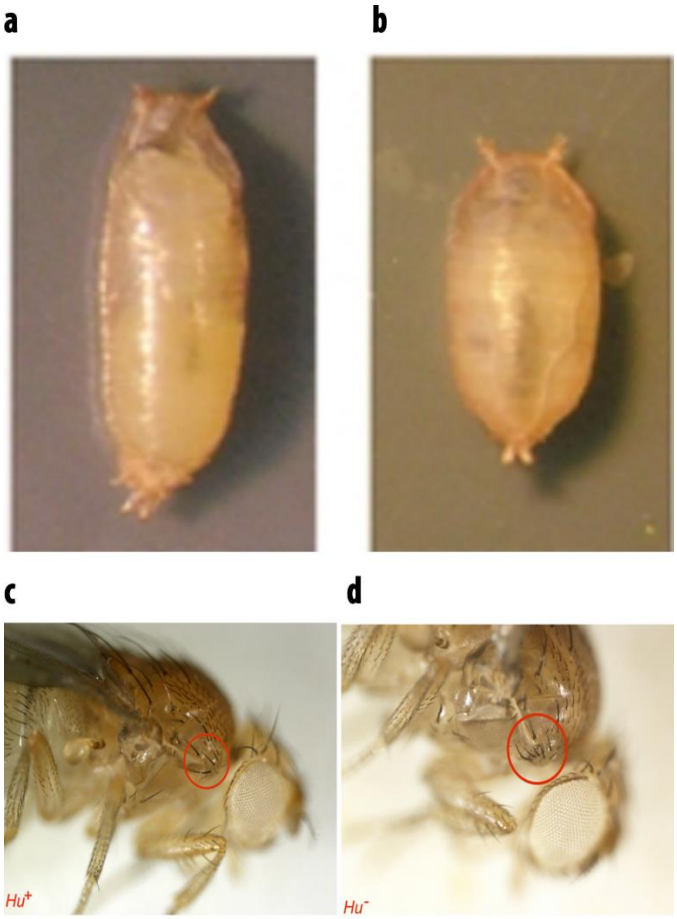

Figure 2.7. Differences between wild type and TM6B balancer flies.

(a) Wild type pupa. **(b)** *Tubby* mutant pupa. Note the shorter and thicker appearance. **(c)** Wild type fly thorax. **(d)** *Humeral* mutant fly thorax. Note the additional macrochaetae on the humeri (red circle).

When the first progenies of transgenic flies hatched, virgin females with red eyes (pKC26w-pUBIQ contains the mini-white reporter gene, see section **2.2.1.9.6**) were collected and then crossed with +/TM6B balancer males **(Figure 2.8)** (kindly provided by the Bjedov Laboratory). TM6B virgin and male flies with red eyes were collected in the F_1 generation, and subsequently crossed *inter se* to generate the balanced stocks **(Figure 2.8)**. The cross scheme was as follows:

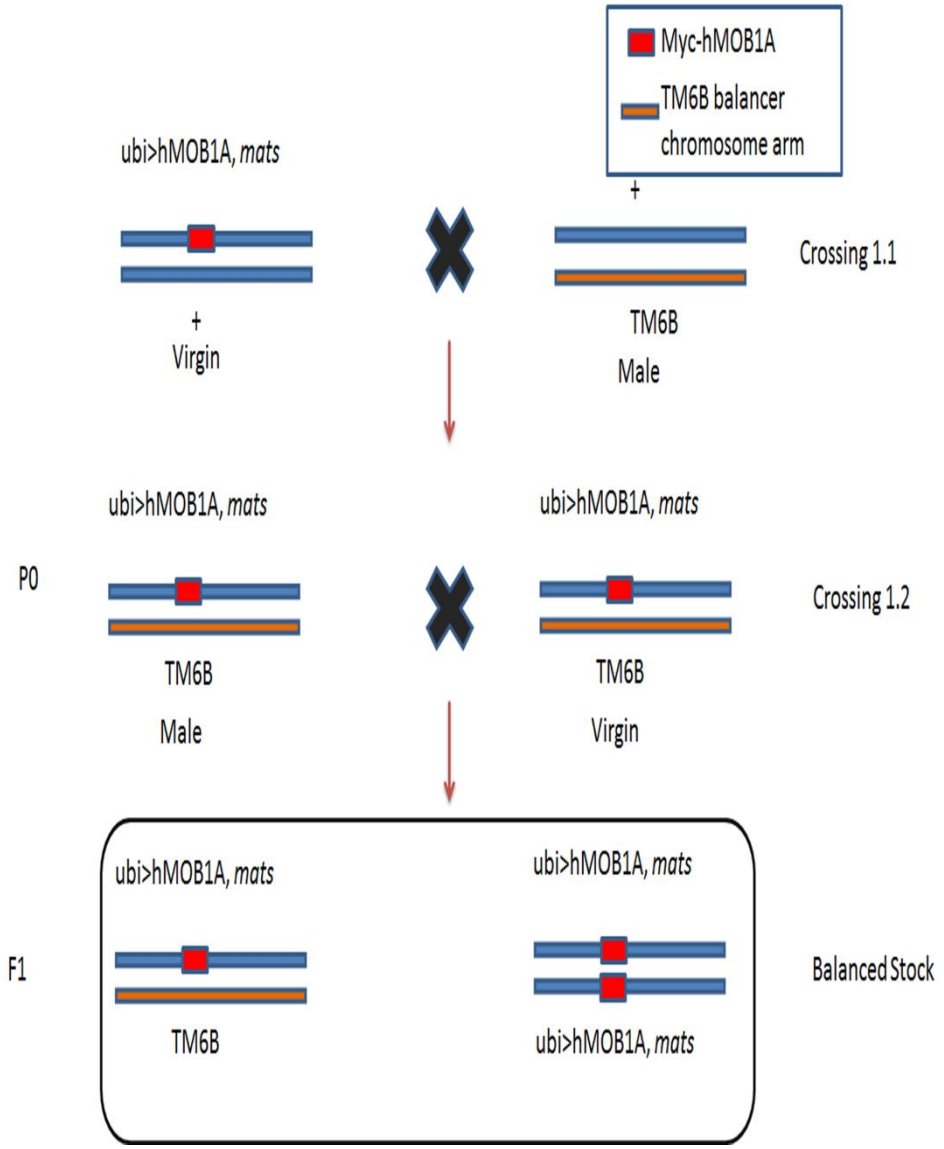

Figure 2.8. The generation of balanced stocks.

Homozygous virgin flies with red eyes were collected and crossed with +/TMB6 balancer flies **(Cross 1.1)**.

2.2.5.3. Recombination of the *mats*^{Roo} allele

The *ubi>myc-hMOB1A* transgenes were recombined with *mats*^{roo} by meiotic recombination as shown in **Figure 2.8**.

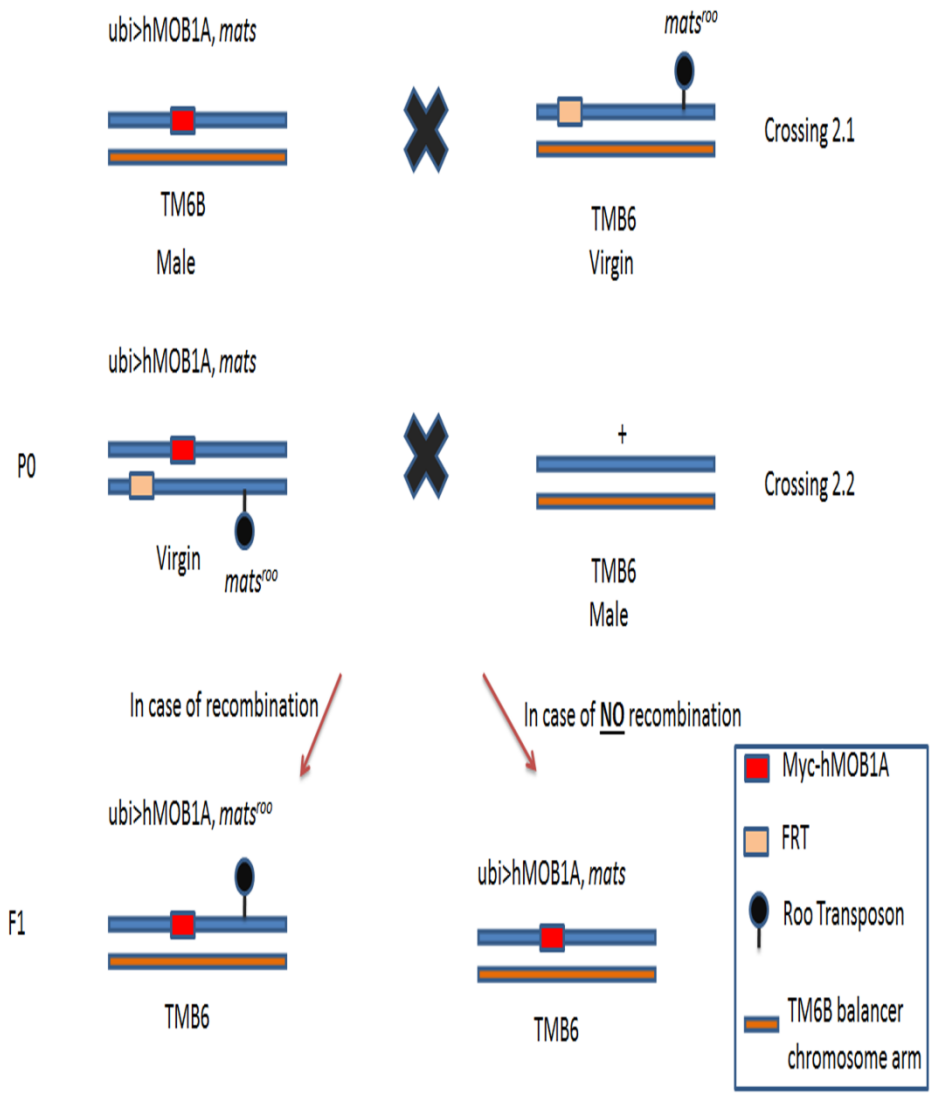

Figure 2.9. Recombination of Roo transposon.

The aim of this cross scheme was to recombine *mats*^{roo} with *ubi>myc-MOB1A*. 15 individual male progeny of the F1 cross were selected and, mated with virgin +/TMB6 to establish stocks. After the crosses had taken, the genomic DNA was extracted from the single males and subjected to PCR to genotype for the Roo transposon. The existence of Roo transposon was confirmed by PCR genotyping **(see Supplementary data, Figure S1).**

Based on the fact that meiotic recombination occurs only in females, virgin homozygous flies with red eyes from **(Figure 2.9)** were selected, which were then crossed with male w;; +/TM6B balancer flies to allow the *mats*^{roo} allele to be exchanged with the endogenous Mats allele **(see Figure 2.9)**. In this crossing, there are two scenarios;

1- If recombination occurs, the *mats*^{roo} gene is recombined into the proximity of the chromosomal arm near on which the hMOB1A gene is integrated (see **Figure 2.9**, "If recombination occurs" scenario)
2- If recombination does not occur, *mats*^{roo} will remain on the same chromosomal arm and the generated flies will have endogenous Mats (see **Figure 2.9**, "If recombination does not occur" scenario).

The main aim of **Figure 2.9** was to recombine the *mats*^{roo} into the proximity of the chromosomal arm near on which the MOB1A gene is integrated so that it has been tested if MOB1A can compensate for Mats loss-of-function.

2.2.5.4. Recombination of the FRT site and Neomycin-based selection for FRT containing recombinants

After the recombination of the *mats*^{roo} allele to our MOB1A constructs, the FRT82B site was recombined to the *mats*^{roo}, *ubi>myc-MOB1A* stocks as depicted in **Figure 2.10.**

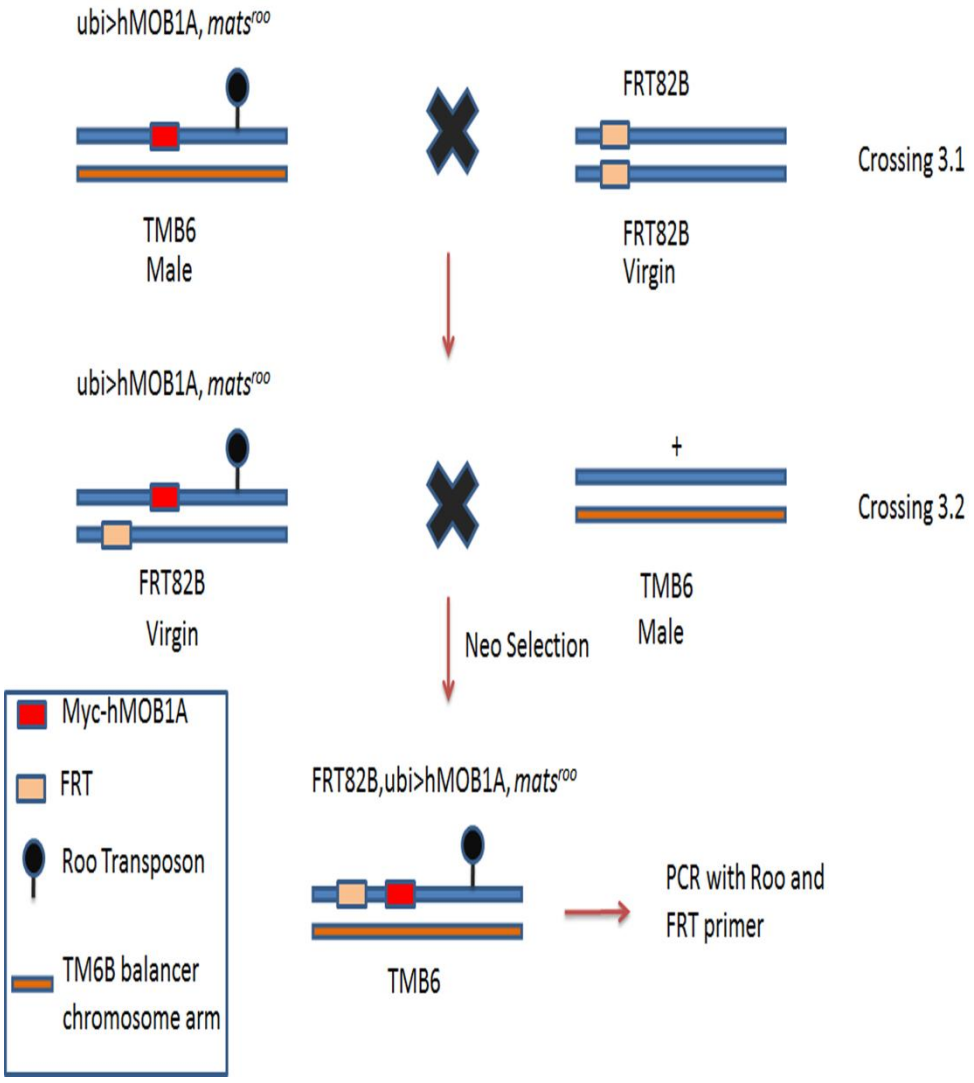

Figure 2.10. Recombination of FRT sites.

Cross scheme to generate the ***FRT82B*** *mats*^{roo}, *ubi>myc-MOB1A* recombinants.

The progeny of the F1 cross were subjected to neomycin selection in order to select for the presence of the neomycin resistance cassette present on the *FRT82B* element (Xu and Rubin 1993).

Crossing was set up as shown in **Figure 2.10**. **Cross 3.2** was performed on medium containing 100 µl of 25mg/ml neomycin solution at 25 ^{o}C. When many eggs became visible on the surface of the food, vials were heat-shocked at 37 ^{o}C for 1 hour 1-2 times per day every day until pupae appeared on the sides of the vials. After balancing, *mats*^{roo} allele and

FRT82B were confirmed by PCR genotyping using primers generated inside *mats* gene (**See supplementary Figure S1 and S2)**.

2.2.5.5. PCR genotyping

All PCR genotyping was carried out as shown in **Table 2.6**. Information about the primers can be found in **section 2.1.5**.

Table 2.6

Reagent	**Volume per reaction**
5 µl	10X Standard Taq Reaction Buffer
1 µl	10 mM dNTPs
1 µl	10 mM Forward Primer
1 µl	10 mM reverse Primer
Variable	Genomic DNA
0.25 µl	Taq DNA Polymerase
To 50 µl	Nuclease-free water

2.2.5.6. Western blotting of whole fly

Three flies per WB lane were frozen at -80 ^{o}C overnight. After freezing, flies were homogenized on ice in 20 µl of 2 x laemmli sample buffer per fly (Bio rad, cat# 1610737) using a Squisher^{TM} manual homogeniser. The samples were then incubated for 5 minutes at 95 ^{o}C, followed by centrifugation at maximum speed in a microcentrifuge. Supernatant was transferred to new eppendorf tubes and the 1 in 20 v/v 1M DTT was added. Equal volumes of samples were analysed by SDS-PAGE, followed by Western blotting, as explained in **(Section 2.2.2.8)**.

2.2.5.7. Genomic DNA preparation from adult flies

Genomic DNA preparations were performed using the Qiagen DNeasy Blood and Tissue kit according to the manufacturer`s instructions (Qiagen, cat#69506). Briefly, flies were collected and frozen in liquid nitrogen. The frozen flies were removed from liquid nitrogen and immediately crushed using micropestle. 180 µl of Buffer ATL was then added to the crushed

flies, followed by the addition of 20 µl of proteinase K before mixing thoroughly by vortexing. The samples were then incubated at 56C for 3 hours while vortexing. After the incubation, 200 µl of Buffer AL and then ethanol (Sigma, cat# E7023-4x4L) were added and mixed by vortexing. The mixture was pipetted into the DNeasy Mini spin column placed in a 2 ml collection tube, following centrifugation at 7,000 x g for 1 minute. The flow-through and collection tubes were discarded. The DNeasy Mini spin columns were placed in new collection tubes and 500 µl of Buffer AW1 was added, followed by centrifugation at 7,000 x g for 1 minute. The flow-through and collection tubes were discarded. The DNeasy Mini spin columns were placed in new collection tube and 500 µl of Buffer AW2 were added, followed by centrifugation at 21,000 x g for 3 minutes. The flow through and collection tubes were discarded once more. The DNeasy Mini columns were placed in 1.5 ml eppendorf tubes and 80 µl of Buffer AE were added onto the DNeasy membrane and centrifuged at maximum speed for 1 minute to elute the DNA. The DNA solution can be stored at -20 ^{o}C. 300 ng DNA was used for PCR genotyping.

2.2.5.8. Generation of mosaic tissues in *Drosophila* using the FLP-FRT system

Genetic mosaic techniques are powerful genetic tools that allow genetic manipulations of gene functions in a subset of cells in tissues (clones) within otherwise unperturbed organism, thus providing a platform to examine genetic changes, which would lead to lethality if applied to the entire organism (Blair 2003).

The FLP-FRT system is one of the most commonly used genetic mosaic techniques. This system is created from yeast and it was first used in *Drosophila* in 1989 (Golic and Lindquist 1989). The FLP-FRT system makes use of the yeast FLP recombinase (FLPase), under the control of a heat-shock inducible promoter, to catalyse recombination between two FRT sites (FLPase recombination target). Thereby, this system generates mitotic clones of homozygous cells in heterozygous tissue. The system is described in **Figure 2.11**.

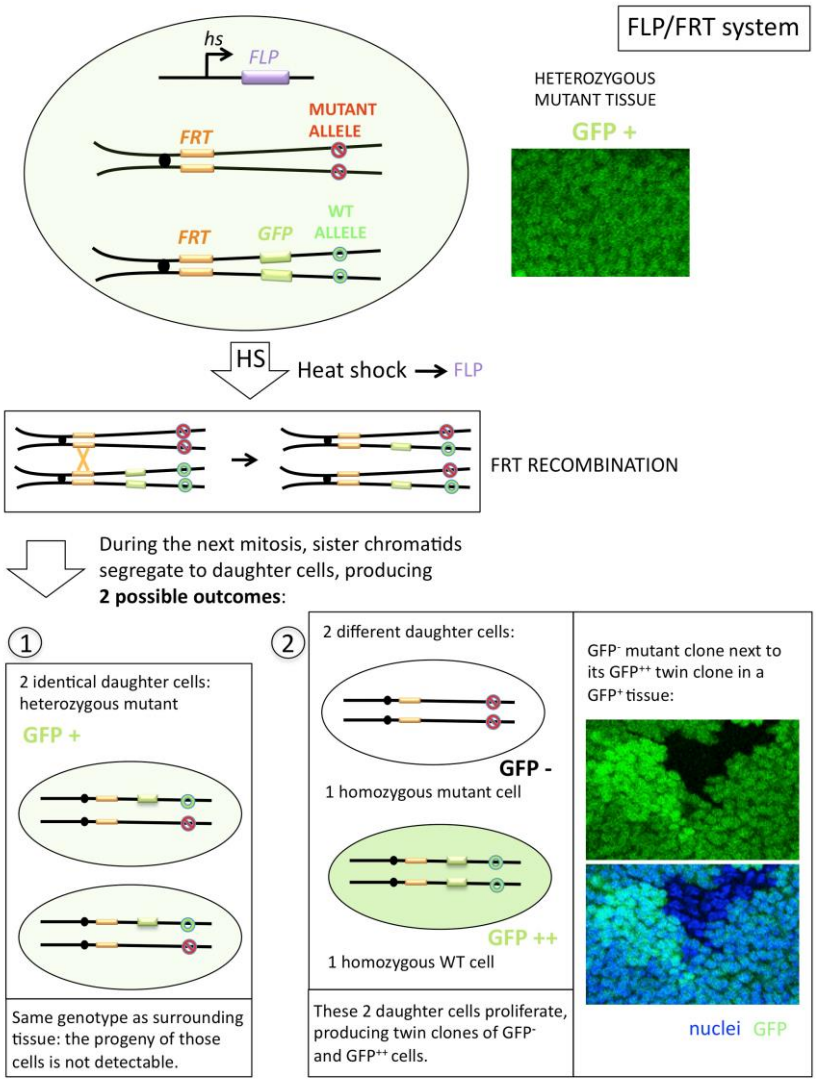

Figure 2.11. The FLP/FRT system.

The pair of chromosomes contain the gene of interest residing distal to FRT transgene near the centromere. One chromosome carries the wild-type allele and a GFP reporter under the control of a given promoter, while the other chromosome bears a mutant allele. The expression of FLPase is induced by heat-shock, ultimately catalysing the recombination of FRT sites between the two homologous chromosomes, thereby generating two chimeric chromosomes, each bearing the two different alleles of gene X on its sister chromatids. Two possible outcomes are observed during the next mitosis. 1. In one possible outcome, two identical daughter cells are produced, each carrying one chromatid of each genotype. These cells are heterozygous mutant for gene X, and expressing GFP. 2. In this possible outcome, two different daughter cells are produced, homozygous wt cells carrying two chromatids with wt allele and GFP, and homozygous mutant cells carrying only X mutant allele. These two different daughter cells can be distinguished by GFP, since homozygous

wt cells express GFP, while homozygous mutant cells does not (Sidor, C., 2012, PhD Thesis, available at http://discovery.ucl.ac.uk/1352451/).

2.2.5.9. Immunostaining of *Drosophila* imaginal discs

Wing or eye imaginal discs were dissected in ice cold PBS. The dissected larvae were then fixed in PBS with 4% formaldehyde at room temperature for 30 minutes. Samples were then washed with two times (10 minutes each) with 0.1% PBST, permeabilised 0.3% PBS-T for 25 minutes and pre-blocked with 10% NGS (normal goat serum) in 0.1% PBS-T for 1 hour, followed by incubation with primary antibody at 4C overnight. Next day, the samples were washed three times (5 minutes per wash) with 0.1% PBS-T and pre-blocked with 10% NGS in 0.1% PBS-T for 25 minutes, followed by incubation with secondary antibody for at least 2 hours. After the incubation, samples were again washed three times with 0.1% PBS-T, before mounting on Vectashield.

3. Results

3.1. Structural and biochemical definition of the importance of MOB1A-NDR, MOB1A-LATS, and MOB1A-MST complex formation

3.1.1. Abstract

In mammals, there are six MOB proteins including MOB1A/B (usually collectively referred as MOB1) and four NDR/LATS kinases: NDR1/2 and LATS1/2. LATS1/2 are closer to Wts and phosphorylate the Yorkie homologue YAP in Hippo signalling; while NDR1/2 are implicated in regulating centrosome duplication, apoptosis, cell cycle, and Hippo signalling. It was found that an N-terminal domain of NDR1/2 (which occurs in the middle of LATS1/2) is responsible for mediating association with MOB1A. Furthermore, it was also shown that MOB1A can also interact with MST1/2 kinases. Although structures of human, *Xenopus*, yeast MOB1, and yeast Mob2-Cbk1 complex are available, it remains elusive how MOB differentially recognize NDR, MST, and LATS subfamilies of kinases. Here, we report the crystal structure of human MOB1A (residues 33-216) in complex with the N-terminal MOB1-binding domain of NDR2 (residues 25-88). Furthermore, we structurally and biochemically characterise the key residues of MOB1A for binding to MST/LATS/NDR kinases. Taken together, our data unveil crucial residues that are required for MOB1A binding to MST/LATS/NDR kinases.

3.1.2. Introduction

Hippo signalling regulates cell proliferation, apoptosis, and cell differentiation from flies to mammals. The final output of the Hippo pathway is to inhibit the transcriptional co-activators Yorkie and YAP/TAZ in *Drosophila* and mammals, respectively (Wei, Shimizu et al. 2007). Essentially, core members of the Hippo pathway include the nuclear Dbf2-related (NDR)/large tumour suppressor (LATS) family of kinases and its activator Mps one binder (MOB) proteins (Hergovich 2011, Avruch, Zhou et al. 2012). In *Drosophila*, Hippo kinase phosphorylates the MOB protein Mats and promotes its interaction with the NDR/LATS kinase Wts (Wei, Shimizu et al. 2007). Upon activation by Hippo and Mats, Wts phosphorylates and inactivates the transcriptional coactivator Yorkie (Avruch, Zhou et al. 2012). In mammals, there are six MOB proteins including MOB1A/B (usually collectively referred as MOB1) and four NDR/LATS kinases: NDR1/2 and LATS1/2 (Hergovich 2011). Mechanistically, the regulation of the mammalian Hippo pathway appears to function in a similar fashion with that of *Drosophila*. Briefly, current evidence suggests that MST (counterpart of Hpo kinase) initiates phosphorylation of MOB1A and then promotes its association with NDR/LATS kinases, therefore resulting in NDR/LATS activation. The activated NDR/LATS kinases subsequently phosphorylate and then inhibit the Yorkie homologue YAP (Hergovich 2013).

It is important to note that complex protein-protein interactome of the Hippo pathway plays crucial role in its regulation (Hergovich 2012). In this context, complex interaction of MOB1A with MST/LATS/NDR kinases seems to be significant with regard to the regulation of the Hippo pathway. MOB1A can associate with all four human LATS/NDR as well as MST kinases (Hergovich 2012). It was only biochemically shown that N-terminal domains of NDR/LATS kinases are essential for the binding of MOB1A with LATS/NDR kinases. However, structural importance of complex formation of MOB1A with NDR/LATS is not known and needs to be addressed.

Here we report the complex formation of MOB1A with NDR/LATS kinases using structural studies. Based on our structural studies, we determine the key residues of MOB1A that is needed for the association with NDR/LATS kinases. To further support our findings from the structural studies, we biochemically prove the importance of the key residues of MOB1A with respect to binding to NDR/LATS kinase. Furthermore, we also report the key residues which is essential for the binding of MOB1A with MST1/2 kinases.

3.1.3. Results - Structural definition of MOB1-NDR2 and MOB1-LATS1 complex formations

To determine the crystal structure of human MOB1A (residues 33-216) in complex with the N-terminal MOB1-binding domain of NDR2 (residues 25-88), MOB1A (33-216) and NDR2 (25-88) were bacterially expressed and purified as outlined in **section 2.2.4.1**. The crystal growth of the purified proteins was carried out as shown in **section 2.2.4.2**. The results are presented in **Figure 3.1**.

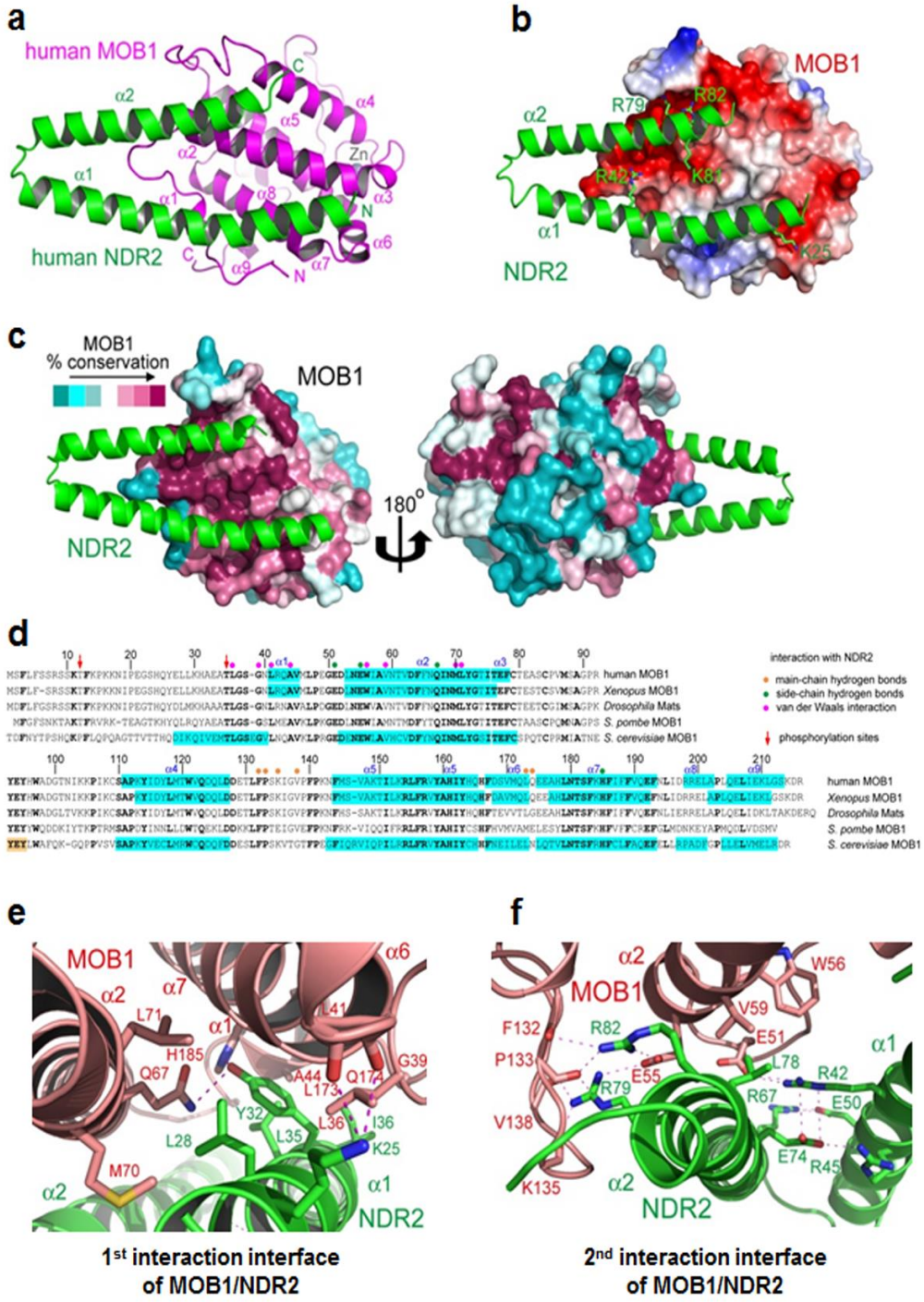

Figure 3.1. The MOB1A/NDR2 structure reveals that MOB1A and NDR2 interact through conserved interfaces.

(a) Overall crystal structure of the complex between human MOB1A (residues 33 to 216) and human NDR2 (residues 25 to 88). MOB1 and NDR2 are coloured in magenta and green, respectively. The Zinc associated with MOB1 is indicated in grey. Secondary structure elements are highlighted. **(b)** The negatively charged surface of MOB1 recognizes positively charged residues on NDR2. The electrostatic surface potential of MOB1 is shown (red: negatively charged residues; blue: positively charged residues). NDR2 is

shown as a ribbon representation coloured in green. **(c)** The MOB1A/NDR2 binding surfaces are highly conserved. The residues of MOB1 are gradually coloured according to conservation scores (dark red: most conserved residues; dark cyan: least conserved residues). NDR2 is shown as a ribbon representation coloured in green. **(d)** Structure based sequence alignment of MOB1A from indicated species. MOB1A residues mediating interactions with NDR2 are marked with brown (main-chain hydrogen bonds), green (side-chain hydrogen bonds) and magenta circles (van der Waals interactions). a helices are painted with cyan background. Thr12 and Thr35 phosphorylation sites are indicated by red arrows. **(e,f)** The interaction interfaces of MOB1A with the a1 (**e**) and a2 (**f**) helices of NDR2. MOB1A and NDR2 and their key interacting residues are shown in pink and green, respectively. Dashed lines represent hydrogen bonds. Side chain nitrogen, oxygen, and sulphur atoms of MOB1A and NDR2 residues are coloured in blue, red and gold, respectively. The hydrogen bond network connecting the a1 and a2 helices of NDR2 is also illustrated in **f**.

We determined the crystal structure of human MOB1A (residues 33-216) in complex with the N-terminal MOB1A-binding domain of NDR2 (residues 25-88) to 2.1 Å resolution **(Supplementary data, Table S1, deposited with the PDB code 4ZUG)**. Noteworthy, the structure of MOB1A in the complex with NDR2 is essentially the same as the published structure of MOB1A in isolation (Stavridi, Harris et al. 2003), while the NDR2 (25-88) fragment bound to MOB1A displays a tong-shaped structure comprising two α helices **(Figure 3.1a)**. MOB1A employs its negatively-charged surface to associate with positively-charged K25/R42/R79/K81/R82 residues on NDR2 **(Figure 3.1b)**. This NDR2-binding surface of MOB1A exhibits a striking level of conservation from yeast to human, while, in contrast, the other part of MOB1A that is not involved in the interaction with NDR2 is much less conserved **(Figure 3.1c)**. Moreover, sequence alignments of MOB1A and NDR2 with their respective functional counterparts reveal that key residues mediating their direct association are highly conserved from yeast to human **(Figure 3.1d)**.

The recognition interface between NDR2 and MOB1A can be divided into two main parts. First, at the interface between the α1 helix of NDR2 and MOB1A, Y32 of NDR2 occupies a central position, and its side-chain hydroxyl group forms hydrogen bonds with Q67 and H185 of MOB1A

(Figure 3.1e). Moreover, K25 of NDR2 makes hydrogen bonds with the main-chains of L173 and Q174 of MOB1A, and residues L28, L35, and I36 of NDR2 interacts with a cluster of residues of MOB1A (L36/G39/L41/A44/M70/L71) by van der Waals forces **(Figure 3.1e)**. Second, at the interface between the α2 helix of NDR2 and MOB1A, L78 of NDR2 makes hydrophobic interactions with W56 and V59 MOB1A, in addition to R79 and R82 of NDR2 forming hydrogen bonds with cluster of residues of NDR2 MOB1A (F132/P133/K135/V138) and a salt bridge with E55 of MOB1A **(Figure 3.1f)**.

Intriguingly, analyses of the sequence alignments of the NDR/LATS kinases revealed that most of the MOB1A-binding residues are conserved in NDR/LATS kinases from yeast to humans **(Figure 3.2a)**. However, we discovered a peculiar subfamily-specific residue of NDR2, namely Y32, that is not present in all NDR/LATS kinases **(Figure 3.2a)**. More specifically, in the NDR-subfamily including human NDR1/2, *Drosophila* Tricornered, *S. cerevisiae* Dbf2/Dbf20/Cbk1, and *S. pombe* Sid2/Orb6, the residue at this key position is an invariant tyrosine **(Figure 3.2a)**. In stark contrast, in the LATS-subfamily including human LATS1/2 and *Drosophila* Wts, a valine or isoleucine occurs at this key position **(Figure 3.2 a).**

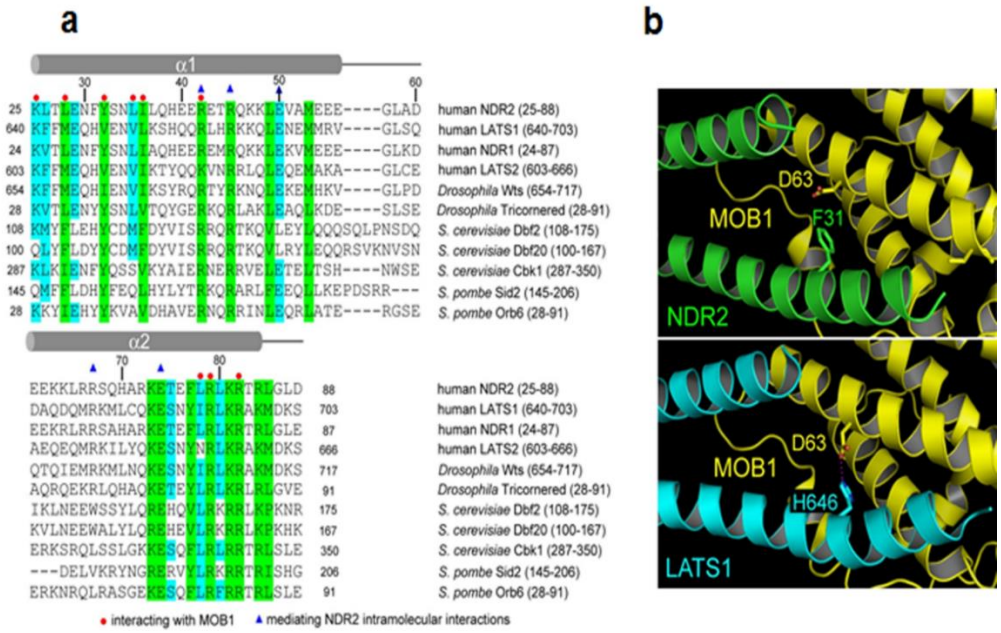

Figure 3.2. Structure based modelling of NDR2 and LATS2 bind to MOB1A through different key residues/mechanisms.

(a) Structure based sequence alignment of the conserved N-terminal regulatory domain of NDR/LATS kinases that is required for MOB1A binding. NDR2 residues mediating interactions with MOB1A are marked with red circles. Residues mediating intramolecular interactions of NDR2 are denoted by blue triangles. Residues conserved from yeast to humans are highlighted in green, while residues conserved in at least seven of the conserved NDR/LATS family members are marked in cyan. a helices are indicated with gray rods. **(b)** Asp63 of MOB1 is involved in LATS1 binding, but does not contribute to the interaction of MOB1A with NDR2. MOB1 is shown in yellow, while NDR2 and LATS1 are indicated in green and blue, respectively. Top panel, Phe31 of NDR2 does not interact with Asp63 of MOB1A. Bottom panel, His646 of LATS1 forms a hydrogen bond with Asp63 of MOB1A.

Significantly, our analysis further determined key residues mediating the interaction of MOB1A with LATS1 and NDR2 **(Figure 3.2)**. To do so, we also studied the recently published structure of MOB1A in complex with a LATS1 fragment (Kim, Tachioka et al. 2016). As shown in **Figure 3.2b**, this revealed that D63 of MOB1A is involved in LATS1-binding but not in NDR2-binding. Specifically, H646 of LATS1 forms a hydrogen bond with D63 of MOB1A, whereas F31 of NDR2, the residue of NDR2 corresponding to H646 of LATS1 **(Figure 3.2a)**, does not interact with D63

of MOB1A **(Figure 3.2b)**. This suggests that the D63 residue of MOB1A plays a specific and pivotal role in the association of LATS1 with MOB1A.

In addition to the structural analyses of NDR/MOB1A and LATS/MOB1A complexes **(Figures 3.1 and 3.2)**, we also sought to determine key residues mediating the interaction of MOB1A with the MST1/2 kinases. To do so, we tested by co-immunoprecipitation assays the interactions of a range of MOB1A mutants with wild-type MST1/2 kinases (Hergovich, A., unpublished data now shown). Considering that negatively charged surfaces of MOB1A are responsible for the interactions with positively charged surfaces of NDR/LATS kinases **(see Figures 3.1 and 3.2)** and that MOB1A interacts with MST1/2 kinases differently than with NDR/LATS (Ni, Zheng et al. 2015, Kim, Tachioka et al. 2016), we hypothesized that potentially positively charged residues of MOB1A are central for complex formation with MST1/2. Therefore, we focused our efforts on studying MOB1A versions carrying point mutations of arginine or lysine. Significantly, this approach proved successfully, since we found that MOB1A(K104E/K105E) does not bind to MST1/2, in contrast to all the other MOB1A mutants tested (Hergovich, A., unpublished data now shown).

Consequently, as next step to further investigate and compare the importance of D63 and K104/K105 residues of MOB1A for binding to MST/NDR/LATS kinases, gel filtration chromatography was performed. The results are shown in **Figure 3.3**.

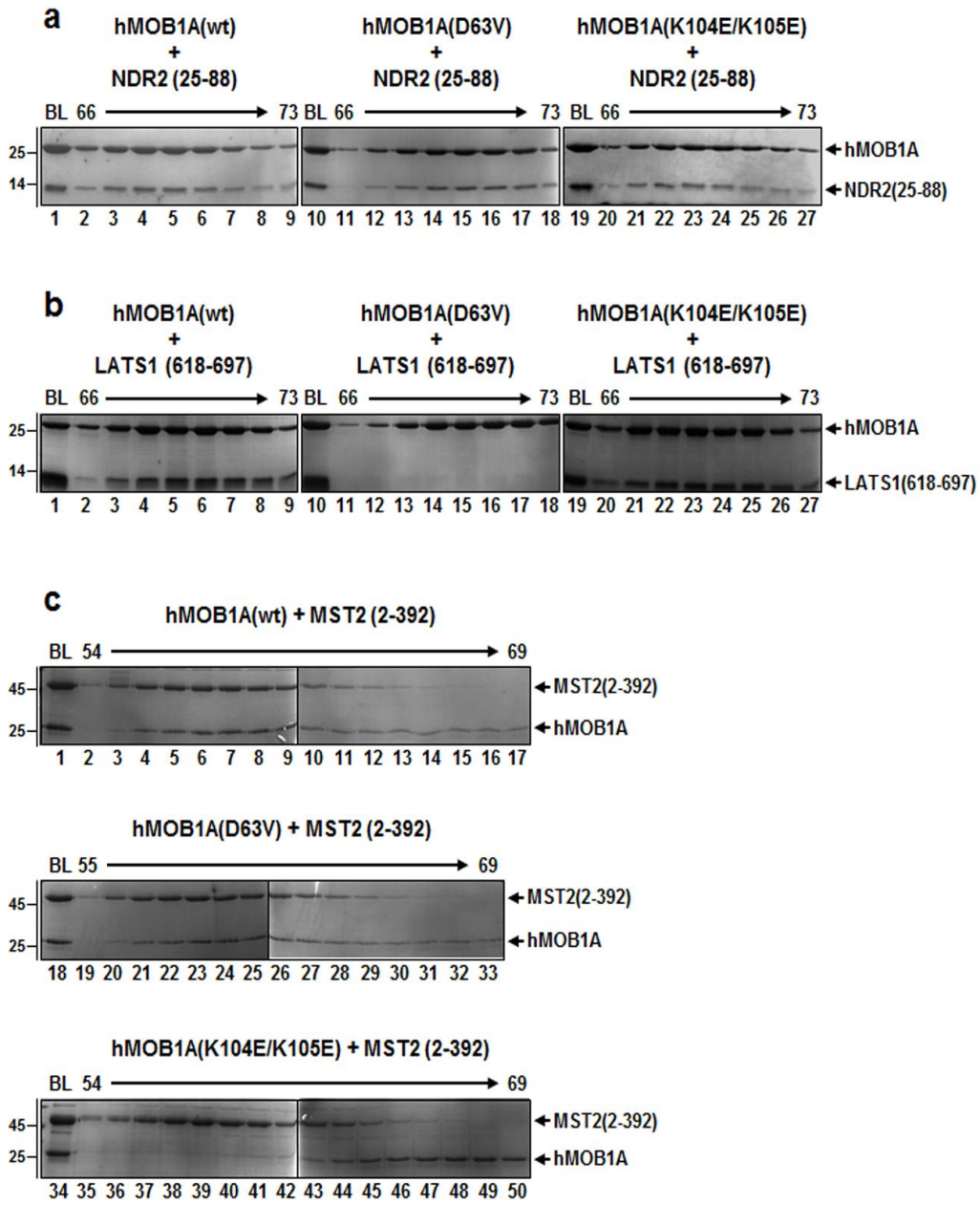

Figure 3. 3. Characterization of MOB1A(D63V) and MOB1A(K104E/K105E) binding to NDR2, LATS1 and MST2 by gel filtration chromatography.

(a-c) Indicated versions of recombinant MOB1A were incubated with recombinant wild-type NDR2(25-88), LATS1(618-697), or MST2(2-392), before loading (BL) onto a Superdex 200 column. To assess LATS1 binding, MST2 phosphorylated MOB1 proteins were used. The indicated fractions from the Superdex 200 column were analyzed by SDS-PAGE followed by coomassie staining. Relative molecular weights are shown. The positions of MOB1A, NDR2, LATS1 and MST2 are indicated on the right. MOB1A(wt), MOB1A(D63V) and MOB1A(K104E/K105E) readily co-fractionated with NDR2 (**a**). Phosphorylated MOB1A(wt) and MOB1A(K104E/K105E) co-eluted with LATS1, while

MOB1A(D63V) did not (**b**). MOB1A(wt) and MOB1A(D63V) co-fractionated with MST2, but MOB1A(K104E/K105E) did not co-elute with MST2 (**c**).

To this end, bacterially expressed and purified full-length MOB1A proteins were incubated with NDR2 (25-88), LATS1 (618-697), or MST2 (2-392) protein fragments, followed by the gel filtration chromatography to analyse complex formation of recombinant proteins **(Figure 3.3)**. Significantly, our findings revealed that D63V and K104E/K105E mutations in MOB1A did not affect the interaction with NDR2 when compared to wild type MOB1A **(Figure 3.3a)**. Furthermore, we found that the D63V mutant of MOB1A, but not the K104E/K105E mutant, bound to LATS1 (618-697) comparable to wild-type MOB1A **(Figure 3.3b)**. In addition, we could show that the K104E/K105E mutant of MOB1A, but not the D63V mutant, displayed a disrupted interaction with MST2 (2-392) **(Figure 3.3c)**.

3.1.4. Results - Characterization of MOB1A mutants with selective binding to MST/NDR/LATS kinases in mammalian cells

To develop research tools that allow us to understand which protein-protein interaction(s) (PPIs) between MOB1A and MST/LATS/NDR are required for YAP-Hippo signalling, cell proliferation and suppression of cellular transformation, we designed and characterized a series of mutants with affected binding of MOB1A to MST/LATS/NDR based on our structural studies **(Section 3.1.3)**. Specifically, we focused on characterising MOB1A variants carrying E51K, D63V, K104E/K105E, E51K/K104E/K105E, or D63V/ K104E/K105E point mutations. The nomenclature of these mutations used in this thesis has been simplified, respectively, as follows: EK (E51K), DV (D63V), KEKE (K104E/K105E), EKKEKE (E51K/K104E/K105E), DVKEKE (D63V/K104E/K105E).

Stavridi et al. (2003) reported that MOB1A has a flat surface rich in acidic residues on one side, which is believed to provide the structural basis for the association with the NDR1/2 and LATS1/2 kinases through electrostatic forces. Stavridi et al. (2003) found that the E51 of MOB1A is conserved from yeast to humans and speculated that this residue is very likely of functional importance. Furthermore, Hergovich et al. (2009) demonstrated that the substitution of Glu51 with Lys (E51K) interferes with the interaction with NDR1/2, highlighting the importance of the E51 residue of MOB1A for the interaction with the NDR1/2 kinases. In addition, based on our structural and biochemical studies **(see section 3.1.2 and 3.1.3 above),** we concluded that MOB1A(DV) displays an abolished interaction with LATS1 **(Figure 3.3)**, while the interactions with NDR2 and MST2 remain fully intact **(Figure 3.3)**. Furthermore, we also discovered that MOB1A (KEKE) displayed an abolished interaction with the MST2, but not with NDR2 and LATS1 **(Figure 3.3)**. Following the discovery of these mutations which appear to be important for the interaction of hMOB1A with MST/LATS/NDR, these mutations were then characterized in mammalian cells using co-immunoprecipitation assays. To this end, hemagglutinin A (HA)-tagged MST1/2, LATS1/2, NDR1/2 and myc-tagged MOB1A variants were co-expressed in HEK 293 cells, followed by immunoprecipitation with

anti-HA 12CA5 antibody, before analyses of protein complexes by Western blotting.

Firstly, the characterization of our MOB1A variants with respect to MST1/2 binding was carried out. The results are presented in **Figure 3.4** below.

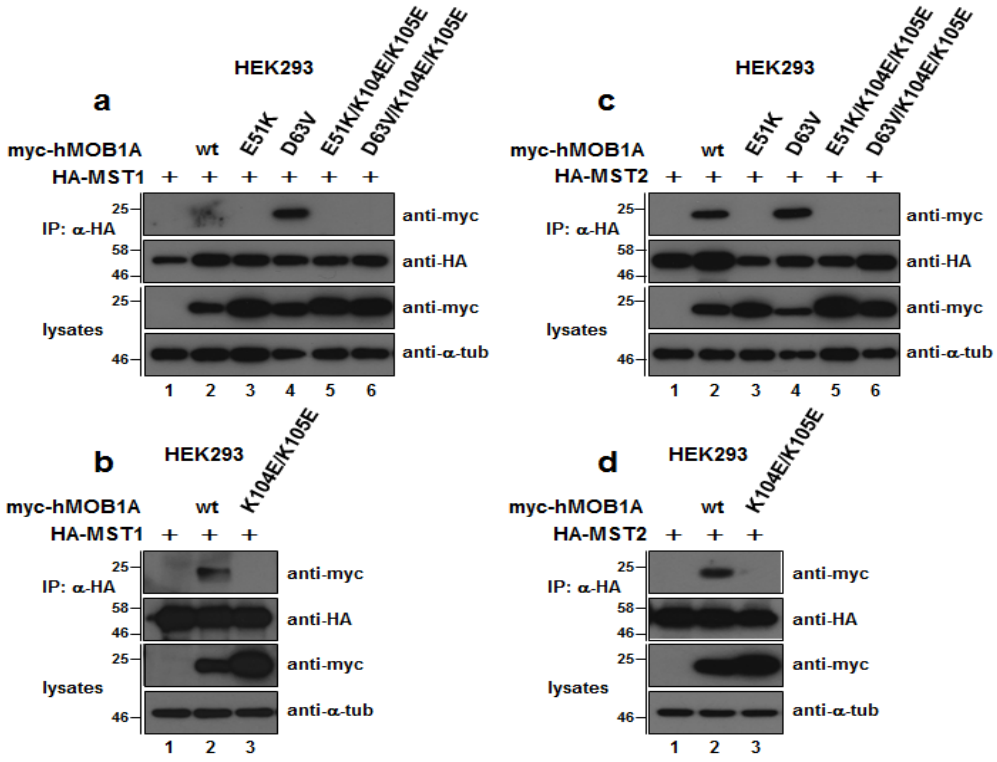

Figure 3.4. Characterization of the interaction of MOB1A variants with MST1/2.

(a-d) Lysates of HEK293 cells expressing full-length HA-MST1 or HA-MST2 wild-type (wt) together with indicated full-length MOB1A versions were subjected to immunoprecipitation (IP) using anti-HA. Complexes were studied by immunoblotting using anti-myc (top) and anti-HA (top middle). Input lysates were analysed with anti-myc (bottom middle) and anti-α-tubulin (bottom). Relative molecular weights are shown. The EK and KEKE mutations caused loss of binding to MST1/2, while the DV mutant bound normally. Complexes were studied by immunoblotting using anti-myc (top) and anti-HA (top middle). Input lysates were probed with anti-myc (bottom middle) and anti-α-tubulin (bottom). Relative molecular weights are shown.

We investigated complex formation of MOB1A(wt) and MOB1A mutants with the MST1/2 kinases in HEK293 **(Figure 3.4)**. To this end, N-terminally tagged versions of HA-MST1 and HA-MST2 were co-expressed with N-terminally tagged versions of myc-MOB1A(wt) and myc-MOB1A mutants, followed by co-immunoprecipitation using anti-HA. These experiments revealed that MOB1A(EK), MOB1(EKKEKE), and MOB1A(DVKEKE) cannot bind to MST1 and MST2 **(Figures 3.4a and 3.4c)**. In sharp contrast, MOB1A(DV) associated with MST1 and MST2 like wild-type MOB1A **(Figures 3.4a and 3.4c)**. Significantly, the MOB1A(KEKE) mutant could not form a complex with neither HA-MST1 nor HA-MST2 **(Figures 3.4b and 3.4d)**. Collectively, these findings suggest that the MOB1A(EK) and MOB1A(KEKE) variants are deficient in MST1/2 binding, while MOB1A(DV) binds normally to MST1/2. Thus, we established in **Figure 3.4** MOB1A mutants that allow us to test the significance of the MST1/2-MOB1A interaction in Hippo signalling. Furthermore, these findings **(Figure 3.4)** also further support our biochemical data presented in **section 3.1.3** above.

Second, the PPIs of our panel of MOB1A mutants with LATS1/2 were examined. The results are shown in **Figure 3.5** below.

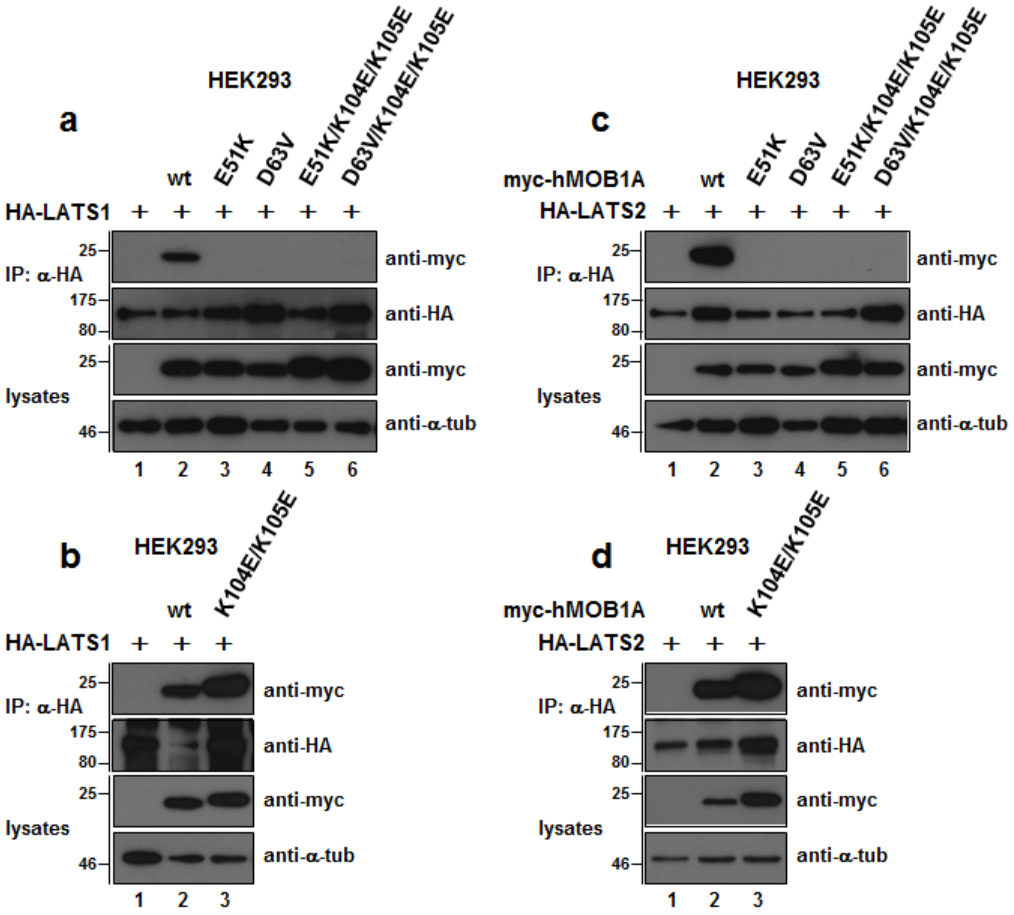

Figure 3.5. Characterization of the interaction of MOB1A variants with the LATS1/2 kinases.

(a-d) Lysates of HEK293 cells expressing full-length HA-tagged LATS1 or LATS2 wild-type (wt) together with the indicated full-length MOB1A versions were subjected to immunoprecipitation (IP) using anti-HA 12CA5 antibody. Complexes were analysed by immunoblotting using anti-myc (top) and anti-HA antibody (top middle). Input lysates were analysed with anti-myc (bottom middle) and anti-a-tubulin antibody (bottom). Relative molecular weights are shown. The EK and DV mutations abolished MOB1 binding to LATS1/2, while the KEKE mutant bound normally. Complexes were analysed by immunoblotting using anti-myc (top) and anti-HA (top middle). Input lysates were analysed with anti-myc (bottom middle) and anti-a-tubulin (bottom). Relative molecular weights are shown.

We investigated complex formation of MOB1A(wt) and MOB1A mutants with the LATS1 and LATS2 kinases in HEK293 cells **(Figure 3.5)**. To this end, N-terminally tagged versions of HA-LATS1 and HA-LATS2 were co-expressed with N-terminally tagged versions of myc-MOB1A wt and

mutants, followed by co-immunoprecipitation using anti-HA. These findings uncovered that only MOB1A(wt) and MOB1A(KEKE) can bind to LATS1 and LATS2, while the remainder mutants did not to interact with LATS1 and LATS2 **(Figure 3.5)**. Collectively, these findings show that the MOB1A(DV) and MOB1A(EK) variants are deficient in LATS1/2-binding, while MOB1A(KEKE) can normally associate with LATS1 and LATS2. Therefore, we established here a foundation that allows us to study the significance of LATS1/2-MOB1A complex formation in Hippo core signalling. Furthermore, our data presented here **(Figure 3.5)** also support the biochemical findings presented in **section 3.1.3**.

Third, the characterization of MOB1A mutants with respect to NDR1/2 binding was carried out. The corresponding results are presented in **Figure 3.6** below.

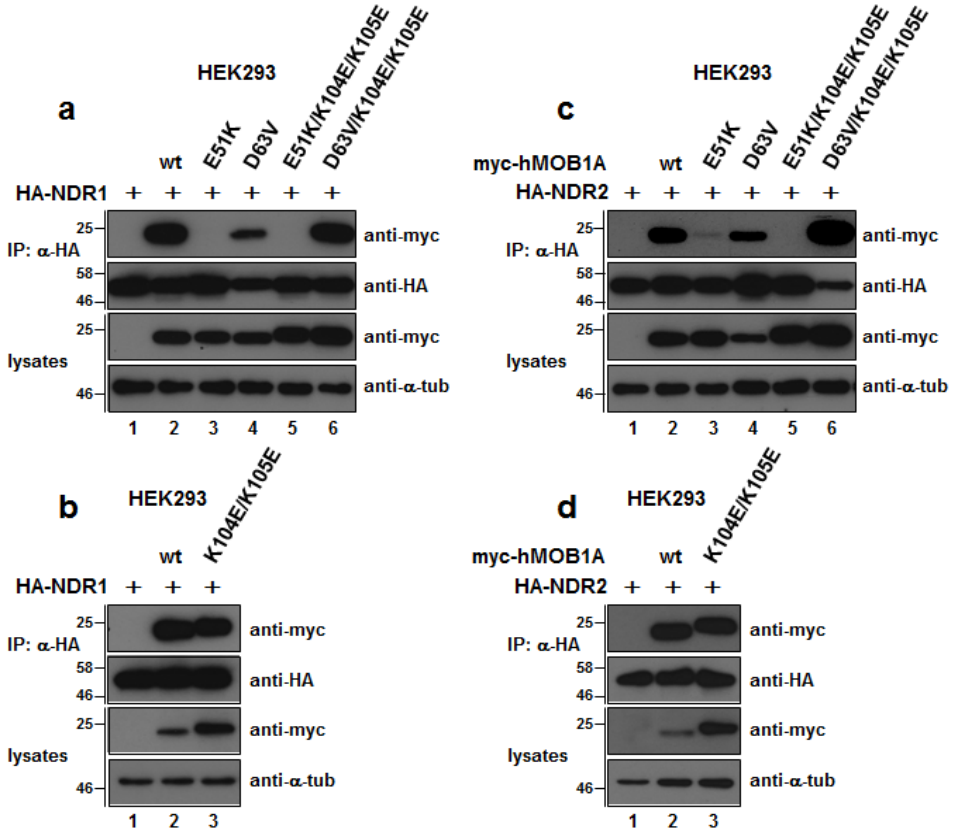

Figure 3.6. Characterization of the interaction of MOB1A variants with NDR1/2.

(a-d) Lysates of HEK293 cells expressing full-length HA-NDR1 or HA-NDR2 wild-type (wt) together with the indicated full-length MOB1A versions were subjected to immunoprecipitation (IP) using anti-HA 12CA5 antibody. Complexes were studied by immunoblotting using anti-myc (top) and anti-HA antibody (top middle). Input lysates were analyzed with anti-myc (bottom middle) and anti-a-tubulin antibody (bottom). Relative molecular weights are shown. Only versions carrying the EK mutation displayed a reduction of binding to NDR1/2. Complexes were examined by immunoblotting using anti-myc (top) and anti-HA (top middle). Input lysates were investigated with anti-myc (bottom middle) and anti-a-tubulin (bottom). Relative molecular weights are shown.

N-terminally tagged versions of HA-NDR1 and HA-NDR2 were co-expressed with N-terminally tagged versions of myc-MOB1A(wt) and myc-MOB1A mutants, followed by co-immunoprecipitation using anti-HA. These findings uncovered that the MOB1A(EK) and MOB1A(EKKEKE) mutants cannot bind to NDR1 and NDR2, while the MOB1A(DV) and MOB1A(DVKEKE) interacted normally with NDR1 and NDR2 when compared to wild-type MOB1A **(Figures 3.6a and 3.6c)**. In addition, we studied the interaction of MOB1A(KEKE) with HA-NDR1 and HA-NDR2, and found that the MOB1A(KEKE) can bind normally to NDR1 and NDR2 **(Figures 3.6b and 3.6d)**. Collectively, our data shown in **Figure 3.6** suggests that only MOB1A(EK) and MOB1A(EKKEKE) are deficient in NDR1/2 binding, while all other mutants tested displayed normal interactions with NDR1/2. Thus, we establish here **(Figure 3.6)** a research tools allowing us to study the significance of the interaction of MOB1A with NDR1/2 in the context of Hippo core signalling.

Taken together, in full agreement with published literature (Stavridi, Harris et al. 2003, Bichsel, Tamaskovic et al. 2004, Bothos, Tuttle et al. 2005, Hergovich, Bichsel et al. 2005, Hergovich, Schmitz et al. 2006, Vichalkovski, Gresko et al. 2008, Hergovich, Kohler et al. 2009, Kohler, Schmitz et al. 2010, Chen, Zhang et al. 2015, Hoa, Kulaberoglu et al. 2016) and the structural/biochemical studies presented in **section 3.1.2** and **3.1.3**, we found that MOB1A(wt) can stably bind to MST1/2, NDR1/2, and LATS1/2 kinases **(Figures 3.4, 3.5, and 3.6)**. More importantly, we characterized a series of selected MOB1A with regard to MST/NDR/LATS

binding. These experiments revealed that the MOB1A(EK) does not to interact with any of the NDR/LATS/MST kinases. In contrast, MOB1A(DV) selectively impaired the binding of MOB1A with LATS1/2, while the MOB1A(DV) normally bound to MST1/2 and NDR1/2 kinases. The MOB1A(KEKE) also interacted normally with LATS1/2 and NDR1/2 kinases, while the KEKE mutations selectively interfered with the interaction of MOB1A with MST1/2 kinases. In addition, the combination of the EK and DV with KEKE were tested for their ability to interact with MST1/2, LATS1/2, and NDR1/2 kinases, respectively. This revealed that the MOB1A(EKKEKE) does not interact stably with any of the tested kinases. The MOB1A(DVKEKE) mutant interacted only with NDR1/2 kinases, but did not bind to any of the other Hippo kinases tested. The binding properties of all mutants tested are summarized in **Figure 3.7**, including an illustration of the location of the key residues in the published structure of MOB1A.

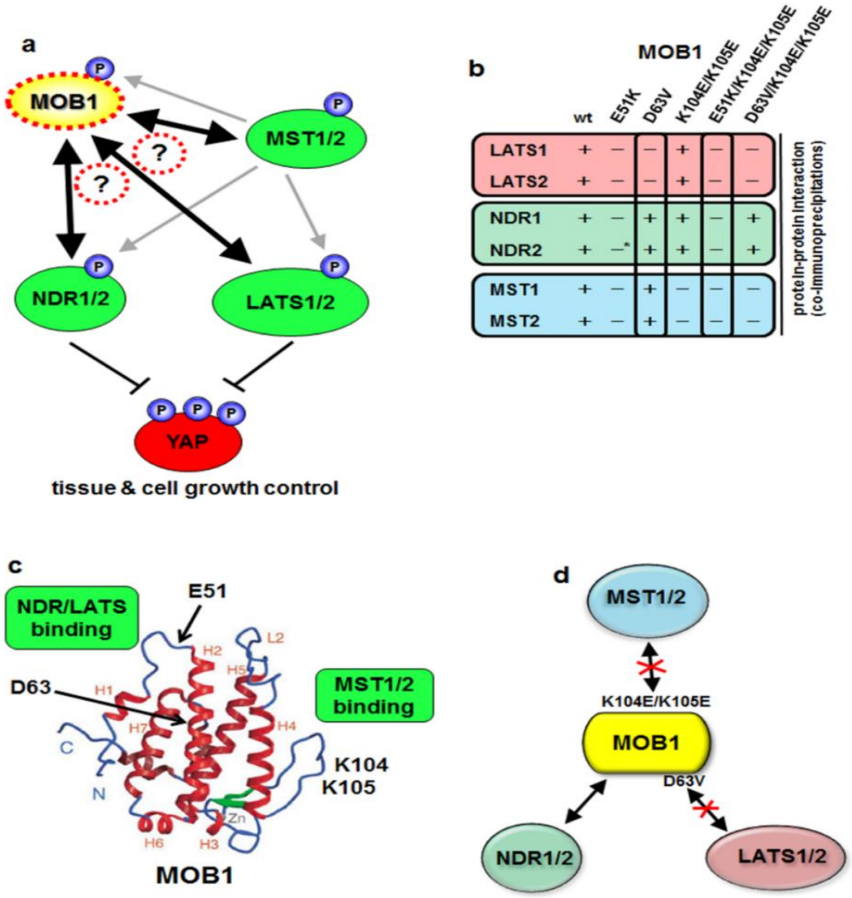

Figure 3.7. Generation of MOB1A variants to dissect the importance of MOB1A interactions with mammalian Hippo core cassette kinases.

(a) Model illustrating two key research questions regarding MOB1A as a hub of mammalian Hippo core signalling: (1) Does MOB1A interact differently with MST1/2, LATS1/2 and NDR1/2 in human? (2) Which interactions of MOB1A with MST1/2, LATS1/2, or NDR1/2 are biologically important in the context of YAP-Hippo signalling? **(b)** Schematic summary of the biochemical and molecular characterization of the indicated MOB1A variants presented in **Figures 3.1 to 3.6**. **(c)** Model of human MOB1A(33-216) depicting the possibly opposing binding sites on MOB1A of NDR/LATS and MST1/2 kinases. Secondary structure elements of MOB1A are highlighted. The locations of Glu51, Asp63, and Lys104/Lys105 in MOB1 are indicated. **(d)** Schematic model of how the differential binding of MOB1A to MST1/2, LATS1/2 and NDR1/2 can be experimentally exploited using the DV and KEKE mutations in order to study the biological importance of these different interactions of MOB1A with Hippo core cassette kinases.

3.1.5. Discussion

Taken together, our structural and biochemical data presented here provide novel insight into the complex formation of MOB1A with the Hippo core kinases, MST1/2, NDR1/2, and LATS1/2 kinases. In our structural studies, we report for the first time the crystal structure of MOB1A-NDR2 complex, encompassing the entire region of NDR2 which is required for binding to MOB1A **(Figure 3.1)**. Our findings revealed that MOB1A utilises its negatively-charged surface to interact with positively charged residues (K25/R42/R79/K81/R82) of NDR2 **(Figure 3.1b)**. Furthermore, we could divide the recognition interface between NDR2 and MOB1A into two sections **(Figures 3.1e and 3.1f)**. At the first interaction interface, Y32 of NDR2 is at a central position with its side-chain hydroxyl group forming hydrogen bonds with Q67 and H185 MOB1A **(Figure 3.1e)**. Moreover, we observed that K25 of NDR2 forms hydrogen bonds with the main-chains of L173 and Q174 of MOB1A, and L28, L35, and I36 of NDR2 associate with L36, G39, L41, A44, M70, and L71 of MOB1A by van der Waals contacts at first interaction interface. At the second interaction interface, we discovered that L78 of NDR2 forms hydrophobic interaction with W56 and V59 of MOB1A and a salt bridge with E55 of MOB1A **(Figure 3.1f)**. Intriguingly, analyses of the sequence alignments of the NDR/LATS kinases revealed that although most of the MOB1-binding residues are conserved in NDR/LATS kinases from yeast to humans **(Figure 3.2a)**, there is a peculiar subfamily-specific residue corresponding to Y32 of NDR2. In the NDR-subfamily including human NDR1/2, *Drosophila* Tricornered, *S. cerevisiae* Dbf2/Dbf20/Cbk1, and *S. pombe* Sid2/Orb6, the residue at this key position is an invariant tyrosine **(Figure 3.2a)**. In stark contrast, in the LATS-subfamily including human LATS1/2 and *Drosophila* Wts, a valine or isoleucine occurs at this key position **(Figure 3.2a).**

Structure based sequence alignment of the conserved N-terminal regulatory domain of NDR/LATS kinases revealed that the D63 residue of MOB1A is essential for binding to LATS1 **(Figure 3.2b),** but not for binding to NDR2 **(Figure 3.2b)**. Sepecifically, we found that H646 of LATS1 makes a hydrogen bond with D63 of MOB1A **(Figure 3.2b, bottom**

model), whereas F31 of NDR2, the corresponding residue to H646 of LATS1, does not interact with D63 of MOB1A **(Figure 3.2b, top model)**.

In addition to the structural analyses of NDR/MOB1A and LATS/MOB1A complexes **(Figures 3.1 and 3.2)**, we also sought to determine key residues mediating the interaction of MOB1A with the MST1/2 kinases. To do so, we tested by co-immunoprecipitation assays the interactions of a range of MOB1A mutants with wild-type MST1/2 kinases (Hergovich, A., unpublished data now shown). Considering that negatively charged surfaces of MOB1A are responsible for the interactions with positively charged surfaces of NDR/LATS kinases **(see Figures 3.1 and 3.2)** and that MOB1A interacts with MST1/2 kinases differently than with NDR/LATS (Ni, Zheng et al. 2015, Kim, Tachioka et al. 2016), we hypothesized that potentially positively charged residues of MOB1A are central for complex formation with MST1/2. Significantly, we showed that MOB1(KEKE) mutant abolished the interaction with MST2 **(Figure 3.3)**, but not with NDR2 and LATS1 **(Figure 3.3)** by gel filtration chromatography.

Initially, to investigate the importance of the residues required for MOB1A binding to MST1/2, LATS1/2, and NDR1/2, we performed gel filtration chromatography using recombinant proteins. Our findings uncovered that the MOB1(DV) did not interact with LATS1, while binding normally to NDR2 and MST2 **(Figure 3.3)**. The MOB1A(KEKE) also displayed a specific loss of interaction (LOI), since MOB1A(KEKE) did not interact with MST2, but associated normally with NDR2 and LATS1 **(Figure 3.3)**.

To further characterize and confirm the importance of the residues important for MOB1A binding to MST1/2, LATS1/2, and NDR1/2, we tested selected mutant versions of MOB1A in HEK293 cells with regard to binding to full length wild-type versions of MST1/2, LATS1/2, and NDR1/2 kinases **(Figures 3.4, 3.5, and 3.6)**. Significantly, this approach confirmed that MOB1A(DV) only displayed a disruption of the association with LATS1/2 kinases, while MOB1A(DV) bound normally to NDR1/2 and

MST1/2 kinases. In contrast, the MOB1A(KEKE) only displayed a disruption of the interaction with MST1/2 kinases, while MOB1A(KEKE) associated normally with NDR1/2 and LATS1/2 kinases. Noteworthy, MOB1A(DVKEKE) only associated with NDR1/2 kinases, while displaying a complete LOI with MST1/2 and LATS1/2 kinases.

Stavridi et al. (2003) showed that E51 of MOB1A is conserved from yeast to humans and speculated that this residue is very likely of functional importance. Furthermore, Hergovich et al. (2009) demonstrated that the substitution of Glu51 with Lys (E51K) interferes with the interaction with NDR1/2, highlighting the importance of the E51 residue of MOB1A for the interaction with the NDR1/2 kinases. Therefore, we also tested MOB1A(EK) with regard to binding to MST1/2, LATS1/2, and NDR1/2 kinases. This allowed us to confirm that MOB1A(EK) does not bind to NDR1/2 kinases. Moreover, we also discovered that MOB1A(EK) cannot associate with the LATS1/2 and MST1/2 kinases.

Hippo signalling represents a MST/LATS/NDR kinase cascade that is tightly regulated by different protein-protein interactions (Hergovich 2012). Very interestingly, MST/LATS/NDR signalling is regulated by members of the MOB protein family. Recent studies reported that MOB1 knockout mice display much bigger tumour that LATS deficient mice, indicating that MOB1 has LATS independent tumour suppressive role possibly including MOB1/MST and/or MOB1/NDR complexes. Thus, it is crucial to understand the complex protein-protein interaction of MOB1A with the Hippo kinases, such as MST1/2, LATS1/2, and NDR1/2. In this context, we define here key residues of MOB1A that are required for binding to MST1/2, LATS1/2, and NDR1/2 by structural and biochemical studies. More specifically, we managed to generate MOB1A LOI versions that display selective LOI with the Hippo core kinases. Therefore, we are establishing here a foundation that allow us to understand the significance of MOB1A-MST1/2, MOB1A-LATS1/2, MOB1A-NDR1/2 complex formation in the context of Hippo core signalling.

3.2. Defining the importance of complex formation of MOB1A with the Hpo, Wts, and Trc kinases in fly cells

3.2.1. Abstract

The mammalian Hippo core cassette consists of MST/LATS/NDR kinases and MOB1, with recent studies suggesting that MOB1A functions as the central hub of Hippo signalling. In *Drosophila*, the Hpo, Warts, and Trc are the functional counterparts of the mammalian MST1/2, LATS1/2, and NDR1/2 kinases, hence, the Hpo, Wts, and Trc kinases function as key players in the fly Hippo pathway. It was established that functional loss of Hpo, Wts, or Trc can be compensated by expression of human MST, LATS1, or NDR1, respectively. Significantly, expression of human MOB1A can also compensate for the loss-of-function of Mats, the fly Mob1 protein. Therefore, we hypothesized that the interaction patterns of MOB1A with Hpo, Warts, and Trc kinases are conserved from flies to human. Interestingly, we report here that the interaction patterns of MOB1A with the Hpo, Warts, and Trc kinases in *Drosophila* cells are highly similar with the patterns observed in human cells.

3.2.2. Introduction

The Hippo pathway was discovered to control cell proliferation, apoptosis, and differentiation (Hergovich 2013); therefore, the Hippo pathway may play crucial role in coordinating these cellular processes. Importantly, *Drosophila* Hippo signalling is regulated by various protein-protein interactions (Hergovich 2012). Even more importantly, it was found that genetic disruption of the core component of the *Drosophila* Hippo pathway result in robust tissue overgrowth. Furthermore, it was found that these overgrowth phenotypes can be rescued by the counterparts of mammalian proteins (Hergovich 2011).

It is not known how *Drosophila* Hippo signalling is tightly regulated by complex protein-protein interactions involving Mats. Therefore, we hypothesized that MOB1A can also interact with the Hpo, Wts, and Trc kinases (the counterparts of the mammalian MST1/2, LATS1/2, and NDR1/2 kinases) in a similar fashion as reported above for their human counterparts (see summary in **Figure 3.7**). Very interestingly, we show here that the interaction patterns of MOB1A with the Hpo, Warts, and Trc in *Drosophila* cells is highly similar with the patterns observed in human cells (see summary in **Figure 3.7**). Thus, our LOI versions of MOB1A will allow us to understand which protein-protein interactions of MOB1A are important for embryogenesis and tumour suppression in *Drosophila*, in addition to studying their importance in human cancer cells.

3.2.3. Results - Characterization of MOB1A mutants with selective binding to the Hpo/Wts/Trc kinases in fly cells

To expand the characterization of our panel of MOB1A versions **(see figure 3.7)**, we characterized the PPIs between MOB1A variants and the Hpo, Warts, and Trc kinases (the *Drosophila* counterparts of the mammalian MST1/2, LATS1/2, NDR1/2 kinases). Through phylogenetic analysis, it has been shown that *Drosophila* Mats (dMOB1) and human MOB1A shares 87 % identity, strongly suggesting that the functions of Mats proteins are conserved from *Drosophila* to humans (Hergovich 2011). Indeed, Lai et al. (2005) reported that loss of function of Mats can be rescued by expression of MOB1A, supporting the notion that the functions of MOB1A are conserved between flies and humans. In addition, it has been shown that the MST1/2 kinases can regulate MOB1A in a similar manner as reported for the regulation of Mats by Hpo in fly cells (Hergovich, 2011; Wei et al, 2007). Furthermore, it has also been reported that MOB1 and Mats can associate with LATS1/2 and NDR1/2, Warts and Trc kinases, respectively. These findings collectively suggest that the functional importance of PPIs between MOB1A and Hippo core kinases are conserved from insects to humans.

First, the PPIs of our selected MOB1A mutants with Hpo were examined. The results are presented in **Figure 3.8** below.

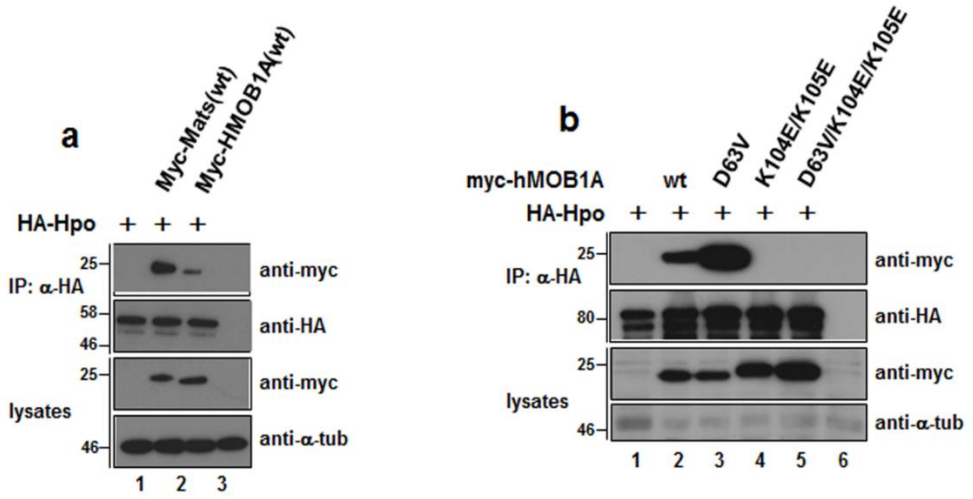

Figure 3.8. Characterization of the interaction of MOB1A variants with the fly Hpo kinase.

(a-b) Lysates of *Drosophila* S2R+ cells expressing full-length HA-Hippo(wt) together with indicated full-length MOB1A versions were subjected to immunoprecipitation (IP) using anti-HA. The KKEE mutations caused loss of binding to Hpo, while the DV mutant bound normally. Complexes were studied by immunoblotting using anti-myc (top) and anti-HA (top middle). Input lysates were probed with anti-myc (bottom middle) and anti-α-tubulin (bottom). Relative molecular weights are shown.

To characterize the interactions of MOB1A(wt) and MOB1A mutants with Hpo, S2R+ cells were co-transfected with N-terminally tagged versions of myc-MOB1A(wt) and myc-MOB1A mutants and HA-Hpo, followed by co-immunoprecipitation using anti-HA antibody. This revealed that Mats and MOB1A(wt) bound similarly to Hpo in S2R+ cells **(Figure 3.8)**, confirming that Mats/Hpo and hMOB1A/Hpo interactions are conserved. As further indicated in **Figure 3.8**, MOB1A(wt) lane and MOB1A(DV), but not the other MOB1A variants, were able to bind to Hpo. Collectively, our data presented in **Figure 3.8** suggest that the MOB1A(KEKE) mutant is deficient in Hpo binding, hence developing a research tool that allow us to understand the role of MOB1A-Hpo complex formation in complex multicellular organism such as *Drosophila*. Noteworthy, the observed interaction pattern in fly cells **(Figure 3.8)** is identical with the one observed in mammalian cells **(Figure 3.7)**.

Second, the PPIs of our selected hMOB1A mutants with Warts were examined. The results are presented in **Figure 3.9** below.

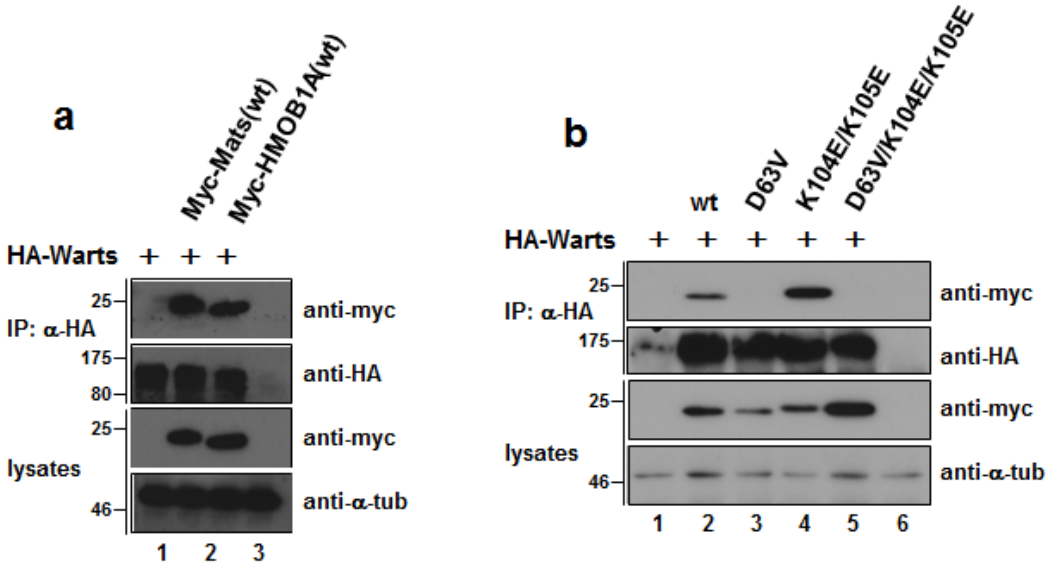

Figure 3.9. Characterization of the interaction of MOB1A variants with the Wts kinase.

(a-b) Lysates of *Drosophila* S2R+ cells expressing full-length HA-Wts(wt) together with indicated full-length MOB1A versions were subjected to immunoprecipitation (IP) using anti-HA. Complexes were analyzed by immunoblotting using anti-myc (top) and anti-HA (top middle). Input lysates were analyzed with anti-myc (bottom middle) and anti-α-tubulin (bottom). Relative molecular weights are shown. The DV mutant did not bind to Warts, while the KEKE mutant bound normally.

To characterize the interactions of MOB1A(wt) and MOB1A mutants with Hpo, S2R+ cells were transfected with N-terminally tagged versions of myc-MOB1A(wt) and myc-MOB1A mutants and HA-Hpo, followed by co-immunoprecipitation using anti-HA antibody. As indicated in **Figure 3.9a,** MOB1A(wt) and Mats were able to bind strongly to Wts. Following that, we characterized the binding of our MOB1A mutants to Wts. This revealed that MOB1A(KEKE) associated with Wts like wild-type MOB1A, while the remaining MOB1A variants did not interact stably with Wts **(Figure 3.9b)**. Collectively, these data suggest that the MOB1A(DV) mutant is deficient in

Wts binding, hence establishing a foundation that allow us to study the significance of MOB1A-Wts complex formation in *Drosophila*. Noteworthy, this interaction pattern is identical with the one observed in mammalian cells **(Figure 3.7)**.

Last, the PPIs of our selected hMOB1A mutants with Trc were examined. The results are illustrated in **Figure 3.10** below.

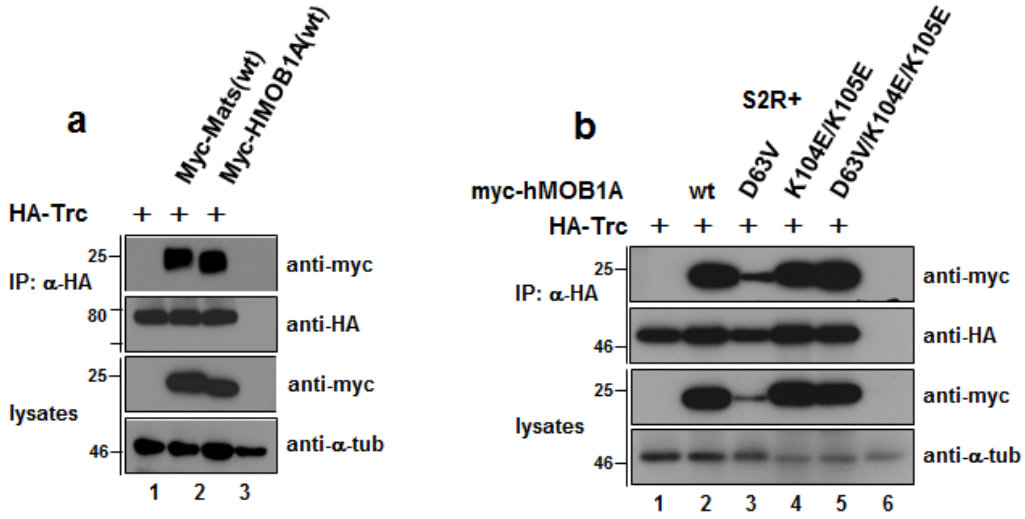

Figure 3.10. Characterization of the interaction of MOB1A variants with the Trc kinase

(a-b) Lysates of *Drosophila* S2R+ cells expressing full-length HA-Trc(wt) together with indicated full-length MOB1A versions were subjected to immunoprecipitation (IP) using anti-HA. Complexes were examined by immunoblotting using anti-myc (top) and anti-HA (top middle). Input lysates were investigated with anti-myc (bottom middle) and anti-α-tubulin (bottom). Relative molecular weights are shown.

To characterize the interactions of MOB1A(wt) and MOB1A mutants and Mats with Trc, S2R+ cells were co-transfected with N-terminally tagged versions of myc-hMOB1A(wt) and myc-MOB1A mutants and HA-Trc, followed by co-immunoprecipitation using anti-HA antibody. As indicated in **Figure 3.10a**, both Mats and MOB1A(wt) were able to associate with Trc. Following that, we characterized the binding of our MOB1A mutants to

Trc. This revealed that all mutants of MOB1A normally bound to Trc like wild-type MOB1A.

Taken together, we show here that MOB1A interacts with the Hpo, Warts, and Hpo kinases in fly cells. In addition, we present the characterization of the interaction patterns of our selected MOB1A versions with the fly Hippo core kinases. This revealed that the MOB1A(DV) can interact with Trc and Hpo, while being unable to associate with Wts. In contrast, MOB1A(KEKE) can interact with Wts and Trc, but does not associate with Hpo. Therefore, we are describing here development of research tools that are suitable to investigate the significance of MOB1A-Hpo, MOB1A-Wts, and MOB1A-Trc complex formation in the context of Mats loss-of-function. Furthermore, our results presented here suggest that the interaction patterns of MOB1A variants in fly cells are nearly identical with the patterns observed in mammalian cells **(Figure 3.11)**.

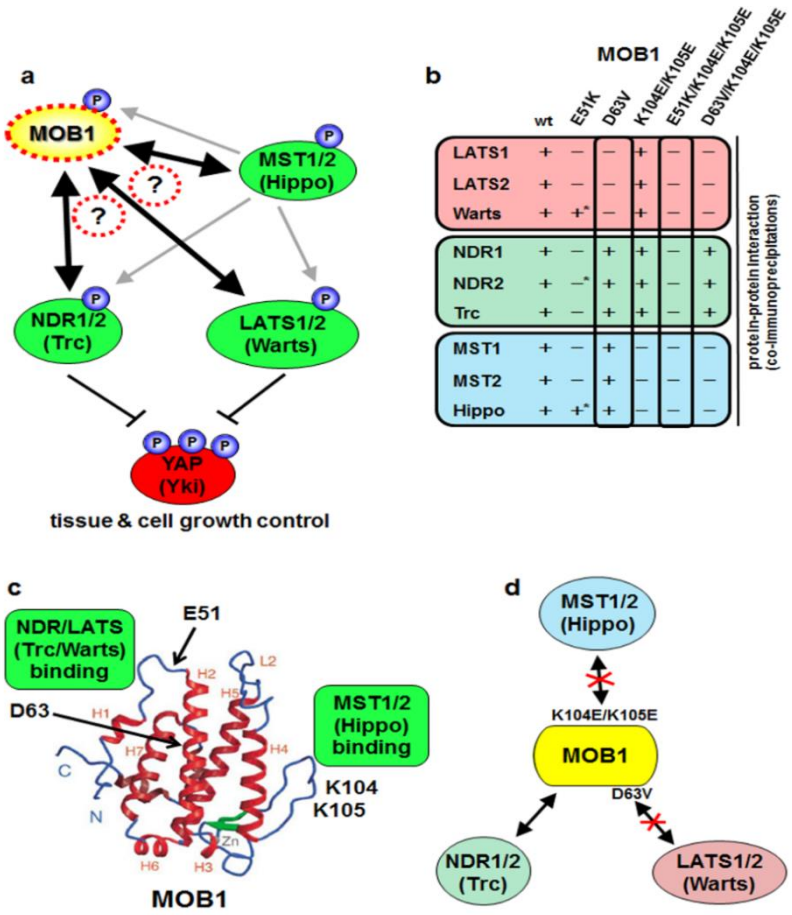

Figure 3.11. Generation of MOB1 variants to dissect the importance of MOB1 interactions with *Drosophila* Hippo core cassette kinases.

(a) Model illustrating two key research questions regarding MOB1 as a hub of *Drosophila* Hippo core signalling: (1) Does MOB1 interact differently with Hippo, Warts and Trc in fly cells? (2) Which interactions of MOB1 with Hippo, Warts, or Trc are biologically important in the context of Yki-Hippo signalling? **(b)** Schematic summary of the biochemical and molecular characterization of the indicated MOB1A variants presented in **Figures 3.8 to 3.10**. **(c)** Model of human MOB1A(33-216) depicting the possibly opposing binding sites on MOB1 of Trc/Warts and Hpo kinases. Secondary structure elements of MOB1 are highlighted. The locations of Asp63, and Lys104/Lys105 in MOB1 are indicated. **(d)** Schematic model of how the differential binding of MOB1 to Hippo, Warts and Trc can be experimentally exploited using the D63V and K104E/K105E mutations in order to study the biological importance of these different interactions of MOB1 with *Drosophila* Hippo core cassette kinases

3.2.4. Discussion

Our structural and biochemical studies of human Hippo core components revealed the identity of key residues in MOB1A that are required for the binding of MOB1A to the MST1/2, LATS1/2, and NDR1/2 kinases **(see section 3.1 above)**. Importantly, our structural and biochemical studies presented above revealed that D63 residue of MOB1A is required for LATS1/2-binding but not NDR1/2-binding, while K104E/K105E residues of MOB1A is key binding residues essential of binding to MST1/2, not LATS1/2 and NDR1/2 kinases. Collectively, these results develop an important tool to study the importance of MOB1A-MST1/2, MOB1A-LATS1/2, and MOB1A-NDR1/2 complex formation in the context of the regulation of Hippo signalling in mammalian cells.

After having revealed the key residues that plays crucial roles in the binding of MOB1A to MST1/2, LATS1/2, and NDR1/2, we asked next whether these residues of MOB1A are also critically important for MOB1A binding to the fly Hpo, Warts, and Trc kinases. To do so, we established first that MOB1A(wt) can interact with the Hpo, Wts, and Trc kinases. We next tested whether the important residues that disrupted binding of MOB1A to the MST1/2, LATS1/2, NDR1/2, respectively, are also important for the interactions of MOB1A with the fly Hippo core kinases Hpo, Wts, and Trc. Significantly, these analyses of PPIs in the fly cell extracts revealed that the interaction patterns in *Drosophila* cells are highly similar with of the patterns observed in mammalian cells. This strongly suggests that the regulation of Hippo core signalling by MOB1A is highly conserved from *Drosophila* to humans. Thus, our selected mutants of MOB1A will allow us to understand which protein-protein interactions are required for embryogenesis, and tissue growth control in *Drosophila*, in addition to performing experiments in human cancer cells.

3.3. Defining phosphorylation patterns of our MOB1A variants by human MST1/2 and fly Hpo kinases

3.3.1. Abstract

The Hippo core pathway is regulated through phosphorylation by MST1 and MST2 kinases. Importantly, recent studies revealed that MST1/2 (Hpo) phosphorylate MOB1A (Mats) at Thr12 and Thr35 in human and *Drosophila*. Our data presented here confirm that MOB1A is phosphorylated at Thr12 and Thr35 by MST1 and MST2 kinases. Thus, we determined next the phosphorylation status of our MOB1A variants by the MST1, MST2, and Hpo kinases, respectively. This revealed that our selected MOB1A variants are normally phosphorylated on Thr12 and Thr35 by MST1, MST2, and Hpo. First, these observations further strengthen the notion that the Hippo pathway is highly conserved from *Drosophila* to humans. Second, our data presented here suggest that any changes in binding patterns of MOB1A versions are very unlikely a consequence of alterations of the phosphorylation status of our selected MOB1A variants.

3.3.2. Introduction

The core of the Hippo pathway consist of MST1/2(Hpo), LATS1/2 (Wts), NDR1/2 (Trc) and MOB1A (Mats) in human (*Drosophila)* cells. In *Drosophila*, Hpo can phosphorylate Mats, thereby enhancing Mats binding to the Wts kinases (Wei, Shimizu et al. 2007). Recent studies revealed that Mats interacts with and regulate Wts allosterically (Lai, Wei et al. 2005, Vrabioiu and Struhl 2015). Moreover, it was also shown that Mats can also interact with Trc and is required for Trc functions in flies (He, Emoto et al. 2005). In mammals, the regulation of Hippo signalling functions in a similar way, though it is more complicated. Praskova *et al*. (2008) identified MOB1A proteins as a substrate of MST1/2. They showed that MST1/2 can phosphorylate MOB1A at Thr12 and Thr35, thereby significantly enhancing the efficiency of MOB1A binding to NTR domains of human NDR1/2 and LATS1/2 kinases (Hergovich, Schmitz et al. 2006, Hergovich, Stegert et al. 2006, Hergovich 2013). On the one hand, the association of MOB1A with NDR/LATS kinases initiates their autophosphorylation in the regulatory T-loop (Bichsel, Tamaskovic et al. 2004, Hergovich, Bichsel et al. 2005, Hergovich, Schmitz et al. 2006, Praskova, Xia et al. 2008, Cook, Hoa et al. 2014, Hoa, Kulaberoglu et al. 2016). On the other hand, binding of MOB1A to NDR/LATS kinases is required for their phosphorylation in the hydrophobic motif by MST1/2 (Praskova, Xia et al. 2008, Hergovich, Kohler et al. 2009, Cook, Hoa et al. 2014, Hoa, Kulaberoglu et al. 2016). Consequently, current evidence suggests that the association of MOB1A with the NDR/LATS kinases is essential for the activation of NDR/LATS kinases. In summary, the binding of MOB1A to NDR/LATS is influenced by MST1/2-mediated phosphorylation of MOB1A (Praskova, Xia et al. 2008, Hergovich 2011), hence one can conclude that MOB1A phosphorylation by MST1/2 plays an important role in the regulation of the Hippo pathway. We therefore examined whether our MOB1A mutants serve as substrates of MST1, MST2, and Hpo, respectively, which revealed that the phosphorylation of our selected MOB1A variants on Thr12 and Thr35 is not significantly changed.

3.3.3. Results - Testing selective MOB1A mutants as MST1/2 substrates

Considering that MST1 and MST2 can function as upstream kinase of MOB1A (Praskova, Xia et al. 2008), we tested whether our MOB1A mutants are phosphorylated by MST1 and MST2 similarly to wild-type MOB1A. To do so, we pursued two lines of *in vitro* kinase assays. First, radioactive *in vitro* kinase assays were performed to measure the total phosphorylation of MOB1A. Second, we utilized specific anti-phospho-antibodies raised against phospho-Thr12 (T12-P) and phosphor-Thr35 (T35-P) to measure MST1/2-mediated MOB1A phosphorylation in our *in vitro* kinase assays.

Prior to the characterization of our MOB1A variants as MST1/2 substrates, recombinant MAL-tagged MOB1A variants were bacterially expressed and then purified as outlined in **section 2.2.2.6** above. Equal amounts of our MAL-MOB1A proteins were analysed by SDS-PAGE followed by Coomassie staining to validate the quality and purity of our protein preparations **(Figure 3.12)**.

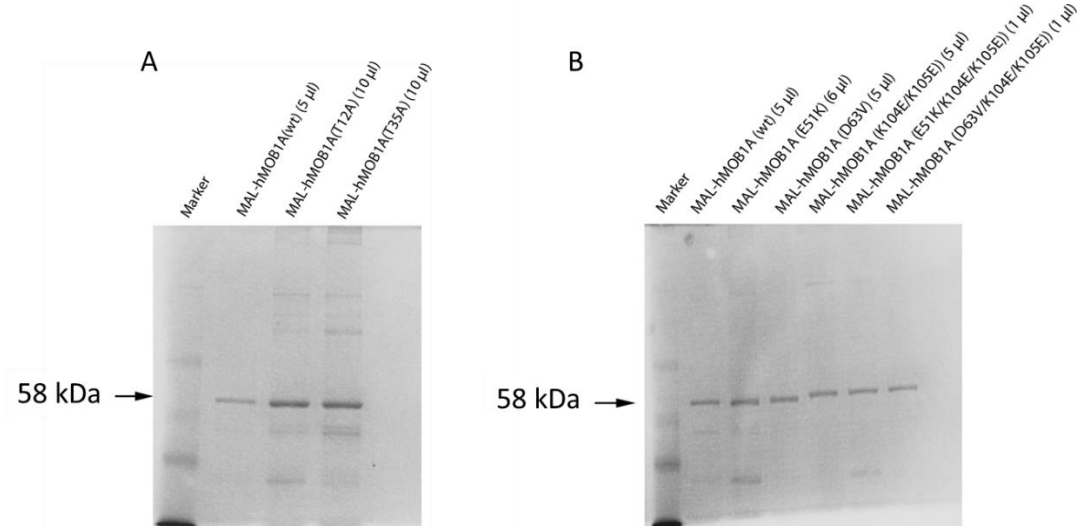

Figure 3.12. Bacterially expressed and purified MAL-MOB1A variants.

All MAL-MOB1A recombinant proteins were bacterially expressed and purified as described in **section 2.2.2.7**. The purified proteins were run on 8 % gel and the gels were stained with Coomassie staining as defined in **section 2.2.2.7**. The location of the recombinant MAL-MOB1A versions are pointed out by an arrow.

After confirming equal quality and purity of our recombinant MAL-MOB1A proteins, equal amounts of recombinant proteins were used as substrates in *in vitro* kinase assays as outlined below.

First, *in vitro* kinase assays using radiolabelled ATP were performed as outlined in **section 2.2.2.6**. The results are presented in **Figure 3.13** below.

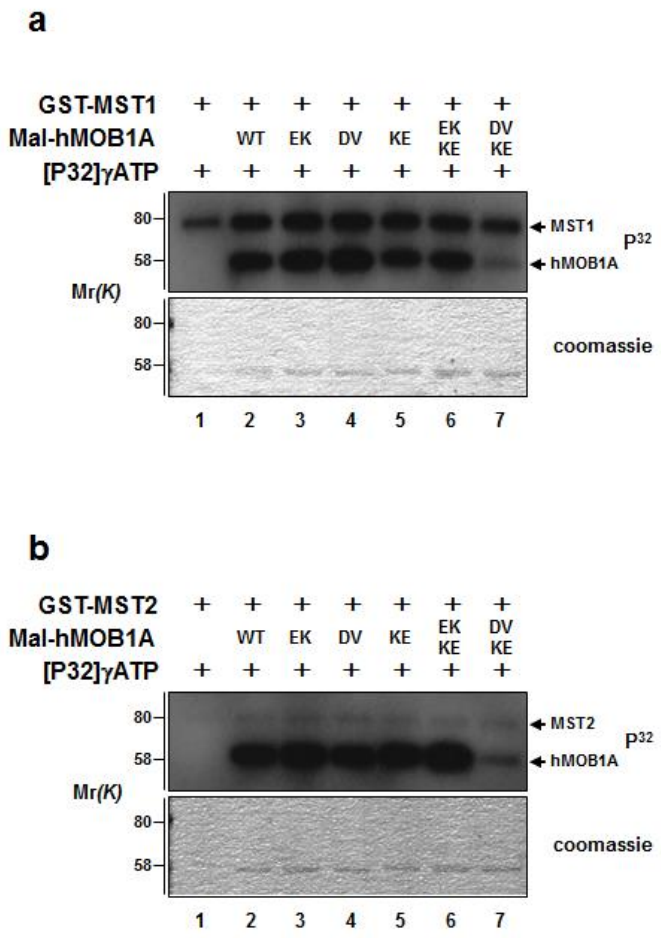

Figure 3.13. Phosphorylation of MOB1A mutants by MST1/2.

GST-tagged full-length MST1 **(a)** and MST2 **(b)** kinases were incubated with purified bacterially expressed MAL-MOB1A proteins as described in **section 2.2.2.6**. As control, GST-MST1 and MST2 were incubated without MAL-MOB1A proteins **(Top panel, lane 1)**. After the kinase reaction, proteins were separated by SDS-PAGE and detected by autoradiography (top panel) or coommassie stain (bottom panel). All MAL-MOB1A variants, except for MOB1A(DVKEKE), displayed the same phosphorylation status. The autophosphorylation of MST1/2 are also visible.

Recombinant GST-tagged MST1 and GST-MST2 kinases were incubated with recombinant MAL-MOB1A variants as substrates using [P32]γATP as a source of ATP, followed by SDS-PAGE and autoradiography. As shown in **Figure 3.13**, all MOB1A mutants tested, except for MOB1A(DVKEKE), were normally phosphorylated by MST1/2 when compared to wild type MOB1A. These results suggest that all MOB1A mutants, with the exception of MOB1A(DVKEKE), serve as MST1/2 substrates like wild-type MOB1A. Considering that MOB1A(EK) and MOB1A(KEKE) were phosphorylated like wild-type MOB1A by MST1/2 **(Figure 3.13)**, although they cannot form a stable complex with MST1/2 **(see section 3.1.4 above)**, these findings further suggested that MOB1A and MST1/2 do not need to stably interact for efficient phosphorylation of hMOB1A by MST1/2. Second, we utilized specific anti-phospho-antibodies raised against phospho-Thr12 (T12-P) and phosphor-Thr35 (T35-P) to measure MST1/2-mediated MOB1A phosphorylation in our *in vitro* kinase assays. However, before testing the phosphorylation status of our MOB1A variants on Thr12 and Thr35, we aimed to validate the specificities of the available anti-T12-P and anti-T35-P antibodies were tested. The results of these specificity tests are presented in **Figure 3.14**.

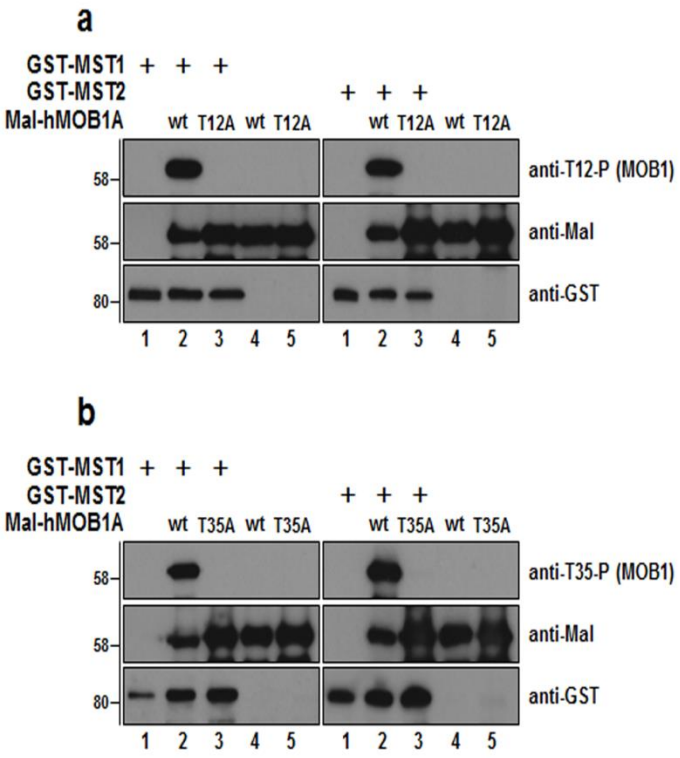

Figure 3.14. Characterization of the anti-Thr12-P and anti-Thr35-P antibodies in the context of MST1/2-mediated phosphorylation of MOB1A.

(a,b) Recombinant full-length GST-MST1 or GST-MST2 wild-type (wt) were incubated with full-length recombinant Mal-MOB1A(wt) or the T12A and T35A phospho-acceptor mutants. Following kinase reactions, the samples were analysed by Western blotting using indicated antibodies. Relative molecular weights are shown. Noteworthy, the anti-T12-P antibody only detected wild-type MOB1A when the kinase assays contained GST-MST1/2, while MOB1A (T12A) was not detected (**a**). The anti-T35-P antibody also specifically detected the phosphorylation of MOB1A on Thr35 (**b**).

Praskova *et al*. showed that MOB1A is phosphorylated at Thr12 and Thr35 by MST1/2. To develop research tools that allow the study of phosphorylation of MOB1A by MST1 and MST2 on Thr12 and Thr35, we characterised antibodies that specifically recognise MOB1A phosphorylated on Thr12 (anti-Thr12-P) and Thr35 (anti-Thr35-P). To test the specificity of these anti-phospho antibodies, we generated phosphor-acceptor mutants carrying Thr12 to Ala (T12A) or Thr35 to Ala (T35A) substitutions, and subsequently compared phosphorylation of recombinant MAL-MOB1A(T12A) and MAL-MOB1A(T35A) with the wild-type MAL-

MOB1A **(Figure 3.14).** *In vitro* kinase assays. *in vitro* kinase assays were performed by incubating recombinant GST-tagged MST1/2 kinases with recombinant MAL-MOB1A variants in the presence of unlabelled ATP, followed by SDS-PAGE and Western blotting using the anti-T12-P and anti-T35-P antibodies. These experiments revealed that MOB1A(wt) display clearly detectable Thr12 and Thr35 phosphorylation **(Figure 3.14, lanes 2)**. Demonstrating the specificity of the anti-phospho antibodies, MOB1A(T12A) and MOB1A(T35A) were not recognized by the anti-T12-P and anti-T35-P antibodies, respectively **(Figure 3.14, compare lanes 2 and 3)**. This confirmed that the anti-T12-P and anti-T35-P antibodies can specifically detect the phosphorylation of MOB1A at Thr12 and Thr35 by MST1 and MST2. Kinase assays that only contained GST-MST1, GST-MST2, or MAL-hMOB1A recombinant proteins were used as additional negative controls **(Figure 3.14)**, further confirming the specificity of the anti-phospho antibodies.

Next, the phosphorylation status of our MOB1A variants by MST1 and MST2 was tested. The results are shown below in **Figure 3.15**.

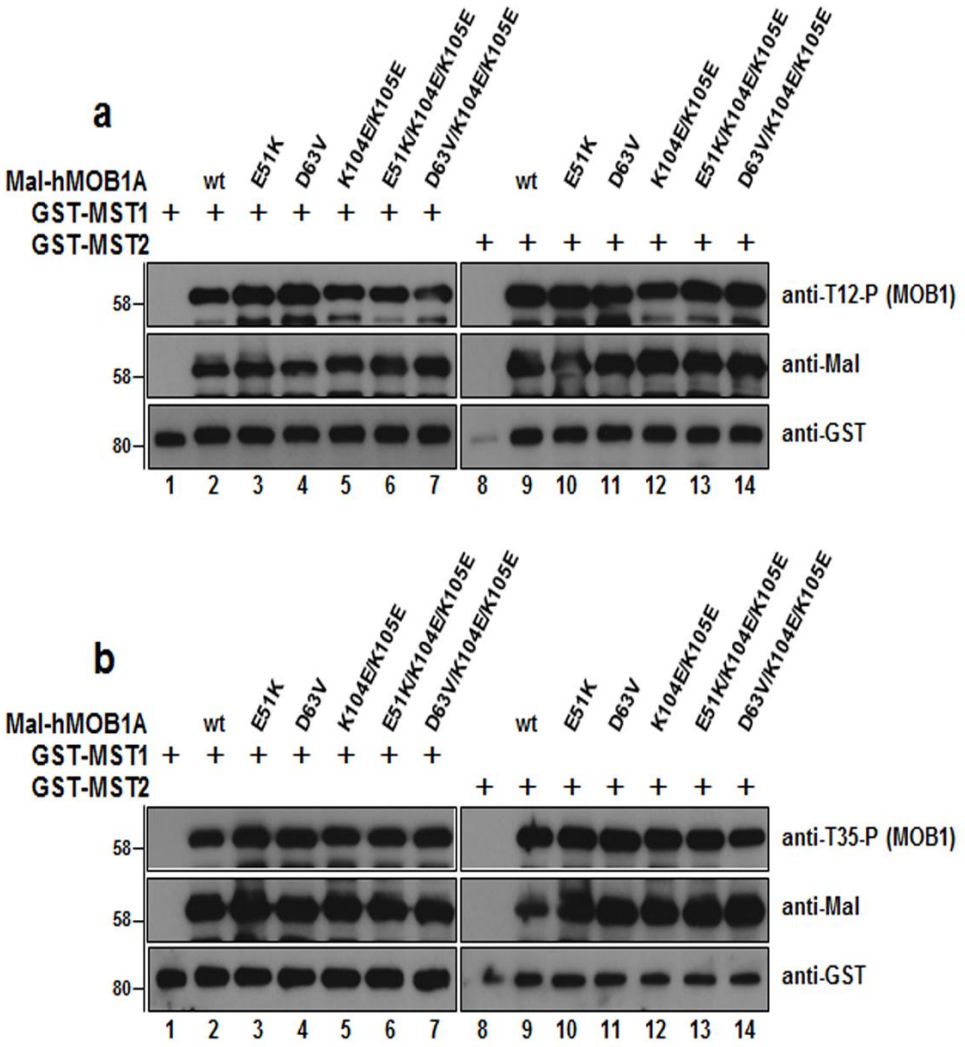

Figure 3.15. Characterization of the MST1/2-mediated phosphorylation of MOB1A variants.

(a,b) Recombinant full-length GST-MST1 or GST-MST2 wild-type (wt) were incubated with indicated full-length recombinant Mal-MOB1A variants. The reactions which only contained MST1 or MST2 were used as control. Following kinase reactions, the samples were analysed by immunoblotting using the specified antibodies. Relative molecular weights are indicated.

More specifically, given the specificity of these phosphor-specific antibodies **(Figure 3.14)**, we sought to determine whether our MOB1A versions are affected with respect to phosphorylation by MST1 and MST2 on Thr12 and Thr35. *In vitro* kinase assays were performed by incubating recombinant GST-MST1 or GST-MST2 kinases with recombinant MAL-

MOB1A variants in the presence of unlabelled ATP, before samples were analysed by SDS-PAGE and Western blotting **(Figure 3.15)**. These experiments showed that our MOB1A versions are phosphorylated on Thr12 and Thr35 by MST1 and MST2 like wild-type MOB1A **(Figure 3.15)**. Collectively, our findings presented in this section suggest that MOB1A and MST1/2 do not need to stably interact for phosphorylation **(Figure 3.7)**. Even more importantly, these findings propose that changes in MST1/2-mediated phosphorylation of MOB1A are very unlikely the cause of the observed alterations of binding patterns of our MOB1A variants.

3.3.4. Results - Testing selective MOB1A mutants as Hpo substrates

Considering that the Thr12 and Thr35 residues of human MOB1A are conserved as Thr12 and Thr35 residues in *Drosophila* Mats protein (the counterpart of human MOB1A) (Lai, Wei et al. 2005), we hypothesized that MOB1A can also be phosphorylated by fly Hpo (the counterpart of human MST1/2). To determine whether MOB1A is also potentially regulated by Hpo in fly cells, the phosphorylation of MOB1A by *Hpo* at Thr12 and Thr35 was tested by using the anti-T12-P and anti-T35-P antibodies. In order to confirm that these anti-phospho-antibodies are also specific in this setting, we compared the phosphorylation of recombinant wild-type MAL-MOB1A with the corresponding phospho-acceptor mutants, MOB1A(T12A) and MOB1A(T35A), respectively **(Figure 3.16)**.

Drosophila S2R+ cells transfected with N-terminally tagged versions of HA-Hpo wild-type were lysed and subjected to overnight IP with anti-HA 12CA5 antibody. Subsequently, *in vitro* kinase assays were performed by incubating immune-purified HA-Hpo with recombinant MAL-MOB1A proteins in the presence of unlabelled ATP. The *in vitro* kinase assay samples were then separated by SDS-PAGE, , followed by Western blotting with anti-T12-P(MOB1) an anti-T35-P(MOB1) antibodies. The results are presented below in **Figure 3.16**.

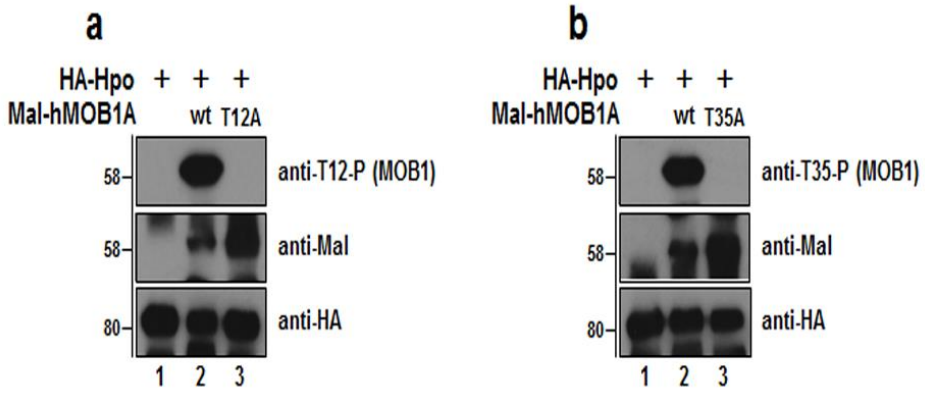

Figure 3.16. Characterization of the anti-Thr12-P and anti-Thr35-P antibodies in the context of Hippo-mediated phosphorylation of MOB1A.

(a-b) Lysates of *Drosophila* S2R+ cells transiently expressing full-length HA-Hpo(wt) were subjected to immunoprecipitation with anti-HA 12CA5 antibody. Immunopurified proteins were then processed for kinase assays without or with the indicated full-length recombinant MOB1A versions. Following kinase reactions, the samples were examined by immunoblotting using the specified antibodies. Relative molecular weights are shown. Importantly, the anti-T12-P and anti-T35-P antibodies specifically detected Hippo-mediated phosphorylation of MOB1A on Thr12 (c) and Thr35 (d).

Significantly, these experiments revealed that Hpo can phosphorylate MOB1A on Thr12 and Thr35 **(Figure 3.16)**. The recombinant MAL-MOB1A(T12A) and MAL-MOB1A(T35A) proteins served as negative controls, showing that the anti-phospho antibodies are specific also when the fly Hpo kinase is used.

Considering that MOB1A is specifically phosphorylated by Hpo **(see Figure 3.16 above)**, we sought next to determine the phosphorylation status of our MOB1A variants is affected by the fly Hpo kinase. The results are presented below in **Figure 3.17**.

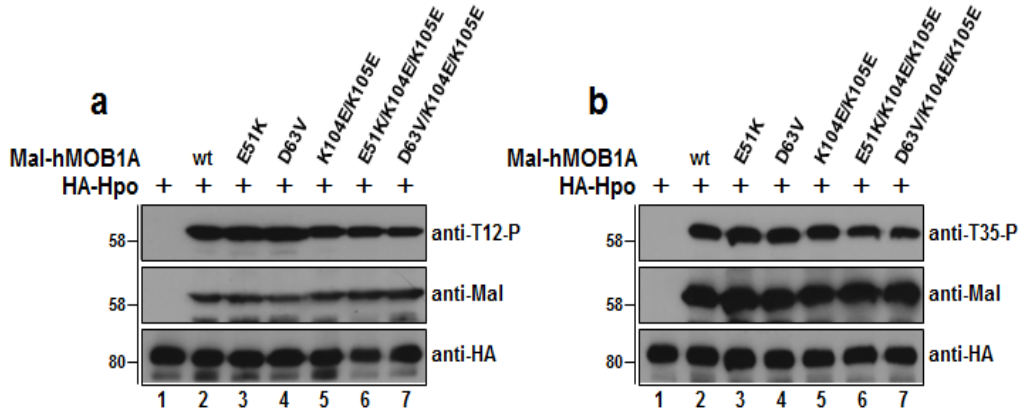

Figure 3.17. Characterization of the MST1/2(Hippo)-mediated phosphorylation of MOB1A variants.

(a-b) Lysates of *Drosophila* S2R+ cells transiently expressing full-length HA-Hpo(wt) were subjected to immunoprecipitation with anti-HA. Immunopurified Hpo was then processed for kinase assays with the indicated full-length recombinant MOB1A versions. Following kinase reactions, the samples were examined by immunoblotting using indicated antibodies. Relative molecular weights are shown.

To test the phosphorylation status of our selected MOB1A variants, HA-Hpo was immune-purified from *Drosophila* S2R+ cells using anti-HA 12CA5 antibody. Immunoprecipitated HA-Hpo was then incubated with recombinant MAL-MOB1A variants in the presence of unlabelled ATP, before processing for SDS-PAGE and immunoblotting with anti-phospho antibodies. As shown in **Figure 3.17**, these experiments revealed that our MOB1A variants are phosphorylated at Thr12 and Thr35 by Hpo very comparable to wild-type MOB1A. Therefore, we can draw the conclusion that the phosphorylation of our MOB1A mutants by Hpo is not significantly affected, as already observed when human MST1 and MST2 were tested **(see section 3.3.3 above) (Figure 3.15)**.

3.3.5. Discussion

Taken together, our study presented here provides novel insights into the phosphorylation of MOB1A by MST1, MST2, and Hpo. Our data presented here confirm that MOB1A is phosphorylated at Thr12 and Thr35 sites by MST1 and MST2 **(Figure 3.14)**. Since MOB1A phosphor-acceptor mutants carrying Thr12 to Ala (T12A) and Thr35 to Ala (T35A) substitutions failed to be phosphorylated by MST1 and MST2 **(Figure 3.14)**, we can be sure that these phosphorylation events are specific. We characterized and defined the important residues that selectively impair the binding of MOB1A to the Hippo core kinases MST1/2(Hpo), LATS1/2(Wts), and NDR1/2(Trc) in mammalian (fly) cells in **section 3.2 and 3.3**. In this section, we tested the phosphorylation of our selected MOB1A variants by MST1, MST2, and Hpo. Significantly, our data presented here uncover that our MOB1A variants are normally phosphorylated on Thr12 and Thr35 by MST1, MST2, and Hpo like wild-type MOB1A **(Figure 3.15 and 3.17)**. Collectively, we can draw the conclusion that MOB1A-MST1/2(Hpo) complex formation is not required for phosphorylation **(Figure 3.7)**. Even more importantly, these findings suggest that changes in MST1/2(Hpo)-mediated phosphorylation of MOB1A are very unlikely the cause of the observed alterations of binding patterns of our MOB1A variants.

3.4. Defining the tumour suppressive roles for MOB1A interactions with Hippo core kinases in human cancer cells

3.4.1. Abstract

The central mammalian Hippo core cassette consists of MST1/2, LATS1/2, NDR1/2 and MOB1, with recent studies of MOB1 knockout mice indicating that MOB1 functions as the central hub of Hippo signalling. More specifically, current evidence suggests that the Hippo core kinases are regulated by various protein-protein interactions with MOB1A as a kind of master regulator of Hippo tumour suppressor signalling. However, it has yet to experimentally shown that the tumour suppressive roles of the Hippo pathway are indeed regulated by interactions of MOB1A with Hippo core kinases. Therefore, we focused on deciphering the complex protein-protein interactions of MOB1 with MST1/2, LATS1/2 and NDR1/2 required for tumour suppression in human cancer cells. Using our MOB1A mutants, we studied the effects of MOB1A expression on the proliferation and anchorage-independent growth of human cancer cells, aiming to establish which MOB1 interactions are required for the tumour suppressive role of MOB1A. Interestingly, we found that wild-type MOB1A functions as tumour suppressor by inhibiting cell proliferation and anchorage-independent growth of human cancer cells. More importantly, we further found that the interaction of MOB1A with MST1/2 or LATS1/2 is not required to suppress proliferation. We also discovered that complex formation of MOB1A with MST1/2 is dispensable for the suppression of anchorage-independent growth of human cancer cells, while the interactions with LATS1/2 and NDR1/2 appear to be essential for the tumour suppressive function of MOB1A.

3.4.2. Introduction

The mammalian Hippo pathway has emerged as an essential tumour suppressor signalling network that controls cellular processes such as cell proliferation, cell death, and cell differentiation to ensure normal tissue development (Halder and Johnson 2011, Hergovich 2013, Yu and Guan 2013). Dysregulation of the Hippo pathway is linked to different types of human cancers (Harvey, Zhang et al. 2013), clearly indicating that mammalian Hippo signalling function as a tumour suppressor pathway. Various genetic and biochemical studies have shown that the Hippo pathway is tightly regulated by various protein-protein interactions. Traditionally, activation of MST1/2 kinases triggers the phosphorylation and subsequently activation of the LATS1/2 kinases and MOB1A. In this regard, the interaction of MOB1A with LATS1/2 is an important step for LATS1/2-mediated phosphorylation and inactivation of YAP/TAZ (Hergovich 2012, Hoa, Kulaberoglu et al. 2016). In its on-state, mammalian Hippo signalling inactivates YAP/TAZ by LATS1/2-stimulated phosphorylation of YAP/TAZ through MST-MOB1A-LATS signalling. However, recent studies identified the NDR1/2 kinases as novel members of the core cassette of the Hippo pathway. More specifically, it was shown that NDR1/2 kinases can phosphorylate YAP on different residues, thereby resulting in the inactivation of YAP by cytoplasmic retention (Zhang, Tang et al. 2015). Furthermore, it was reported that NDR1/2 function as downstream of MST1, MST2, and MST3, and regulated by MOB1A binding (Hergovich, Stegert et al. 2006, Hergovich 2011, Hergovich 2013). Therefore, like LATS1/2, the NDR1/2 kinases can also function in Hippo core signalling as upstream kinases of YAP.

Taken together, mammalian Hippo signalling is regulated by complex protein-protein interactions and phosphorylation events. However, it is currently unknown how Hippo signalling is controlled by the various protein-protein interactions of MOB1 with Hippo core kinases. In this context, studies of MOB1 knockout mice already indicate that MOB1 functions as a central hub of Hippo signalling in tumour suppression, since (Nishio, Hamada et al. 2012, Nishio, Sugimachi et al. 2016) (Harvey, Zhang

et al. 2013). These studies further suggest that MOB1A has LATS1/2 and MST1/2 independent tumour suppressive functions possibly including the interaction of MOB1 with NDR1/2. Therefore, it is crucial to understand how MOB1A, as a central hub of Hippo signalling, differentially associate with the Hippo core kinases MST1/2, LATS1/2, and NDR1/2, thereby play important roles in tumour suppression. Therefore, we used our MOB1A variants as defined in **Sections 3.1, 3.2, 3.3** to test which protein-protein interactions of MOB1 with Hippo core kinases are required for the suppression of cell proliferation and cellular transformation. Interestingly, our findings revealed that the association of MOB1A with MST1/2 or LATS1/2 is not essential for the suppression of cell proliferation. Moreover, we uncovered that the interaction of MOB1A with MST1/2 is dispensable for the suppression of anchorage-independent growth of human cancer cells, while the interactions with LATS1/2 and NDR1/2 appear to be essential for the tumour suppressive function of MOB1A

3.4.3. Results

Mammalian Hippo signalling can be regulated through complex protein-protein interactions of MOB1 with the Hippo core kinases MST1/2, LATS1/2, and NDR1/2 kinases. Considering that MOB1 deficient mice develop larger tumours with a broader range of tumour types than that of mice deficient for LATS1/2 or MST1/2, one can draw the conclusion that MOB1 functions as central hub of core Hippo signalling and has LATS1/2 and MST1/2 independent tumour suppressive functions possibly including the interaction of MOB1 with NDR1/2. Thus, we exploited our MOB1A variants as defined in **Sections 3.1, 3.2, 3.3** to understand which protein-protein interactions of MOB1 with Hippo core kinases are essential for the suppression of cell proliferation and cellular transformation. To do so, we investigated two cell biological processes of human cancer cells. First, we examined whether MOB1 can function as a tumour suppressor by regulating cell proliferation. Second, we sought to study whether MOB1 can suppress anchorage-independent growth.

To address our first aim, we generated human breast cancer MCF-7 cells stably expressing our MOB1A mutants forms as outlined in **section 2.2.3.5**. Lysates of transgenic MCF-7 cells were analysed by Western blotting to confirm the expression of our MOB1 versions **(Figure 3.18a)**. Subsequently, cell proliferation rates of these cell pools were determined. The results are presented in **Figure 3.18** below.

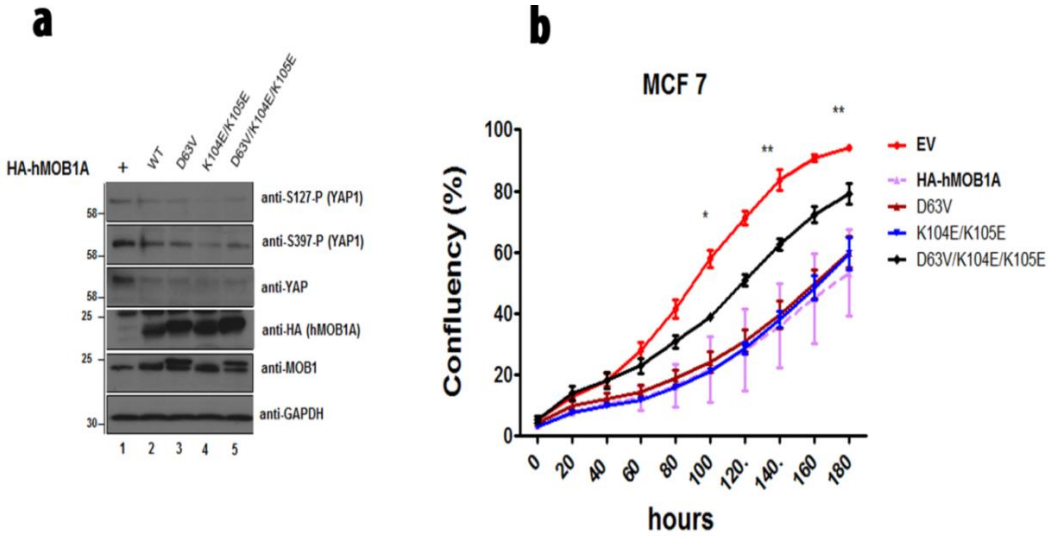

Figure 3.18. MOB1A functions as tumour suppressor by decreasing cell proliferation.

(a) Lysates of MCF-7 cells stably expressing indicated cDNAs were processed for immunoblotting using indicated antibodies. Noteworthy, in spite of empty vector **(lane 1)**, overexpression of the indicated hMOB1As **(lanes 2, 3, 4, and 5)** resulted in the decreased levels of total YAP1 comparable to empty vector **(lane 1)**. Relative molecular weights are shown. **(b)** In parallel, the proliferation of MCF-7 cells stably expressing indicated cDNAs was monitored using IncuCyte live cell imaging for the indicated time periods. Data represent the average of three experiments performed in triplicates using cell pools that were generated independently three times (n=3, **p*<0.05; ***p*<0.01; ****p*<0.001; ns, not significant, compared to EV). Of note, all cell pools expressing indicated MOB1A variants displayed decreased cell proliferation compared to empty vector expressing cells.

To test whether MOB1A can function as a tumour suppressor by suppressing human cancer cell proliferation, we stably expressed our MOB1A mutants in MCF-7 cells **(Figure 3.18a)**, and then monitored the proliferation of these cell pools stably expressing our MOB1A mutants **(Figure 3.18b)**. Importantly, this revealed that MOB1A(wt) can function as a tumour suppressor by decreasing cell proliferation of human cancer cells **(Figure 3.18b, violet line)**. We further observed that the levels of total and phosphorylated YAP1 were decreased upon expression of MOB1A(wt) **(Figure 3.18a, compare lanes 1 and 2).** Surprisingly, expression of MOB1A(DV) or MOB1A(KEKE) resulted in decreased YAP1 levels and suppression of cell proliferation **(Figure 3.18)**, suggesting that the

interaction of MOB1A with LATS1/2 or MST1/2, respectively, is dispensable for this tumour suppressive function of MOB1A. In contrast, cells expressing MOB1A(DVKEKE) did not suppress cell proliferation like wild-type MOB1A **(Figure 3.18b, compare black and violet lines)**, although YAP1 protein levels were decreased like in cells expressing wild-type MOB1A **(Figure 3.18a, compare lanes 2 and 5)**. This finding indicates that the combined loss of binding to LATS1/2 and MST1/2 by MOB1A is impairing the tumour suppressive function of MOB1A without affecting the suppression of YAP1. Nevertheless, since MOB1A(DVKEKE) expressing cells still decrease proliferation and YAP1 levels when compared to empty vector (EV) expressing controls **(Figure 3.18b, compare red and black lines)**, this finding further suggests that in addition to MST1/2 and LATS1/2 other YAP1 regulators are likely to be supported by MOB1A. Considering that MOB1A(DVKEKE) still binds normally to the NDR1/2 kinases (see **sections 3.1, 3.2, 3.3**), it is quite likely that in our proliferation setting NDR1/2 remain their function as YAP regulators.

Taken together, we report here that MOB1A can function as a tumour suppressor by controlling the YAP1 onco-protein. Furthermore, by using our hMOB1A mutants we could address which protein-protein interactions of MOB1 with Hippo core kinases are required for cell proliferation, which revealed that the association of MOB1A with MST1/2 or LATS1/2 is not essential for the suppression of cell proliferation. Furthermore, our data revealed that NDR1/2 function as YAP regulator in cell proliferation setting **(Figure 3.18)**.

Next, to address our second aim, we generated MCF-7 cells stably expressing our MOB1A variants. Lysates of infected MCF-7 cells were analysed by Western Blotting to confirm expression of our MOB1A versions **(Figure 3.19a)**. Subsequently, anchorage-independent growth assays were performed as described in **(section 2.2.3.7)**. The results are presented in **Figure 3.19** below.

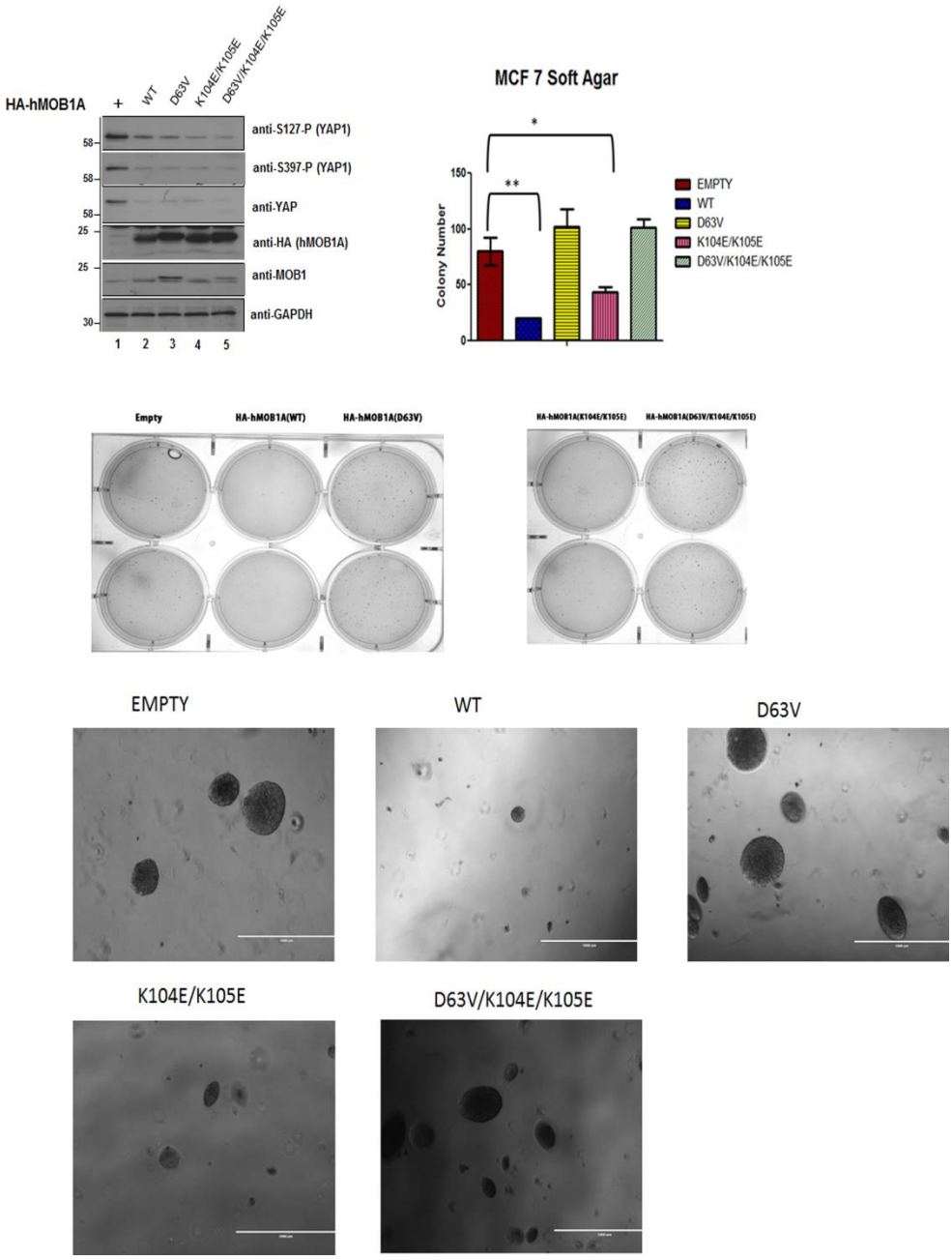

Figure 3. 19. MOB1A can suppress proliferation and anchorage-independent growth of human cancer cells through different interactions with Hippo core cassette kinases.

(a) Immunoblotting with indicated antibodies of cell lysates derived from MCF-7 human breast cancer cells stably expressing the indicated HA-MOB1 variants or empty vector (EV). Relative molecular weights are indicated. **(b)** Quantifications of the soft agar growth assays shown in **c**. The average of three experiments performed in duplicates is shown (n=3, *p<0.05; **p<0.01; ***p<0.001; ns, not significant, compared to EV). P values are as follows: EV vs WT is 0.0014, EV vs DV is 0.7526, EV vs KEKE is 0.0245, EV vs DVKEKE is 0.1143 **(d)** Representative images are displayed.

To test whether MOB1A expression can play a role in suppressing anchorage-independent growth of human cancer cells, we infected MCF-7 cells with retrovirus expressing MOB1A(wt) or EV and subsequently set up anchorage independent assay as described in **section 2.2.3.7**. Importantly, we discovered that MOB1A expression can significantly inhibit anchorage independent growth of MCF-7 cells **(Figure 3.19)**. It has been shown that YAP1 overexpression can effectively induce anchorage independent growth of non-tumour breast cancer MCF10A cells (Overholtzer, Zhang et al. 2006). Thus, we examined the levels of total YAP expression in our cell pools, revealing that total YAP1 expression is dramatically decreased in MOB1A(wt) expressing cells compared to empty vector controls **(Figure 3.19a, compare lanes 1 and 2)**.

Next, we asked which protein-protein interactions of MOB1A with Hippo core kinases are required for suppressing anchorage-independent growth of MCF-7 cells. To do so, we tested cell pools expressing our MOB1A mutants in anchorage independent growth assays **(Figure 3.19)**. We found that MOB1A(KEKE) expression can effectively inhibit anchorage independent growth as observed in MOB1A(wt) expressing cells **(Figure 3.19)**. In stark contrast, expression of MOB1A(DV) or MOB1A(DVKEKE) failed to inhibit anchorage-independent growth **(Figure 3.19)**, suggesting that the interaction of MOB1A with the LATS1/2 kinases is essential for this tumour suppressive function of MOB1A.

Taken together, in full support of our cell proliferation experiments **(Figure 3.18)**, we show here that MOB1A(wt) can function as a tumour suppressor by inhibiting anchorage independent growth of MCF-7 cancer cells. Furthermore, our data revealed that complex formation of MOB1A with MST1/2 is dispensable for these tumour suppressive functions of MOB1A, while the interactions of MOB1A with the LATS1/2 and NDR1/2 kinases are required for the suppression of cellular transformation phenotypes of MCF-7 cells.

3.4.4. Discussion

The Hippo pathway is known as a master regulator of organ size control regulating cell, proliferation, death and cellular transformation (Harvey, Zhang et al. 2013, Hergovich 2013, Yu and Guan 2013, Johnson and Halder 2014). Uncontrolled cell proliferation, death, cellular transformation are regarded as main hallmarks of cancer development (Hanahan and Weinberg 2011). Mammalian Hippo signalling is tightly regulated by complex protein-protein interactions of MOB1 with the Hippo core kinases MST1/2, LATS1/2, and NDR1/2 kinases. However, very little is known about how MOB1, as central hub of the Hippo pathway, differentially associates with MST1/2, LATS1/2, and NDR1/2 and thereby potentially plays diverse tumour suppressive roles. In this regard, we molecularly characterized the interactions of MOB1A with MST1/2, LATS1/2, and NDR1/2 as outlined in **sections 3.1, 3.2, and 3.3.** Here, to cell biologically investigate the roles of MOB1A in tumour suppression, we generated MCF-7 cells stably expressing MOB1A(wt) and subsequently analysed cell proliferation rates and anchorage independent growth. Interestingly, our results revealed that MOB1A can function as a tumour suppressor by dramatically decreasing cell proliferation and anchorage independent growth **(Figures 3.18 and 3.19)**. Considering that the total protein levels of the proto-oncoprotein YAP1 also decreased upon MOB1A(wt) expression **(Figures 3.18a and 3.19a)**, it is tempting to draw the conclusion that the diminished proliferation and anchorage-independent growth of MCF-7 cells expressing MOB1A(wt) was caused by the decrease in YAP1 levels.

Even more importantly, we used our MOB1A mutants to address which protein-protein interactions of MOB1A with Hippo core kinases are required for the suppression of cell proliferation and anchorage-independent growth of human cancer cells **(Figures 3.18 and 3.19)**. Furthermore, on the one hand, our cell proliferation experiments uncovered that the interaction of MOB1A with MST1/2 or LATS1/2 is not essential for suppressing proliferation. On the other hand, our anchorage independent growth assay revealed that complex formation of MOB1A with MST1/2 is dispensable for the suppression of anchorage-independent growth of human cancer cells,

while the interactions with LATS1/2 and NDR1/2 appear to be required for the tumour suppressive function of MOB1A.

3.5. Defining the tumour suppressive roles of MOB1A interactions with the Hippo core kinases in *Drosophila melanogaster*

3.5.1. Abstract

In *Drosophila*, the Hippo pathway is an essential signalling cascade which is required for normal development and tissue growth control. The central Hippo core cassette in *Drosophila* consists of the Hippo core kinases Hpo, Wts, and Trc (the counterparts of human MST1/2, LATS1/2, and NDR1/2), as well as Mats (the counterpart of human MOB1A/B). A recent study showed that loss-of-function of Mats results in embryonic homozygous lethality and severe tissue overgrowth phenotype in mosaic eyes, suggesting that Mats functions as a central hub of fly Hippo signalling. Very interestingly, the same study also showed that the tissue overgrowth phenotype caused by Mats loss-of-function can be rescued by expression of human MOB1A, suggesting that the regulation of Hippo signalling by MOB1A/Mats is highly conserved from *Drosophila* to humans. Therefore, we sought to determine whether MOB1A expression can also rescue the homozygous lethality driven by Mats loss-of-function. Indeed, we discovered that the homozygous lethality caused by *mats* loss-of-function can be rescued by MOB1A expression. We therefore used the *MOB1A* rescue of the *mats* mutation in flies as a paradigm to test the importance of MOB1A interaction with its partners by introducing into flies *MOB1A* transgenes bearing various mutations. Intriguingly, the study of these flies revealed that the Hippo/MOB1A interaction is neither required for life nor for tumour suppression (suppression of tissue overgrowth), while the other interactions of MOB1A with Hippo core cassette kinases are essential in a context-dependent manner.

3.5.2. Introduction

The coordination of cell growth, proliferation, and death determines the appropriate number of cell in tissue and thereby organ size (Harvey, Zhang et al. 2013). Dysregulation of these processes can result in cancer development (Harvey, Zhang et al. 2013). Recent studies discovered Hippo signalling as a master regulator of these processes in *Drosophila melanogaster*. *Drosophila* Hippo core signalling consists of the Hippo core kinases Hpo, Wts, Trc, as well as the signal transducer Mats (Hergovich 2016). Mechanistically, Hpo phosphorylates and thereby activates Wts and Mats (Yang, Cron et al. 2002). The complex composed of Mats/Warts then phosphorylates and thereby inhibits Yorkie (the counterpart of human YAP/TAZ) (Hergovich 2013). The phosphorylation of Mats by Hpo seems to play a crucial role in promoting the association of Mats with Wts and ultimately the activation of Warts (Wei, Shimizu et al. 2007, Zheng, Wang et al. 2015), although this activation model has been challenged recently (Vrabioiu and Struhl 2015). Moreover, it was also shown that Mats also can associate with Trc and that complex formation of Trc with Mats can play an important role in the regulation of fly wing development (He, Emoto et al. 2005, Hergovich 2012, Hergovich 2016). Indeed, Mats mutant cells in fly wing display phenotypes that are typical of Trc and Wts deficiency (He, Emoto et al. 2005), strongly suggesting that Mats can be essential for Trc and Warts signalling.

Taken together, *Drosophila* Hippo signalling is regulated by various protein-protein interactions involving the Mats (aka dMOB1) as a central signal transducer. Recent findings actually show that the core components of the Hippo pathway are evolutionally conserved from *Drosophila* to humans (Geng, He et al. 2000, Wu, Huang et al. 2003, Lai, Wei et al. 2005, Hergovich 2011). However, it is currently unknown how the *Drosophila* Hippo pathway is regulated by the protein-protein interactions of Mats/dMOB1 with the Hippo core kinases. Specifically, it is vital to understand how Hpo/Wts/Trc kinase signalling is regulated by Mats. A recent report using conformation sensors proposed that the Wts/Mats complex formation is required for allosteric Wts activation, while the

Hpo/Mats interaction seem to be dispensable (Vrabioiu and Struhl 2015). However, these findings are solely based on FRET conformation sensors and the actual molecular basis of Wts activation by Mats remains unknown. Hence, experimental evidence using full-length proteins carrying selective manipulations is yet outstanding. We report here that the expression of MOB1A(wt) can rescue the homozygous lethality driven by Mats loss-of-function. Moreover, our study of MOB1A variants in transgenic flies revealed that the Hippo/MOB1A interaction is neither required for viability nor for tumour suppression. In contrast, the interactions of MOB1A with the other Hippo core cassette kinases Wts and Trc are essential in a context-dependent manner.

3.5.3. Results – The characterisation of *mats* loss-of-function and transgenic flies expressing MOB1A variants

Lai et al (2005) observed that *mats* loss-of-function causes embryonic lethality, with increased cell proliferation and tissue overgrowth in mosaic clones. More importantly, they showed that expression of human MOB1A(wt) in Mats mutant clones compensated for the *mats* loss-of-function in larval eye discs (Lai, Wei et al. 2005). Since MOB1A expression can rescue *mats* loss-of-function phenotype in mosaic clones, we speculated that MOB1A expression may compensate for the embryonic lethality caused by *mats* loss-of-function. To test this hypothesis, we generated transgenic flies expressing myc-tagged MOB1A(wt) under the control of the *ubiquitin 63E* promoter (*ubi>myc-hMOB1A(wt)*. Furthermore, to understand which PPIs between MOB1A and Wts, Trc, Hpo are required to prevent embryonic lethality, we also generated transgenic flies expressing our MOB1A variants in the same locus using the ΦC31 integrase system. However, before we could test whether the embryonic lethality caused by *mats* loss of function can be rescued by MOB1A(wt) expression, we confirmed that *mats* trans-heteroallelic combinations result in the homozygous embryonic lethality in our setting. The crosses outlined in **Figure 3.20**.

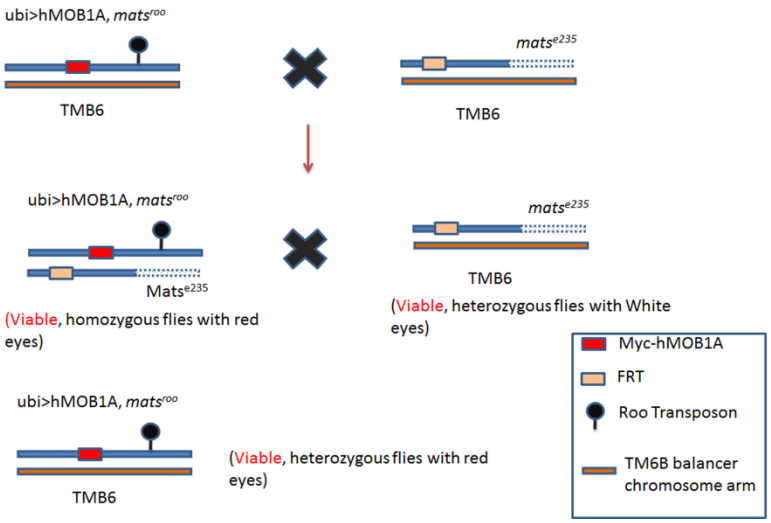

Figure 3.20. Confirmation of the homozygous lethality caused by *mats* loss-of-function.

The aim of this cross was to confirm that the lethality is caused by *mats* loss-of-function, independently of additional mutations in in the available *mats* mutants stocks. Female virgin w;; FRT82B, $mats^{roo}$/ TM6B flies were crossed with male w;; FRT82B, $mats^{e235}$/ TM6B flies as outlined. After this crossing, only heterozygous flies developed to adulthood, while homozygous flies failed to develop

To confirm that the homozygous lethality driven by *mats* results from *mats* loss-of-function, flies carrying two independent *mats* mutant alleles ($mats^{roo}$ and $mats^{e235}$) were crossed **(Figure 3.20)**. The $mats^{e235}$ mutant allele was generated by P-element mobilisation (Lai, Wei et al. 2005), which is the process of imprecise transposon excision leading to deletion of surrounding genomic sequences. $mats^{235}$ results in deletion of most of the *mats* coding sequence. The $mats^{roo}$ mutant allele is an insertion of a 428 base pair Roo transposon at the beginning of the *mats* third exon (Lai, Wei et al. 2005), leading to premature termination of the Mats protein. Both alleles are though to be null for the *mats* locus. As expected, these alleles failed to complement each other, confirming the lethality of the *mats* mutations (**Figure 3.20).**

After confirming that *mats* loss-of-function results in homozygous embryonic lethality **(see section 3.5.3 above)**, we sought to test whether *MOB1A(wt)* can compensate for the embryonic lethality driven by *mats* loss-of-function. To do so, the $mats^{roo}$ transgene was recombined into the proximity of the chromosomal arm where our MOB1A(wt) transgene was integrated **(see section 2.2.5.3)**. MOB1A(wt) and MOB1A variants were inserted on third chromosome at cytological location 89E11 using the ΦC31 integrase-mediated transgenesis system, which utilises the recombination between an attP docking site and the bacterial attachment attB site **(Figure 3.21a)**. For the recombination of the $Mats^{Roo}$ transgene, Virgin w;; ubi>myc-hMOB1A, endogenous Mats/ FRT82B, $Mats^{roo}$ flies were crossed with male +/TM6B flies **(see section 2.2.5 for further details)**. Importantly, to ensure that MOB1A(wt) and MOB1A mutants are expressed equally, we performed Western blot analysis of transgenic flies **(see Figure 3.21b)**. Our results presented in **Figure 3.21b** show that MOB1A(wt) and MOB1A variants are expressed equally. After the required recombination

and confirmation of equal expression of our MOB1A variants in the different fly lines, we performed the crosses presented in **Figure 3.21c**.

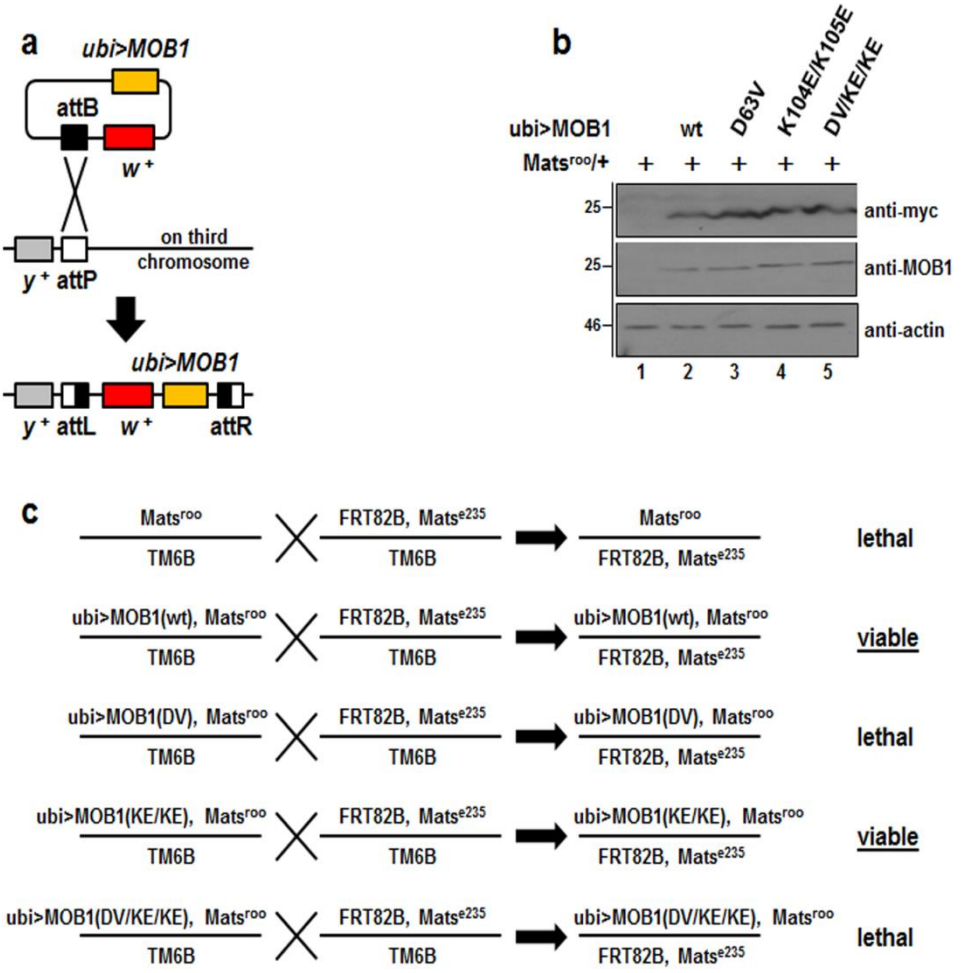

Figure 3.21. Ubiquitous expression of human MOB1(wt) or MOB1(K104E/K105E) rescues larval lethality of *mats* deficient flies.

(a) Schematic representation of the generation of MOB1A transgenic flies. Plasmids which can ubiquitously express N-terminally myc-tagged wild-type (wt) or mutant human MOB1 (*ubi>-myc-hMOB1A*) were inserted into an identical genome location (attP site at 89E11 on chromosome 3) using ΦC31-mediated recombination. **(b)** Whole flies of indicated genotypes were analysed by Western blotting. Equal expression of the myc-tagged MOB1A transgenes was observed. DV/KE/KE, D63V/K104E/K105E. **(c)** Genetic schemes illustrating how we tested which MOB1A transgenes can rescue the larval lethality of Mats deficient flies. wt, wild-type; DV, D63V; KE/KE, K104E/K105E; DV/KE/KE, D63V/K104E/K105E. Adult flies expressing myc-MOB1A(wt) or myc-MOB1A(K104E/K105E) in a *mats* null ($mats^{roo}/mats^{e235}$) genetic background are viable and fertile, indicating that the interaction of MOB1 with Hippo is dispensable for normal

fly development. In contrast, adult flies expressing myc-MOB1A(D63V) or myc-MOB1A(D63V/K104E/K105E) in a *mats* null background were not observed, indicating that the interaction of MOB1 with Wts is essential for normal fly development.

To determine whether MOB1A can rescue the embryonic lethality caused by *mats* loss-of-function, w;; ubi>myc-MOB1A(wt), $mats^{roo}$/ TM6B flies were mated with w;; FRT82B, $mats^{e235}$/ TM6B flies as outlined in **Figure 3.20**. This cross revealed that homozygous embryonic lethality caused by Mats loss-of-function can be rescued by transgenic ubiquitous expression of human MOB1A (wt) **(Figure 3.21c, first cross)**.

We identified and characterized MOB1A variants with respect to binding to Hpo, Wts, and Trc (defined in **sections 3.2 and 3.3** above). Therefore, considering further that MOB1A(wt) can rescue the homozygous lethality caused by homozygous *mats* loss-of-function **(Figure 3.21c, first cross)**, we sought to test which PPIs of MOB1A with the Hippo core kinases are required to prevent embryonic lethality of Mats null flies. To do so, we generated transgenic flies expressing our MOB1A mutants from one fixed chromosomal location **(Figure 3.21a)** and performed compensation crossings, as shown in **Figure 3.21 c**. As expected, transgenic flies expressing MOB1A(DV) or MOB1A(DVKEKE) failed to compensate for the lethality driven by *mats* loss-of-function **(Figure 3.21c)**. In stark contrast, transgenic flies expressing MOB1A(KEKE) were viable and fertile in a *mats* null background, hence indicating that expression of MOB1A(KEKE) fully compensates for *mats* loss-of-function like flies expressing wild-type MOB1A **(Figure 3.21c)**. Considering that MOB1A(DV) is deficient in binding to Wts, while MOB1A(KEKE) does not associate with Hpo **(see section 3.2 above)**, these results collectively indicate that the binding of MOB1A to Wts is necessary for normal fly development, while complex formation between MOB1A and Hpo is dispensable.

3.5.4. Results – The characterisation of transgenic flies expressing MOB1A variants in mosaic fly tissues

We showed above that two independent mutant *mats* alleles result in homozygous lethality in *Drosophila*. Furthermore, we found that expression of MOB1A(wt) or MOB1A(KEKE) can rescue for homozygous lethality caused by *mats* loss-of-function, while expression of MOB1A (DV) or MOB1A(DVKEKE) cannot compensate for *mats* loss-of-function **(see sections 3.5.3)**. To further characterise our lines of transgenic mutant flies, clonal analysis was performed. These genetic mosaic analyses allowed us to analyse mutant phenotypes of an essential genes at different tissue levels. Specifically, using genetic mosaic approaches, patches of homozygous mutant tissues can be generated in a heterozygous background. To achieve this in our settings, FRT sites were recombined into the long arm of the third chromosome of our transgenic flies **(see section 2.2.5.4)**. Consequently, upon expression of the FLP recombinase somatic crossovers can be achieved **(see section 2.2.5.8)**. We recombined the FRT sites as described in **section 2.2.5.4**. After the FRT recombination, the mosaic flies were generated as described in **section 2.2.5.8** to test three different FLP approaches: adult eye, the imaginal discs eye, the imaginal discs wing.

First, we examined the functions of our MOB1A variants in *Drosophila* adult eye development. The results of adult eye are presented in **Figure 3.22** below.

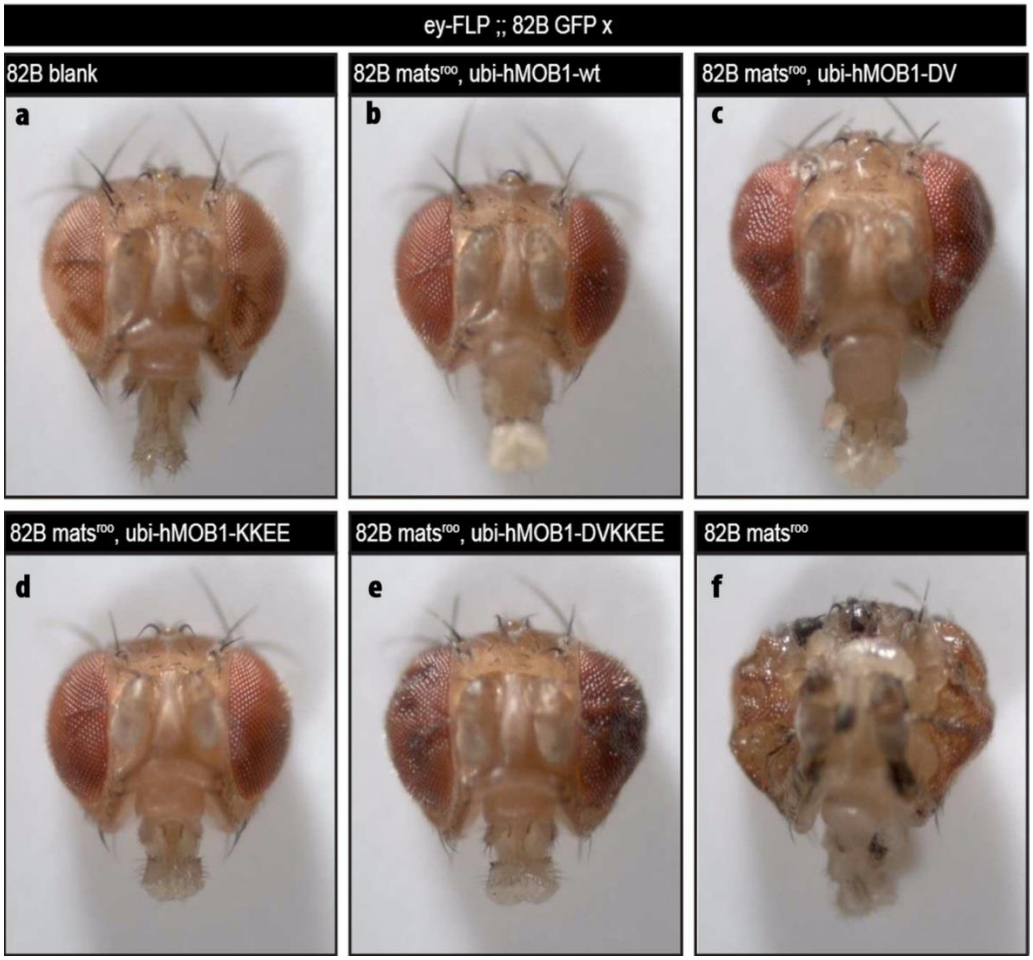

Figure 3.22. Ubiquitous expression of human MOB1(wt) or MOB1(K104E/K105E) rescues tissue overgrowth phenotype driven by Mats loss-of-function

Briefly, virgin ey-FLP;;FRT82B GFP/TM6B were crossed with ey-FLP;;FRT82B GFP/TM6B **(a)** w;; FRT82B,ubi>MOB1A(WT), Mats^{roo}/TMB6 **(b)**, w;; FRT82B,ubi>MOB1A(DV), *mats^{roo}*/TMB6 **(c)**, w;; FRT82B,ubi>MOB1A (KEKE), Mats^{roo}/TMB6 **(d)**, w;; FRT82B,ubi>MOB1A (DVKEKE), *mats^{roo}*/TMB6 **(e)**, and w;; FRT82B, *mats^{roo}*/TMB6. *mats* loss-of-function caused by *mats^{roo}* result in severe overgrowth phenotype **(f).** This severe overgrowth phenotype can be rescued by expression of MOB1A(wt) **(b)** or MOB1A(KEKE) **(d),** while MOB1A(DV) **(c)** and MOB1A(DVKEKE) **(e)** display overgrowth phenotype compared to control **(a).**

In the first instance, we targeted the formation of *mats* clones to the eye imaginal disc (the larval epithelial structure giving rise to the adult eye) by expressing FLPase under the control of the eye-specific *eyeless* promoter (*eyFLP*, Newsome, TP et al Development 2000).

Our findings further confirmed that Mats loss-of-function caused by the transgene *mats*^{roo} developed severe overgrowth eye phenotype (Lai, Wei et al. 2005) **(Figure 3.22f)** and this severe overgrowth eye phenotype can be rescued by the expression of MOB1A(wt) (Lai, Wei et al. 2005) **(Figure 3.22b)**. Furthermore, our findings revealed that the expression of MOB1A(KEKE) fully rescued the severe overgrowth eye phenotype like flies expressing MOB1A(wt) **(Figure 3.22b and 3.22d)**, while the expression of MOB1A(DV) or MOB1A(DVKEKE) failed to completely compensate for the severe overgrowth phenotype **(Figure 3,22c and 3.22e)**. Taken together, in full agreement with our compensation crossing regarding normal fly development **(Figure 3.21c)**, MOB1A(wt) or MOB1A(KEKE) can functionally replace Mats in both *Drosophila* embryogenesis and eye development, while MOB1A(DV) or MOB1(DVKEKE) cannot rescue for *mats* loss-of-function. These findings reveal that the Hippo/MOB1A interaction is neither required for fly development nor for tumour suppression. In contrast, the interactions of MOB1A with the other Hippo core cassette kinases Wts and Trc are essential in a context-dependent manner. Interestingly, flies expressing MOB1A(DV) or MOB1A(DVKEKE) with eye specific Mats loss-of-function did not display as severe tissue overgrowth phenotypes as observed upon Mats loss-of-function alone **(Figure 3.21)**. Considering that MOB1A(DV) or MOB1A(DVKEKE) can still bind to Trc, these observations imply that complex formation of MOB1A with Trc possibly can help to regulate tissue growth to some extent.

Traditionally, the final output of *Drosophila* Hippo signalling is to restrict cell proliferation by inhibiting the transcriptional co-activator Yki. To monitor Yki activity, two well-characterised Yki targets Expanded (*Ex*) and *Diap* are commonly used as readout (Huang, Wu et al. 2005, Hamaratoglu, Willecke et al. 2006). Therefore, we used the Yki target genes *Ex* as a readout for Yki activity. Specifically, we examined the functions of our MOB1A variants in imaginal discs wing and eye by monitoring Yki activity using the target gene *Ex*. we dissected wing and eye imaginal discs,

after generating mosaic flies, and immunostained with *Ex* antibodies **(summarized in section 2.2.5.8 and 2.2.5.9)**.

We generated clones in the wing and eye imaginal discs by expressing FLPase under the control of the *heat shock protein 70* (*hsp70 – hsFLP*) and eye-specific *eyeless* (*eyFLP)* promoters, respectively. The results of wing and eye imaginal discs are presented in **Figure 3.23** and **3.24** below.

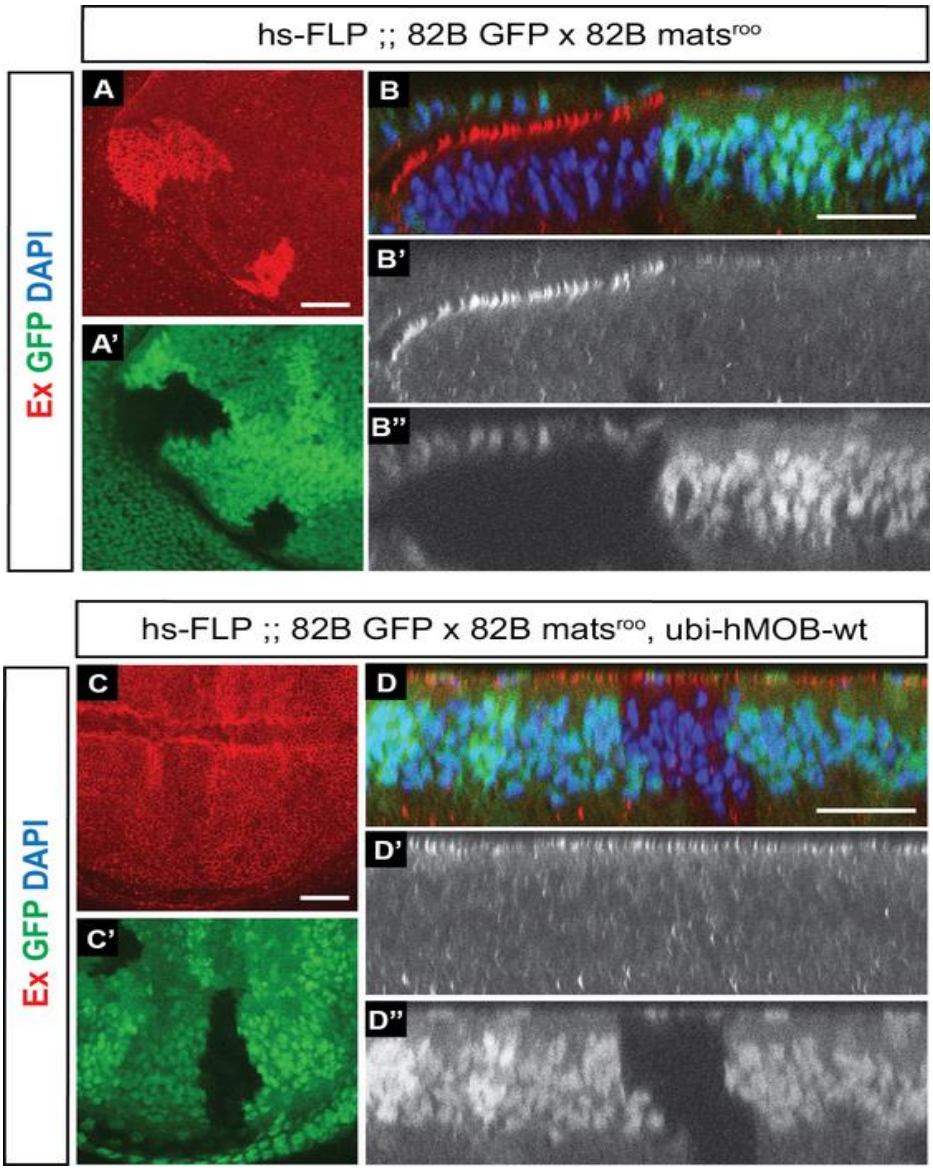

Figure 3.23. Ubiquitous expression of the MOB1A(wt) transgene restores *ex* upregulation in *mats^{roo}* mutant clones in wing imaginal discs.

(A, A', C, C') Maximum intensity projections of the apical region of wing imaginal discs containing *mats*^{roo} clones (negatively marked by GFP), immunostained for *Ex* protein in red. **(B, B', B'', D, D', D'').** X-Z confocal sections through the same wing discs shown in **A** and **C**. Nuclei are stained with DAPI (blue). *Ex* protein levels increase markedly in Mats^{roo} clones **(A, B)**, but this increase is rescued by expressing of MOBA(wt) transgene **(C, D)**. Larvae were heat-shocked at 3 days after egg laying, and dissected as wandering L3s (approximately day 7). All scale bars are 20 µm. These studies were performed in collaboration with the Tapon Labaratory. Pictures were kindly provided by Dr. Maxine Holder.

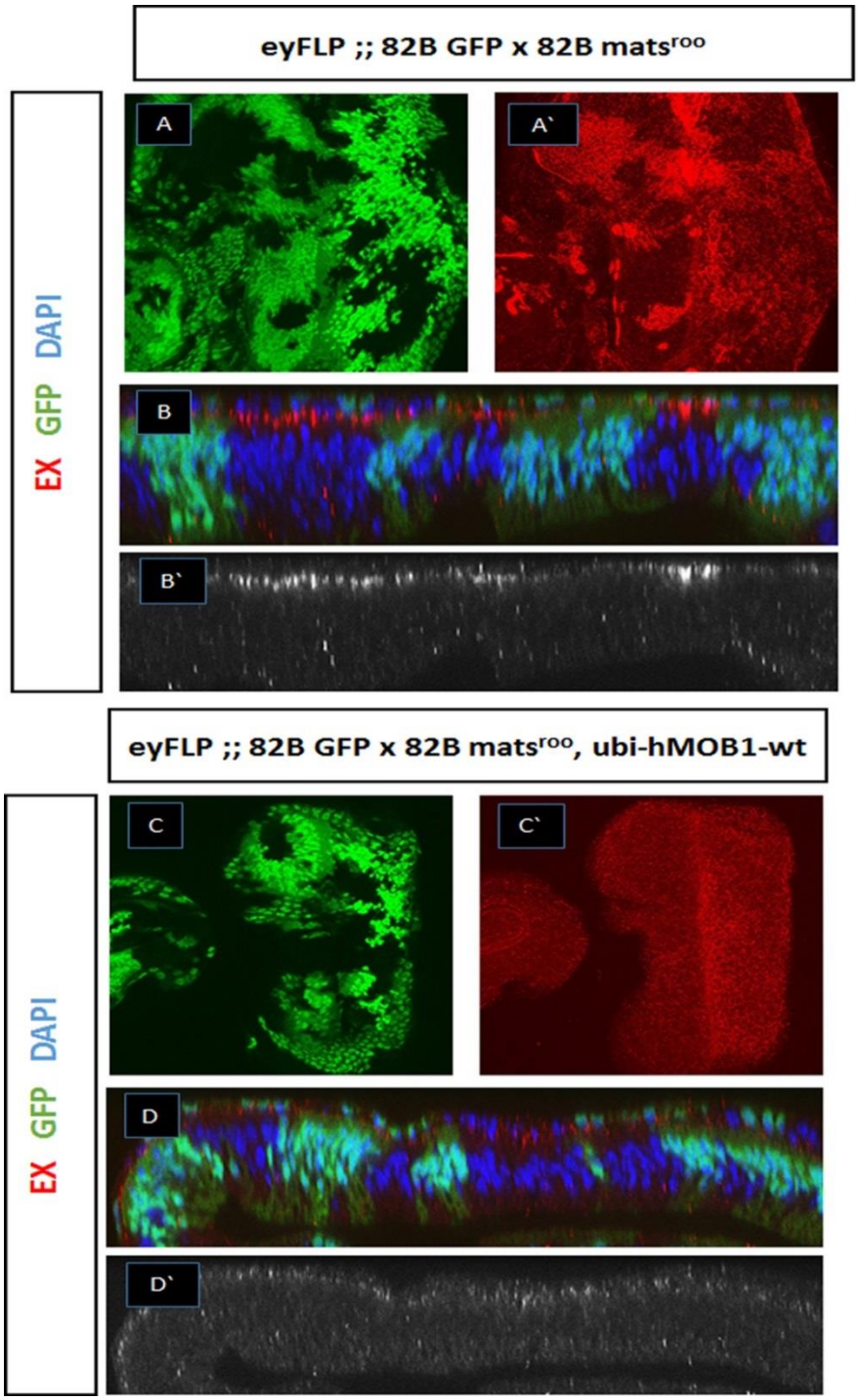

Figure 3.24. Ubiquitous expression of MOB1A(wt) transgene rescues *Ex* upregulation in *mats^{roo}* mutant clones in the eye imaginal discs.

(A, A', C, C') Maximum intensity projections of the apical region of eye imaginal discs containing *mats^{roo}* clones (negatively marked by GFP), immunostained for *Ex* protein. **(B, B', D, D')**. X-Z confocal sections through the same eye discs shown in A and C. Nuclei are stained with DAPI. *Ex* protein levels increase markedly in Mats^{roo} clones **(A, B)**, but this increase is rescued by expressing the MOB1A(wt) transgene **(C, D)**. Larvae were heat-shocked at 3 days after egg laying, and dissected as wandering L3s (approximately day 7).

All scale bars are 20 µm. These studies were performed in collaboration with the Tapon Labaratory. Pictures were kindly provided by Dr. Maxine Holder.

Our findings reported in **section 3.5.5.1** revealed that Mats loss-of-function drives tissue overgrowth phenotype in the eye **(Figure 3.22f)**. Furthermore, we also confirmed that tissue overgrowth phenotype caused by Mats loss-of-function can be rescued by the expression of MOB1A(wt) **(Figure 3.22b)**. The final output of *Drosophila* Hippo signalling is to negatively regulate Yki. Therefore, we used the Yki target gene *Ex* as a readout, which is a well-established readout for monitoring Yki activity (Hamaratoglu, Willecke et al. 2006). Our findings revealed that Mats loss-of-function result in strong upregulation of *Ex* protein in the wing and eye imaginal discs **(Figure 3.23** and **3.24)**. Moreover, we confirmed that *Ex* upregulation driven by Mats loss-of-function can be rescued by the expression of MOB1A(wt) **(Figure 3.23** and **3.24)**. We next used our MOB1A variants to address which PPIs of MOB1A with Hippo core kinases is required for the regulation of Yki activity. The results are presented in **Figure 3.25** and **3.26** below.

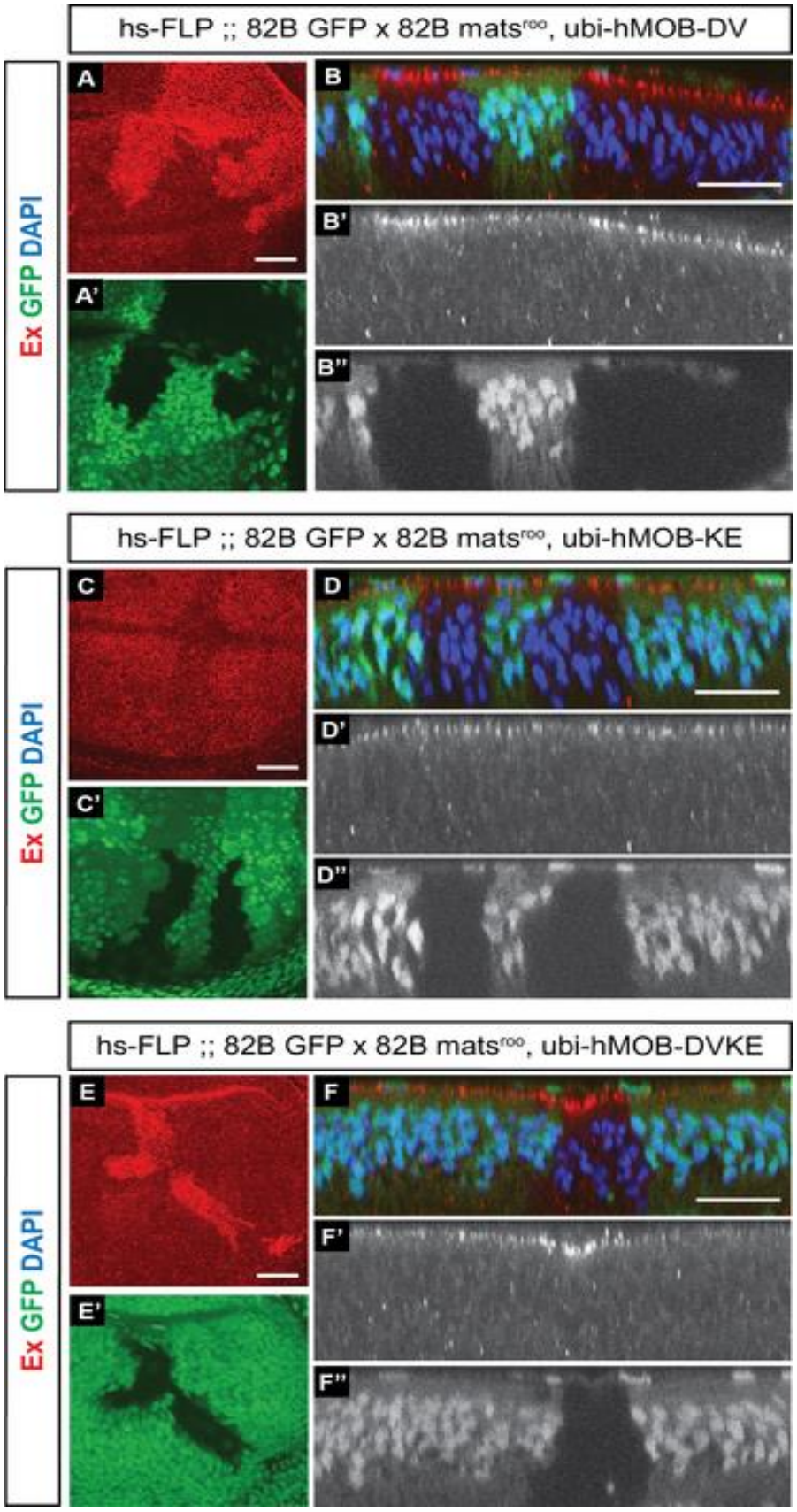

Figure 3.25. Expression of MOB1A(KEKE) restores normal *Ex* levels in *mats^{roo}* mutant clones in the wing imaginal disc, while expression of MOB1A(DV) or MOB1A(DVKEKE) does not.

(A, A', C, C', E, E') Maximum intensity projections of the apical region of wing imaginal discs containing *mats*^{roo} clones (negatively marked by GFP in green), immunostained for *Ex* protein in red. **(B, B', B'', D, D', D'', F, F', F'')** X-Z confocal sections through the same wing discs shown in **A**, **C** and **E**. Nuclei are stained with DAPI in blue. *Ex* protein levels still increase in *mats*^{roo} clones in the presence of the MOBA(DV) and MOB1A(DVKEKE) transgenes **(A, B, E, F)**, but not in the presence of the MOB1A(KEKE) transgene **(C, D)**. Larvae were heatshocked at 3 days after egg laying, and dissected as wandering L3s (approximately day 7). All scale bars are 20 μm. These studies were performed in collaboration with the Tapon Labaratory. Pictures were kindly provided by Dr. Maxine Holder.

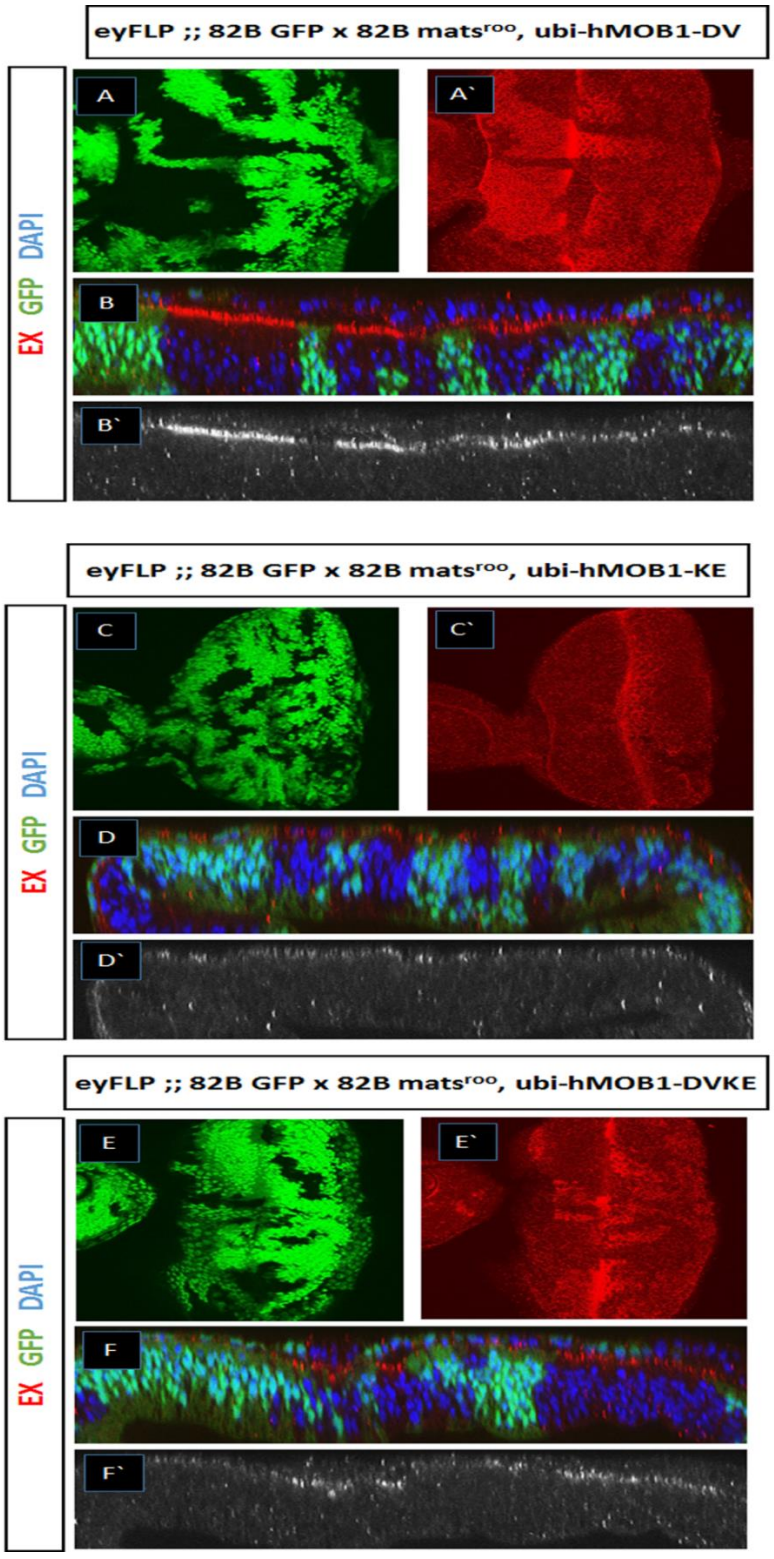

Figure 3.26. Expression of MOB1A(KEKE) restores normal *Ex* levels in *mats*^{roo} mutant clones in the eye imaginal disc, while expression of MOB1A(DV) or MOB1A(DVKEKE) does not.

(A, A', C, C', E, E') Maximum intensity projections of the apical region of eye imaginal discs containing Mats^{roo} clones (negatively marked by GFP), immunostained for *Ex* protein.

(B, B', D, D', F, F') X-Z confocal sections through the same wing discs shown in A, C and E. Nuclei are stained with DAPI. *Ex* protein levels still increase in *mats*^{roo} clones in the presence of the MOB1A(DV) and MOB1A(DVKEKE) transgenes **(A, B, E, F)**, but not in the presence of the MOB1A(KEK1) transgene **(C, D)**. Larvae were heat-shocked at 3 days after egg laying, and dissected as wandering L3s (approximately day 7). All scale bars are 20 µm. These studies were performed in collaboration with the Tapon Labaratory. Pictures were kindly provided by Dr. Maxine Holder.

We previously identified and characterized MOB1A variants with respect to binding to Hpo, Wts, and Trc **(see sections 3.2 and 3.3)**. Considering further that expression of MOB1A(wt) can rescue the tissue overgrowth phenotype caused by Mats loss-of-function **(Figure 3.22)**, we sought to test which PPIs of MOB1A with the Hippo core kinases are required for the regulation of Yki activity. To do so, we generated mosaic clones in the wing and eye imaginal discs and monitored Yki activity through *Ex* expression levels **(Figure 3.24)**. Importantly, our findings revealed that *mats* null mutant clones with MOB1A(DV) or MOB1A(DVKEKE) expression displayed the elevated *Ex* expression **(Figures 3.25 and 3.26)** as observed in Mats null clones **(Figures 3.23 and 3.24)**. In contrast, upon expression of MOB1A(KEKE) in Mats deficient clones, we could not detect any significant increase of *Ex* expression **(Figures 3.25 and 3.26)**. Therefore, the data shown in **Figures 3.25** and **3.26** suggest collectively that only MOB1A(KEKE) or MOB1A(wt) expression is sufficient to suppress Yki activity in Mats mutant clones. Taken together, these findings further indicate that Hpo/MOB1A complex formation is not important for the regulation of Yki activity, while Wts/MOB1A and possibly also Trc/MOB1A complex formations are required for tissue growth by regulating Yki activity in our experimental settings.

3.5.3. Discussion

Hippo signalling in *Drosophila* regulates tissue growth by the coordination of cell proliferation, and apoptosis (Zhao, Li et al. 2010). Current evidence proposes that *Drosophila* Hippo signalling is tightly regulated by complex protein-protein interactions of Mats with the Hpo, Wts, and Trc kinases (Hergovich 2011, Hergovich 2016). Recent studies showed that the functions of Mats are highly conserved from *Drosophila* to humans, since Mats loss-of-function can be compensated by the expression of human MOB1A (Lai, Wei et al. 2005). However, it has remained unknown how Mats, as a central hub of the Hippo pathway, differentially interacts with the Hippo core kinases Hpo, Wts, and Trc and thereby potentially regulate tissue growth through different signalling branches. In a recent study, Vrabioiu et al. (2015) proposed that Mats/Wts complex formation is essential for Wts activation, while Mats/Hpo complex formation is dispensable for Wts activation. However, these findings (Vrabioiu and Struhl 2015) are solely based on conformational sensors. In contrast, Ni *et al.* (2015) reported that complex formation of MST1/2(Hpo) with MOB1A is crucial for LATS1/2(Wts) activation.

Therefore, we decided to investigate the regulatory interactions of Mats/MOB1 with the central Hippo core kinase cassette. First, we defined the molecular characteristic of the MOB1A interactions with Hpo(MST1/2), Wts(LATS1/2), and Trc(NDR1/2) as described in **section 3.2, 3.2, and 3.3.** Second, we studied MOB1A interactions in human cancer cell lines as outlined in **section 3.4.** Third**,** to develop research tools that allow us to investigate the roles for MOB1A interactions with Hippo core kinases in tissue growth, we generated transgenic flies expressing full-length versions of our MOB1A variants and subsequently profiled the viability, tissue overgrowth phenotype, and Yki target gene expression in these fly lines. Importantly, we found that the expression of human MOB1A(wt) can rescue the homozygous lethality caused by *mats* loss-of-function. Our findings further revealed that Hpo/MOB1A complex formation is not required for normal fly development, while the other interactions of MOB1A with the Wts and Trc kinases appear to be required for fly development. To further

consolidate our findings, we generated mosaic fly tissues expressing our MOB1A transgenes in *mats* null clones. This revealed that expression of MOB1A(wt) can prevent the tissue overgrowth phenotype driven by Mats loss-of-function. In addition, we also tested our MOB1A variants and found that Hpo/MOB1A complex formation is dispensable, while the other interactions of MOB1A with Hippo core cassette kinases are essential to prevent tissue overgrowth in adult fly eyes. Lastly, we studied *Ex* expression as a readout to monitor Yki activity in *mats* deficient tissues expressing our MOB1A transgenes. As expected, our findings revealed that Mats loss-of-function results in upregulation of *Ex* proteins, while human MOB1A(wt) can decrease the upregulation of *Ex* to normal level in *mats* mutant clones, thereby showing that MOB1A(wt) expression can also rescue for *mats* loss-of-function in these settings. Significantly we also showed that Hpo/MOB1A complex formation is dispensable for the regulation of *Ex* levels in a Mats loss-of-function background. In contrast, the other interactions of MOB1A with the Hippo core kinases seem to be essential for the regulation of *Ex* upon the Mats loss-of-function. Taken together, our study of MOB1A variants in transgenic flies revealed that the Hpo/MOB1A interaction is neither required for life nor for tumour suppression (the regulation of tissue overgrowth), while the interactions of MOB1A with the other Hippo core cassette kinases Wts and Trc are essential.

Moreover, we noted two interesting aspects of our *in vivo* data. Firstly, while MOB1A/Hpo PPI disruption did not have a detectable effect on MOB1A function in the context of an otherwise wild type MOB1A (*MOB1A(KEKE)* mutant), we observed that, in the context of disrupted MOB1A/Wts interaction (*MOB1A(DVKEKE)* mutant), the Hpo/MOB1A interaction did affect MOB1A function. This is illustrated by the fact that, in the eye overgrowth assay, the *MOB1A(DVKEKE)* flies were noticeably more overgrown than *MOB1A(DV)* flies (compare the more wrinkled appearance of the head in **Figure 3.22e** with **Figure 3.22c**). Furthermore, in the wing clone experiments, we noticed that, while Ex levels were elevated in both the *MOB1A(DVKEKE)* and *MOB1A(DV)* situations, the *MOB1A(DVKEKE)* clones showed a high frequency of clone delamination

and loss in the wing pouch, indicative of a strong overgrowth phenotype and similar to the full *mats* mutant phenotype (Maxine Holder, personal communication). Thus, in the context of a weakened MOB1A function, loss of the MOB1A/Hpo interaction does reduce MOB1A *in vivo* function.

The second interesting aspect of our *in vivo* work is that, while the *MOB1A(DVKEKE)* rescued flies showed a strong eye overgrowth phenotype and *Ex* upregulation **(Figures 3.22e, 3.25e, 3.26e)**, these phenotypes were markedly weaker than the full *mats* loss-of-function phenotypes **(compare Figure 3.22f with 3.22e)**, suggesting *MOB1A(DVKEKE)* can partially rescue the *mats* mutant phenotype. This could be due to several reasons. Firstly, as the MOB1A/Trc is not disrupted in the MOB1A(DVKEKE) mutant, the ability of this construct to partially rescue the *mats* mutant phenotype could be mediated by the MOB1A/Trc weakly repressing Yki activity. Indeed, Trc has been proposed to function partially redundantly with Wts, at least in some contexts (He, Emoto et al. 2005). Secondly, despite the fact that the MOB1A(DVKEKE) mutant is severely impaired in its ability to bind Wts, it is nevertheless possible that some low-affinity Wts binding activity remains, which could be sufficient to partially rescue the *mats* mutant when MOB1A(DVKEKE) is overexpressed *in vivo*. To distinguish between these possibilities, we could deplete Trc in the context of the *MOB1A(DVKEKE)* rescue experiments to test for phenotypic enhancement. In addition, we could generate and introduce into flies mutations that either selectively disrupt the MOB1A/Trc or both the MOB1A/Trc and MOB1A/Wts interactions to test their ability to fully or partially rescue the *mats* phenotype.

4. Final discussion

Hippo signalling has emerged as a tumour suppressor pathway regulating cellular processes such as cell proliferation, apoptosis, and differentiation (Hergovich 2016). Importantly, Hippo signalling is highly conserved from *Drosophila* to humans and is tightly regulated by complex protein-protein interactions involving complex formations of the MOB1A/B (Mats/dMOB1) signal transducer with the Hippo core kinases MST1/2(Hpo), LATS1/2(Wts), and NDR1/2(Trc) (Hergovich 2012).

Recent studies of Mats (aka dMOB1). revealed that Mats loss-of-function results in more severe overgrowth phenotypes than Wts loss-of-function in *Drosophila* (Tao, Zhang et al. 1999, Lai, Wei et al. 2005). In fully support of this, studies of MOB1 knockout mice reported that MOB loss-of-function results in the most dramatic tumour formation comparing to that of other Hippo components (Nishio, Sugimachi et al. 2016). Altogether, these findings suggest that MOB1(Mats/dMOB1) is the most important element of Hippo core signalling and functions as a master tumour suppressor. However, the molecular mechanism how MOB1(Mats) functions as a master tumour suppressor in Hippo signalling is not completely understood. These findings collectively suggest that MOB1(Mats) has LATS(Wts) independent tumour suppressor functions possibly including MOB1(Mats)/MST1/2(Hpo) or/and MOB1(Mats)/NDR1/2(Trc) complexes.

4.1. Final discussion - from structural biology to cell culture

Our data presented in **section 3.1** provide, for the first time, crystal structures of the MOB1A-NDR2 complex, revealing key residues that are required for binding of MOB1A to NDR kinases. Specifically, our findings uncovered that MOB1A employs its negatively-charged surface to associate with positively charged residues of NDR2. Significantly, our structure based sequence alignment of different members of the NDR/LATS kinase family also revealed a single key residue of MOB1A that is required for binding of MOB1A to LATS1 kinase, but not to the NDR2 kinase.

In addition to our structural analysis of NDR/LATS kinases, considering further that **(i)** negatively charged surfaces of MOB1A are responsible for the interactions with positively charged surfaces of NDR/LATS kinases and **(ii)** that MOB1 interacts with MST1/2 differently than with NDR/LATS (Praskova, Xia et al. 2008, Kohler, Schmitz et al. 2010, Ni, Zheng et al. 2015, Tang, Gill et al. 2015), we selectively mutated positively charged residues of MOB1A and tested their binding properties. This resulted in the discovery of two key residues of MOB1A that are essential for binding of MOB1A to the MST1/2 kinases.

To further profile the importance of the key residues that are selectively required for binding to the MST1/2, LATS1/2, and NDR1/2 kinases, we generated mutant forms of MOB1A carrying substitutions of selected residues and tested their binding properties to full-length MST1/2, LATS1/2, and NDR1/2 kinases in mammalian cells **(see section 3.1)**. Significantly, these experiments established the importance of selected residues of MOB1A that are selectively essential for binding of MOB1A to the MST1/2, LATS1/2, and NDR1/2 kinases. Specifically, we discovered that D63 of MOB1A forms a hydrogen bonds with H646 of LATS1, while D63 of MOB1A is not important for binding to the corresponding residue F31 of NDR2. Supportively, our biochemical experiments show that mutant forms of MOB1A carrying D63 to V (D63V) substitutions completely abolish the binding of MOB1A to LATS1/2, but not to NDR1/2, suggesting that the binding of MOB1A to the LATS1/2 and NDR1/2 kinases is selectively supported by different key residues. In addition, our biochemical experiments revealed that mutant versions of MOB1A carrying K104/K105 to E (K104E/K105E) substitution abrogate the binding of MOB1A to the MST1/2 kinase, but not to the LATS1/2 and NDR1/2 kinases. However, it is currently unknown how MOB1A interacts through these two residues with MST1/2 on the structural level. Therefore, the definition of crystal structures of the MOB1/MST complex are now warranted in order to help us understand the detailed molecular mechanism of the MOB1/MST complex formation.

The core components of the Hippo pathway are highly conserved from *Drosophila* to humans (Hergovich, Stegert et al. 2006, Hergovich 2016). Considering that expression of wild-type human MOB1A can compensate for the tissue overgrowth phenotype caused by Mats/dMOB1 in *Drosophila* (Lai, Wei et al. 2005), we hypothesized that the regulation of the Hippo core kinases by Mats/dMOB1 is also conserved from *Drosophila* to humans. Significantly, in support of this hypothesis, our findings presented in **section 3.2** revealed that the interaction patterns of MOB1A with the fly Hippo core kinases Hpo, Wts, and Trc in *Drosophila* cells are highly similar with the patterns observed in mammalian cells. Specifically, using human cells and proteins, we showed that D63 of MOB1A is required for associating with LATS1/2, but not with NDR1/2 and MST1/2, while K104E/K105E of MOB1A is essential for binding to MST1/2, but not to NDR1/2 and LATS1/2. Thus, we also tested MOB1A variants carrying substitutions of selected residues with regard to binding to full-length Hpo, Wts, and Trc kinases in fly cells. Significantly, our findings revealed that MOB1A carrying D63 to V (D63V) substitution disrupts the association with Wts, but not with Trc and Hpo, while MOB1A carrying K104/K105 to E (K104E/K105E) substitutions abrogate the interaction with Hpo, but not with Trc and Wts. These findings are fully consistent with the findings observed in mammalian cells. Our structure based sequence alignment of the conserved N-terminal regulatory domain of NDR/LATS kinases further showed that the H646 and F31 residues of LATS1 and NDR2, respectively, are conserved in *Drosophila* Wts and Trc, respectively, thereby suggesting that D63 of MOB1A also makes a hydrogen bond with the His residue of Wts that corresponds to H646 in human LATS1. Furthermore, our biochemical experiments showed that the positively charged K104 and K105 residues are essential for binding to Hpo. However, further structural studies are now required to provide insights into the complex formation of MOB1A with the fly Hippo core kinases. Collectively, these observations support our notion that the regulation of Hippo core signalling by MOB1A (Mats) is highly conserved from *Drosophila* to humans.

In **sections 3.1, and 3.2**, we characterized and defined the important residues that selectively impair the binding of MOB1A to the Hippo core kinases MST1/2(Hpo), LATS1/2(Wts), and NDR1/2(Trc) in mammalian (fly) cells. Considering that MOB1A(Mats) is regulated through phosphorylation by MST1/2(Hpo), we examined also the phosphorylation status of our selected MOB1A variants by MST1, MST2, and Hpo as a complementary approach to our characterisation of MOB1A variants. Significantly, our findings presented in **section 3.3** show that all our MOB1A variants are normally phosphorylated on Thr12 and Thr35 by MST1, MST2, and Hpo like wild-type MOB1A. Considering that MOB1A(KEKE) does not stably interact with MST1/2 and Hpo, but is phosphorylated by MST1/2 and Hpo like wild-type MOB1A, we are tempted to conclude that MOB1A-MST1/2(Hpo) complex formation is not essential for MST1/2(Hpo)-mediated phosphorylation of MOB1A. Even more importantly, these findings suggest that changes in MST1/2(Hpo)-mediated phosphorylation of MOB1A are very unlikely the cause of the observed alterations of binding patterns of our MOB1A variants.

Taken together, our findings presented in **sections 3.1, 3.2, and 3.3** allowed us to establish novel research tools to study the biological significance of the interactions of MOB1A with the Hippo core kinases MST1/2(Hpo), LATS1/2(Wts), and NDR1/2(Trc) kinases in the context of mammalian and fly Hippo core signalling.

4.2. Final discussion - from human cells and *Drosophila melanogaster*

After characterizing the residues of MOB1A that selectively play crucial roles in binding to the Hippo core kinases MST1/2(Hpo), LATS1/2(Wts), and NDR1/2(Trc), we investigated the selected roles of MOB1A in tumour suppression in **section 3.4**. Significantly, we discovered that MOB1A functions as a tumour suppressor by inhibiting cell proliferation and anchorage-independent growth of human breast cancer cells. Our cell proliferation-based experiments showed that the association of MOB1A

with MST1/2 or LATS1/2 is not required for suppressing cell proliferation of human breast cancer cells. Our anchorage-independent growth experiments revealed that the interaction of MOB1A with MST1/2 is not essential for the suppression of anchorage-independent growth of breast cancer cells, while complex formation of MOB1A with LATS1/2 and NDR1/2 appear to be required for the tumour suppressive function of MOB1A in this setting. More specifically, our findings revealed that disruption of the interaction of MOB1A with the LATS1/2 or MST1/2 kinases results in decreased YAP1 levels and suppression of cell proliferation, suggesting that the interaction of MOB1A with LATS1/2 or MST1/2, respectively, is dispensable for this tumour suppressive function of MOB1A. In contrast, our findings showed that disruption of the interaction of MOB1A with both LATS1/2 and MST1/2 does not suppress cell proliferation like wild-type MOB1A, although YAP1 protein levels are decreased like in cells expressing wild-type MOB1A. This finding indicates that the combined loss of binding to LATS1/2 and MST1/2 by MOB1A is impairing the tumour suppressive function of MOB1A without affecting the suppression of YAP1. Nevertheless, since disruption of the interaction of MOB1A with both LATS1/2 and MST1/2 still decrease proliferation and YAP1 levels when compared to controls, this finding further suggests that in addition to MST1/2 and LATS1/2 other YAP1 regulators are likely to be supported by MOB1A. In this context, it is quite likely that in our proliferation setting NDR1/2 maintain their function as YAP regulators, which would explain why YAP1 levels are consistently downregulated irrespective of the type of MOB1A variant that was expressed.

In addition to addressing the roles of MOB1A in cancer cells, we also examined the roles of MOB1A in *Drosophila melanogaster*. Our findings presented in **section 3.5** revealed, for the first time, that expression of wild-type human MOB1A can rescue for the homozygous lethality caused by Mats/dMOB1 loss-of-function. Moreover, our results uncovered that complex formation of MOB1A with Hpo is dispensable, while the interactions of MOB1A with Wts and Trc are required for normal fly embryogenesis/development. Our findings presented in **section 3.5** further

show that complex formation of MOB1A with the Wts and Trc kinases is required for tissue growth control in the adult fly eye, while the Hpo/MOB1A interaction is dispensable in this context. Importantly, our findings in **section 3.5** further revealed that Mats/dMOB1 loss-of-function in wing and eye imaginal discs leads to elevated *Ex* expression, which is a well-established readout for Yki activity (the counterpart of human YAP1). In this regard, we found that the upregulation of *Ex* can be reversed by expression of wild-type human MOB1A, further confirming that the functions of Mats/dMOB1 are conserved from *Drosophila* to humans. Moreover, our data indicate that MOB1A with a disruption in Hpo/MOB1A complex formation can still suppress the upregulation of *Ex*, while disruption of the interaction between Wts and MOB1A does not reverse elevated *Ex* expression in Mats mutant clones. Collectively, these findings revealed that stable Hpo/MOB1A complex formation is not important for the regulation of Yki activity, while Wts/MOB1A and possibly also Trc/MOB1A complex formations are required for tissue growth control by regulating Yki activity in our experimental settings.

Taken together, our experimental results performed in both mammalian cells and *Drosophila* reveal that complex formation of MST1/2(Hpo) with MOB1A is dispensable, while interaction of MOB1A with LATS1/2(Wts) is required for tumour suppression (suppression of tissue overgrowth) in human cells and *Drosophila*. Our findings are fully consistent with the findings of Vrabioiu *et al.* (2015). Using chimeric sensor proteins, Vrabioiu *et al.* (2015) reported that Wts/Mats complex formation is required for Wts activation, while the Hpo/Mats interaction appears to be dispensable for the activation of Wts, and hence Hippo signalling. However, Ni *et al.* (2015) reported that MST/MOB1 complex formation is required for the activation of the LATS kinases. However, latter evidence (Ni, Zheng et al. 2015) is solely based on structural biology and biochemistry using truncated protein versions. Noteworthy, our results presented in this thesis do not support their notion, namely that MST/MOB1 complex formation is essential. One explanation of this discrepancy might be that they only studied truncated proteins and did not test the interaction patterns using full-length proteins in

tissue culture cells. In our research, we used full-length versions of all the proteins tested and investigated their functions in mammalian cells as well as *Drosophila melanogaster*. Thus, we are very tempted to conclude that evidence only based on structural and biochemical studies can be quite misleading, and therefore observations should also be confirmed cell biologically using even multicellular organisms if possible.

4.3. Future outlook

Studies of knockout mice revealed that MOB1 loss-of-function results in a range of different cancers in mice (Nishio, Sugimachi et al. 2016). Thus, a future key question should be the investigation of PPIs of MOB1 with the MST1/2, LATS1/2, and NDR1/2 kinases described herein in mouse tissues with MOB1 loss-of-function. Specifically, one should consider to use our MOB1A variants described herein to address which protein-protein interactions of MOB1 with the MST1/2, LATS1/2, NDR1/2 kinases are required for the suppression of cancer development. In this regard, we are confident that the use of the newly-developed gene engineering technology CRISPR-Cas9 (Jinek, Chylinski et al. 2012) has a great potential to lead the way. In addition to MOB1 functioning as a central regulator of Hippo core signalling, recent studies reported that MOB1 can be involved in the regulation of microtubule dynamics (Florindo, Perdigao et al. 2012). Thus, protein-protein interactions of MOB1 with the Hippo core kinases MST1/2, LATS1/2, and NDR1/2 might play important roles in regulating microtubule dynamics as well. It is noteworthy that MOB1 can also bind to PRAJA2 and DOCK8 proteins to regulate different cellular processes (Mou, Praskova et al. 2012, Lignitto, Arcella et al. 2013). On the one hand, PRAJA2 was shown to bind to and ultimately ubiquitylate MOB1, thereby playing a role in glioblastoma multiform growth (Lignitto, Arcella et al. 2013). On the other hand, phosphorylation of MOB1A by the MST1/2 kinases was shown to promote the binding of MOB1A to the DOCK8 guanyl nucleotide exchanger (Mou, Praskova et al. 2012). Consequently, MOB1 can be involved in different cellular processes in addition to Hippo signalling. Considering our findings, namely that MOB1 is tightly associated through

protein-protein interactions with the Hippo core kinases MST1/2, LATS1/2, and NDR1/2, one should consider to investigate whether any of the interactions of MOB1 with these kinases are potentially affecting DOCK8 and PRAJA2-dependent signalling outputs. Thus, discovery of the key residues that are selectively required for binding to the MST1/2, LATS1/2, and NDR1/2 kinases should provide an excellent platform to address such key questions in the future.

In my thesis, we discovered the key residues that is required for binding to the MST1/2, LATS1/2, and NDR1/2 kinases and established important and novel research tools to study the importance of protein-protein interactions of MOB1A with the MST1/2, LATS1/2, and NDR1/2 kinases in MOB1-regulated cellular processes. Moreover, we also managed to integrate human MOB1A(wt) into the Mats loss-of-function flies and showed that human MOB1A(wt) can rescue homozygous lethality caused by the Mats loss-of-function. Furthermore, we also successfully integrated our selective MOB1A variants into the Mats loss-of-function flies, thereby establishing novel research tools to study the importance of protein-protein interactions of MOB1A with the Hpo, Wts, and Trc kinases in different signalling concepts.

5. References

Abdollahpour, H., G. Appaswamy, D. Kotlarz, J. Diestelhorst, R. Beier, A. A. Schaffer, E. M. Gertz, A. Schambach, H. H. Kreipe, D. Pfeifer, K. R. Engelhardt, N. Rezaei, B. Grimbacher, S. Lohrmann, R. Sherkat and C. Klein (2012). "The phenotype of human STK4 deficiency." Blood **119**(15): 3450-3457.

Alarcon, C., A. I. Zaromytidou, Q. R. Xi, S. Gao, J. Z. Yu, S. Fujisawa, A. Barlas, A. N. Miller, K. Manova-Todorova, M. J. Macias, G. Sapkota, D. J. Pan and J. Massague (2009). "Nuclear CDKs Drive Smad Transcriptional Activation and Turnover in BMP and TGF-beta Pathways." Cell **139**(4): 757-769.

Attrill, H., K. Falls, J. L. Goodman, G. H. Millburn, G. Antonazzo, A. J. Rey, S. J. Marygold and F. Consortium (2016). "FlyBase: establishing a Gene Group resource for Drosophila melanogaster." Nucleic Acids Research **44**(D1): D786-D792.

Avruch, J., D. W. Zhou, J. Fitamant, N. Bardeesy, F. Mou and L. R. Barrufet (2012). "Protein kinases of the Hippo pathway: Regulation and substrates." Seminars in Cell & Developmental Biology **23**(7): 770-784.

Bandyopadhyay, S., C. Y. Chiang, J. Srivastava, M. Gersten, S. White, R. Bell, C. Kurschner, C. H. Martin, M. Smoot, S. Sahasrabudhe, D. L. Barber, S. K. Chanda and T. Ideker (2010). "A human MAP kinase interactome." Nature Methods **7**(10): 801-U850.

Bardin, A. J. and A. Amon (2001). "Men and sin: What's the difference?" Nature Reviews Molecular Cell Biology **2**(11): 815-826.

Baumgartner, R., I. Poernbacher, N. Buser, E. Hafen and H. Stocker (2010). "The WW Domain Protein Kibra Acts Upstream of Hippo in Drosophila." Developmental Cell **18**(2): 309-316.

Benhamouche, S., M. Curto, I. Saotome, A. B. Gladden, C. H. Liu, M. Giovannini and A. I. McClatchey (2010). "Nf2/Merlin controls progenitor homeostasis and tumorigenesis in the liver." Genes & Development **24**(16): 1718-1730.

Bichsel, S. J., R. Tamaskovic, M. R. Stegert and B. A. Hemmings (2004). "Mechanism of activation of NDR (nuclear Dbf2-related) protein kinase by the hMOB1 protein." Journal of Biological Chemistry **279**(34): 35228-35235.

Blair, S. S. (2003). "Genetic mosaic techniques for studying Drosophila development." Development **130**(21): 5065-5072.

Boggiano, J. C., P. J. Vanderzalm and R. G. Fehon (2011). "Tao-1 phosphorylates Hippo/MST kinases to regulate the Hippo-Salvador-Warts tumor suppressor pathway." Dev Cell **21**(5): 888-895.

Bothos, J., R. L. Tuttle, M. Ottey, F. C. Luca and T. D. Halazonetis (2005). "Human LATS1 is a mitotic exit network kinase." Cancer Research **65**(15): 6568-6575.

Camargo, F. D., S. Gokhale, J. B. Johnnidis, D. Fu, G. W. Bell, R. Jaenisch and T. R. Brummelkamp (2007). "YAP1 increases organ size and expands undifferentiated progenitor cells." Current Biology **17**(23): 2054-2060.

Campbell, M. and B. Ganetzky (2013). "Identification of Mob2, a Novel Regulator of Larval Neuromuscular Junction Morphology, in Natural Populations of Drosophila melanogaster." Genetics **195**(3): 915-+.

Chen, C. L., K. M. Gajewski, F. Hamaratoglu, W. Bossuyt, L. Sansores-Garcia, C. Y. Tao and G. Halder (2010). "The apical-basal cell polarity determinant Crumbs regulates Hippo signaling in Drosophila." Proceedings of the National Academy of Sciences of the United States of America **107**(36): 15810-15815.

Chen, C. T., A. Feoktistova, J. S. Chen, Y. S. Shim, D. M. Clifford, K. L. Gould and D. McCollum (2008). "The SIN Kinase Sid2 Regulates Cytoplasmic Retention of the S. pombe Cdc14-like Phosphatase Clp1." Current Biology **18**(20): 1594-1599.

Chen, D. H., Y. T. Sun, Y. K. Wei, P. J. Zhang, A. H. Rezaeian, J. Teruya-Feldstein, S. Gupta, H. Liang, H. K. Lin, M. C. Hung and L. Ma (2012). "LIFR is a breast cancer metastasis suppressor upstream of the Hippo-YAP pathway and a prognostic marker." Nature Medicine **18**(10): 1511-U1105.
Chen, Q., N. L. Zhang, R. Xie, W. Wang, J. Cai, K. S. Choi, K. K. David, B. Huang, N. Yabuta, H. Nojima, R. A. Anders and D. J. Pan (2015). "Homeostatic control of Hippo signaling activity revealed by an endogenous activating mutation in YAP." Genes & Development **29**(12): 1285-1297.
Cohen, S. N., A. C. Y. Chang and L. Hsu (1972). "Nonchromosomal Antibiotic Resistance in Bacteria - Genetic Transformation of Escherichia-Coli by R-Factor DNA." Proceedings of the National Academy of Sciences of the United States of America **69**(8): 2110-&.
Colman-Lerner, A., T. E. Chin and R. Brent (2001). "Yeast Cbk1 and Mob2 activate daughter-specific genetic programs to induce asymmetric cell fates." Cell **107**(6): 739-750.
Cook, D., L. Y. Hoa, V. Gomez, M. Gomez and A. Hergovich (2014). "Constitutively active NDR1-PIF kinase functions independent of MST1 and hMOB1 signalling." Cellular Signalling **26**(8): 1657-1667.
Cordenonsi, M., F. Zanconato, L. Azzolin, M. Forcato, A. Rosato, C. Frasson, M. Inui, M. Montagner, A. R. Parenti, A. Poletti, M. G. Daidone, S. Dupont, G. Basso, S. Bicciato and S. Piccolo (2011). "The Hippo Transducer TAZ Confers Cancer Stem Cell-Related Traits on Breast Cancer Cells." Cell **147**(4): 759-772.
Cornils, H., R. S. Kohler, A. Hergovich and B. A. Hemmings (2011). "Human NDR Kinases Control G(1)/S Cell Cycle Transition by Directly Regulating p21 Stability." Molecular and Cellular Biology **31**(7): 1382-1395.
Dan, I., N. M. Watanabe and A. Kusumi (2001). "The Ste20 group kinases as regulators of MAP kinase cascades." Trends in Cell Biology **11**(5): 220-230.
de Souza, P. L., W. Liauw, M. Links, S. Pirabhahar, G. Kelly and L. G. Howes (2006). "Phase I and pharmacokinetic study of weekly NV06 (Phenoxodiol (TM)), a novel isoflav-3-ene, in patients with advanced cancer." Cancer Chemotherapy and Pharmacology **58**(4): 427-433.
Deak, P., M. M. Omar, R. D. C. Saunders, M. Pal, O. Komonyi, J. Szidonya, P. Maroy, Y. Zhang, M. Ashburner, P. Benos, C. Savakis, I. SidenKiamos, C. Louis, V. N. Bolshakov, F. C. Kafatos, E. Madueno, J. Modolell and D. M. Glover (1997). "P-element insertion alleles of essential genes on the third chromosome of Drosophila melanogaster: Correlation of physical and cytogenetic maps in chromosomal region 86E-87F." Genetics **147**(4): 1697-1722.
Del Re, D. P., Y. F. Yang, N. Nakano, J. Cho, P. Y. Zhai, T. Yamamoto, N. L. Zhang, N. Yabuta, H. Nojima, D. J. Pan and J. Sadoshima (2013). "Yes-associated Protein Isoform 1 (Yap1) Promotes Cardiomyocyte Survival and Growth to Protect against Myocardial Ischemic Injury." Journal of Biological Chemistry **288**(6): 3977-3988.
Di Agostino, S., G. Sorrentino, E. Ingallina, F. Valenti, M. Ferraiuolo, S. Bicciato, S. Piazza, S. Strano, G. Del Sal and G. Blandino (2016). "YAP enhances the pro-proliferative transcriptional activity of mutant p53 proteins." Embo Reports **17**(2): 188-201.
Dong, J. X., G. Feldmann, J. B. Huang, S. Wu, N. L. Zhang, S. A. Comerford, M. F. Gayyed, R. A. Anders, A. Maitra and D. J. Pan (2007). "Elucidation of a universal size-control mechanism in Drosophila and mammals." Cell **130**(6): 1120-1133.
Emoto, K., J. Z. Parrish, L. Y. Jan and Y. N. Jan (2006). "The tumour suppressor Hippo acts with the NDR kinases in dendritic tiling and maintenance." Nature **443**(7108): 210-213.

Emsley, P. and K. Cowtan (2004). "Coot: model-building tools for molecular graphics." Acta Crystallographica Section D-Biological Crystallography **60**: 2126-2132.
Evans, D. G. (2009). "Neurofibromatosis 2 [Bilateral acoustic neurofibromatosis, central neurofibromatosis, NF2, neurofibromatosis type II]." Genet Med **11**(9): 599-610.
Ewing, R. M., P. Chu, F. Elisma, H. Li, P. Taylor, S. Climie, L. McBroom-Cerajewski, M. D. Robinson, L. O'Connor, M. Li, R. Taylor, M. Dharsee, Y. Ho, A. Heilbut, L. Moore, S. Zhang, O. Ornatsky, Y. V. Bukhman, M. Ethier, Y. Sheng, J. Vasilescu, M. Abu-Farha, J. P. Lambert, H. S. Duewel, I. I. Stewart, B. Kuehl, K. Hogue, K. Colwill, K. Gladwish, B. Muskat, R. Kinach, S. L. Adams, M. F. Moran, G. B. Morin, T. Topaloglou and D. Figeys (2007). "Large-scale mapping of human protein-protein interactions by mass spectrometry." Molecular Systems Biology **3**.
Fang, X. and P. N. Adler (2010). "Regulation of cell shape, wing hair initiation and the actin cytoskeleton by Trc/Fry and Wts/Mats complexes." Dev Biol **341**(2): 360-374.
Fish, M. P., A. C. Groth, M. P. Calos and R. Nusse (2007). "Creating transgenic Drosophila by microinjecting the site-specific phi C31 integrase mRNA and a transgene-containing donor plasmid." Nature Protocols **2**(10): 2325-2331.
Fleming, J. K., J. M. Wojciak, M. A. Campbell and T. Huxford (2011). "Biochemical and Structural Characterization of Lysophosphatidic Acid Binding by a Humanized Monoclonal Antibody." Journal of Molecular Biology **408**(3): 462-476.
Florindo, C., J. Perdigao, D. Fesquet, E. Schiebel, J. Pines and A. A. Tavares (2012). "Human Mob1 proteins are required for cytokinesis by controlling microtubule stability." Journal of Cell Science **125**(13): 3085-3090.
Frenz, L. M., S. E. Lee, D. Fesquet and L. H. Johnston (2000). "The budding yeast Dbf2 protein kinase localises to the centrosome and moves to the bud neck in late mitosis." Journal of Cell Science **113**(19): 3399-3408.
Galliot, B. and L. Ghila (2010). "Cell Plasticity in Homeostasis and Regeneration." Molecular Reproduction and Development **77**(10): 837-855.
Genevet, A., M. C. Wehr, R. Brain, B. J. Thompson and N. Tapon (2010). "Kibra Is a Regulator of the Salvador/Warts/Hippo Signaling Network." Developmental Cell **18**(2): 300-308.
Geng, W., B. He, M. Wang and P. N. Adler (2000). "The tricornered gene, which is required for the integrity of epidermal cell extensions, encodes the drosophila nuclear DBF2-Related kinase." Genetics **156**(4): 1817-1828.
Golic, K. G. and S. Lindquist (1989). "The Flp Recombinase of Yeast Catalyzes Site-Specific Recombination in the Drosophila Genome." Cell **59**(3): 499-509.
Gomez, M., V. Gomez and A. Hergovich (2014). "The Hippo pathway in disease and therapy: cancer and beyond." Clinical and translational medicine **3**: 22.
Gomez, M., V. Gomez and A. Hergovich (2014). "The Hippo pathway in disease and therapy: cancer and beyond." Clin Transl Med **3**: 22.
Goulev, Y., J. D. Fauny, B. Gonzalez-Marti, D. Flagiello, J. Silber and A. Zider (2008). "SCALLOPED interacts with YORKIE, the nuclear effector of the hippo tumor-suppressor pathway in Drosophila." Current Biology **18**(6): 435-441.
Groth, A. C., M. Fish, R. Nusse and M. P. Calos (2004). "Construction of transgenic Drosophila by using the site-specific integrase from phage phi C31." Genetics **166**(4): 1775-1782.
Halder, G. and R. L. Johnson (2011). "Hippo signaling: growth control and beyond." Development **138**(1): 9-22.
Hamaratoglu, F., M. Willecke, M. Kango-Singh, R. Nolo, E. Hyun, C. Y. Tao, H. Jafar-Nejad and G. Halder (2006). "The tumour-suppressor genes NF2/Merlin and

Expanded act through Hippo signalling to regulate cell proliferation and apoptosis." Nature Cell Biology **8**(1): 27-U29.
Hanahan, D. and R. A. Weinberg (2011). "Hallmarks of Cancer: The Next Generation." Cell **144**(5): 646-674.
Hansen, C. G., T. Moroishi and K. L. Guan (2015). "YAP and TAZ: a nexus for Hippo signaling and beyond." Trends Cell Biol **25**(9): 499-513.
Hao, Y. W., A. Chun, K. Cheung, B. Rashidi and X. L. Yang (2008). "Tumor suppressor LATS1 is a negative regulator of oncogene YAP." Journal of Biological Chemistry **283**(9): 5496-5509.
Harvey, K. F., C. M. Pfleger and I. K. Hariharan (2003). "The Drosophila Mst ortholog, hippo, restricts growth and cell proliferation and promotes apoptosis." Cell **114**(4): 457-467.
Harvey, K. F., X. M. Zhang and D. M. Thomas (2013). "The Hippo pathway and human cancer." Nature Reviews Cancer **13**(4): 246-257.
He, Y., K. Emoto, X. Fang, N. Ren, X. Tian, Y. N. Jan and P. N. Adler (2005). "Drosophila Mob family proteins interact with the related tricornered (Trc) and warts (Wts) kinases." Mol Biol Cell **16**(9): 4139-4152.
He, Y., K. Emoto, X. L. Fang, N. Ren, X. J. Tian, Y. N. Jan and P. N. Adler (2005). "Drosophila Mob family proteins interact with the related Tricornered (Trc) and Warts (Wts) kinases." Molecular Biology of the Cell **16**(9): 4139-4152.
Heallen, T., Y. Morikawa, J. Leach, G. Tao, J. T. Willerson, R. L. Johnson and J. F. Martin (2013). "Hippo signaling impedes adult heart regeneration." Development **140**(23): 4683-+.
Heallen, T., M. Zhang, J. Wang, M. Bonilla-Claudio, E. Klysik, R. L. Johnson and J. F. Martin (2011). "Hippo Pathway Inhibits Wnt Signaling to Restrain Cardiomyocyte Proliferation and Heart Size." Science **332**(6028): 458-461.
Helias-Rodzewicz, Z., G. Perot, F. Chibon, C. Ferreira, P. Lagarde, P. Terrier, J. M. Coindre and A. Aurias (2010). "YAP1 and VGLL3, Encoding Two Cofactors of TEAD Transcription Factors, Are Amplified and Overexpressed in a Subset of Soft Tissue Sarcomas." Genes Chromosomes & Cancer **49**(12): 1161-1171.
Hergovich, A. (2011). "MOB control: reviewing a conserved family of kinase regulators." Cell Signal **23**(9): 1433-1440.
Hergovich, A. (2011). "MOB control: Reviewing a conserved family of kinase regulators." Cellular Signalling **23**(9): 1433-1440.
Hergovich, A. (2012). "Mammalian Hippo signalling: a kinase network regulated by protein-protein interactions." Biochemical Society Transactions **40**: 124-128.
Hergovich, A. (2013). "Regulation and functions of mammalian LATS/NDR kinases: looking beyond canonical Hippo signalling." Cell and Bioscience **3**.
Hergovich, A. (2016). "The Roles of NDR Protein Kinases in Hippo Signalling." Genes **7**(5).
Hergovich, A., S. J. Bichsel and B. A. Hemmings (2005). "Human NDR kinases are rapidly activated by MOB proteins through recruitment to the plasma membrane and phosphorylation." Molecular and Cellular Biology **25**(18): 8259-8272.
Hergovich, A., R. S. Kohler, D. Schmitz, A. Vichalkovski, H. Cornils and B. A. Hemmings (2009). "The MST1 and hMOB1 Tumor Suppressors Control Human Centrosome Duplication by Regulating NDR Kinase Phosphorylation." Current Biology **19**(20): 1692-1702.
Hergovich, A., D. Schmitz and B. A. Hemmings (2006). "The human tumour suppressor LATS1 is activated by human MOB1 at the membrane." Biochemical and Biophysical Research Communications **345**(1): 50-58.

Hergovich, A., M. R. Stegert, D. Schmitz and B. A. Hemmings (2006). "NDR kinases regulate essential cell processes from yeast to humans." Nature Reviews Molecular Cell Biology **7**(4): 253-264.
Hoa, L., Y. Kulaberoglu, R. Gundogdu, D. Cook, M. Mavis, M. Gomez, V. Gomez and A. Hergovich (2016). "The characterisation of LATS2 kinase regulation in Hippo-YAP signalling." Cellular Signalling **28**(5): 488-497.
Hoa, L., Y. Kulaberoglu, R. Gundogdu, D. Cook, M. Mavis, M. Gomez, V. Gomez and A. Hergovich (2016). "The characterisation of LATS2 kinase regulation in Hippo-YAP signalling." Cell Signal **28**(5): 488-497.
Hong, W. and K. L. Guan (2012). "The YAP and TAZ transcription co-activators: key downstream effectors of the mammalian Hippo pathway." Semin Cell Dev Biol **23**(7): 785-793.
Hou, M. C., D. A. Guertin and D. McCollum (2004). "Initiation of cytokinesis is controlled through multiple modes of regulation of the Sid2p-Mob1p kinase complex." Molecular and Cellular Biology **24**(8): 3262-3276.
Hou, M. C., D. J. Wiley, F. Verde and D. McCollum (2003). "Mob2p interacts with the protein kinase Orb6p to promote coordination of cell polarity with cell cycle progression." Journal of Cell Science **116**(1): 125-135.
Huang, J. B., S. Wu, J. Barrera, K. Matthews and D. J. Pan (2005). "The Hippo signaling pathway coordinately regulates cell proliferation and apoptosis by inactivating Yorkie, the Drosophila homolog of YAP." Cell **122**(3): 421-434.
Huang, W., X. B. Lv, C. Y. Liu, Z. Y. Zha, H. Zhang, Y. Jiang, Y. Xiong, Q. Y. Lei and K. L. Guan (2012). "The N-terminal Phosphodegron Targets TAZ/WWTR1 Protein for SCF beta-TrCP-dependent Degradation in Response to Phosphatidylinositol 3-Kinase Inhibition." Journal of Biological Chemistry **287**(31): 26245-26253.
Hwang, E., K. S. Ryu, K. Paakkonen, P. Guntert, H. K. Cheong, D. S. Lim, J. O. Lee, Y. H. Jeon and C. Cheong (2007). "Structural insight into dimeric interaction of the SARAH domains from Mst1 and RASSF family proteins in the apoptosis pathway." Proceedings of the National Academy of Sciences of the United States of America **104**(22): 9236-9241.
Ivanov, A. A., F. R. Khuri and H. A. Fu (2013). "Targeting protein-protein interactions as an anticancer strategy." Trends in Pharmacological Sciences **34**(7): 393-400.
Jansen, J. M., M. F. Barry, C. K. Yoo and E. L. Weiss (2006). "Phosphoregulation of Cbk1 is critical for RAM network control of transcription and morphogenesis." Journal of Cell Biology **175**(5): 755-766.
Jia, D. Y., M. Soylemez, G. Calvin, R. Bornmann, J. Bryant, C. Hanna, Y. C. Huang and W. M. Deng (2015). "A large-scale in vivo RNAi screen to identify genes involved in Notch-mediated follicle cell differentiation and cell cycle switches." Scientific Reports **5**.
Jia, J. H., W. S. Zhang, B. Wang, R. Trinko and J. Jiang (2003). "The Drosophila Ste20 family kinase dMST functions as a tumor suppressor by restricting cell proliferation and promoting apoptosis." Genes & Development **17**(20): 2514-2519.
Jiao, S., H. Z. Wang, Z. B. Shi, A. M. Dong, W. J. Zhang, X. M. Song, F. He, Y. C. Wang, Z. Z. Zhang, W. J. Wang, X. Wang, T. Guo, P. X. Li, Y. Zhao, H. B. Ji, L. Zhang and Z. C. Zhou (2014). "A Peptide Mimicking VGLL4 Function Acts as a YAP Antagonist Therapy against Gastric Cancer (vol 25, pg 166, 2014)." Cancer Cell **25**(3): 406-406.
Jin, H. S., H. S. Park, J. H. Shin, D. H. Kim, S. H. Jun, C. J. Lee and T. H. Lee (2011). "A novel inhibitor of apoptosis protein (IAP)-interacting protein, Vestigial-like (Vgl)-4,

counteracts apoptosis-inhibitory function of IAPs by nuclear sequestration." Biochemical and Biophysical Research Communications **412**(3): 454-459.
Jinek, M., K. Chylinski, I. Fonfara, M. Hauer, J. A. Doudna and E. Charpentier (2012). "A Programmable Dual-RNA-Guided DNA Endonuclease in Adaptive Bacterial Immunity." Science **337**(6096): 816-821.
Johnson, R. and G. Halder (2014). "The two faces of Hippo: targeting the Hippo pathway for regenerative medicine and cancer treatment." Nature Reviews Drug Discovery **13**(1): 63-79.
Johnson, R. and G. Halder (2014). "The two faces of Hippo: targeting the Hippo pathway for regenerative medicine and cancer treatment." Nature reviews. Drug discovery **13**(1): 63-79.
Johnston, L. H., S. L. Eberly, J. W. Chapman, H. Araki and A. Sugino (1990). "The Product of the Saccharomyces-Cerevisiae Cell-Cycle Gene Dbf2 Has Homology with Protein-Kinases and Is Periodically Expressed in the Cell-Cycle." Molecular and Cellular Biology **10**(4): 1358-1366.
Justice, R. W., D. F. Woods and P. J. Bryant (1999). "The warts tumor suppressor gene is required for normal cell cycle and patterning in the developing Drosophila eye." Molecular Biology of the Cell **10**: 46a-46a.
Justice, R. W., O. Zilian, D. F. Woods, M. Noll and P. J. Bryant (1995). "The Drosophila tumor suppressor gene warts encodes a homolog of human myotonic dystrophy kinase and is required for the control of cell shape and proliferation." Genes Dev **9**(5): 534-546.
Kanai, M., K. Kume, K. Miyahara, K. Sakai, K. Nakamura, K. Leonhard, D. J. Wiley, F. Verde, T. Toda and D. Hirata (2005). "Fission yeast MO25 protein is localized at SPB and septum and is essential for cell morphogenesis." Embo Journal **24**(17): 3012-3025.
Kango-Singh, M., R. Nolo, C. Tao, P. Verstreken, P. R. Hiesinger, H. J. Bellen and G. Halder (2002). "Shar-pei mediates cell proliferation arrest during imaginal disc growth in Drosophila." Development **129**(24): 5719-5730.
Kelly, M. G., G. Mor, A. Husband, D. M. O'Malley, L. Baker, M. Azodi, P. E. Schwartz and T. J. Rutherford (2011). "Phase II Evaluation of Phenoxodiol in Combination With Cisplatin or Paclitaxel in Women With Platinum/Taxane-Refractory/Resistant Epithelial Ovarian, Fallopian Tube, or Primary Peritoneal Cancers." International Journal of Gynecological Cancer **21**(4): 633-639.
Kim, S. Y., Y. Tachioka, T. Mori and T. Hakoshima (2016). "Structural basis for autoinhibition and its relief of MOB1 in the Hippo pathway." Scientific Reports **6**.
Kohler, R. S., D. Schmitz, H. Cornils, B. A. Hemmings and A. Hergovich (2010). "Differential NDR/LATS Interactions with the Human MOB Family Reveal a Negative Role for Human MOB2 in the Regulation of Human NDR Kinases." Molecular and Cellular Biology **30**(18): 4507-4520.
Lai, Z. C., X. M. Wei, T. Shimizu, E. Ramos, M. Rohrbaugh, N. Nikolaidis, L. L. Ho and Y. Li (2005). "Control of cell proliferation and apoptosis by Mob as tumor suppressor, Mats." Cell **120**(5): 675-685.
Landau, M., I. Mayrose, Y. Rosenberg, F. Glaser, E. Martz, T. Pupko and N. Ben-Tal (2005). "ConSurf 2005: the projection of evolutionary conservation scores of residues on protein structures." Nucleic Acids Research **33**: W299-W302.
Laskowski, R. A., M. W. Macarthur, D. S. Moss and J. M. Thornton (1993). "Procheck - a Program to Check the Stereochemical Quality of Protein Structures." Journal of Applied Crystallography **26**: 283-291.
Lau, A. N., S. J. Curtis, C. M. Fillmore, S. P. Rowbotham, M. Mohseni, D. E. Wagner, A. M. Beede, D. T. Montoro, K. W. Sinkevicius, Z. E. Walton, J. Barrios, D. J. Weiss, F. D. Camargo, K. K. Wong and C. F. Kim (2014). "Tumor-propagating cells and

Yap/Taz activity contribute to lung tumor progression and metastasis (vol 33, pg 468, 2014)." Embo Journal **33**(13): 1502-1502.
Lee, J. H., T. S. Kim, T. H. Yang, B. K. Koo, S. P. Oh, K. P. Lee, H. J. Oh, S. H. Lee, Y. Y. Kong, J. M. Kim and D. S. Lim (2008). "A crucial role of WW45 in developing epithelial tissues in the mouse." Embo Journal **27**(8): 1231-1242.
Lee, K. W., S. S. Lee, S. B. Kim, B. H. Sohn, H. S. Lee, H. J. Jang, Y. Y. Park, S. Kopetz, S. S. Kim, S. C. Oh and J. S. Lee (2015). "Significant Association of Oncogene YAP1 with Poor Prognosis and Cetuximab Resistance in Colorectal Cancer Patients." Clinical Cancer Research **21**(2): 357-364.
Li, Q., S. X. Li, S. Mana-Capelli, R. J. R. Flach, L. V. Danai, A. Amcheslavsky, Y. C. Nie, S. Kaneko, X. H. Yao, X. C. Chen, J. L. Cotton, J. H. Mao, D. McCollum, J. Jiang, M. P. Czech, L. Xu and Y. T. Ip (2014). "The Conserved Misshapen-Warts-Yorkie Pathway Acts in Enteroblasts to Regulate Intestinal Stem Cells in Drosophila." Developmental Cell **31**(3): 291-304.
Li, W., J. Cooper, L. Zhou, C. Y. Yang, H. Erdjument-Bromage, D. Zagzag, M. Snuderl, M. Ladanyi, C. O. Hanemann, P. B. Zhou, M. A. Karajannis and F. G. Giancotti (2014). "Merlin/NF2 Loss-Driven Tumorigenesis Linked to CRL4(DcAF1)-Mediated Inhibition of the Hippo Pathway Kinases Latsl and 2 in the Nucleus." Cancer Cell **26**(1): 48-60.
Lignitto, L., A. Arcella, M. Sepe, L. Rinaldi, R. Delle Donne, A. Gallo, E. Stefan, V. A. Bachmann, M. A. Oliva, C. T. Storlazzi, A. L'Abbate, A. Brunetti, S. Gargiulo, M. Gramanzini, L. Insabato, C. Garbi, M. E. Gottesman and A. Feliciello (2013). "Proteolysis of MOB1 by the ubiquitin ligase praja2 attenuates Hippo signalling and supports glioblastoma growth." Nature Communications **4**.
Liu-Chittenden, Y., B. Huang, J. S. Shim, Q. Chen, S. J. Lee, R. A. Anders, J. O. Liu and D. J. Pan (2012). "Genetic and pharmacological disruption of the TEAD-YAP complex suppresses the oncogenic activity of YAP." Genes & Development **26**(12): 1300-1305.
Liu, B., Y. G. Zheng, F. Yin, J. Z. Yu, N. Silverman and D. J. Pan (2016). "Toll Receptor-Mediated Hippo Signaling Controls Innate Immunity in Drosophila." Cell **164**(3): 406-419.
Liu, C. Y., Z. Y. Zha, X. Zhou, H. Zhang, W. Huang, D. Zhao, T. T. Li, S. W. Chan, C. J. Lim, W. J. Hong, S. M. Zhao, Y. Xiong, Q. Y. Lei and K. L. Guan (2010). "The Hippo Tumor Pathway Promotes TAZ Degradation by Phosphorylating a Phosphodegron and Recruiting the SCF beta-TrCP E3 Ligase." Journal of Biological Chemistry **285**(48): 37159-37169.
Lu, L., Y. Li, S. M. Kim, W. Bossuyt, P. Liu, Q. Qiu, Y. D. Wang, G. Halder, M. J. Finegold, J. S. Lee and R. L. Johnson (2010). "Hippo signaling is a potent in vivo growth and tumor suppressor pathway in the mammalian liver." Proceedings of the National Academy of Sciences of the United States of America **107**(4): 1437-1442.
Luca, F. C. and M. Winey (1998). "MOB1, an essential yeast gene required for completion of mitosis and maintenance of ploidy." Molecular Biology of the Cell **9**(1): 29-46.
Manning, S. A. and K. F. Harvey (2015). "Warts Opens Up for Activation." Developmental Cell **35**(6): 666-668.
Mccoy, A. J., R. W. Grosse-Kunstleve, P. D. Adams, M. D. Winn, L. C. Storoni and R. J. Read (2007). "Phaser crystallographic software." Journal of Applied Crystallography **40**: 658-674.
Meng, Z., T. Moroishi and K. L. Guan (2016). "Mechanisms of Hippo pathway regulation." Genes Dev **30**(1): 1-17.

Meng, Z., T. Moroishi and K. L. Guan (2016). "Mechanisms of Hippo pathway regulation." Genes & Development **30**(1): 1-17.
Meng, Z. P., T. Moroishi and K. L. Guan (2016). "Mechanisms of Hippo pathway regulation." Genes & Development **30**(1): 1-17.
Meng, Z. P., T. Moroishi, V. Mottier-Pavie, S. W. Plouffe, C. G. Hansen, A. W. Hong, H. W. Park, J. S. Mo, W. Q. Lu, S. C. Lu, F. Flores, F. X. Yu, G. Halder and K. L. Guan (2015). "MAP4K family kinases act in parallel to MST1/2 to activate LATS1/2 in the Hippo pathway." Nature Communications **6**.
Miller, E., J. Y. Yang, M. DeRan, C. L. Wu, A. I. Su, G. M. C. Bonamy, J. Liu, E. C. Peters and X. Wu (2012). "Identification of Serum-Derived Sphingosine-1-Phosphate as a Small Molecule Regulator of YAP." Chemistry & Biology **19**(8): 955-962.
Millward, T., P. Cron and B. A. Hemmings (1995). "Molecular-Cloning and Characterization of a Conserved Nuclear Serine(Threonine) Protein-Kinase." Proceedings of the National Academy of Sciences of the United States of America **92**(11): 5022-5026.
Mou, F., M. Praskova, F. Xia, D. Van Buren, H. Hock, J. Avruch and D. W. Zhou (2012). "The Mst1 and Mst2 kinases control activation of rho family GTPases and thymic egress of mature thymocytes." Journal of Experimental Medicine **209**(4): 741-759.
Murakami, H., T. Mizuno, T. Taniguchi, M. Fujii, F. Ishiguro, T. Fukui, S. Akatsuka, Y. Horio, T. Hida, Y. Kondo, S. Toyokuni, H. Osada and Y. Sekido (2011). "LATS2 Is a Tumor Suppressor Gene of Malignant Mesothelioma." Cancer Research **71**(3): 873-883.
Murakami, M., M. Nakagawa, E. N. Olson and O. Nakagawa (2005). "A WW domain protein TAZ is a critical coactivator for TBX5, a transcription factor implicated in Holt-Oram syndrome." Proceedings of the National Academy of Sciences of the United States of America **102**(50): 18034-18039.
Neely, G. G., K. Kuba, A. Cammarato, K. Isobe, S. Amann, L. Y. Zhang, M. Murata, L. Elmen, V. Gupta, S. Arora, R. Sarangi, D. Dan, S. Fujisawa, T. Usami, C. P. Xia, A. C. Keene, N. N. Alayari, H. Yamakawa, U. Elling, C. Berger, M. Novatchkova, R. Koglgruber, K. Fukuda, H. Nishina, M. Isobe, J. A. Pospisilik, Y. Imai, A. Pfeufer, A. A. Hicks, P. P. Pramstaller, S. Subramaniam, A. Kimura, K. Ocorr, R. Bodmer and J. M. Penninger (2010). "A Global In Vivo Drosophila RNAi Screen Identifies NOT3 as a Conserved Regulator of Heart Function." Cell **141**(1): 142-153.
Nehme, N. T., J. Pachlopnik Schmid, F. Debeurme, I. Andre-Schmutz, A. Lim, P. Nitschke, F. Rieux-Laucat, P. Lutz, C. Picard, N. Mahlaoui, A. Fischer and G. de Saint Basile (2012). "MST1 mutations in autosomal recessive primary immunodeficiency characterized by defective naive T-cell survival." Blood **119**(15): 3458-3468.
Ni, L. S., Y. G. Zheng, M. Hara, D. J. Pan and X. L. Luo (2015). "Structural basis for Mob1-dependent activation of the core Mst-Lats kinase cascade in Hippo signaling." Genes & Development **29**(13): 1416-1431.
Nishio, M., K. Hamada, K. Kawahara, M. Sasaki, F. Noguchi, S. Chiba, K. Mizuno, S. O. Suzuki, Y. Y. Dong, M. Tokuda, T. Morikawa, H. Hikasa, J. Eggenschwiler, N. Yabuta, H. Nojima, K. Nakagawa, Y. Hata, H. Nishina, K. Mimori, M. Mori, T. Sasaki, T. W. Mak, T. Nakano, S. Itami and A. Suzuki (2012). "Cancer susceptibility and embryonic lethality in Mob1a/1b double-mutant mice." Journal of Clinical Investigation **122**(12): 4505-4518.
Nishio, M., K. Sugimachi, H. Goto, J. Wang, T. Morikawa, Y. Miyachi, Y. Takano, H. Hikasa, T. Itoh, S. O. Suzuki, H. Kurihara, S. Aishima, A. Leask, T. Sasaki, T. Nakano, H. Nishina, Y. Nishikawa, Y. Sekido, K. Nakao, K. Shin-ya, K. Mimori and A. Suzuki (2016). "Dysregulated YAP1/TAZ and TGF-beta signaling mediate

hepatocarcinogenesis in Mob1a/1b-deficient mice." Proceedings of the National Academy of Sciences of the United States of America **113**(1): E71-E80.
Oh, H. J., K. K. Lee, S. J. Song, M. S. Jin, M. S. Song, J. H. Lee, C. R. Im, J. O. Lee, S. Yonehara and D. S. Lim (2006). "Role of the tumor suppressor RASSF1A in Mst1-mediated apoptosis." Cancer Res **66**(5): 2562-2569.
Otwinowski, Z. and W. Minor (1997). "Processing of X-ray diffraction data collected in oscillation mode." Macromolecular Crystallography, Pt A **276**: 307-326.
Overholtzer, M., J. Zhang, G. A. Smolen, B. Muir, W. Li, D. C. Sgroi, C. X. Deng, J. S. Brugge and D. A. Haber (2006). "Transforming properties of YAP, a candidate oncogene on the chromosome 11q22 amplicon." Proceedings of the National Academy of Sciences of the United States of America **103**(33): 12405-12410.
Pantalacci, S., N. Tapon and P. Leopold (2003). "The Salvador partner Hippo promotes apoptosis and cell-cycle exit in Drosophila." Nature Cell Biology **5**(10): 921-927.
Pobbati, A. V., S. W. Chan, I. Lee, H. W. Song and W. J. Hong (2012). "Structural and Functional Similarity between the Vgll1-TEAD and the YAP-TEAD Complexes." Structure **20**(7): 1135-1140.
Polesello, C., S. Huelsmann, N. H. Brown and N. Tapon (2006). "The Drosophila RASSF homolog antagonizes the hippo pathway." Curr Biol **16**(24): 2459-2465.
Ponchon, L., C. Dumas, A. V. Kajava, D. Fesquet and A. Padilla (2004). "NMR solution structure of Mob1, a mitotic exit network protein and its interaction with an NDR kinase peptide." Journal of Molecular Biology **337**(1): 167-182.
Ponnusamy, S., S. P. Selvam, S. Mehrotra, T. Kawamori, A. J. Snider, L. M. Obeid, Y. Shao, R. Sabbadini and B. Ogretmen (2012). "Communication between host organism and cancer cells is transduced by systemic sphingosine kinase 1/sphingosine 1-phosphate signalling to regulate tumour metastasis." Embo Molecular Medicine **4**(8): 761-775.
Poon, C. L., J. I. Lin, X. Zhang and K. F. Harvey (2011). "The sterile 20-like kinase Tao-1 controls tissue growth by regulating the Salvador-Warts-Hippo pathway." Dev Cell **21**(5): 896-906.
Poon, C. L., J. I. Lin, X. Zhang and K. F. Harvey (2011). "The sterile 20-like kinase Tao-1 controls tissue growth by regulating the Salvador-Warts-Hippo pathway." Developmental cell **21**(5): 896-906.
Praskova, M., F. Xia and J. Avruch (2008). "MOBKL1A/MOBKL1B phosphorylation by MST1 and MST2 inhibits cell proliferation." Current Biology **18**(5): 311-321.
Rauskolb, C., G. H. Pan, B. V. V. G. Reddy, H. Y. Oh and K. D. Irvine (2011). "Zyxin Links Fat Signaling to the Hippo Pathway." Plos Biology **9**(6).
Ribeiro, P. S., F. Josue, A. Wepf, M. C. Wehr, O. Rinner, G. Kelly, N. Tapon and M. Gstaiger (2010). "Combined functional genomic and proteomic approaches identify a PP2A complex as a negative regulator of Hippo signaling." Mol Cell **39**(4): 521-534.
Robinson, B. S., J. Huang, Y. Hong and K. H. Moberg (2010). "Crumbs Regulates Salvador/Warts/Hippo Signaling in Drosophila via the FERM-Domain Protein Expanded." Current Biology **20**(7): 582-590.
Rock, J. M., D. Lim, L. Stach, R. W. Ogrodowicz, J. M. Keck, M. H. Jones, C. C. L. Wong, J. R. Yates, M. Winey, S. J. Smerdon, M. B. Yaffe and A. Amon (2013). "Activation of the Yeast Hippo Pathway by Phosphorylation-Dependent Assembly of Signaling Complexes." Science **340**(6134): 871-875.
Rual, J. F., K. Venkatesan, T. Hao, T. Hirozane-Kishikawa, A. Dricot, N. Li, G. F. Berriz, F. D. Gibbons, M. Dreze, N. Ayivi-Guedehoussou, N. Klitgord, C. Simon, M. Boxem, S. Milstein, J. Rosenberg, D. S. Goldberg, L. V. Zhang, S. L. Wong, G.

Franklin, S. M. Li, J. S. Albala, J. H. Lim, C. Fraughton, E. Llamosas, S. Cevik, C. Bex, P. Lamesch, R. S. Sikorski, J. Vandenhaute, H. Y. Zoghbi, A. Smolyar, S. Bosak, R. Sequerra, L. Doucette-Stamm, M. E. Cusick, D. E. Hill, F. P. Roth and M. Vidal (2005). "Towards a proteome-scale map of the human protein-protein interaction network." Nature **437**(7062): 1173-1178.
Santucci, M., T. Vignudelli, S. Ferrari, M. Mor, L. Scalvini, M. L. Bolognesi, E. Uliassi and M. P. Costi (2015). "The Hippo Pathway and YAP/TAZ-TEAD Protein-Protein Interaction as Targets for Regenerative Medicine and Cancer Treatment." Journal of Medicinal Chemistry **58**(12): 4857-4873.
Schuldiner, O., D. Berdnik, J. M. Levy, J. S. Wu, D. Luginbuhl, A. Camille and L. Q. Luo (2008). "piggyBac-based mosaic screen identifies a postmitotic function for cohesin in regulating developmental axon pruning." Developmental Cell **14**(2): 227-238.
Shimizu, T., L. L. Hot and Z. C. Lai (2008). "The mob as tumor suppressor gene is essential for early development and regulates tissue growth in drosophila." Genetics **178**(2): 957-965.
Simons, M. and M. Mlodzik (2008). "Planar Cell Polarity Signaling: From Fly Development to Human Disease." Annual Review of Genetics **42**: 517-540.
Song, H., K. K. Mak, L. Topol, K. S. Yun, J. X. Hu, L. Garrett, Y. B. Chen, O. Park, J. Chang, R. M. Simpson, C. Y. Wang, B. Gao, J. Jiang and Y. Z. Yang (2010). "Mammalian Mst1 and Mst2 kinases play essential roles in organ size control and tumor suppression." Proceedings of the National Academy of Sciences of the United States of America **107**(4): 1431-1436.
Staley, B. K. and K. D. Irvine (2012). "Hippo signaling in Drosophila: Recent advances and insights." Developmental Dynamics **241**(1): 3-15.
Stavridi, E. S., K. G. Harris, Y. Huyen, J. Bothos, P. M. Verwoerd, S. E. Stayrook, N. P. Pavletich, P. D. Jeffrey and F. C. Luca (2003). "Crystal structure of a human Mob1 protein: Toward understanding mob-regulated cell cycle pathways." Structure **11**(9): 1163-1170.
Stegert, M. R., A. Hergovich, R. Tamaskovic, S. J. Bichsel and B. A. Hemmings (2005). "Regulation of NDR protein kinase by hydrophobic motif phosphorylation mediated by the mammalian Ste20-like kinase MST3." Molecular and Cellular Biology **25**(24): 11019-11029.
Strano, S., E. Munarriz, M. Rossi, L. Castagnoli, Y. Shaul, A. Sacchi, M. Oren, M. Sudol, G. Cesareni and G. Blandino (2001). "Physical interaction with Yes-associated protein enhances p73 transcriptional activity." Journal of Biological Chemistry **276**(18): 15164-15173.
Tang, F., J. Gill, X. Ficht, T. Barthlott, H. Cornils, D. Schmitz-Rohmer, D. Hynx, D. Zhou, L. Zhang, G. Xue, M. Grzmil, Z. Yang, A. Hergovich, G. A. Hollaender, J. V. Stein, B. A. Hemmings and P. Matthias (2015). "The kinases NDR1/2 act downstream of the Hippo homolog MST1 to mediate both egress of thymocytes from the thymus and lymphocyte motility." Sci Signal **8**(397): ra100.
Tao, J. Y., D. F. Calvisi, S. Ranganathan, A. Cigliano, L. L. Zhou, S. Singh, L. J. Jiang, B. A. Fan, L. Terracciano, S. Armeanu-Ebinger, S. Ribback, F. Dombrowski, M. Evert, X. Chen and S. P. S. Monga (2014). "Activation of beta-Catenin and Yap1 in Human Hepatoblastoma and Induction of Hepatocarcinogenesis in Mice." Gastroenterology **147**(3): 690-701.
Tao, W. F., S. Zhang, G. S. Turenchalk, R. A. Stewart, M. A. R. St John, W. L. Chen and T. Xu (1999). "Human homologue of the Drosophila melanogaster lats tumour suppressor modulates CDC2 activity." Nature Genetics **21**(2): 177-181.

Tapon, N., K. F. Harvey, D. W. Bell, D. C. R. Wahrer, T. A. Schiripo, D. A. Haber and I. K. Hariharan (2002). "salvador promotes both cell cycle exit and apoptosis in Drosophila and is mutated in human cancer cell lines." Cell **110**(4): 467-478.
Thibault, S. T., M. A. Singer, W. Y. Miyazaki, B. Milash, N. A. Dompe, C. M. Singh, R. Buchholz, M. Demsky, R. Fawcett, H. L. Francis-Lang, L. Ryner, L. M. Cheung, A. Chong, C. Erickson, W. W. Fisher, K. Greer, S. R. Hartouni, E. Howie, L. Jakkula, D. Joo, K. Killpack, A. Laufer, J. Mazzotta, R. D. Smith, L. M. Stevens, C. Stuber, L. R. Tan, R. Ventura, A. Woo, I. Zakrajsek, L. Zhao, F. Chen, C. Swimmer, C. Kopczynski, G. Duyk, M. L. Winberg and J. Margolis (2004). "A complementary transposon tool kit for Drosophila melanogaster using P and piggyBac." Nature Genetics **36**(3): 283-287.
Udan, R. S., M. Kango-Singh, R. Nolo, C. Y. Tao and G. Halder (2003). "Hippo promotes proliferation arrest and apoptosis in the Salvador/Warts pathway." Nature Cell Biology **5**(10): 914-920.
Vichalkovski, A., E. Gresko, H. Cornils, A. Hergovich, D. Schmitz and B. A. Hemmings (2008). "NDR Kinase Is Activated by RASSF1A/MST1 in Response to Fas Receptor Stimulation and Promotes Apoptosis." Current Biology **18**(23): 1889-1895.
Vrabioiu, A. M. and G. Struhl (2015). "Fat/Dachsous Signaling Promotes Drosophila Wing Growth by Regulating the Conformational State of the NDR Kinase Warts." Developmental Cell **35**(6): 737-749.
Vrabioiu, A. M. and G. Struhl (2015). "Fat/Dachsous Signaling Promotes Drosophila Wing Growth by Regulating the Conformational State of the NDR Kinase Warts." Dev Cell **35**(6): 737-749.
Watson, K. L. (1995). "Drosophila Warts - Tumor-Suppressor and Member of the Myotonic-Dystrophy Protein-Kinase Family." Bioessays **17**(8): 673-676.
Wei, X., T. Shimizu and Z. C. Lai (2007). "Mob as tumor suppressor is activated by Hippo kinase for growth inhibition in Drosophila." Embo Journal **26**(7): 1772-1781.
Weiss, E. L., C. Kurischko, C. Zhang, K. Shokat, D. G. Drubin and F. C. Luca (2002). "The Saccharomyces cerevisiae Mob2p-Cbk1p kinase complex promotes polarized growth and acts with the mitotic exit network to facilitate daughter cell-specific localization of Ace2p transcription factor." Journal of Cell Biology **158**(5): 885-900.
Winn, M. D. (2003). "An overview of the CCP4 project in protein crystallography: an example of a collaborative project." Journal of Synchrotron Radiation **10**: 23-25.
Wu, S., J. B. Huang, J. X. Dong and D. J. Pan (2003). "hippo encodes a Ste-20 family protein kinase that restricts cell proliferation and promotes apoptosis in conjunction with salvador and warts." Cell **114**(4): 445-456.
Xiao, L., Y. H. Chen, M. Ji and J. X. Dong (2011). "KIBRA Regulates Hippo Signaling Activity via Interactions with Large Tumor Suppressor Kinases." Journal of Biological Chemistry **286**(10): 7788-7796.
Xin, M., Y. Kim, L. B. Sutherland, M. Murakami, X. X. Qi, J. McAnally, E. R. Porrello, A. I. Mahmoud, W. Tan, J. M. Shelton, J. A. Richardson, H. A. Sadek, R. Bassel-Duby and E. N. Olson (2013). "Hippo pathway effector Yap promotes cardiac regeneration." Proceedings of the National Academy of Sciences of the United States of America **110**(34): 13839-13844.
Xin, M., Y. Kim, L. B. Sutherland, X. X. Qi, J. McAnally, R. J. Schwartz, J. A. Richardson, R. Bassel-Duby and E. N. Olson (2011). "Regulation of Insulin-Like Growth Factor Signaling by Yap Governs Cardiomyocyte Proliferation and Embryonic Heart Size." Science Signaling **4**(196).
Xu, T. and G. M. Rubin (1993). "Analysis of Genetic Mosaics in Developing and Adult Drosophila Tissues." Development **117**(4): 1223-1237.

Xu, T. A., W. Y. Wang, S. Zhang, R. A. Stewart and W. Yu (1995). "Identifying Tumor Suppressors in Genetic Mosaics - the Drosophila Lats Gene Encodes a Putative Protein-Kinase." Development **121**(4): 1053-1063.
Yang, J., P. Cron, V. Thompson, V. M. Good, D. Hess, B. A. Hemmings and D. Barford (2002). "Molecular mechanism for the regulation of protein kinase B/Akt by hydrophobic motif phosphorylation." Molecular Cell **9**(6): 1227-1240.
Yang, Y. F., V. Gupta, L. L. Ho, B. Zhou, Q. C. Fan, Z. Y. Zhu, W. X. Zhang and Z. C. Lai (2008). "Both upstream and downstream intergenic regions are critical for the mob as tumor suppressor gene activity in Drosophila." Febs Letters **582**(12): 1766-1770.
Yu, F. X. and K. L. Guan (2013). "The Hippo pathway: regulators and regulations." Genes & Development **27**(4): 355-371.
Yu, F. X., Y. F. Zhang, H. W. Park, J. L. Jewell, Q. Chen, Y. T. Deng, D. J. Pan, S. S. Taylor, Z. C. Lai and K. L. Guan (2013). "Protein kinase A activates the Hippo pathway to modulate cell proliferation and differentiation." Genes & Development **27**(11): 1223-1232.
Yu, F. X., B. Zhao, N. Panupinthu, J. L. Jewell, I. Lian, L. H. Wang, J. G. Zhao, H. X. Yuan, K. Tumaneng, H. R. Li, X. D. Fu, G. B. Mills and K. L. Guan (2012). "Regulation of the Hippo-YAP Pathway by G-Protein-Coupled Receptor Signaling." Cell **150**(4): 780-791.
Yu, J. Z., Y. G. Zheng, J. X. Dong, S. Klusza, W. M. Deng and D. J. Pan (2010). "Kibra Functions as a Tumor Suppressor Protein that Regulates Hippo Signaling in Conjunction with Merlin and Expanded." Developmental Cell **18**(2): 288-299.
Zanconato, F., M. Cordenonsi and S. Piccolo (2016). "YAP/TAZ at the Roots of Cancer." Cancer Cell **29**(6): 783-803.
Zhang, L., F. Y. Tang, L. Terracciano, D. Hynx, R. Kohler, S. Bichet, D. Hess, P. Cron, B. A. Hemmings, A. Hergovich and D. Schmitz-Rohmer (2015). "NDR Functions as a Physiological YAP1 Kinase in the Intestinal Epithelium." Current Biology **25**(3): 296-305.
Zhang, N. L., H. B. Bai, K. K. David, J. X. Dong, Y. G. Zheng, J. Cai, M. Giovannini, P. T. Liu, R. A. Anders and D. J. Pan (2010). "The Merlin/NF2 Tumor Suppressor Functions through the YAP Oncoprotein to Regulate Tissue Homeostasis in Mammals." Developmental Cell **19**(1): 27-38.
Zhang, W. J., Y. J. Gao, P. X. Li, Z. B. Shi, T. Guo, F. Li, X. K. Han, Y. Feng, C. Zheng, Z. Y. Wang, F. M. Li, H. Q. Chen, Z. C. Zhou, L. Zhang and H. B. Ji (2014). "VGLL4 functions as a new tumor suppressor in lung cancer by negatively regulating the YAP-TEAD transcriptional complex." Cell Research **24**(3): 331-343.
Zhao, B., L. Li, Q. Y. Lei and K. L. Guan (2010). "The Hippo-YAP pathway in organ size control and tumorigenesis: an updated version." Genes & Development **24**(9): 862-874.
Zhao, B., L. Li, K. Tumaneng, C. Y. Wang and K. L. Guan (2010). "A coordinated phosphorylation by Lats and CK1 regulates YAP stability through SCF beta-TRCP." Genes & Development **24**(1): 72-85.
Zhao, B., L. Li, L. Wang, C. Y. Wang, J. D. Yu and K. L. Guan (2012). "Cell detachment activates the Hippo pathway via cytoskeleton reorganization to induce anoikis." Genes & Development **26**(1): 54-68.
Zhao, B., X. Wei, W. Li, R. S. Udan, Q. Yang, J. Kim, J. Xie, T. Ikenoue, J. Yu, L. Li, P. Zheng, K. Ye, A. Chinnaiyan, G. Halder, Z. C. Lai and K. L. Guan (2007). "Inactivation of YAP oncoprotein by the Hippo pathway is involved in cell contact inhibition and tissue growth control." Genes & Development **21**(21): 2747-2761.

Zhao, B., X. Ye, J. D. Yu, L. Li, W. Q. Li, S. M. Li, J. J. Yu, J. D. Lin, C. Y. Wang, A. M. Chinnaiyan, Z. C. Lai and K. L. Guan (2008). "TEAD mediates YAP-dependent gene induction and growth control." Genes & Development **22**(14): 1962-1971.
Zheng, Y. G., W. Wang, B. Liu, H. Deng, E. Uster and D. J. Pan (2015). "Identification of Happyhour/MAP4K as Alternative Hpo/Mst-like Kinases in the Hippo Kinase Cascade." Developmental Cell **34**(6): 642-655.
Zhou, D. W., C. Conrad, F. Xia, J. S. Park, B. Payer, Y. Yin, G. Y. Lauwers, W. Thasler, J. T. Lee, J. Avruch and N. Bardeesy (2009). "Mst1 and Mst2 Maintain Hepatocyte Quiescence and Suppress Hepatocellular Carcinoma Development through Inactivation of the Yap1 Oncogene." Cancer Cell **16**(5): 425-438.
Zhou, D. W., Y. Y. Zhang, H. Wu, E. Barry, Y. Yin, E. Lawrence, D. Dawson, J. E. Willis, S. D. Markowitz, F. D. Camargo and J. Avruch (2011). "Mst1 and Mst2 protein kinases restrain intestinal stem cell proliferation and colonic tumorigenesis by inhibition of Yes-associated protein (Yap) overabundance." Proceedings of the National Academy of Sciences of the United States of America **108**(49): E1312-E1320.

Supplementary Data

Supplementary Table S1 Data collection and refinement statistics.

R_{merge} = R_{merge} = $\Sigma_h\Sigma_i |I_{h,i} – I_h|/\Sigma_h\Sigma_i I_{h,i}$ for the intensity (I) of observation i of reflection h. R factor = $\Sigma||F_{obs}| - |F_{calc}||/\Sigma|F_{obs}|$, where F_{obs} and F_{calc} are the observed and calculated structure factors, respectively. R_{free} = R factor calculated using 5% of the reflection data chosen randomly and omitted from the start of refinement. RMSD, root-mean-square deviations from ideal geometry. Data for the highest resolution shell are shown in parentheses.

Table S1: Data collection and refinement statistics

Data collection	
Space group	$P2_12_12_1$
Unit-cell parameters	*a*=57.5 Å, *b*=94.4 Å, *c* =102.2 Å; α=β=γ=90°
Number of molecules/asymmetric unit	2
Resolution range (Å)	50-2.10 (2.18-2.10)
Completeness (%)	99.6 (100.0)
Redundancy	6.9 (6.4)
Total observations	226,859
Unique reflections	32,723
R_{merge} (%)	10.0 (61.3)
I/σ_I	16.3 (3.1)
Refinement	
R_{work} (%)	15.3
R_{free} (%)	24.4
Overall B factor	42.3
RMSD bond lengths (Å)	0.013
RMSD bond angles (°)	1.507

Ramanchandran plot (favored, allowed, disallowed, %)	99.0, 0.6, 0.4
Final model (Number of protein/solvent atoms)	4,149/267

Supplementary Figure S1 PCR genotyping.

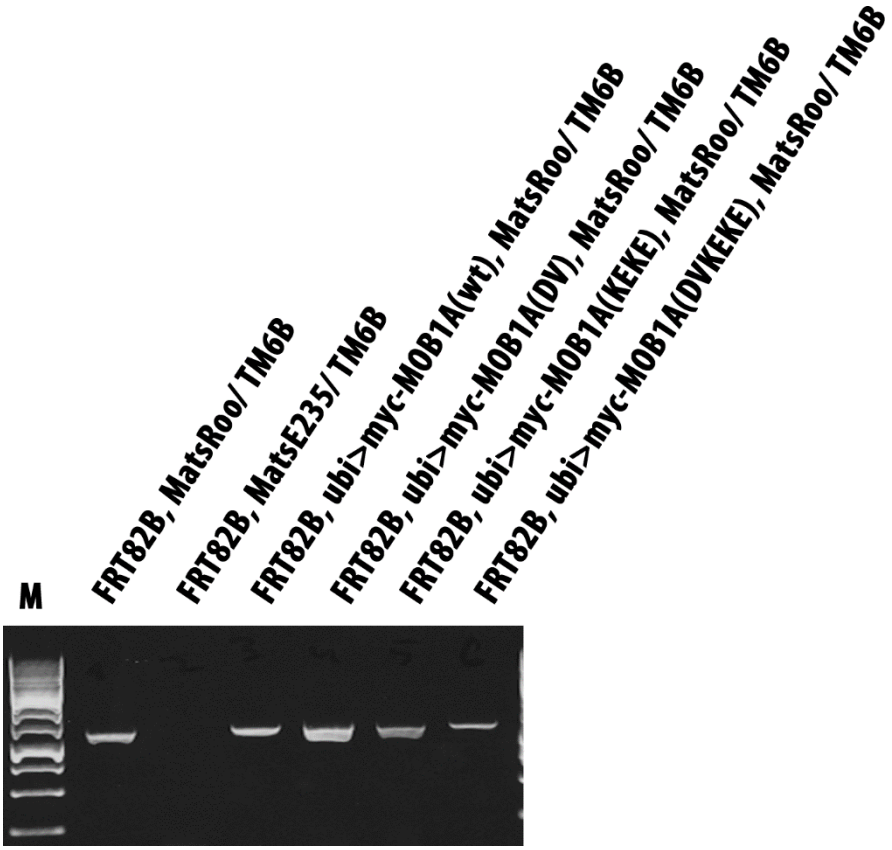

Figure S1: PCR genotyping of the indicated flies. The primers Roo Internal 1 and 97 **(specified in section 2.1.5)** was used to confirm the Roo transposon.

Supplementary Figure S2 PCR genotyping.

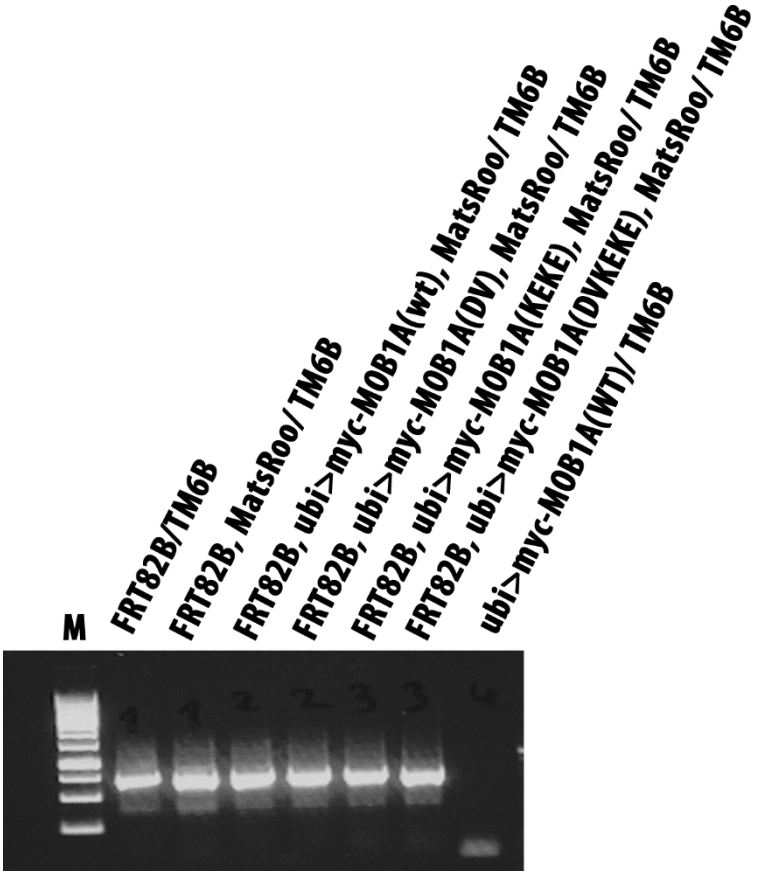

Figure S2: PCR genotyping of the indicated flies. The primers Neo2 f and hsp70_FRT r **(specified in section 2.1.5)** was used to confirm the FRT site.

Appendix 2

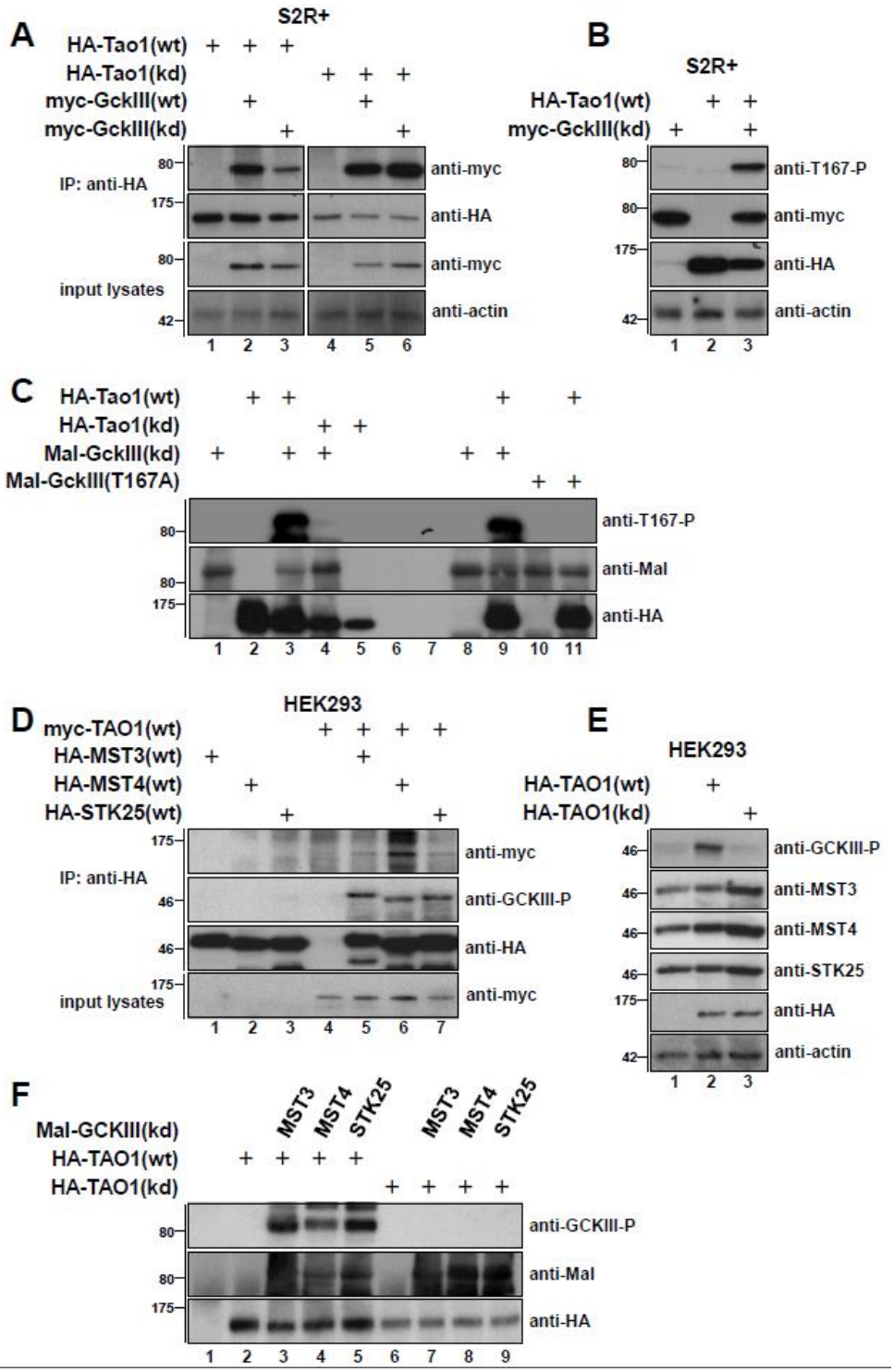

Appendix Figure 1: The TAO1 kinase phosphorylate GCKIII kinases on their T-loop phosphorylation site in fly and human cells.

(A) Lysates of *Drosophila* S2R+ cells expressing full-length HA-Tao1 wild-type (wt) or kinase-dead (kd) together with indicated full-length GckIII versions were subjected to immunoprecipitation (IP) using anti-HA 12CA5 antibody. Complexes were analysed by

immunoblotting using anti-myc (top) and anti-HA (top middle). Input lysates were analysed with anti-myc (bottom middle) and anti-actin (bottom).

(B) S2R+ cells were transfected with indicated versions of fly Tao1 and GckIII, before whole cell extracts were processed for Western blotting using anti-T167-P (top), anti-myc (top middle), anti-HA (bottom middle) and anti-actin (bottom).

(C) Lysates of S2R+ cells transiently expressing full-length HA-Tao1 variants were subjected to immunoprecipitation with anti-HA 12CA5 antibody. Immunopurified proteins were then processed for kinase assays without or with the indicated recombinant full-length and kinase-dead Mal-GckIII version. Following kinase reactions, the samples were examined by immunoblotting using the specified antibodies. Importantly, the anti-T167-P antibody specifically detected Tao1-mediated phosphorylation of GckIII on Thr167 (compare lanes 3, 9 and 11).

(D) Lysates of human HEK293 cells expressing full-length HA-GCKIII variants (MST3, MST4 or STK25) together with indicated full-length myc-TAO1 were subjected to IP using anti-HA, before Western blot analysis of complexes and input lysates using indicated antibodies.

(E) HEK293 cells were transfected with indicated versions of human TAO1, before whole cell extracts were processed for Western blotting using the specified antibodies. Noteworthy, increased T-loop phosphorylation of human GCKIII kinases was observed upon TAO1 overexpression.

(F) Lysates of HEK293 cells transiently expressing full-length human HA-TAO1 variants were subjected to immunoprecipitation with anti-HA. Immunopurified kinases were then processed for kinase assays without or with the indicated recombinant full-length and kinase-dead Mal-GCKIII versions (MST3, MST4 or STK25). Following kinase reactions, the samples were examined by immunoblotting using the specified antibodies. Importantly, TAO1-mediated T-loop phosphorylation of human GCKIII kinases was only observed when wild-type TAO1 was incubated with kinase-dead GCKIII kinases. Relative molecular weights are shown.

To determine whether GckIII is potentially directly regulated by Tao1 in fly cells, we investigated Tao1/GckIII complex formation in *Drosophila* S2R+ cells **(Appendix Fig. 1A)**. N-terminally tagged versions of HA-Tao1 and myc-GckIII were co-expressed, followed by immunoprecipitation using anti-HA. This revealed that irrespective of their activity status Tao1 and GckIII can form a complex in fly cells, as judged by the co-immunoprecipitation of wild-type and kinase-dead variants **(Appendix Fig. 1A)**. Next, considering that Tao1 can function as upstream kinase of Hippo

(Poon, Lin et al. 2011), we sought to test whether Tao1 can also act as upstream kinase of the Hippo-like GckIII kinase. To do so, we pursued two lines of research. First, we examined in fly cells the level of T-loop (Thr167) phosphorylation on GckIII upon Tao1 co-expression **(Appendix Fig. 1B)**. Second, we studied Tao1-mediated phosphorylation of recombinant full-length GckIII *in vitro* **(Appendix Fig. 1C)**. The phosphorylation of kinase-dead GckIII was elevated upon Tao1 expression (Appendix Fig. 1B) and *in vitro* the T-loop phosphorylation of GckIII was dependent on Tao1 kinase activity **(Appendix Fig. 1C)**. Significantly, these experiments collectively showed that fly Tao1 can phosphorylate GckIII on Thr167 in the activation T-loop in cells and *in vitro* **(Appendix Fig. 1B and 1C)**.

Considering that GckIII is conserved between flies and humans, we asked next whether human TAO1 can also interact with and phosphorylate MST3, MST4 and/or STK25, the three human counterparts of fly GckIII, hence collectively termed hGCKIII. The corresponding human cDNAs were expressed in human HEK293 cells and TAO1/hGCKIII complex formation was assessed by co-immunoprecipitation experiments (Fig. XD). Furthermore, the T-loop phosphorylation of endogenous hGCKIII was studied in cells transiently overexpressing HA-TAO1(wt) or HA-TAO1(kd) **(Appendix Fig. 1E)**, and the phosphorylation of recombinant full-length kinase-dead hGCKIII versions by TAO1 was investigated *in vitro* (Appendix Fig. 1). These experiments jointly revealed, like observed for fly Tao1/GckIII **(Appendix Fig. 1A-C)**, that human TAO1 and hGCKIII can form complexes **(Appendix Fig. 1D)**, and even more importantly, that human TAO1 phosphorylates all three hGCKIII kinases on their T-loop regulatory site **(Appendix Fig. 1E and 1F)**. Taken together, our data presented in **Appendix Fig. 1** suggest that GCKIII kinases are *bona fide* substrates of TAO1 in fly and human cells.